Analysis of cuticular hydrocarbons in forensically important blowflies using mass spectrometry and its application in Post Mortem Interval estimations

A thesis submitted by

Hannah Elizabeth Moore

to

Keele University

For the degree of Doctor of Philosophy

June 2013

Abstract

Forensic entomology relies on accurate identification of forensically important blowflies to species level, preceded by ageing the Calliphorid specimens present on a cadaver to determine the post-mortem interval (PMI). The task of identifying blowflies based on morphological criteria can be challenging due to complex keys, limited diagnostic features in the immature stages and poor preservation of entomological samples. Therefore, the larvae will mostly be reared to adult flies to confirm identification, which is a time consuming process.

This thesis presents work examining the cuticular hydrocarbon (CHC) profiles of three forensically important blowfly species in the UK, *Lucilia sericata*, *Calliphora vicina* and *Calliphora vomitoria* with two main aims to this study. Firstly to establish if CHC analysis could be used to determine whether the three species yield characteristic profiles, allowing for identification to be achieved. The second aim was to examine the hydrocarbon profiles over time to determine if chemical changes occurred at certain points in time, giving an indication of age. The CHCs were extracted from all life stages (empty egg cases, larvae, pupae, empty puparial cases and adult flies) and analysed using gas chromatography – mass spectrometry (GC-MS) and Direct-analysis-in-Real-Time MS (DART-MS). Statistical interpretation was applied in the form of principal component analysis (PCA) and preliminary Artificial Neural Networks (ANN). Results showed species-specific characteristics within the chromatograms in all life stages, meaning distinctions can be made between the three species, even in 1st instar larvae. Significant chemical changes were observed within the hydrocarbon profiles over time, hence accurate ageing could be established for larvae, empty puparial cases and adult flies. Early results show great potential to utilise this technique and to develop it into a highly useful identification and ageing tool.

Acknowledgements

I would like to start by thanking my principal PhD supervisor, Dr Falko Drijfhout, for his endless guidance and support through my studies. He gave me this amazing opportunity and allowed me the freedom to choose my own research paths. He has been inspirational and I have learnt an enormous amount from his vast knowledge base.

My thanks also go to…

ACORN from Keele University, for funding part of my research.

Dr Craig Adam, my second supervisor, who not only helped me with the statistical side of my research, but also improved my writing skills.

Dr Peter Haycock, to whom I owe a great deal, for had he not given me a chance all those years ago, I would have never started my undergraduate studies at Keele. I hope my academic progress has given him the confidence to allow other students the same opportunities.

Deena van Logchem for his help in the laboratory during his time at Keele.

Dr Martin Hall, Dr Cameron Richards, Amoret Whittaker and Dr Andrew Hart, for their advice, inspiration and support.

Dr John Butcher for his contribution on the artificial neural network results. On a personal note, I would like to thank him for being so patient with me over the last four years and for keeping a smile on my face. Everything is reachable with him by my side.

The Winston Churchill Memorial Trust for awarding me the opportunity of a life time.

My whole PhD experience has been one of complete enjoyment. I have always been highly passionate about my research and over the duration of my studies it has developed, changed direction and reshaped itself into a fascinating project which I am enormously proud to present.

List of Content

List of Figures

List of Tables

List of Equations

List of Abbreviations

CHC	Cuticular Hydrocarbon
HC	Hydrocarbon
C. vicina	*Calliphora vicina*
C. vomitoria	*Calliphora vomitoria*
L. sericata	*Lucilia sericata*
PMI	Post-Mortem Interval
PMI_{min}	minimum Post-Mortem Interval
PMI_{max}	maximum Post-Mortem Interval
TOC	Time of Colonization
PIA	Period of Insect Activity
ADD	Accumulated Degree Days
ADH	Accumulated Degree Hours
RH	Relative Humidity
MP	Mobile Phase
SP	Stationary Phase
GC-MS	Gas Chromatography - Mass Spectrometry
LC-MS	Liquid Chromatography - Mass Spectrometry
DART-MS	Direct Analysis in Real Time - Mass Spectrometry
TOF	Time of Flight
FID	Flame Ionisation Detector
PCA	Principal Component Analysis
PCs	Principal Components
ANN	Artificial Neural Networks
SOM	Self-Organizing Map
LDA	Linear Discriminant Analysis
C_x:H	*n*-alkane
$_xMeC_y$:H	Methyl branched alkane
C_x:1	Alkene

C$_x$:2   Alkadiene

DMDS   Dimethyl Disulfide

[M]$^+$ Molecular ion

Chapter 1

Introduction

1. Background

Forensic entomology is a branch of forensic science that uses insects and their arthropod relatives that inhabit decomposing human remains to aid legal investigation [1–3]. The use of forensic entomology can be dated back to the 13th century when it was first used by Sung Tźu, a Chinese lawyer and death investigator (cited in [3]). Between the 13th and 19th century scientists were discovering new areas in biology and since then forensic entomology became a scientific branch of its own. The first time it was used in the courtroom was in France in 1850 [3] and although it has been around for all these years, it is only in the last few decades that its true forensic potential is being utilised.

The wealth of information that forensic entomology provides is vast and it can be divided into three areas [4]:

1) Medicolegal forensic entomology

2) Urban forensic entomology

3) Stored product pest forensic entomology

For the purpose of this research, only medicolegal forensic entomology will be considered. Medicolegal forensic entomology focuses on necrophagous insects that infest decomposing remains, involved in criminal investigations [5]. A branch within medicolegal forensic entomology is forensic entomotoxicology, which can be used to establish whether the deceased had taken drugs and/or toxins prior to death as the growth rate of the larvae can be accelerated or retarded, depending on the drug [6]. Medicolegal forensic entomology does not just cover insect infestation of the deceased. It also covers cases of myiasis [7–9], which is the infestation of live vertebrates with Diptera larvae, usually associated with cases of neglect where open wounds are colonized [8]. However, the study of myiasis is a separate line of forensic entomology and therefore will not be covered in this thesis.

When a corpse is discovered, the time since death, otherwise known as Post Mortem Interval (PMI), needs to be determined. A medical pathologist can usually give an accurate PMI up to 72 hours after death depending on the state of the body and the climate (the milder the conditions the faster the decomposition process) [10]. However, the longer the body is discovered after this window of time, the more inaccurate the PMI will be, which is where insect evidence can be utilised, often with a great deal of success.

Due to the abundance of insects that inhabit decomposing remains, they offer a variety of forensic evidence. In particular, the first inhabitants, known to be the blowfly [3], can provide information ranging from an estimation of how long a person has been

dead [10], to determining whether the deceased had taken drugs prior to death [2]. The quality of the evidence is dependent on accurate insect identification and a thorough understanding of entomology and the biology of blowflies [11].

If a forensic entomologist has knowledge of the blowfly species present, the respective development times for that particular species and how it is affected by temperature and other environmental conditions, a minimum Post Mortem Interval (PMI_{min}) can be obtained. The estimation depends on correct identification , a high degree of accuracy of the environmental conditions the insects are thought to have been exposed to and the reliability and credibility of experimental data used when performing the calculations [11].

A cadaver will attract many insects ranging from flies (Diptera) to Wasps (Hymenoptera) [3] as the corpse progresses through the decomposition process, known as succession (see also 1.3). This succession pattern of insects on decomposing remains has been well studied and flies, in particular, the blowfly (Calliphoridea) are known to be the early colonizers, arriving very quickly after death [12] making them the prominent insects used for PMI estimations.

If the species are incorrectly identified this would result in the PMI_{min} estimation being either too short or too long, risking potential conflicts with other evidence [6,11]. It is also essential to estimate the age of the oldest developing blowfly present on the body in order to determine the PMI_{min} calculation. These are the initial key factors a forensic entomologist has to undertake when presented with a crime scene.

The female blowflies will lay eggs in any open wounds (if present) or in the body's natural and moist orifices such as the ears, eyes, nose, genitalia. This process occurs in waves so there will be a continuous wave of larvae hatching at different times. A

forensic entomologist is able to make a PMI_{min} estimation based on the life cycle stages of the insect species found at the body. The PMI involves a mathematical calculation that has many variables contributing to it (ambient air temperature, mass maggot temperature etc.) so when all these are taken into account, a reliable measurement of time since death can be estimated.

Methods currently used to estimate the PMI_{min} includes two main processes:

1) For the early PMI estimations, the oldest insect specimens that have developed on the carrion must be identified and aged.

2) For late PMI estimations, the succession patterns of arthropods present on the carrion must be examined [13].

1.1 Stages of decomposition

The extent of the body's decomposition determines which insects are present. The body goes through different changes in temperature and moisture as it decomposes, as well as emitting various Volatile Organic Compounds (VOCs) and bacteria, which attract the flies [6]. These changes make it hospitable for different insects at different times. The five stages of decomposition and insects associated with them are briefly outlined below [2]:

1) **Fresh**: Adult blowflies are the first to arrive, feeding and laying eggs on the body.

2) **Bloated**: The body bloats and expands due to a buildup of gases produced by the cells and organs breaking down. Maggot masses may begin to form and more flies,

such as the flesh flies (Sarcophagidae), will start to arrive as well as beetles (Coleoptera), which prey on the larvae and feed off the body.

3) **Decay**: The body will deflate and the buildup of gases may have caused the skin to split. Maggot masses may be abundantly present, attracting more beetles to pray on them. Early colonizers could be in the post-feeding stage and begin to migrate away from the body to find a suitable place to pupate.

4) **Post-Decay**: Predominantly skin, hair, cartilage and bones are left. Some beetles may be present feeding on these.

5) **Skeletal**: Bones and hair remain and no insects will be present.

1.2 The life cycle of the blowfly

As the blowfly is the most important insect when it comes to estimating the time since colonisation, their life cycle has been well studied [14–19]. The cycle has six stages of development from the egg to the adult fly, undergoing a complete metamorphosis, as seen in Figure 1.1.
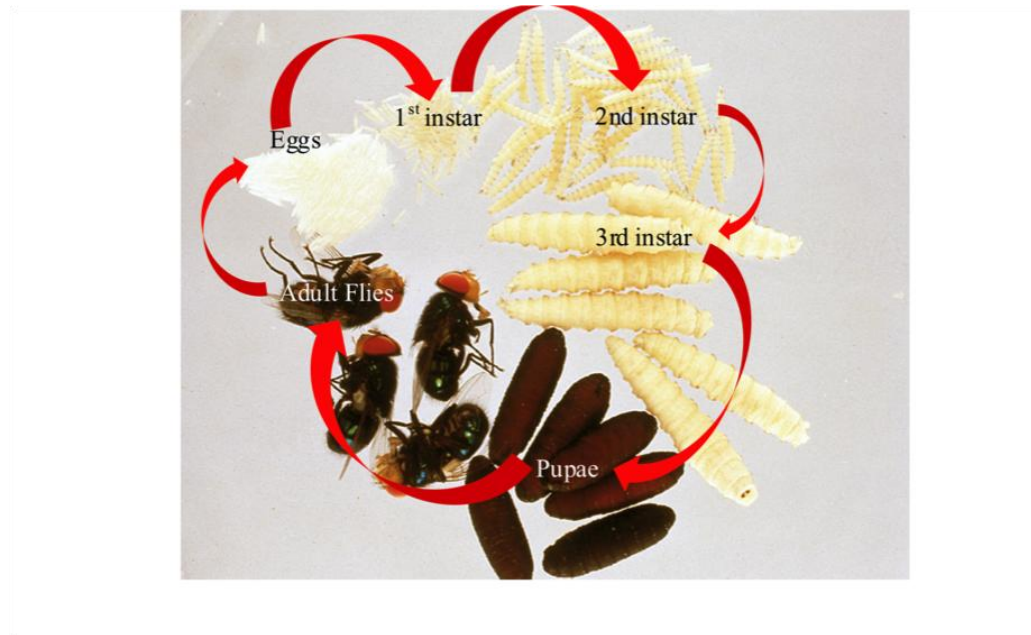
Figure 1.1: The life cycle of the blowfly, taken and adapted with permission from Dr Martin Hall

During the three larval stages, known as 1st instar, 2nd instar and 3rd instar, the larvae increase in size as they develop. A further stage that occurs before pupation is known as the post-feeding stage, where larvae stop feeding and migrate away from the body seeking cool, dark and damp conditions in order to pupate. Adult flies then eclose from the puparial cases and the cycle continues.

1.3 Factors influencing PMI

The succession pattern is defined as the order in which arthropods arrive at decomposing remains [20] and it has been widely studied [20–25].

As mentioned before, when a forensic entomologist attends a crime scene it is crucial they can identify two aspects. Firstly, the species of the insect needs to be determined. The easiest way of doing this is rearing the immature stages, collected at a crime scene,

to adult flies as it can be challenging to morphologically identify the larvae to species level in these larval stages [26]. The reason that identification is so important is because different species of insects have different life stage timings therefore to utilise the correct developmental information, correct identification is first required [27] and misidentifications can lead to inaccurate PMI estimations.

Secondly, the forensic entomologist must be able to age the oldest life stages present for time since colonization to be established. Time since colonization is the estimation based on the age of the insects present when the body is discovered. This is then compiled with other influential factors to calculate the PMI_{min}. Figure 1.2 summarises the relationships of insect development (PMI_{min}), time since colonization (TOC), period of insect activity (PIA), ecological succession and maximum PMI (PMI_{max}) [28].
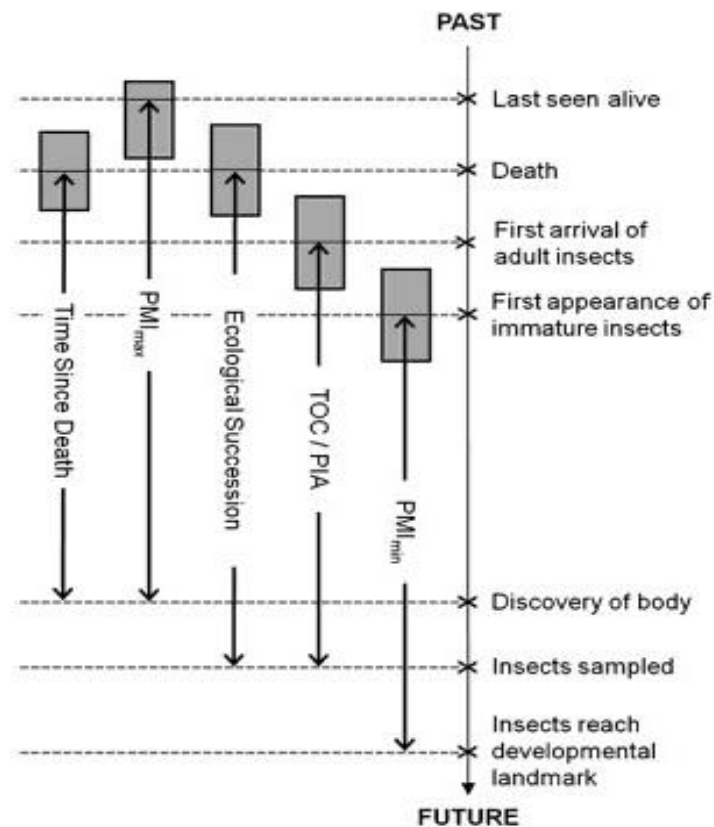
Figure 1.2: Summary of the relationships of insect development (PMI_{min}), time since colonization (TOC), period of insect activity (PIA), ecological succession and maximum PMI (PMI_{max}). The shaded regions represent windows of prediction associated with estimates of the time since death [28]

Although there are various methods used for ageing larvae, they are all based on the knowledge that the rate of development is dependent on temperature. A measurement of the length and weight of larvae is considered as an indication of age [6,11]. This information is then combined with environmental data, toxicology reports, medical examiner autopsy reports and the state in which the body was found (clothed, partly buried etc) to give an estimation of the age of the immature larvae, and therefore an estimated PMI_{min}.

Since larval growth rate is a function of temperature, many studies have been carried out to provide data on the effects that various temperatures have on larvae development [15–19,29,30]. A growth chart commonly used is the isomorphen-diagram of which an example is shown in Figure 1.3. The graph shows the effect temperature has on the development of the blowfly species, *Lucilia sericata*.
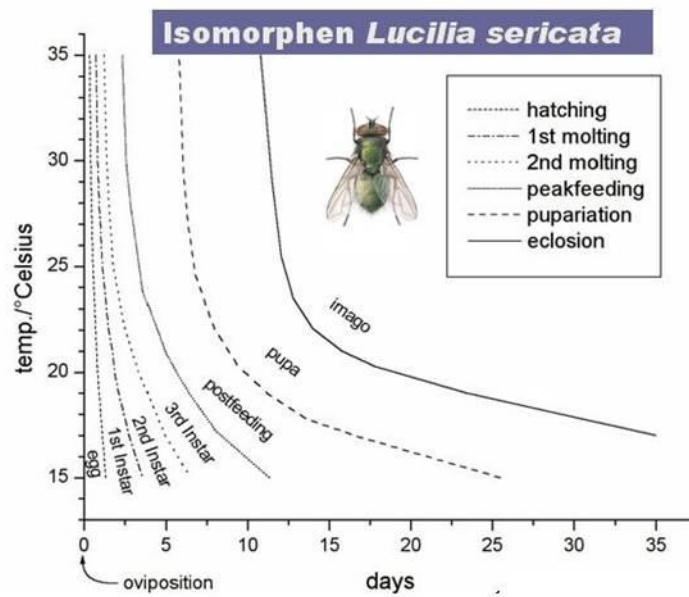
Figure 1.3: Isomorphen diagram of the *L. sericata* - taken from Grassberger and Reiter [16]

From the literature it is clear that forensic entomologists are realising the need to find new means of calculating the PMI_{min} to compliment the current methods [31–35].

1.4 New developments in forensic entomology

The first crucial step a forensic entomologist has to undertake when presented with a crime scene is to identify the insects present. Closely related carrion can have substantially different development rates and therefore a misidentification can lead to inaccurate PMI estimations. The current method used for identification are keys which are based on morphological features within different insect species. These require the

analysts to be very familiar with the anatomical characteristics of insects. However, most of the identification keys found in literature are for adult flies, because identifying larvae to species level can be complex and requires specialised taxonomic knowledge. Larvae collected at a crime scene are therefore reared to adult flies, which can be a time consuming process. One way to compliment current identification methods is DNA-based analysis [31].

DNA-based techniques have been applied in the field of forensic entomology for over a decade. Sperling and co-workers [31] were the first to suggest the idea for the purpose of species identification in forensic entomology and many more literature papers have since proceeded [27,32,34–42]

Recently studies are investigating the potential of using DNA-based techniques to also age forensically important carrion such as work from Tarone & Foran, [43], which examined the gene expression during the development of the blowfly *Lucilia sericata*, to improve the precision of age estimations. Zehner and colleagues [44] looked into the potential of using gene expression analysis as an age estimation tool for *Calliphora vicina* puparia. Their results gave age specific expression patterns, allowing for the puparia to be aged in three stages: the beginning, the middle and at the end of their metamorphosis.

DNA has shown to be a sound identification tool when applied to forensically important blowflies, as well as showing great potential for ageing some of the life stages. However, DNA-based techniques have a few disadvantages which could limit their use in the field. The analyst must be a technical expert and the process can be time consuming and expensive.

1.5 Cuticular Hydrocarbons (CHC)

One technique that may have the potential to give the same accuracy as DNA-based techniques for species identification as well as a potential ageing tool is Cuticular Hydrocarbon (CHC) analysis.

The cuticle of insects is covered by a layer of epicuticular waxes, consisting of hydrocarbons, fatty acids, alcohols, waxes, glycerides, phospholipids and glycolipids. This cuticular lipid layer prevents desiccation as well as penetration of micro-organisms [45]. Hydrocarbons predominate in this layer in many species of insects [46] and are found to be very stable [47]. There is a vast number of different hydrocarbons and possible combinations, indicating that potentially, each species of insect should have its own unique hydrocarbon profile, often referred to as a fingerprint [48–50].

Hydrocarbons are long linear molecules and are observed in their saturated and unsaturated form in insects and can have one or more methyl groups attached to the chain length. In the saturated form, *n*-alkanes (or paraffins) consist of all the carbons being joined together with single bonds but they may have one or more methyl groups present. In the unsaturated form (olefins), one (alkene), two (alkadiene) or three (alkatriene) double bonds maybe present along the length of the chain. Olefins can be in the form of two isomeric structures, referred to as *cis*-alkenes (*Z*-alkenes) or *trans*-alkenes (*E*-alkenes) [47].

Insect hydrocarbons are usually made up of *n*-alkanes, *Z*-alkenes and methyl branched alkanes, of which examples are given in Figure 1.4:

A

B

C

D
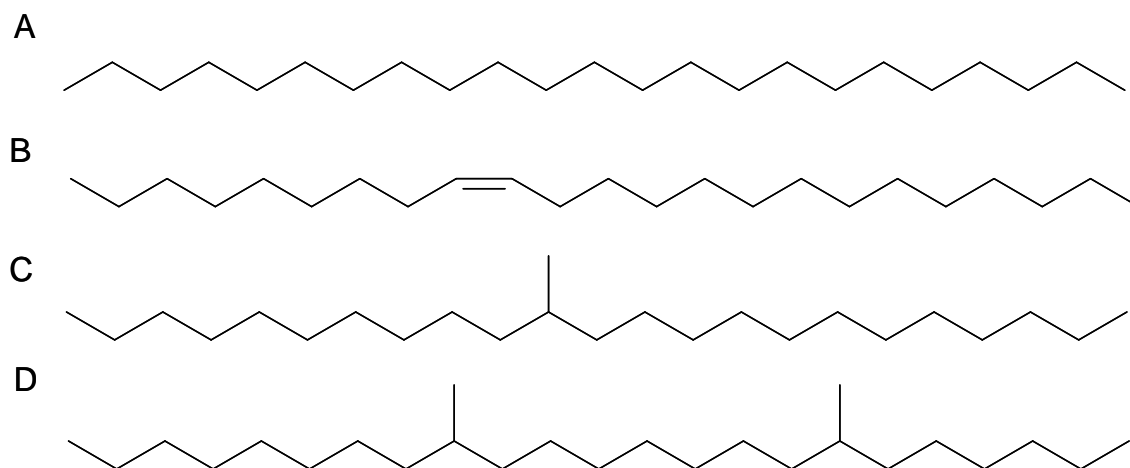
Figure 1.4: Linear long chain cuticular hydrocarbons – A) Linear alkane: Tricosane, B) *Z*-Alkene: (*Z*9)-tricosene, C) Mono methyl branched alkane: 11-methyltricosane, D) Dimethyl branched alkane: 9,17-dimethyltricosane.

The epicuticular lipids serve a variety of roles in different insects (e.g. in ants they are used for communication and recognition of their own colony nest mates [48]), but their primary function is to protect against dessication [51]. This is achieved by the structure of the *n*-alkanes which allows them to be closely packed [52].

1.5.1 Chemical analysis of Cuticular Hydrocarbons

The number of studies on cuticular chemistry has greatly increased over the past 20 years, especially concerning the hydrocarbons of social insects (ants [48], bees [53], termites [54] and wasps [55]). Due to the widespread availability and popularity of Gas

Chromatography-Mass Spectrometry (GC-MS), the majority of the studies carried out on CHCs have benefited from this well established technique that provides separation, identification and is user-friendly [56]. This technique was used primarily to analyse the hydrocarbons from the three blowfly species examined and presented in this thesis and it will be explained in more detail in chapter 2, section 2.2 to 2.4.

1.5.2 Cuticular hydrocarbons in (forensic) entomology

Researchers in the field of entomology have successfully demonstrated the technique of using hydrocarbons as a means of species identification for ants [48,57,58]; termites [54]; cockroaches [49]; mosquitos [59]; grasshoppers [60,61]; wasps [55]; honeybees [53]; beetles [62–65] and flies [66]. Guillem and co-workers [67] proposed to address the difficulty of morphological identification by using chemo-taxonomy. The two ant species, *Myrmica sabuleti* and *M. scabrinodis,* are morphologically very similar. Their hydrocarbon profiles were examined to see if this could provide a solution and a quick means of differentiating between the two species. They discovered that by observing the presence or absence of two species-specific compounds, they could accurately identify the two ants.

CHC's have also been utilised in the field of entomology for ageing [60,68–74] and gender identification [60,69,72,74–78]. Trabalon and colleagues [79] examined the cuticular hydrocarbons of adult *C. vomitoria* with relation to age and sex. Using Principal Component Analysis (PCA), they were able to distinguish between different groups based on relative proportions of male and female hydrocarbons. Young adult flies could be distinguished from old ones and males could be distinguished from

females, with the sex pheromones (alkenes) being the main class of compounds allowing for this distinction.

Recent studies on Diptera have also shown that hydrocarbons have the potential to be used for taxonomic purposes [50,66,72] as well as a potential ageing tool [80–82]. Roux and co-workers [80] were the first to carry out a complete ontogenetical study of three forensically important blowflies (*C. vicina, C. vomitoria* and *Protophormia terraenovae*) using Gas Chromatography with a Flame Ionisation Detector (GC-FID), producing results that have shown the potential to utilise the hydrocarbons for a forensic entomological application. The discrimination analysis they carried out allowed for clear differentiations between the life stages (larvae, post-feeding larvae, puparia and adult fly).

Additional work from Zhu and co-workers [81] also showed potential to use hydrocarbons with a forensic entomology application by firstly analysing the larvae of *Chrysomya rufifacies* using GC-FID and GC-MS [81] and then following this up by looking at the weathering effects of hydrocarbons extracted from the empty puparial cases of *C. megacephala* [82]. The study on the *C. rufifacies* larvae gave results allowing for ageing to be established by adopting the simple statistical analysis of taking the peak area of nonacosane (C29:H) and dividing it by the peak area of eight other selected peaks, giving a peak ratio compared to C29:H. This ratio was seen to significantly increase with age and was followed up by modelling the results using exponential or power functions. However, the peak ratios can vary considerably between individuals and the method of the analyst selecting eight other peaks can be seen as being a rather subjective means of analysis. This *C. megacephala* empty puparial case study [80] looked into determining the weathering time using hydrocarbons to enable ageing, which would be of particular use in scenarios where a

body is highly decomposed and the only entomological evidence that remains are the empty puparial cases, which are notoriously difficult, if not impossible to age. GC-MS was used to analyse the hydrocarbons and significant changes of the abundances of the compounds in relation to weathering time was observed. Interestingly, the abundance of the even numbered low molecular weight *n*-alkanes (C22:H, C24:H, C26:H) increased with time which could allow for an approximate age to be established up to 90 days.

1.6 Rationale of research

A major problem in the field of forensic entomology is the complexity of PMI estimations involving many different factors such as species identification, ageing the oldest life stage present, environmental conditions prior to the discovery of the body, condition of the body (clothed etc), location of the body and potential intake of toxins which can alter the rate of development for larvae. If any of these steps are factored incorrectly, the PMI calculation will be misleading and therefore the time of death will be unreliable. Species identification alone is a complex procedure that must be carried out by a highly experienced taxonomist/forensic entomologist and even then, some insects can be impossible to identify to species level, especially in the larval stages.

A potential application of hydrocarbon analysis is to identify and age forensically important blowflies. If the hydrocarbon profiles are found to be species-specific and distinguishable at different ages, this could provide a reliable method that can complement the current methods used for taxonomic and ageing purposes. This has the potential to therefore enhance the accuracy of PMI estimations. The technique of hydrocarbon analysis also has the potential of drastically cutting time in criminal

investigations as it could potentially eliminate the need to rear the larvae to adult flies to enable correct species identification. If successful, one chromatogram would be sufficient to facilitate the age of the insect, alongside the species identification.

The main aim of the research presented in this thesis is therefore to determine whether the cuticular hydrocarbons could be used to distinguish between the three forensically important blowfly species for the UK, *Calliphora vicina*, *Calliphora vomitoria* and *Lucilia sericata* and to investigate further if the CHCs could be utilised to establish the age of all six life stages of these three blowfly species.

References

[1]   J. Amendt, R. Krettek, C. Niess, R. Zehner, and H. Bratzke, Forensic entomology in Germany, Forensic Science International 113 (2000) 309–14.

[2]   R. Hart, A, J., Whitaker, A, P., Hall, M, J, The use of forensic entomology in criminal investigations: How it can be of benefit to SIOs, The Journal of Homicide and Major Incident Investigation 4 (2008) 37–48.

[3]   M. Benecke, A brief history of forensic entomology, Forensic Science International 120 (2001) 2–14.

[4]   E.P. Catts and M.L. Goff, Forensic entomology in criminal investigations, Annual Review of Entomology 37 (1992) 253–272.

[5]   M.I. Marchenko, Medicolegal relevance of cadaver entomofauna for the determination of the time of death, Forensic Science International 120 (2001) 89–109.

[6]   J. Amendt, R. Krettek, and R. Zehner, Forensic entomology, Naturwissenschaften 91 (2004) 51–65.

[7]   J.R. Stevens, The evolution of myiasis in blowflies (Calliphoridae), International Journal for Parasitology 33 (2003) 1105–1113.

[8]   J.R. Stevens and J.F. Wallman, The evolution of myiasis in humans and other animals in the Old and New Worlds (part I): Phylogenetic analyses, Trends in Parasitology 22 (2006) 129–36.

[9]   D. Otranto and J.R. Stevens, Molecular approaches to the study of myiasis-causing larvae, International Journal for Parasitology 32 (2002) 1345–60.

[10]   D.E. Gennard, *Forensic Entomology*, John Wiley & Sons Ltd (2007).

[11]   A. Gunn, *Essential Forensic Biology*, John Wiley & Sons Ltd (2006).

[12]   G.S. Anderson, Determining time of death using blow fly eggs in the early postmortem interval, International Journal of Legal Medicine 118 (2004) 240–1.

[13]   J. Amendt, C.P. Campobasso, E. Gaudry, C. Reiter, H.N. LeBlanc, and M.J.R. Hall, Best practice in forensic entomology-standards and guidelines, International Journal of Legal Medicine 121 (2007) 90–104.

[14]   S.L. VanLaerhoven, Blind validation of postmortem interval estimates using developmental rates of blow flies, Forensic Science International 180 (2008) 76–80.

[15]   M. Grassberger and C. Reiter, Effect of temperature on development of the forensically important holarctic blow fly *Protophormia terraenovae* (Robineau-Desvoidy) (Diptera: Calliphoridae), Forensic Science International 128 (2002) 177–82.

[16]   M. Grassberger and C. Reiter, Effect of temperature on *Lucilia sericata* (Diptera: Calliphoridae) development with special reference to the isomegalen- and isomorphen-diagram, Forensic Science International 120 (2001) 32–6.

[17]   G.S. Anderson, Minimum and maximum development rates of some forensically important Calliphoridae (Diptera), Journal of Forensic Sciences 45 (2000) 824–32.

[18]   J.H. Byrd and J.C. Allen, The development of the black blow fly, *Phormia regina* (Meigen), Forensic Science International 120 (2001) 79–88.

[19]   S. Niederegger, J. Pastuschek, and G. Mall, Preliminary studies of the influence of fluctuating temperatures on the development of various forensically relevant flies, Forensic Science International 199 (2010) 72–78.

[20]   S. Matuszewski, D. Bajerlein, S. Konwerski, and K. Szpila, An initial study of insect succession and carrion decomposition in various forest habitats of Central Europe, Forensic Science International 180 (2008) 61–9.

[21]   S.C. Voss, H. Spafford, and I.R. Dadour, Annual and seasonal patterns of insect succession on decomposing remains at two locations in Western Australia, Forensic Science International 193 (2009) 26–36.

[22]   J. Wang, Z. Li, Y. Chen, Q. Chen, and X. Yin, The succession and development of insects on pig carcasses and their significances in estimating PMI in south China, Forensic Science International 179 (2008) 11–8.

[23]   M.A. O'Flynn, The succession and rate of development of blowflies in carrion in Southern Queensland and the application of these data to forensic entomology, Journal of the Australian Entomological Society 22 (1983) 137–148.

[24]   C.P. Campobasso, G. Di Vella, and F. Introna, Factors affecting decomposition and Diptera colonization, Forensic Science International 120 (2001) 18–27.

[25]   J.-P. Michaud and G. Moreau, Predicting the visitation of carcasses by carrion-related insects under different rates of degree-day accumulation, Forensic Science International 185 (2009) 78–83.

[26]   Z. Adams and M.J.R. Hall, Methods used for the killing and preservation of blowfly larvae, and their effect on post-mortem larval length, Forensic Science International 138 (2003) 50–61.

[27]   C. Ames, B. Turner, and B. Daniel, Estimating the post-mortem interval (I): The use of genetic markers to aid in identification of Dipteran species and subpopulations, International Congress Series 1288 (2006) 795–797.

[28]   M.H. Villet and J. Amendt, Forensic Pathology Reviews, in: Forensic Pathology Reviews 6, ed., E.E. Turk, Springer Science and Business Media (2011) 213–237.

[29]   K. Clark, L. Evans, and R. Wall, Growth rates of the blowfly, *Lucilia sericata*, on different body tissues, Forensic Science International 156 (2006) 145–9.

[30]   S.E. Donovan, M.J.R. Hall, B.D. Turner, and C.B. Moncrieff, Larval growth rates of the blowfly, *Calliphora vicina*, over a range of temperatures, Medical and Veterinary Entomology 20 (2006) 106–14.

[31]   F.A. Sperling, G.S. Anderson, and D. a Hickey, A DNA-based approach to the identification of insect species used for postmortem interval estimation., Journal of Forensic Sciences 39 (1994) 418–27.

[32]   Y. Malgorn and R. Coquoz, DNA typing for identification of some species of Calliphoridae. An interest in forensic entomology, Forensic Science International 102 (1999) 111–9.

[33]   M. Mazzanti, F. Alessandrini, A. Tagliabracci, J.D. Wells, and C.P. Campobasso, DNA degradation and genetic analysis of empty puparia: genetic identification limits in forensic entomology, Forensic Science International 195 (2010) 99–102.

[34]   M.L. Harvey, I.R. Dadour, and S. Gaudieri, Mitochondrial DNA cytochrome oxidase I gene: potential for distinction between immature stages of some forensically important fly species (Diptera) in Western Australia, Forensic Science International 131 (2003) 134–9.

[35]   J.F. Wallman and S.C. Donnellan, The utility of mitochondrial DNA sequences for the identification of forensically important blowflies (Diptera : Calliphoridae) in Southeastern Australia, Forensic Science International 120 (2001) 60–67.

[36]   L.M. Cainé, F.C. Real, M.I. Saloña-Bordas, M.M. de Pancorbo, G. Lima, T. Magalhães, and F. Pinheiro, DNA typing of Diptera collected from human corpses in Portugal, Forensic Science International 184 (2009) e21–23.

[37]   J.D. Wells and F.A.H. Sperling, DNA-based identification of forensically important Chrysomyinae (Diptera : Calliphoridae), Forensic Science International 120 (2001) 110–115.

[38]   S.T. Ratcliffe, D.W. Webb, R.A. Weinzievr, and H.M. Robertson, PCR-RFLP identification of Diptera (Calliphoridae, Muscidae and Sarcophagidae)-a generally applicable method, Journal of Forensic Sciences 48 (2003) 783–5.

[39]   S. Vincent, J.M. Vian, and M.P. Carlotti, Partial sequencing of the cytochrome oxydase b subunit gene I: a tool for the identification of European species of blow flies for postmortem interval estimation, Journal of Forensic Sciences 45 (2000) 820–3.

[40]   H. Schroeder, H. Klotzbach, S. Elias, C. Augustin, and K. Pueschel, Use of PCR–RFLP for differentiation of calliphorid larvae (Diptera, Calliphoridae) on human corpses, Forensic Science International 132 (2003) 76–81.

[41]   J. Stevens and R. Wall, Genetic relationships between blowflies (Calliphoridae) of forensic importance, Forensic Science International 120 (2001) 116–123.

[42]   A.R. Oliveira, A. Farinha, M.T. Rebelo, and D. Dias, Forensic entomology: Molecular identification of blowfly species (Diptera: Calliphoridae) in Portugal, Forensic Science International: Genetics Supplement Series 3 (2011) e439–e440.

[43]   A.M. Tarone and D.R. Foran, Gene expression during blow fly development: improving the precision of age estimates in forensic entomology, Journal of Forensic Sciences 56 (2011) S112–S122.

[44]   R. Zehner, J. Amendt, and P. Boehme, Gene expression analysis as a tool for age estimation of blowfly puparia, Forensic Science International: Genetics Supplement Series 2 (2009) 292–293.

[45]   A.G. Gibbs and E.L. Crockett, The Biology of Lipids: Integrative and Comparative Perspectives, Integrative and Comparative Biology 38 (1998) 265–267.

[46] A. Gibbs and J.G. Pomonist, Physical properties of insect cuticular hydrocarbons : The effects of chain length, methyl-branching and unsaturation, Comparative Biochemistry and Physiology 112B (1995) 243–249.

[47] F.P. Drijfhout, Cuticular Hydrocarbons: A new tool in forensic entomology, in: Current Concepts in Forensic Entomology, eds., J. Amendt, C.P. Campobasso, M.L. Goff, and M. Grassberger, Springer (2010) pp. 179–203.

[48] S.J. Martin, H. Helanterä, and F.P. Drijfhout, Colony-specific hydrocarbons identify nest mates in two species of Formica ant, Journal of Chemical Ecology 34 (2008) 1072–80.

[49] C. Everaerts, J.P. Farine, and R. Brossut, Changes of species specific cuticular hydrocarbon profiles in the cockroaches *Nauphoeta cinerea* and *Leucophaea maderae* reared in heterospecific groups, Behavioral Ecology and Sociobiology (1997) 145–150.

[50] G. Ye, K. Li, J. Zhu, G. Zhu, and C. Hu, Cuticular hydrocarbon composition in pupal exuviae for taxonomic differentiation of six necrophagous flies, Journal of Medical Entomology 44 (2007) 450–6.

[51] G.J. Blomquist and A.G. Bagnères, *Insect Hydrocarbons: Biology, Biochemistry, and Chemical Ecology*, Cambridge University Press (2010).

[52] A.G. Gibbs, Water-Proofing Properties of Cuticular Lipids, American Zoologist 38 (1998) 471–482.

[53] B.K. Lavine and M.N. Vora, Identification of Africanized honeybees, Journal of Chromatography. A 1096 (2005) 69–75.

[54] M.I. Haverty, M.S. Collins, L.J. Nelson, and B.L. Thorne, Cuticular hydrocarbons of termites of the British Virgin Islands, Journal of Chemical Ecology 23 (1997) 927–964.

[55] U.R. Bernier, D.A. Carlson, and C.J. Geden, Analysis of the Cuticular Hydrocarbons from Parasitic Wasps of the Genus *Muscidifurax*, Journal of the American Society for Mass Spectrometry 9 (1998) 320–332.

[56] S.J. Martin and F.P. Drijfhout, How reliable is the analysis of complex cuticular hydrocarbon profiles by multivariate statistical methods? Journal of Chemical Ecology 35 (2009) 375–82.

[57] T. Akino, K. Yamamura, S. Wakamura, and R. Yamaoka, Direct behavioral evidence for hydrocarbons as nestmate recognition cues in *Formica japonica* (Hymenoptera: Formicidae), Applied Entomology and Zoology 39 (2004) 381–387.

[58] M. Tissot, D.R. Nelson, and D.M. Gordon, Qualitative and quantitative differences in cuticular hydrocarbons between laboratory and field colonies of *Pogonomyrmex barbatus*, Comparative Biochemistry and Physiology. Part B, Biochemistry and Molecular Biology 130 (2001) 349–58.

[59] G.I. Anyanwu, D.H. Molyneux, and A. Phillips, Variation in cuticular hydrocarbons among strains of the *Anopheles gambiae* sensu stricto by analysis of cuticular hydrocarbons using gas liquid chromatography of larvae, Memórias do Instituto Oswaldo Cruz 95 (2000) 295–300.

[60]   T. Tregenza, S.H. Buckley, V.L. Pritchard, and R.K. Butlin, Inter- and intra-population effects of sex and age on epicuticular composition of meadow grasshopper,*Chorthippus parallelus*, Journal of Chemical Ecology 26 (2000) 257–278.

[61]   R.F. Chapman and K.E. Espelies, Use of Cuticular Lipids in Grasshopper Taxonomy: A Study of Variation in *Schistocerca shoshone* (Thomas), Biochemical Systematics and Ecology 23 (1995) 383–398.

[62]   K. Lockey, Insect hydrocarbon chemotaxonomy: Cuticular hydrocarbons of adult and larval *epiphysa* species blanchard and adult *Onymacris unguicularis* (HAAG) (tenebrionidae: Coleoptera), Comparative Biochemistry and Physiology Part B: Comparative Biochemistry 102 (1992) 451–470.

[63]   J.E. Baker, Developmental changes in cuticular lipids of the black carpet beetle, *Attagenus megatoma*, Insect Biochemistry 9 (1979) 335–339.

[64]   M. Page, L.J. Nelson, G.J. Blomquist, and S.J. Seybold, Cuticular hydrocarbons as chemotaxonomic characters of pine engraver beetles (*Ips* spp.) in the *grandicollis* subgeneric Group, Journal of Chemical Ecology 23 (1997) 1053–1099.

[65]   K. Lockey, Insect hydrocarbon classes: Implications for chemotaxonomy, Insect Biochemistry 21 (1991) 91–97.

[66]   R. Urech, G.W. Brown, C.J. Moore, and P.E. Green, Cuticular hydrocarbons of buffalo fly, *Haematobia exigua*, and chemotaxonomic differentiation from horn fly, *H. irritans*, Journal of Chemical Ecology 31 (2005) 2451–61.

[67]   R.M. Guillem, F.P. Drijfhout, and S.J. Martin, Using chemo-taxonomy of host ants to help conserve the large blue butterfly, Biological Conservation 148 (2012) 39–43.

[68]   F. Savarit and J.-F. Ferveur, Temperature affects the ontogeny of sexually dimorphic cuticular hydrocarbons in *Drosophila melanogaster*, The Journal of Experimental Biology 205 (2002) 3241–9.

[69]   W.V. Brown, H.A. Rose, M.J. Lacey, and K. Wright, The cuticular hydrocarbons of the giant soil-burrowing cockroach *Macropanesthia rhinoceros* saussure (Blattodea: Blaberidae: Geoscapheinae): analysis with respect to age, sex and location, Comparative Biochemistry and Physiology. Part B, Biochemistry and molecular biology 127 (2000) 261–77.

[70]   P.T. Desena ML, Clark JM, Edman JD, Symington SB, Scott TW, Clark GG, Potential for aging female *Aedes aegypti* (Diptera : Culicidae) by gas chromatographic analysis of cuticular hydrocarbons, including a field evaluation, Journal of Medical Entomology 36 (1999) 811–823.

[71]   L.E. Hugo, B.H. Kay, G.K. Eaglesham, N. Holling, and P. a Ryan, Investigation of cuticular hydrocarbons for determining the age and survivorship of Australasian mosquitoes, The American Journal of Tropical Medicine and Hygiene 74 (2006) 462–74.

[72]   W.V. Brown, R. Morton, and J.P. Spradbery, Cuticular hydrocarbons of the old world screw-worm fly, *Chrysomya bezziana* Villeneuve (Diptera: Calliphoridae). Chemical characterization and quantification by age and sex, Comparative Biochemistry and Physiology Part B: Comparative Biochemistry 101 (1992) 665–671.

[73] M.L. Desena, J.D. Edman, J.M. Clark, S.B. Symington, and T.W. Scott, *Aedes aegypti* (Diptera: Culicidae) Age Determination by Cuticular Hydrocarbon Analysis of Female Legs, Journal of Medical Entomology 36 (1999) 824–830.

[74] C.J.D. Chen C.S., Mulla M.S., March R.B., Cuticular hydrocarbon patterns in *Culex-quinquefasciatus* as influenced by age and sex and geography, Bulletin of the Society for Vector Ecology 15 (1990) 129–139.

[75] S. Mpuru, G.J. Blomquist, C. Schal, M. Roux, M. Kuenzli, G. Dusticier, J.L. Clément, and A.G. Bagnères, Effect of age and sex on the production of internal and external hydrocarbons and pheromones in the housefly, *Musca domestica*, Insect Biochemistry and Molecular Biology 31 (2001) 139–55.

[76] L.L. Jackson and R.J. Bartelt, Cuticular Hydrocarbons of Sex, Insect Biochemistry 16 (1986) 433–439.

[77] S. Steiner, N. Hermann, and J. Ruther, Characterization of a female-produced courtship pheromone in the parasitoid *Nasonia vitripennis*, Journal of Chemical Ecology 32 (2006) 1687–702.

[78] C. Marican, L. Duportets, S. Birman, and J.M. Jallon, Female-specific regulation of cuticular hydrocarbon biosynthesis by dopamine in *Drosophila melanogaster*, Insect Biochemistry and Molecular Biology 34 (2004) 823–30.

[79] M. Trabalon, M. Campan, J.L. Clement, C. Lange, and M.T. Miquel, Cuticular hydrocarbons of *Calliphora vomitoria* (Diptera): Relation to age and sex, General and Comparative Endocrinology 85 (1992) 208–216.

[80] O. Roux, C. Gers, and L. Legal, Ontogenetic study of three Calliphoridae of forensic importance through cuticular hydrocarbon analysis, Medical and Veterinary Entomology 22 (2008) 309–17.

[81] G.H. Zhu, G.Y. Ye, C. Hu, X.H. Xu, and K. Li, Development changes of cuticular hydrocarbons in *Chrysomya rufifacies* larvae: potential for determining larval age, Medical and Veterinary Entomology 20 (2006) 438–44.

[82] G.H. Zhu, X.H. Xu, X.J. Yu, Y. Zhang, and J.F. Wang, Puparial case hydrocarbons of *Chrysomya megacephala* as an indicator of the postmortem interval, Forensic Science International 169 (2007) 1–5.

Chapter 2

Techniques and Data Analysis

2. Introduction

This chapter covers the theory and principles of the analytical instruments and computational techniques used to analyse and interpret the data presented in this thesis. Before describing the analytical instrumentation, an understanding of chromatography is needed and this shall be covered in section 2.1. The primary analytical technique used in this thesis was Gas Chromatography – Mass Spectrometry (GC-MS). GC-MS will be discussed as its isolated techniques (GC and MS) and the principal components that make up each instrument, before explaining the technique in its hyphenated form and how to interpret the data it provides.

The statistical method of Principal Component Analysis (PCA) will also be briefly described. This method was applied to the data obtained from the GC chromatograms to help visualise any trends in the dataset. Although PCA was the primary technique used for the results presented in this thesis, the computational intelligence technique of

Artificial Neural Networks (ANN) was applied to a dataset to examine its potential of analysing this type of data. The technique and results shall be presented in chapter 7.

2.1 Chromatography

Chromatography is a general term used to describe a variety of analytical chemical separation techniques that are widely applied in many branches of science [1]. Chromatography requires two phases in order to separate analytes from complex mixtures; a stationary phase (SP - solid or liquid) and a mobile phase (MP - liquid or gas) which is passed over the immobile stationary phase. All the techniques of chromatography can be subcategorized depending on the physical state of the SP and MP [2].

There are five mechanisms underlying separation in chromatography:

1) *Adsorption Chromatography*

2) *Partition Chromatography*

3) *Ion-exchange Chromatography*

4) *Molecular exclusion Chromatography*

5) *Affinity Chromatography*

A

Solute adsorbed on surface of stationary phase

B

Cross section of open tubular column

Solute dissolved in liquid phase bonded to the surface of column

C

Mobile anions held near cations that are covalently attached to stationary phase

Small molecules penetrate pores of particles

Anion-exchange resin; only anions can be attracted to it

D

Large molecules are excluded

E

One kind of molecule in complex mixture becomes attached to molecule that is covalently bound to stationary phase

All other molecules simply wash through

Figure 2.1: Diagram showing the five mechanisms of chromatography, A: Adsorption Chromatography, B: Partition Chromatography, C: Ion-exchange Chromatography, D: Molecular exclusion chromatography and E: Affinity Chromatography. Taken with permission from Harris [3]

1) Adsorption Chromatography:

Adsorption chromatography (often referred to as liquid-solid chromatography) (Figure 2.1A) was the first to be developed by Tswett in 1906 (cited in [2]), who successfully separated the pigments of leaves on a polar SP. The mobile phase used in adsorption chromatography can either be a liquid or a gas. Since analytes are adsorbed differently onto the surface of a porous solid SP they can be separated. The analytes attraction to the SP will depend on its polarity. Polar analytes will be most attracted to a polar SP, and will therefore be adsorbed more than the less polar analytes. This leads to the polar analytes being retained on the column for longer, thus giving separation of the analytes from a mixture [2]. The two most common adsorbents used in adsorption chromatography are silica gel and alumina [4]. Silica (less polar than alumina) is often the choice of the two adsorbents due to its wider range of forms. Silica gel and alumina both contain OH groups, which can lead to specific interactions taking place between the SP and the analytes; Van der Waals' (i.e. dipole-dipole interactions, hydrogen bonding and/or London dispersion forces) [1]. Adsorption chromatography is usually used to separate relatively non-polar compounds since very polar compounds do not always display good separation using this technique [4].

2) Partition Chromatography:

Partition chromatography (Figure 2.1B) is based on the principle of separating out components in a mixture according to their solubilities [1]. A solid support (e.g. silica gel) with a large surface area contains the chemically bonded liquid SP. The differing solubilities that the analytes exhibit with the SP and MP leads to the separation of compounds in a mixture. Analytes favouring the SP will be retained for longer and

therefore travel through the system at a much slower speed than those that are more soluble in the MP.

3) Ion-exchange Chromatography:

Ion-exchange chromatography (Figure 2.1C) is based on the principal of separating out components in a mixture according to their charge. Ions are retained on the SP according to their ionic interactions [5]. Ionic functional groups within the SP will interact with the analyte ions carrying an opposite charge and will therefore be retained for longer than ions yielding the same charge.

4) Molecular Exclusion Chromatography:

Molecular exclusion chromatography (Figure 2.1D) separates analytes according to their physical properties i.e. size. It is often applied to large molecules such as proteins. The technique is useful in separating larger molecules from small molecules, with the larger ones eluting first and the smaller ones being retained in the pores of the SP.

5) Affinity Chromatography:

Affinity chromatography (Figure 2.1E) is a liquid purification technique often used in biological systems [6]. To separate analytes, interacting molecules are immobilised onto a solid support which then acts as the SP. The affinity ligand (name given to the immobilized molecule) then binds to specific compounds in a mixture and the analytes of interest will be retained due to an interaction with the ligand of the SP [7]. Affinity chromatography can be specific, where ligands will bind to specific analytes of interest, or general, where the ligands bind to particular groups of analytes sharing similar properties.

2.2 Gas Chromatography (GC)

Chromatography techniques are often categorised by the physical state of the mobile phase used. The two types are:

1) *Liquid Chromatography (LC)*

2) *Gas Chromatography (GC)*

For the purpose of this research, GC was the chromatographic technique used to analyse the samples. It is therefore discussed in greater detail below.

2.2.1 Instrumentation

Gas chromatography is an analytical technique where the MP is a gas (commonly helium). A schematic instrumental setup of a gas chromatograph (GC) can be seen in Figure 2.2. The four main components of a GC are the injector, the column, the oven and the detector. A carrier gas is continuously flowing through the system and it is important to have a leak-free environment. The SP sits within the column, which is held in the oven of the GC. The vapourised components (resulting from a heated injector port) contained within the MP interact with the SP according to their differing volatility and affinity at ranging temperatures. Compounds that are more volatile will have little chemical interaction with the column and will travel quicker than those of a lower volatility. This leads to the separation of different components of a sample and this process is called elution [2]. The eluting components then produce a signal in the processing unit component of the instrument which are displayed as peaks on a chromatogram.

28
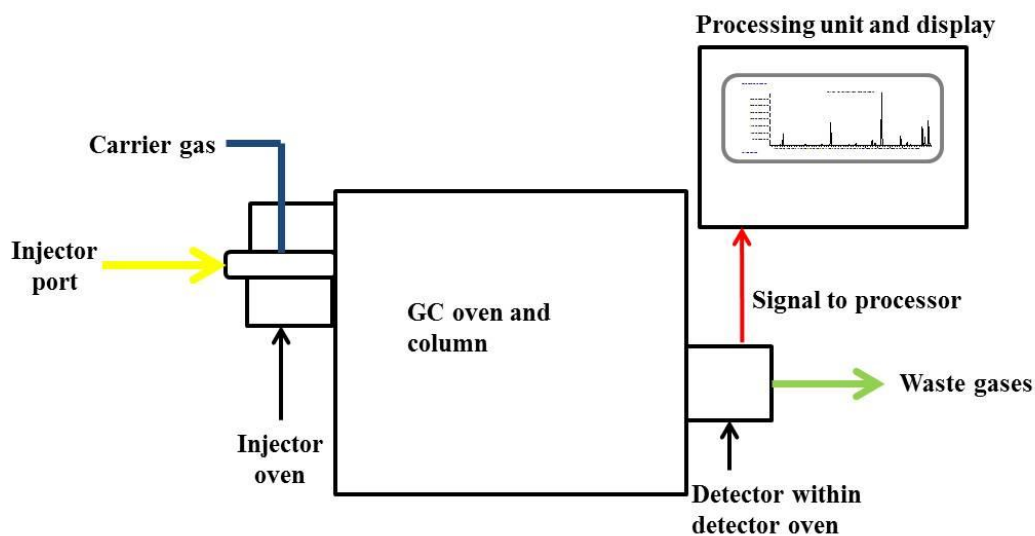
Figure 2.2: A schematic diagram of a Gas Chromatograph

2.2.1.1 Split/Splitless injector

To enable a sample to be analysed on a GC system, it must be in the form of a gas. Therefore when a sample is introduced into the GC system via the heated injector port, it is vaporised. Two common injection techniques are:

1) Split

2) Splitless

The split mode is used for very concentrated samples as only some of the vaporised analytes will reach the column and the rest are removed from the system via the split outlet (Figure 2.3). It is therefore ideal for samples that cannot be diluted. It is also the method used to avoid column overloading because the volume that will reach the column can be adjusted. For example, if 1 μL of a liquid solution was injected using the split mode, only vaporised analytes in the order of nanoliters will enter the column [8]

29

The split / splitless injector
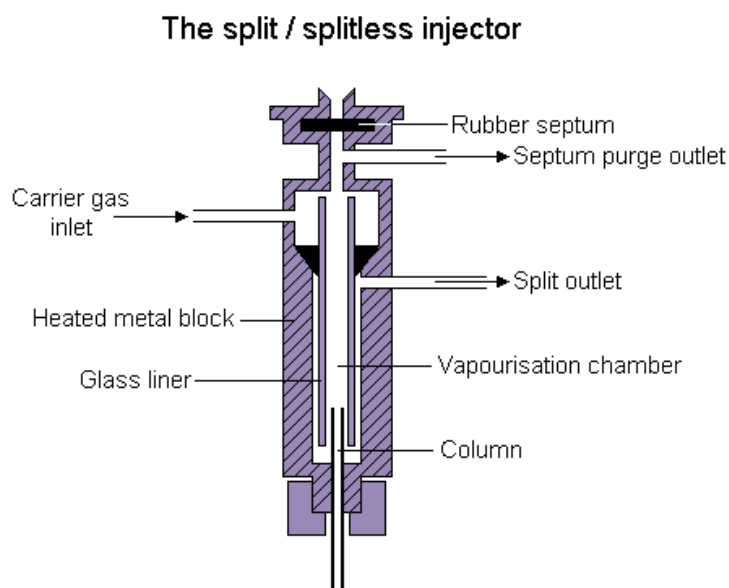
Figure 2.3: Diagram of a split/splitless injector. Edited version [9]

Split mode is the preferred method of injecting as it gives sharper peaks but for this work, splitless mode was used for all sample injections due to their relatively low concentrations. Splitless mode is opposite to split mode in that all of the injected compounds will pass through to the column so it is commonly used for less concentrated samples or trace analysis. Splitless mode gives higher sensitivity than split injection and can be carried out using the same system, so long as the split outlet is closed prior to sample injection [8]. The split valve is then opened between 30 second and 1 minute after injection.

Once the sample is vaporised it gets carried by the mobile phase (carrier gas) into the column. The carrier gas is inert and therefore will not chemically interact with the SP. However it must be highly purified because any impurities such as oxygen or water could chemically interact with the SP within the column and could destroy the SP or greatly interfere with its performance.

2.2.1.2 Column

There are generally two types of columns, packed and capillary. A packed column has the SP (bound to a large surface area) packed inside a stainless steel tube.

A capillary column was used in the analysis of this work. They are thin fused silica open tubes which are internally lined with the stationary liquid phase (see Figure 2.4).
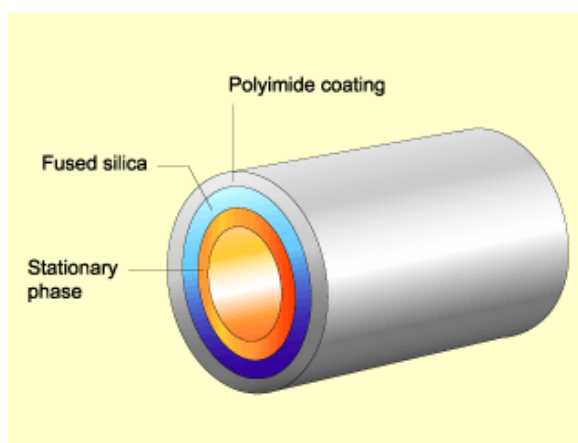
Figure 2.4: A schematic diagram of a capillary column [10]

Fused silica is commonly used as it is the most inert material available due to its high purity [11]. Fine walled columns of this material are highly flexible and the straight fused silica can be easily coiled enabling installation of very long columns (up to 100 m) into the GC oven. The SP in the column is where the separation of compounds takes place, therefore it is very important to choose the right one for the target analytes, both in terms of type of SP, as well as the amount of SP. Packed columns can cope with much higher sample capacity and are often advantageous when analysing gas samples.

31

However the efficiency of the capillary column means it is often the column of choice due to its peak separation abilities [12].

Within the capillary column the SP consists of a silica backbone with functional groups attached which dictate the polarity of the SP. There are a wide variety of SP's available, all with varying chemical composition. For a more polar column, polyethylene glycol (carbowax) and phenyl cyanopropyl substituted polysiloxanes are used due to their affinity for compounds that are hydrogen-bonded or contain functional groups [13]. The dimethylsiloxane polymers are a very good general purpose column for a range of applications due to their high temperature limit and low column bleed. With these columns, analytes are separated primarily according to their boiling points, with the low boiling point components eluting from the column first and the high boiling point analytes eluting last. This type of column therefore elutes components according to polarity as well as in order of the number of carbons present in its structure, e.g. for example in the GC chromatogram of a blowfly, the hydrocarbons will elute from the column in increasing order of the number of carbons, heptadecane (C17:H), octadecane (C18:H), nonadecane (C19:H), eicosane (C20:H) etc [2].

There are some limitations of using a polyimide coated column when analysing high boiling point compounds. Polyimide will not be stable at high temperatures (>390 ˚C) and will become brittle. This therefore limits the analysis to only detecting chain lengths of approximately 35 to 40 carbons. Higher temperature columns can detect much larger compounds than this, as examined by Akino [14], where they were able to detect up to 48 carbons, but they can be unstable.

2.2.1.3 Column temperature

The column sits coiled inside the oven of the GC and the column temperature will vary depending on the nature of the sample analytes. As temperature has an influence on separation, using the correct temperature for the analytes of interest is vital. It can be carried out in two different modes:

1) *Isothermal*

2) *Linear temperature programming*

In isothermal mode, the column is kept at a constant temperature. In this case, analytes with a lower interaction affinity to the SP will travel through the column at a higher speed, therefore separation is achieved because analytes with a higher interaction affinity which will be retarded [12]. This technique is advantageous when analysing components of similar boiling points but has the disadvantage of producing broader peaks if compounds are present with a wide range of boiling points. For the results presented in this thesis, a linear programmed temperature system is adopted because the boiling points extend over a large range and this method ensures all analytes are eluted from the column as well as producing good separation.

If the temperature were to remain constantly low, it would achieve good separation but the compounds would take a long time to move through the column, which decreases the resolution of the peaks, resulting in a broad appearance and some of the high boiling point compounds may not even elute off the column at all. However, if the temperature of the column remained constantly high, it would ensure all analytes of interest passed through quickly but analytes would not be separated and therefore the data analysis might be impaired.

33

Therefore, samples can be analysed using a programmed temperature mode. The temperature programming system begins at a relatively low ambient temperature of around 40-50 ˚C before being increased at a fixed amount per minute until it reaches a temperature of around 300 ˚C where it is held.

The faster the temperature rate, the closer together the peaks will be, giving less resolution. It is usually advisable to carry out some method development prior to sample injection by using a solution of standards to ensure an adequate temperature program is developed. The method of including a high final temperature is also a very efficient way of column cleaning, ensuring no contaminants or unwanted components are left on the column after a sample has been analysed.

2.2.2 Chromatogram

The end of the column terminates at the detector, where the eluting analytes are detected, generating an electrical signal detector response which is based on the concentration of the sample. This is displayed on a data system in the form of a chromatogram (Figure 2.5), which is a plot of time vs detector response
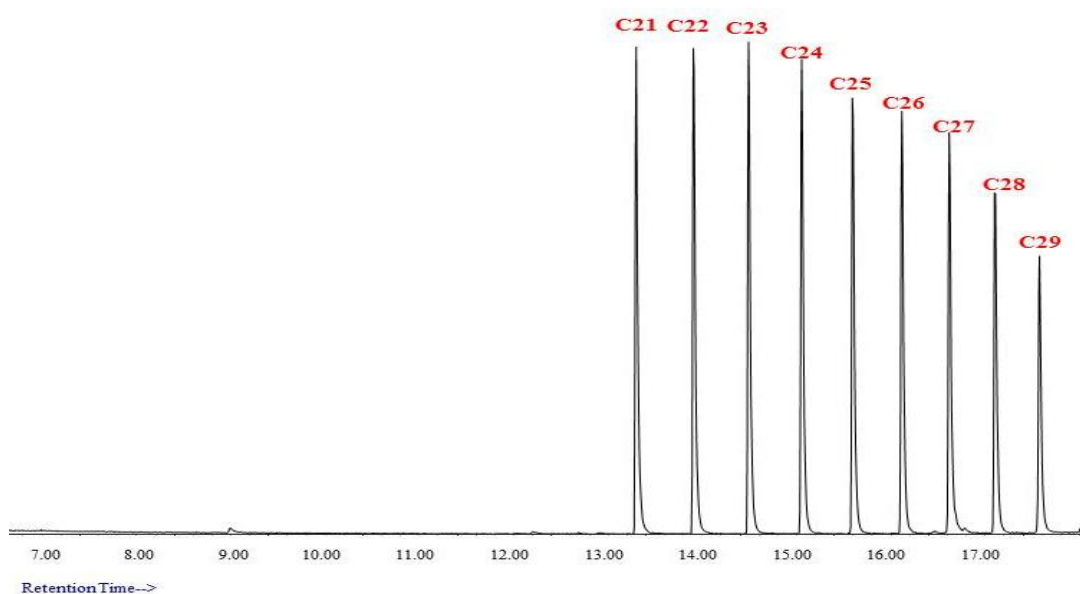
Figure 2.5: Example chromatogram of an alkane standard solution ranging from heneicosane to nonacosane

The time taken for a compound to elute from the column is called the retention time which generates qualitative information [15]. Retention times are characteristic for a particular compound because different compounds elute at different times depending on their boiling point. The retention time is displayed on the x-axis and the y-axis shows the abundance of the separated analytes. The peak area provides quantitative information of the concentration for each compound present.

A value often used in chromatographic analysis is the Kovats Index [16].The Kovats Index is the value obtained from an equation (equation 2.1) and allows for the identification of compounds in GC analysis. In calculating the Kovats Index, the retention time of e.g. a branched methyl hydrocarbon, is normalised to the retention time of standard *n*-alkanes. The value specifies the number of carbons in the backbone

35

of the chain as well as giving an indication of the identification of the unknown branched hydrocarbon [16].

$$I=100[n+(N - n) \frac{log \ t'r_{(unknown)} - \log t'r_{(n)}}{log \ t'r_{(N)} - \log t'r_{(n)}}]$$

Equation 2.1: The Kovats equation for isothermal chromatography, where I = Kovats Index, n = the number of carbon atoms in the smaller *n*-alkane, N = the number of carbon atoms in the larger *n*-alkane and t'r = the adjusted retention time.

2.3 Mass Spectrometry (MS)

Mass Spectrometry (MS) is an analytical technique that generates gas-phase ions and separates them out according to their mass-to-charge ratio (*m/z*). The MS separates ions due to their ease of manipulation in contrast to neutral molecules. The signal of these ions is then detected and sent to a data system, which generates a mass spectrum which gives structural information about the molecules from their molecular mass as well as characteristic fragmentation patterns [17]. MS allows for excellent selectivity which is very important when carrying out quantitative trace analysis [18].

2.3.1 Instrumentation

The mass spectrometer is made-up of three main components:

1) Ion source

2) Analyser

3) Detector
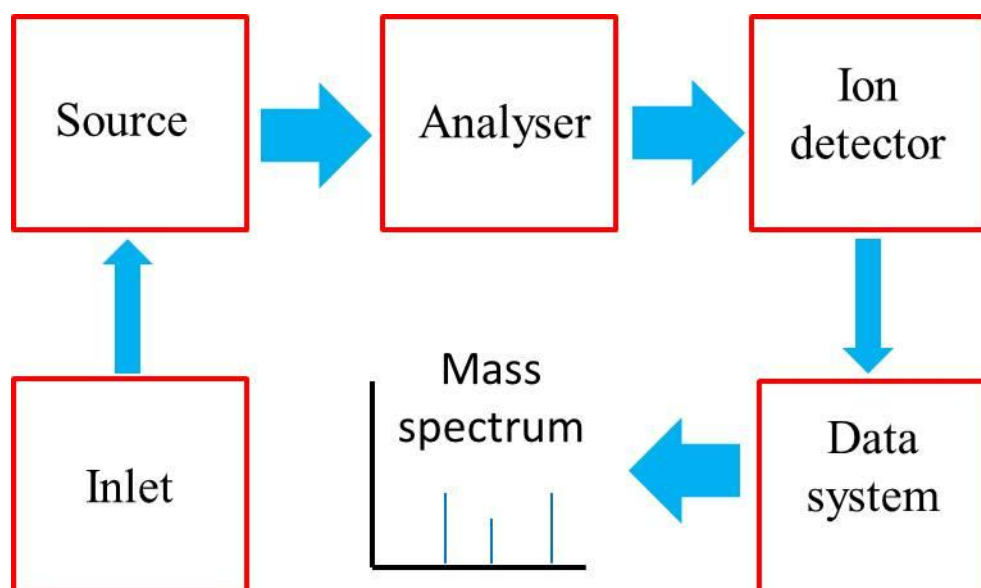
Figure 2.6: Diagram showing the components that make up a mass spectrometer

Figure 2.6 shows the schematic set-up of the MS set-up. Each component is described below.

2.3.1.1 Ion source

The analyte of interest is ionised in the ion source which is accomplished by the loss or gain of a charge [19]. There are a number of ionisation techniques that have been developed which can be utilised in MS, such as Electrospray Ionisation (ESI), Atmospheric Pressure Chemical Ionisation (APCI), Chemical Ionisation (CI) and Electron Ionisation (EI). The latter two techniques are predominantly used in GC-MS analysis. EI (Figure 2.7) was the ionisation technique used in this work and will be described in more detail.
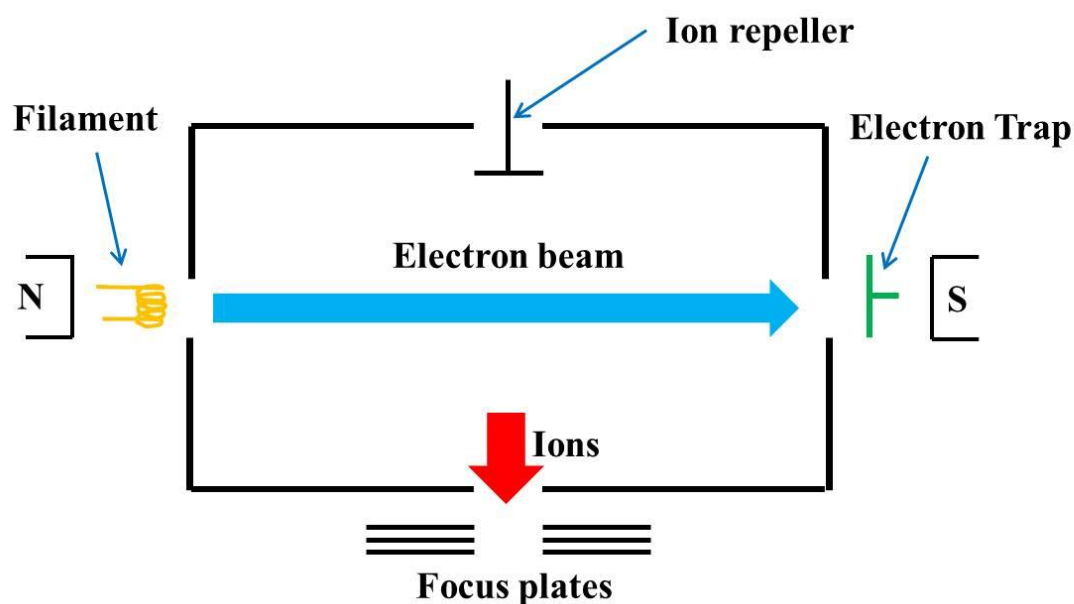
Figure 2.7: Diagram illustrating the process of electron ionisation.

Electron Ionisation

Some of the ionisation techniques can lead to extensive fragmentation and electron ionisation is one of these. It is therefore considered a "hard" ionisation technique and it is likely the molecular ion will be fragmented and not always observed [19].

EI works well with gas-phase molecules and is therefore ideal when used in conjunction with GC. A metal coil (filament) which is electrically heated generates electrons which are accelerated forward (see Figure 2.7). They "collide" with the analyte molecules leading to the loss of an electron, producing a charged Molecular ion $[M^{+\cdot}]$ (see Equation 2.2) which hereafter fragments into a mixture of cations and neutral fragments [20].

$$M + e^- \rightarrow M^{\cdot+} + 2e^-$$
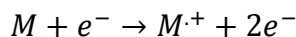
Equation 2.2: Equation showing the process of electron ionization

Most ions after fragmentation hold a charge that corresponds to the loss of an electron during this process. These ions give structural information. The molecular ion (if present but often fragmented) will be the ion of the highest m/z ratio, giving the molecular weight of the analyte.

Once the ions have passed through the ionisation source they are kept moving through the instrument from the driving force of an ion repeller, a metal plate carrying a small positive charge, into the mass analyser.

2.3.1.2 Mass analyser

The mass analyser separates the ions, produced in the ion source, according to their m/z ratio and numerous techniques have been developed for this. Some examples of popular mass analysers used in MS are Quadrupole Ion Trap, Time-of-Flight and linear Quadrupole [19][21]. The latter two were used for the results presented in this thesis and are therefore described in more detail.

Quadrupole:

The quadrupole is made up of four metal rods (hyperbolic shaped) (see Figure 2.8), which sit parallel to one another. A Direct Current (DC) voltage and an oscillating

Radio Frequency (RF) voltage are applied across the rods, with opposite pairs yielding opposite charges [12]. The variation of the electronic field alters the path of some of the ions leading to specific ions of interest (selected and separated by their *m/z* ratio) making it through the quadrupole to the detector while the others are deflected out of the quadrupole because the alterations of the voltage cause them to become unstable [20].
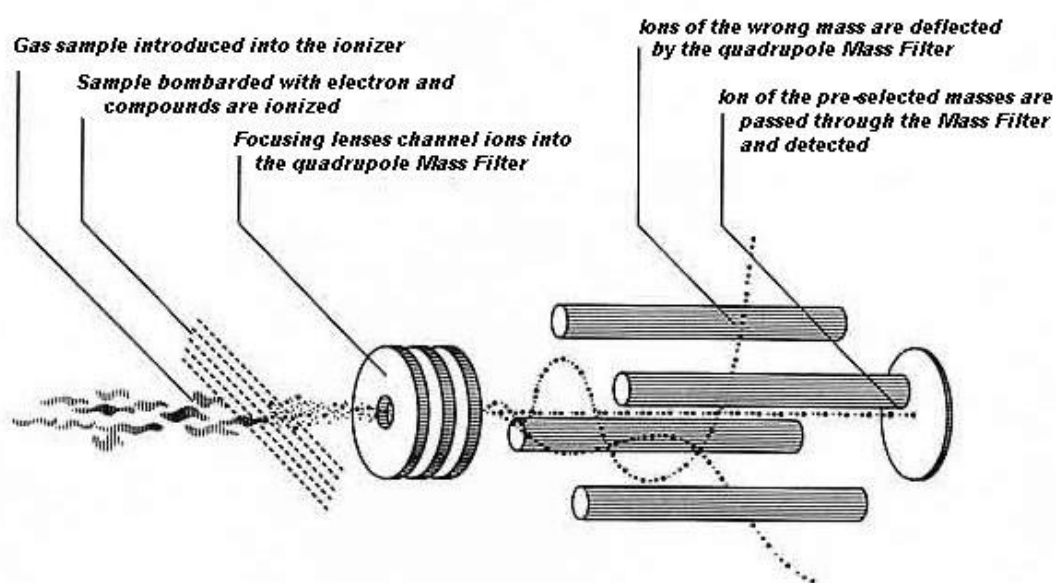
Figure 2.8: A schematic diagram of a quadrupole analyser (and ion source) [22]

Quadrupoles are widely used in Liquid Chromatography-Mass Spectrometry (LC-MS) and Gas Chromatography-Mass Spectrometry (GC-MS) systems.

2.3.1.3 Ion detector

A signal is received as an ion (after passing through the mass analyser) strikes the detector which is then amplified. The ion detector measures the abundance of each ion

that passes through the system from the mass analyser and this measured abundance is converted into a mass spectrum, consisting of masses and peak intensities [20].

Mass spectrometry provides quantitative and qualitative analysis with low limits of detection (ppm/ppb), and therefore excellent sensitivity. When the molecular weight is combined with the fragmentation patterns, identification as well as structural information of unknown analytes can be established [17].

2.4 Gas Chromatography – Mass Spectrometry (GC-MS)

The result of combining the two analytical techniques of Gas Chromatography (GC) and Mass Spectrometry (MS) produces a very powerful and user-friendly analytical instrument. Over the years it has become the number one analysis choice in many branches of science owing to its ability to separate, detect and identify a large number of molecular compounds [12].

The sample is injected into the GC via the injector port and the vaporised samples get carried onto the column of the GC by the mobile phase. The non-polar hydrocarbons being analysed in this thesis will interact strongly with the column (like-for-like) so a linear temperature program is applied to aid separation of the analytes. The lower molecular weight hydrocarbons (and therefore lower boiling point) will elute off the column first with the high boiling point compounds eluting last. The temperature program is gradually ramped up and then held at a high temperature, ensuring all analytes and impurities are removed from the column, before returning back to ambient temperature. The compounds then remain in the gas phase as they leave the GC oven, via the heated transfer line. These separated analytes pass into the MS where they are

ionised by electron ionisation. The ions are pushed through the system into the quadrupole analyser where they are measured according to their *m/z* ratio. The ions are then detected and plotted into a mass spectrum showing the masses against the peak intensities. The end result is of a GC chromatogram (Figure 2.9) with each peak detected in the GC displacing its own mass spectrum (Figure 2.10) enabling identification and structural information.
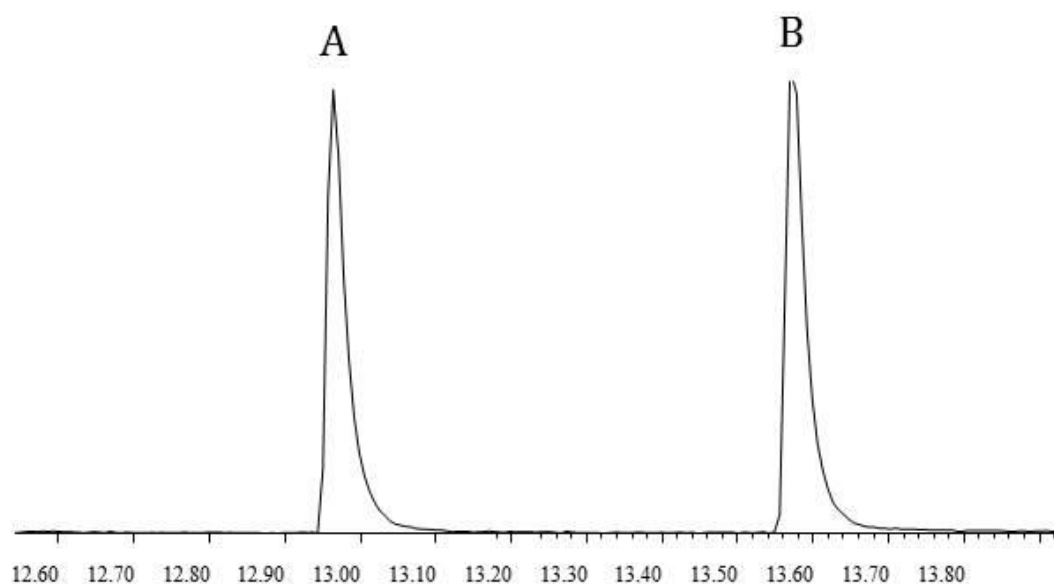
Figure 2.9: Part of a GC chromatogram of two alkane standards, A: Heneicosane, B: Docosane

Figure 2.9 shows a section of the chromatogram of two alkane standards, heneicosane ($M^{+.} = 296$) and docosane ($M^{+.} = 310$) with their respective mass spectra given in Figure 2.10 and Figure 2.11. The identification of hydrocarbons using their mass spectra is described in section 2.5.
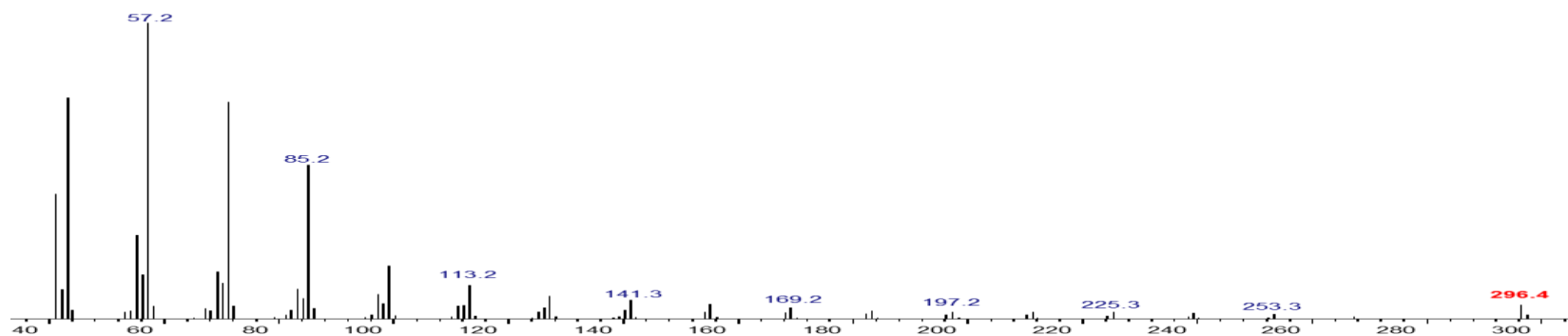
Figure 2.10: Mass spectrum of heneicosane (peak A of the chromatogram in Figure 2.9)
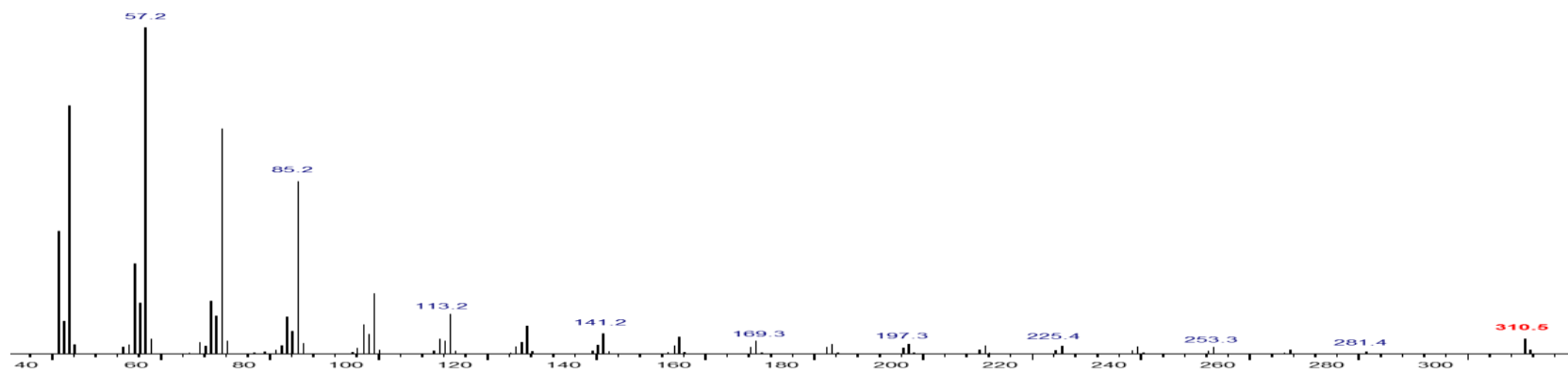
Figure 2.11: Mass spectrum of docosane (peak B of the chromatogram in Figure 2.9)

2.5 GC-MS data analysis and identification of cuticular hydrocarbons

Due to the complex mixtures extracted from the cuticles of blowflies, GC is needed to separate out the analytes followed by MS to identify the compounds.

The mass spectrum reveals the mass of the molecule as well as the masses of fragmented ions [23]. The molecular ion [$M^{+ \cdot}$] of a molecule gives invaluable information for identification purposes. However, much of the time it is not present in the spectrum due to it being unstable when it has undergone EI. In most of the *n*-alkanes present in the profile of a blowfly, the $M^{+ \cdot}$ is present and it is essential to identify the chain length. The *n*-alkanes also have a characteristic profile in the mass spectrum, as seen in Figure 2.10 and 2.11. To correctly identify the position of the methyl group in methyl-branched alkanes and the chain length, mechanisms of the fragmentation are required.

Diagnostic ions in the mass spectrum can be used to determine the position of the methyl HC group. The position of the diagnostic ions in methyl-branched hydrocarbons are caused by a fragmentation mechanism called Sigma-bond dissociation (σ). When *n*-alkanes are ionised the C-C bond length is increased, leading to a decrease in the bond dissociation energy. This enables fragmentation to take place preferentially at carbon atoms that are more highly substituated. The ion with the higher abundance will be more stable to hold the charge, whilst the other fragment becomes a radical [23].

Although the molecular ion is often not observed in most methyl branched alkanes, a [M-15]$^+$ ion is nearly always present which corresponds to the loss of the methyl group (M relates to the molecular ion and 15 [CH_3] relates to the molecular weight of a methyl group being cleaved off).

Similar methyl branched HCs can elute at the same retention time, resulting in a combined mass spectrum. An example of this is seen in mass spectrum shown in Figure 2.12, where an 11MeC25:H co-eluted with a 13MeC25:H.

Figure 2.12 and 2.13 show examples of how methyl-branched alkanes are identified from their mass spectra (both taken from the eggs of the *L. sericata*). As mentioned, Figure 2.12 shows the mass spectrum of 11MeC25:H and 13MeC25:H eluting at the same retention time. The observation of ions pairs is due to the loss of a hydrogen atom, as reported by Biemann, cited in McCarthy et al [24]. The intensity of ions $m/z = 168/169$, $m/z = 196/197$ and $m/z = 224/225$ are greater abundance than the surrounding ions. This is because fragmentation reveals where the chain has cleaved and is therefore indicative of the position of the methyl group. The ions $m/z = 168/169$ and $m/z = 224/225$ correspond to the 11MeC25:H isomer where these two ions are paired together due to fragmentation at the eleventh and twelfth position (from left to right of the chain. 168/169) and the fifteenth position (from right to left of the chain, 224/225). The ions $m/z = 196/197$ corresponds to the 13MeC25:H. There is no fragment pair for this methyl because the position of the thirteenth carbon is the same site from both ends of the chain.
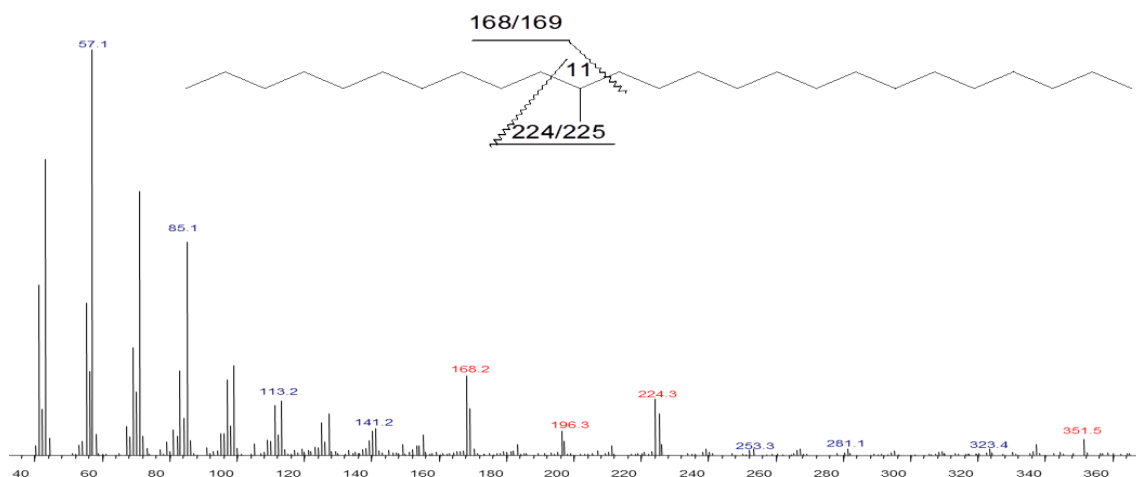
Figure 2.12: Mass spectrum of an 11MeC25:H and 13MeC25:H

The [M-15]$^+$ shown in Figure 2.12 is ion $m/z = 351$ and it can be used to calculate the M$^{+\cdot}$ ion which in this case is ion $m/z = 366$. This corresponds to a compound containing 26 carbons, but as it's a monomethyl-branched compound, the chain length backbone contains 25 carbons.

A common methyl branched hydrocarbon observed in the blowflies examined for this research is 2-Methyl. An example of the mass spectrum is given in Figure 2.13, showing 2MeC24:H. Ion $m/z = 309/310$ shows increased intensity, which corresponds to the [M-43]$^+$ ion (M relates to the molecular ion and 43 [C$_3$H$_7$] relates to the weight of the carbon and hydrogen atoms being cleaved off). In this particular example, both 2-Methyl (Figure 2.13) and 4-Methyl (Figure 2.14) have the same diagnostic ion of $m/z = 309/310$ present in their mass spectra. They will also both have visible ions at the [M-15]$^+$ due to the loss of a methyl group. However, there is a noticeable increase in the abundance of $m/z = 43$ in the mass spectrum of 2-Methyl (Figure 2.13). This ion is

not observed in the mass spectrum shown in Figure 2.14, but it will be present in a much lower abundance in comparison.
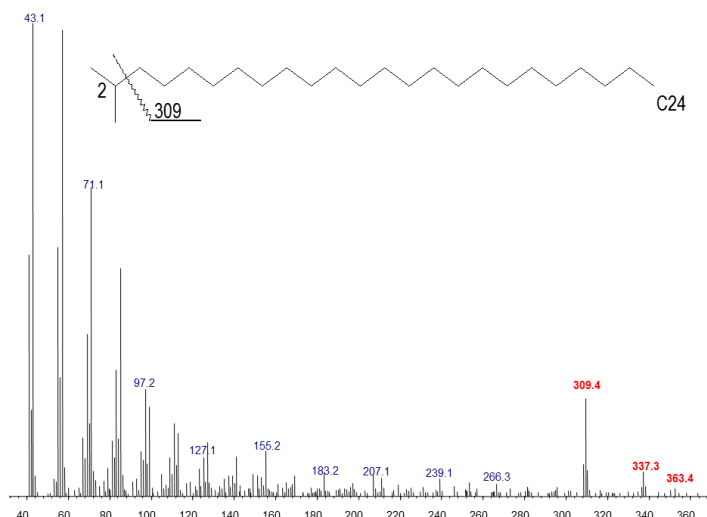
Figure 2.13: Mass spectrum of 2-Methyltetracosane from the GC-MS of the eggs of *L. sericata*

However, the mass spectrum of the 4-Methyl shows an increased intensity of $m/z = 70$ equal to an amount similar or greater than the intensity $m/z = 69$ due to the cleavage of the C_4-C_5 bond, which is observed in the mass spectrum of 4MeC30:H (Figure 2.14). In Figure 2.13, the ion $m/z = 70$ is not of sufficient intensity to support an explanation of the spectrum being the 4-Methyl isomer. The spectrum is instead matching a 2-Methyl isomer [25][26]. The m/z [M-15] $^+$ and M$^{+\cdot}$ are shown to be ion $m/z = 337$ and $m/z = 352$ respectively revealing a 2MeC24:H.
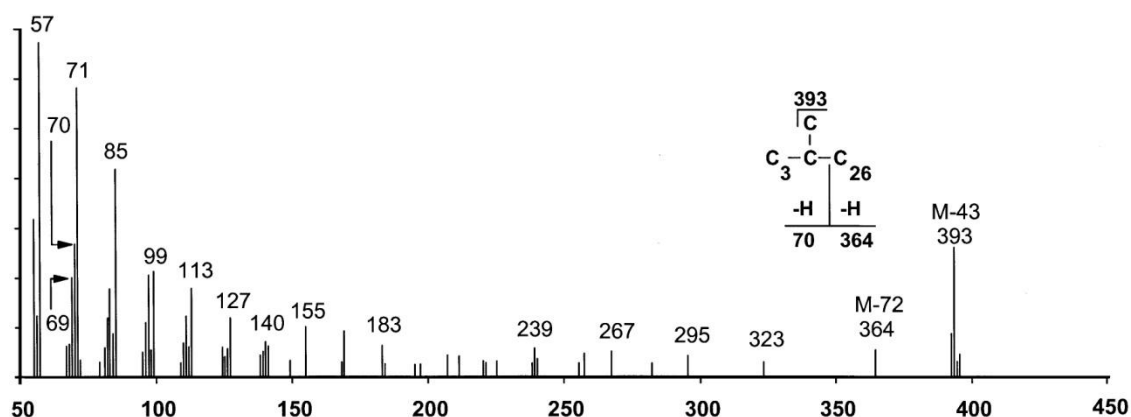
Figure 2.14: Mass spectrum of 4MeC30:H taken from Tissot et al. [26]

2.6 New MS developments

The main analytical instrument used for the results presented in this thesis was GC-MS. For many years, this has proven to be a sound technique for analysing hydrocarbons [25–30]. However, over recent years, a number of ambient ionisation techniques have been developed in mass spectrometry [31]. The main two techniques that have become most established are Desorption Electrospray Ionisation (DESI) (developed in 2004) and Direct Analysis in Real Time (DART) (developed in 2005) [32]. These two novel techniques are highly advantageous as they greatly reduce analysis time since they require minimal or no sample preparation because they are carried out by direct sampling in the open atmosphere [31].

DESI has similar characteristics to Electrospray Ionisation (ESI). The ionisation occurs by a pneumatically assisted needle producing a spray of charged microdroplets (of an appropriate solvent) which interact with the surface of the sample of interest [33][34].

In DART, ionisation takes place directly on the sample surface when it is placed in a stream of helium (for a detailed description of DART-MS see chapter 7).

Preliminary results were obtained from DART-MS. Further information on this particular technique is presented in chapter 7.

2.7 Multivariate analysis: Introduction

When analysing a sample of any nature with an analytical technique, often a large amount of information can be gathered even from a single GC trace. For the hydrocarbon analysis of an insect, the amount of compounds present ranges from approximately 30 to 50 and each compound yields a retention time and peak area. The retention time (and related mass spectrum) allows for identification of the compound whilst the peak area corresponds to the concentration. Due to the volume of information extracted from a single GC chromatogram, multivariate analysis was required as it condenses data which can then be visualised in the form of a scatter plot for ease of interpretation.

The primary type of multivariate analysis selected for this research was Principal Component Analysis (PCA) which is briefly explained below.

2.7.1 Principal Component Analysis (PCA)

PCA is a technique used for reducing correlated data sets from large numbers of samples, making them more manageable and allowing for any trends within the data to be revealed. This is done by grouping data according to statistically significant similarities using principal components. To understand the plots presented in this thesis

a brief summary is given, however for further details on PCA, the reader is referred to reference [35].

The relative peak areas in the GC data from each sample is described by a linear combination of principal components, each of which is weighted by a specific set of numbers, known as the loadings (or scores). The first principal component (PC1) describes the largest amount of variation within a dataset whilst the second and successive principal components reveal additional variation, each of successively less significance [36]. Each principal component has a corresponding eigenvalue which displays the value of variance within a dataset, as a percentage [37]. The eigenvalue is used to determine the number of principal components that need to be applied to the dataset. It is favourable when data can be described by the least number of principal components, since the principal components decrease in significance, leading to the exclusion of some data. For the results presented in this thesis, 4 to 6 principal components were seen to be sufficient to describe the main variations, thus greatly reducing the datasets from the original site of the input data.

The output of a PCA calculation is usually compiled into a scatter-plot using the loadings (or scores) of two selected principal components. This enables any clustering to be easily visualised, signifying samples that are similar to each other. The Euclidean distance can be calculated to measure the distance between two points, given by Pythagoras' theorem [35]. This technique is calculated using the loading values allowing for comparison based on all principal components.

PCA was the principal statistical analysis technique used in this thesis because of its capability of classifying patterns within data and its user friendly approach, in

conjunction with Excel. However, some preliminary results were also obtained for Artificial Neural Networks analysis which is a new emerging field in the analysis of complex data. These results are presented in chapter 7 to illustrate the potential it holds for data analysis of this nature.

References

[1]   A. Langford, J. Dean, R. Reed, D. Holmes, J. Weyers, and A. Jones, *Practical Skills in Forensic Science*, Pearson, UK (2005).

[2]   H.M. McNair and J.M. Miller, *Basic Gas Chromatography*, Wiley, UK (2009).

[3]   D.C. Harris, *Quantitative Chemical Analysis*, W.H. Freeman and Company, New York (2002).

[4]   R.J. Hurtubise, Adsorption Chromatography, in: Encyclopedia of chromatography, (2004) ed., J. Cazes, Update Supplement, Marcel Dekker Inc. USA (2002) 17–20.

[5]   J. Weiss, *Ion Chromatography*, VCH Verlagsgesellschaft mbH, Germany and VCH Publishers, USA (1995).

[6]   W.H. Scouten, Chromatography, Affinity, in: Encyclopedia of polymer science and technology, Wiley, UK (2002) 580–598.

[7]   D.S. Hage and W. Clarke, Affinity chromatography: An overview, in: Encyclopedia of Chromatography (2004) ed., J. Cazes, Update Supplement, Marcel Dekker Inc., USA (2002) 40–43.

[8]   K. Grob, *Split and Splitless Injection for Quantitative Gas Chromatography*, Wiley VCH, Germany (2001).

[9]   Accessed in November 2011
        http://teaching.shu.ac.uk/hwb/chemistry/tutorials/chrom/gaschrm.htm, .

[10]   Accessed in March 2012
        http://online.cit.edu.au/toolboxes/labtech/Laboratory/StudyNotes/snTheGCColumn.htm, .

[11]   E.L. Grob and E.F. Barry, *Modern practice of gas chromatography*, Wiley, UK, (2004).

[12]   M. McMaster and C. McMaster, *GC/MS: A practical user's guide*, Wiley VCH, Germany, (1998).

[13]   H.M. McNair and J.M. Miller, Basic gas chromatography: Techniques in analytical chemistry, Wiley, UK (1997).

[14]   T. Akino, Cuticular hydrocarbons of *Formica truncorum* (Hymenoptera: Formicidae): Description of new very long chained hydrocarbon components, Applied Entomology and Zoology 41 (2006) 667–677.

[15]   F.W. Karasek and R.E. Clement, *Basic Gas Chromatography - Mass Spectrometry: principles and techniques*, Elsevier, NL (1988).

[16]   D.A. Carlson, U.R. Bernier, and B.D. Sutton, Elution patterns from capillary GC for methyl-branched alkanes, Journal of Chemical Ecology 24 (1998) 1845–1865.

[17] G. McMahon, *Analytical Instrumentation: A guide to laboratory, portable and miniaturized instruments*, Wiley, UK, (2007).

[18] W.M.A. Niessen, *Liquid Chromatography-Mass Spectrometry*, Taylor and Francis Group, USA (2006).

[19] E. Hoffmann and V. Stroobant, *Mass spectrometry: Principles and applications*, Wiley, UK, (2008).

[20] E. Hoffmann, J. Charette, and V. Stroobant, *Mass spectrometry: Principles and applications*, Wiley, UK (1999).

[21] W. Henderson and J.S. McIndoe, *Mass spectrometry of inorganic and organometallic compounds*, Wiley, UK (2005).

[22] Accessed on April 2012 http://www.extrel.com/products/theoryofoper.php, .

[23] F.W. McLafferty and F. Turecek, *Interpretation of Mass Spectra*, University Science Books, USA (1993).

[24] E.D. Mccarthy, J. Han, and M. Calvin, Hydrogen atom transfer in mass spectrometric fragmentation patterns of saturated aliphatic hydrocarbons, in: Analytical Chemistry (1968) 1475–1480.

[25] D.R. Nelson and R.E. Lee, Cuticular lipids and desiccation resistance in overwintering larvae of the goldenrod gall fly, *Eurosta solidaginis* (Diptera: Tephritidae)., Comparative Biochemistry and Physiology. Part B, Biochemistry and Molecular Biology 138 (2004) 313–20.

[26] M. Tissot, D.R. Nelson, and D.M. Gordon, Qualitative and quantitative differences in cuticular hydrocarbons between laboratory and field colonies of *Pogonomyrmex barbatus*, Comparative Biochemistry and Physiology. Part B, Biochemistry and Molecular Biology 130 (2001) 349–58.

[27] G.H. Zhu, G.Y. Ye, C. Hu, X.H. Xu, and K. Li, Development changes of cuticular hydrocarbons in *Chrysomya rufifacies* larvae: potential for determining larval age, Medical and Veterinary Entomology 20 (2006) 438–44.

[28] R. Urech, G.W. Brown, C.J. Moore, and P.E. Green, Cuticular hydrocarbons of buffalo fly, *Haematobia exigua*, and chemotaxonomic differentiation from horn fly, *H. irritans*, Journal of Chemical Ecology 31 (2005) 2451–61.

[29] G. Ye, K. Li, J. Zhu, G. Zhu, and C. Hu, Cuticular hydrocarbon composition in pupal exuviae for taxonomic differentiation of six necrophagous flies, Journal of Medical Entomology 44 (2007) 450–6.

[30] S.J. Martin, H. Helanterä, and F.P. Drijfhout, Colony-specific hydrocarbons identify nest mates in two species of Formica ant, Journal of Chemical Ecology 34 (2008) 1072–80.

[31] L. Vaclavik, T. Cajka, V. Hrbek, and J. Hajslova, Ambient mass spectrometry employing direct analysis in real time (DART) ion source for olive oil quality and authenticity assessment, Analytica Chimica Acta 645 (2009) 56–63.

[32]   J. Hajslova, T. Cajka, and L. Vaclavik, Challenging applications offered by direct analysis in real time (DART) in food-quality and safety analysis, Trends in Analytical Chemistry 30 (2011) 204–218.

[33]   M. Morelato, A. Beavis, A. Ogle, P. Doble, P. Kirkbride, and C. Roux, Screening of gunshot residues using desorption electrospray ionisation-mass spectrometry (DESI-MS), Forensic Science International (2011).

[34]   Z. Miao and H. Chen, Direct analysis of liquid samples by Desorption Electrospray Ionization-Mass Spectrometry (DESI-MS), Journal of the American Society for Mass Spectrometry 20 (2009) 10–9.

[35]   R.G. Brereton, *Chemometrics: Data analysis for the laboratory and chemical plant*, Wiley, Chichester UK (2003).

[36]   C.D. Adam, S.L. Sherratt, and V.L. Zholobenko, Classification and individualization of black ballpoint pen inks using principal component analysis of UV-vis absorption spectra, Forensic Science International 174 (2008) 16–25.

[37]   J.N. Miller and J.C. Miller, *Statistics and Chemometrics for analytical chemistry*, Pearson, UK (2005).

Chapter 3

Methods and Materials

3. Fly rearing

Lucilia sericata:

A colony of *L. sericata* was kindly supplied by the Natural History Museum in London (geographical origin, Hayward's Heath, West Sussex, UK, 51°00'18"N:00°05'09E"). This colony of *L. sericata* was used for larvae and puparial case extractions. A second colony was later supplied by Kate Barnes from Derby University (originated from Castaway Tackle, Unit 8b, Chieftain Way, Tritton Road, Lincoln, but regularly supplemented by wild flies caught in Lincoln city.) This supply of *L. sericata* was used for adult fly and egg extractions. The flies were reared in the laboratory and maintained in a rearing cage under standard environmental conditions (23±1 ˚C with RH ~ 70%) with a 14:10h light cycle. They were supplied with sugar, water and milk powder. Pig's liver (or pork chop for the later experiments) was used as an ovisposition medium

which was placed on a petri-dish with damp cotton wool to prevent the meat from drying out.

Calliphora vicina:

Two sources of *C. vicina* were used for the duration of this project. The first was supplied by Katherine Davies from Portsmouth University (geographical location, Anglesea building car park, Anglesea road, Portsmouth, PO1 3DJ). This colony was used for pupal and empty puparial case extractions. The second colony came from Scott Hayward's research group (geographical location, Birmingham campus. Collected in the summer of 2009, but regularly replenished with wild caught individuals.) This particular colony was used for larvae, adult fly and egg extractions. The flies were reared in the laboratory and maintained in a rearing cage under standard environmental conditions (23±1˚C with RH ~ 70%) with a 14:10h light cycle. They were supplied with sugar, water and milk powder. Pigs liver (or pork chop for the later experiments) was used as an ovisposition medium which was placed on a petri-dish with damp cotton wool to prevent the meat from drying out.

Calliphora vomitoria:

Two colonies of *C. vomitoria* were used for experimental work. The first was supplied by the Natural History Museum – Bartley Road, woodlands, New Forest, 50˚55'22"N:01˚33'18"W). The first colony was primarily used for puparial case experiments. The second colony was supplied by Scott Hayward's research group at Birmingham University and originated from a fishing tackle shop in Birmingham city

centre. This colony was used for larvae, adult fly and egg extractions The flies were reared in the laboratory and maintained in a rearing cage under standard environmental conditions (23±1˚C with RH ~ 70%) with a 14:10h light cycle. They were supplied with sugar, water and milk powder. Pigs liver (or pork chop for the later experiments) was used as an ovisposition medium which was placed on a petri-dish with damp cotton wool to prevent the meat from drying out.

3.1 Larvae rearing

Once eggs were laid on the oviposition medium, the Petri dish containing the meat was placed into small lunch boxes with a large hole cut into the lids and covered with muslin to allow a good air flow to circulate and to prevent a build-up of ammonia, given off as a by-product when the larvae feed. Each box has a small layer of sawdust to allow the larvae to pupate. When the larvae hatched and the oviposition meat had been eaten, they were fed on minced beef because it was less potent and easier to handle and store when used on a daily basis. The larval instars were established by looking at the number of posterior spiracles slits.

3.2 Sample preparation

The methodology, which was developed at the beginning of the project, was aimed to be kept simple so a non-expert could carry out the hydrocarbon extractions from any life stage of the blowflies with ease. This sampling method was then applied to the six life stages of the three blowflies used in this work. To compensate for any variation

within the extractions, 10 replicates were always taken from each extraction period, of every life stages (with the exception of the egg experiments, see 3.2.1).

3.2.1 Hydrocarbon extraction

Empty egg cases:

Once the flies had laid eggs on the oviposition medium, the meat was removed from the rearing cage and put into an incubator at 22 ˚C. When the larvae had hatched the empty egg cases were removed from the meat using a fine paint brush and put into an open Petri dish where they were stored in the laboratory until the hydrocarbons were extracted. Liquid extraction with hexane was used to extract the hydrocarbons from the egg case cuticle. Egg cases were pooled together due to their size to acquire a suitable concentration when analysed on the GC-MS. Each sample required ~30 egg shells and these were placed into a clean 2 mL GC vial and fully submerged with hexane (150 μL). The extract was left for 10-15 minutes before being transferred to a 300 μL flat bottomed insert and left until completely dry. All samples were stored dry in the refrigerator at 4 ˚C until they were required for analysis. The dried extract was then reconstituted in 10 μL of hexane before being manually injected into the GC-MS. Due to the empty egg case results being obtained at the end of the laboratory experimental period for this research, only 2 repeats per daily extraction were taken because the fly colonies were very old and no longer laying a sufficient quantity of eggs. As they were preliminary results, the extraction days were chosen at random.

Larvae:

When needed, larvae were pooled together to ensure the concentration was sufficient enough for the GC-MS to detect the hydrocarbons and for each day the extraction was replicated 10 times ($n = 10$). As the larvae become older, and therefore larger in size, fewer were required for the extractions. The larvae were extracted daily upon emergence from the egg to pupation. Emergence of the egg was regarded as day 1. Larvae were placed into a 2 mL GC vial with hexane ensuring that the insects were fully submerged. It was then left for 10 to 15 minutes where after the hexane extract was transferred to a silica gel column. The larvae were the only life stage needed to have column chromatography applied to (see 3.3) due to contaminants the larvae encounter when feeding on meat. The eluted column extract was collected in a clean vial and the hexane was left to evaporate until the extract could be transferred to a 300 µL flat bottomed insert and left to dry down completely. All samples were stored dry in the refrigerator at 4 ˚C until they were required for analysis. The dried extract was then reconstituted in 30 µL of hexane before GC-MS analysis apart from the first 2 sampling days which were reconstituted in 20 µL of hexane (due to the larvae being so small in size and therefore requiring a higher concentration for sampling). The latter were manually injected into the GC-MS (hexane could have evaporated slightly before the sample is analysed meaning the autosampler may not be able to draw up the extract from the insert) while the remaining samples were introduced to the GC-MS via the autosampler. Tables 3.1 to 3.3 show the number of larvae used per sample, per day for all three species.

Table 3.1: Number of larvae taken daily during *L. sericata* larval extractions at 23±1˚C

Day	Instar	Number of larvae added to each sample $n = 10$
1	1st	~30
2	2nd instar	10
3	2nd instar	5
4	3rd instar	3
5 to 10	3rd instar and post-feeding	2

Table 3.2: Number of larvae taken daily during *C. vicina* larval extractions at 22±1˚C

Day	Instar	Number of larvae added to each sample $n = 10$
1	1st	~20
2	2nd instar	9
3	3rd instar	5
4 & 5	3rd instar	3
6 to 10	Post-feeding	2

Table 3.3: Number of larvae taken daily during *C. vomitoria* larval extractions at 22±1˚C

Day	Instar	Number of larvae added to each sample $n = 10$
1	1st	~30
2	2nd instar	~15
3	2nd/3rd instar	7
4 & 5	3rd instar	3
6 to 10	3rd instar	2
11 to 14	Post-feeding	2

Puparia:

Puparia extractions for *C. vicina* and *L. sericata* were carried out in a similar way to the empty egg case samples. Extractions were replicated 10 times ($n = 10$) and were carried out daily until eclosion, using two cases per sample. The cases were added to a 2 mL GC vial and submerged with hexane (350 μL) for 10-15 minutes. The hexane extract was collected in a clean 2 mL vial and the hexane was left to evaporate until the extract could be transferred to a 300 μL flat bottomed insert and left to dry down completely. All samples were stored dry in the refrigerator at 4 ˚C until they were required for analysis. The dried extract was then reconstituted in 30 μL of hexane before GC-MS analysis which was carried out using the autosampler.

Puparial case:

The hydrocarbon extractions of the empty puparial cases for all three species were carried out using the same methodology as the pupae extractions. Two cases were used per replicate. The cases were added to a 2 mL GC vial and submerged with hexane (350 μL) for 10-15 minutes. The hexane extract was collected in a clean 2 mL vial and the hexane was left to evaporate until the extract could be transferred to a 300 μL flat bottomed insert and left to dry down completely. All samples were stored dry in the refrigerator at 4 ˚C until they were required for analysis. The dried extract was then reconstituted in 30 μL of hexane before GC-MS analysis which was carried out using the autosampler.

Puparial cases were extracted weekly for the first 8 weeks then monthly until 9 months. They were stored in open plastic lunchboxes in the laboratory environment (23±1˚C

with RH ~ 60%) with a 14:10h light cycle. Week 1 is on the seventh day once the adult fly had emerged from the puparial case, with week 2 on the 14th day etc.

Blind samples were also taken from empty puparial cases that had been collected from fly colonies over the duration of rearing and stored in open plastic lunchboxes in the laboratory environment (23±1˚C with RH ~ 60%) with a 14:10h light cycle. The same extraction protocol was followed by a colleague for the blind samples.

Adult fly:

When extracting the hydrocarbons from the female adult flies, one fly per extraction was used and ten repeats were obtained per extraction period ($n = 10$). For this particular experiment, the adult flies were extracted on the day of eclosing (day 1), day 5, day 10, day 20 and day 30. The flies for this experiment were maintained in a smaller rearing cage for ease of capture and were placed into a 2 mL GC vial and submerged with hexane (500 μL). The extract was left for 10-15 minutes then transferred to a clean 2 mL GC vial and dried down until it could be transferred to a 300 μL flat bottomed insert and left to dry down completely. All samples were stored dry in the refrigerator at 4 ˚C until they were required for analysis. The dried extract was then reconstituted in 150 μL of hexane before GC-MS analysis which was carried out using the autosampler.

3.3 Column chromatography

In order to separate out the polar compounds from the non-polar hydrocarbons, column chromatography was used on larval extracts as this stage were found to contain the highest number of polar contaminants. The column was prepared by using a Pasteur pipette which was plugged with glass wool and then layered with approximately 1 cm of silica gel (see Figure 3.1). The column was first wetted with 100 µL of hexane before the extract containing the insect specimen was transferred onto the column and an additional 500 µL of hexane was then added. The eluted hexane was collected into a clean 2 mL GC vial and the extract was left to evaporate to dryness. The extracts were redissolved in 10 µL (for manual injections) and 20 µL (for autosampler injections) of hexane and a 2 µL aliquot was injected into the GC-MS.

1)   2)   3)

Figure 3.1: Column chromatography: 1) Pasteur pipette being plugged with glass wool 2) Silica gel being added 3) Finished Pasteur pipette complete with glass wool, silica gel and a pupae ready to be extracted.

3.4 Chemical Analysis: Gas Chromatography – Mass Spectrometry

For the first 2 days of larval extractions and the egg shell extraction, samples were injected manually into the GC-MS. From day 3 onwards for larvae, pupae, pupal case and adult flies, extracts were introduced into the GC-MS using the autosampler. Chemical analysis of all extracts was carried out on an Agilent Technologies 6890N Network GC system with a split/splitless injector at 250 ˚C, a Restek Rxi-1MS capillary column, containing an SP of 100% Polydimethyl siloxane (30m x 0.25 mmID, 0.25μm film thickness) and coupled to an Agilent 5973 Network Mass Selective Detector. The GC was coupled to a computer and the data was processed with Agilent Chemstation software. Elution was carried out with helium at 1mL/min. The oven temperature was programmed to be held at 50 ˚C for 2 minutes then ramped to 200 ˚C at 25 ˚C /min, then from 200 ˚C to 260 ˚C at 3 ˚C /min and finally from 260 ˚C to 320 ˚C at 20 ˚C /min where it was held for 2 minutes. The mass spectrometer was operated in Electron Ionisation at 70 eV, scanning from 40 – 500 amu at 1.5 scans s^{-1}. Hydrocarbons were identified using a library search (NIST08), the diagnostic fragmented ions and the Kovats Index.

An *n*-alkane standard solution, ranging from heneicosane (C21:H) to tetracotane (C40:H) was analysed on the GC-MS under the parameters stated above.

3.5 Methylthiolation

A methylthiolation reaction (adapted from [1]) was carried out on the adult flies of *C. vicina*, *C. vomitoria* and *L. sericata* to establish the double bond position of the alkenes. A basic reaction mechanism is shown in Figure 3.2 for *Z*7C27:1. Due to the

low concentration of alkenes in samples extracted from the other life stages, the decision was taken to carry out a dimethyl disulfide (DMDS) derivatization on the adult fly samples only, as they contained a much higher concentration of alkenes. It is therefore assumed the double bond positions remain the same during the immature life stages of the three species.

Three flies were extracted from each of the three species in the usual way using a liquid extraction of hexane in individual vials and left to dry down. 100 μL of hexane was then added to each vial and these were added together for each species to ensure a sufficient concentration of product was gathered. Each extract then had 100 μL of iodine solution (5% in ether) added and 100 μL of dimethyl disulfide (DMDS). The solutions will turn brown in colour and the iodine acts as a catalyst for the reaction. Nitrogen was passed over each solution before being capped and left overnight at 40 °C.
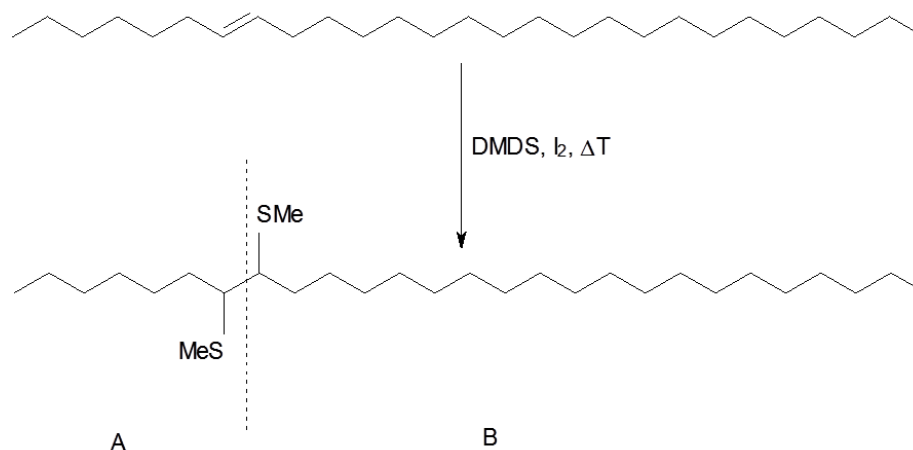
Figure 3.2: Basic reaction scheme of 7-heptacosene with DMDS [2]. The dashed line illustrates where the molecule is expected to break along the chain in the mass spectrometry to give fragment A and B (see appendix 14)

Iodine initially reacts with DMDS forming a methylthio-iodide, which will subsequently react with the double bond in the alkene. The second DMDS molecule reacts with the obtained intermediate, sulphonium-iodide. Iodide also acts as the catalysts in this step to regenerate methylthio-iodide [2].

The fragments (A and B) seen in Figure 3.2 are shown in the mass spectrum in appendix 14. They diagnostic ions are circled and they allowing for the double bond position to be determined. Fragment A (m/z 145) is, $C_7H_{14}SMe$. Fragment B (m/z 327) is $C_{20}H_{40}SMe$. As the DMDS derivatives are quite stable, the molecular ion ($M^{+\cdot}$) is usually visible, which in the case of appendix 14, is m/z 472, $C_{27}H_{54}(SMe)_2$.

To work up the reaction, a few drops of a saturated aqueous solution of $Na_2S_2O_3$ were added to the mixtures to quench the reaction until they were colourless, which removed the iodine. This will give an organic aqueous layer and a white deposit is also formed. The organic layer is extracted off and 2 μL of the solution is injected into the GC-MS. A normal hydrocarbon GC-MS program was used with the alteration of increasing the injector temperature to 325 ˚C and holding the final temperature (325 ˚C) for 15 minutes to ensure the heavier DMDS adducts elute off the column.

3.6 Solvents

Hexane (HPLC grade), purchased from Fisher Scientific, was used for extracting the hydrocarbons from the insect's cuticle.

Silica gel for flash chromatography was purchased from BDH, UK and used in column chromatography to separate the non-polar compounds from the polar compounds present in the insect hexane extracts.

An *n*-alkanes standard solution was purchased from Fluka, Germany.

The DMDS and Iodine solutions were purchased from Sigma-Aldrich Co. The iodine was saturated with ether (also purchased from Sigma-Aldrich Co).

3.7 Principal Component Analysis

The statistical analysis was carried out using multivariate add-ins to Microsoft Excel, which was written by Tom Thurston using an original development by Les Erskine [3]. All data were normalised to a mean of zero and a standard deviation of unity prior to the PCA calculation. Prior to PCA the peak areas were integrated using the Agilent Chemstation software, with the main focus being hydrocarbons. The *n*-alkanes were generally examined from C20:H to C33:H and the lower molecular weight compounds (C15:H to C19:H) were excluded from analysis (with the exception of the pupae for species identification). The reasoning for this was these volatile hydrocarbons are more variable and could introduce scatter within the PCA data. Many were also observed in trace amounts and all hydrocarbons with a peak area of less than 0.5% were excluded from the PCA datasets.

The PCA output is usually interpreted using a scatter-plot where the relative contributions of two principal components (here called the loadings) to each chromatogram are displayed. This facilitates the grouping of chemically similar samples, which will be represented by similar loadings. It is essential that several replicates for each sample are analysed so that any variation arising from genuine chemical variability may be distinguished from the natural random variation in these loadings. In this work ten replicates were taken on most occasions (with the exception

of empty egg cases). In all datasets apart from the empty egg cases, six principal components were generated (three for empty egg cases due to such a small dataset). All possible combinations of PCs were then plotted (starting with PC3 vs PC2) until the best separation was obtained between the extraction days. For each day, it is expected to see a cluster of points on the PCA plot. If that cluster is tight then the experimental repeatability is good and the system is not subject to significant variation in composition over that time-span. If the scatter is large then this may be an indicator of dynamic chemical changes occurring at that time.

References

[1]   D.A. Carlson, C.S. Roan, R.A. Yost, and J. Hector, Dimethyl disulfide derivatives of long chain alkenes, alkadienes, and alkatrienes for gas chromatography/mass spectrometry, Analytical Chemistry 61 (1989) 1564–1571.

[2]   F.C. Griepink, "Analysis of the Sex Pheromones of *Symmetrischema tangolias* and *Scrobipalpuloides absoluta*," Wageningen University, 1996.

[3]   R.G. Brereton, *Chemometrics: Data Analysis for the Laboratory and Chemical Plant*, Wiley, Chichester UK, 2003.

Chapter 4

Species identification using Cuticular Hydrocarbons

4. Introduction

One of the first steps in establishing the minimum Post-Mortem Interval (PMI_{min}) is to identify all insects present on human remains [1], as growth rate is dependent on the species. Identification is therefore needed in order to utilise the correct developmental data. When insects are incorrectly identified, PMI estimations can be inaccurate due to the variability in growth rates between taxa.

The identification of larvae is possible using morphological techniques but it can be challenging [1] and an experienced entomologist is required to carry out the procedure.

The analysis of hydrocarbons on insect cuticles offers a means to compliment the current identification techniques and has the potential to be applied to unknown specimens [2] or to confirm the species identification if there is uncertainty. Hydrocarbons have been found to be species-specific in a number of insect orders e.g. Blattodea, Coleoptera and Hymenoptera [3–7]. Each species of insect yields a

characteristic hydrocarbon profile so they are often used in chemotaxonomic studies for this purpose. Hence, hydrocarbon analysis has the potential to complement current identification methods used for Calliphoridae, especially for the more challenging life stages such as eggs and empty egg shell cases, first instar larvae and puparial cases, which can all be difficult to morphologically characterise. It could also be developed to assist with the identification of more difficult families such as the Sarcophagidae. The larvae of the flesh fly are particularly difficult to distinguish using morphological criteria alone, and the only way to successfully identify them is to rear them to adulthood, which may cause delays in criminal investigations. Sarcophagidae females are notoriously difficult to identify, as many keys refer to male genitalia only. Therefore if established, hydrocarbon analysis may form a useful identification tool for specimens at the larval stages, as well as adult flies.

4.1 Aims and Objectives

The aim of this study was to identify three forensically important blowfly species (*Calliphora vicina, Lucilia sericata* and *Calliphora vomitoria*) common in the UK, over the six stages of their life cycle [Figure 4.1, egg (empty cases), 1st instar, 2nd instar and 3rd instar larvae, puparia and adult flies] by analysing their hydrocarbon profiles using the analytical technique of Gas Chromatography – Mass Spectrometry (GC-MS). Results will also be presented for the empty puparial cases as these can be the only entomological evidence present at older crime scenes, therefore correct identification of the cases can give invaluable information as to which species inhabited the cadavers.
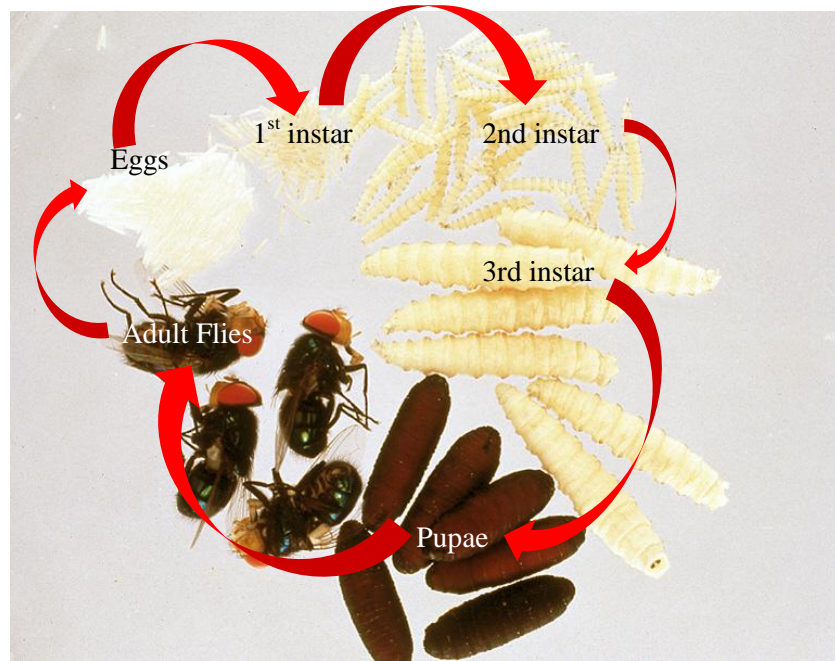
Figure 4.1: Life cycle of a blowfly, taken and adapted with permission from Dr Martin Hall.

Results for each species in each life stage will be presented by showing characteristic differences in their chromatograms as well as using multivariate statistical analysis in the form of Principal Component Analysis (PCA) to help interpret and visualise the results collected from the GC-MS analysis.

4.2 Egg cases

The female blowfly will initially concentrate oviposition in the natural orifices of human remains, such as the eyes, ears, nose, genitals, or any open wounds that maybe present. If eggs are the only insect evidence collected at a crime scene, it is likely they will be reared to 3rd instar larvae or ideally to adult flies to confirm their identification. However, confident early identification of this life stage can provide valuable information and allow for more timely PMI estimations [8] which can aid police

72

investigations. They can also give an indication of whether the body has been moved because the presence of eggs of a Diptera specific to a certain geographical location, differing from where the body was discovered, might suggest the victim was killed in a different location and has been moved since death [8,9].

Currently, the best method of identifying an egg is with the aid of a Scanning Electron Microscope (SEM) [8,10]. The eggs are elongated and curved at the ends, with an opening running along the centre of the chorion which splits at egg hatching (Figure 4.2).
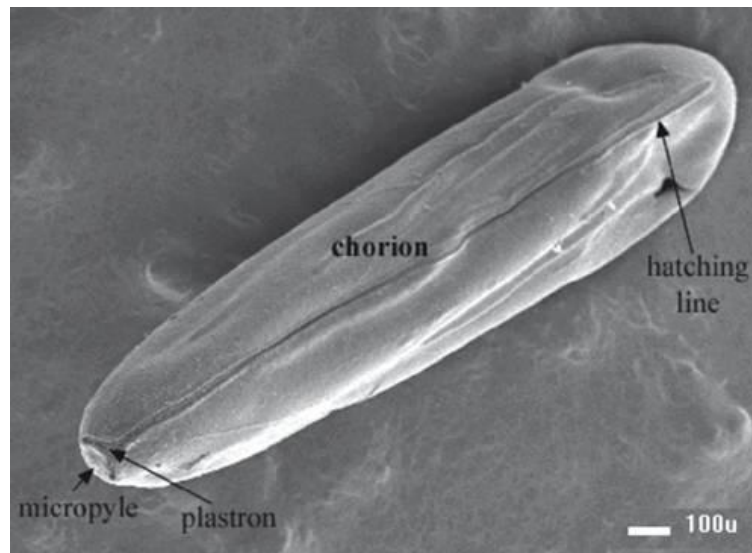
Figure 4.2: SEM image showing the morphology of a blowfly egg, with key features labelled. Image taken with kind permission of Springer Science and Business Media [11]

Another technique that has been published is the use of light microscopy and staining the egg with potassium permanganate [12]. This technique has the advantage of being rapid whilst also using the lower cost method of light microscopy. However, up to the present time, this is the only study that uses this technique on fly eggs in the literature.

It can be a complex and time-consuming procedure using SEM to determine characteristics on an egg in order to distinguish the species. In comparison, hydrocarbon analysis offers a relatively simple method for identification.

It is very difficult to identify an empty egg case, since they no longer hold their shape and have a split along the hatching line. This makes the characteristics within the surface of the egg (chorion) difficult to visualise using SEM imaging, and it may not be possible to distinguish any key features that can determine the identification. Since the empty egg cases are more challenging to identify using the current method of microscopy, only the empty egg case results shall be presented in this chapter.

4.2.1 Results and Discussion for egg cases

GC-MS analysis:

The hydrocarbons were extracted from the empty egg cases of *L. sericata*, *C. vicina* and *C. vomitoria*, obtaining preliminary results. They were analysed using GC-MS (refer to chapter 3, section 3.2.1). The egg cases were pooled together due to their size to acquire a suitable concentration for GC-MS analysis. PCA was then applied to a dataset consisting of the peak areas taken from the chromatograms (refer to chapter 3, section 3.6). Since the extractions of empty egg cases were carried out at the end of the laboratory experimental period for this research, it was only possible to obtain 2 replicates per daily extraction ($n = 2$), because the fly colonies were old and the females were no longer laying a sufficient quantity of eggs. Table 4.1 summarises the compound classes extracted from the egg cases for all three species and illustrates the different chemical compositions for each species.

Table 4.1: Hydrocarbon composition for each species, showing the number and percentage of *n*-alkanes, alkenes and methyl branched alkanes that each species yielded.

	L. sericata	*%*	*C. vicina*	*%*	*C. vomitoria*	*%*
Alkanes	7	28	5	18	7	21
Alkenes	4	16	3	11	6	18
Methyl branched HC	14	56	20	71	21	62
Total HCs	**25**	**100**	**28**	**100**	**34**	**100**

N.B. The data used to accumulate table 4.1 and 4.2 was obtained from 5-day old empty egg cases of *C. vomitoria* and *L. sericata* and 2-day old empty egg cases of *C. vicina*.

The HC profile of all three species are composed of medium to high boiling point hydrocarbons which include *n*-alkanes ranging from C23:H to C31:H, alkenes and mono- and di-methyl branched alkanes (see appendix 1 for list of all compounds extracted). The lower retention time compounds in the chromatogram (Figure 4.3) for all three species were mainly polar compounds. As this research primarily focused on hydrocarbons, these polar compounds were excluded from the analysis. The middle section of the chromatogram is predominantly made up of *n*-alkanes, ranging from C23:H to C27:H, as well as methyl branched alkanes and alkenes. The higher end of the chromatogram comprises of long chain *n*-alkanes (C28:H to C31:H), although they are often not observed in a sufficient concentration (*L. sericata* contained C31:H in an adequate concentration but in the two Calliphora species, the *n*-alkanes were only detected up to a chain length of C29:H. Heptacosane (C27:H) and nonacosane (C29:H) were present in substantial amounts in all three species. *C. vomitoria* contains the highest number of alkenes in its hydrocarbon profile and both species of Calliphora have considerably more methyl branched hydrocarbons than *L. sericata*.

The *n*-alkanes were excluded from the PCA dataset as they introduced substantial scatter within the replicates of *C. vicina* (also seen in results presented in chapters 5 and 6 for this particular species).

The reader is referred to appendices 2 to 9 for example mass spectra of mono-methyl alkanes, di-methyl alkanes and alkenes.

Table 4.2: List of the compounds extracted and used for subsequent PCA analysis from the egg cases of *C. vomitoria*, *L. sericata* and *C. vicina,* along with the Kovats Index to aid identification. (Peak numbers relate to peaks in Figure 4.3)

Peak no.	Peak Identification	Kovats iu	*L. sericata* n=2 %	*C. vicina* n=2 %	*C. vomitoria* n=2 %
1	2-Methyltetracosane	2463	ND	6.09±2.57	3.45±0.95
2	Pentacosene[1]	2469	2.74±0.58	1.60±0.06	3.97±3.39
3	Pentacosene[1]	2476	ND	ND	3.48±2.85
4	9+11-Methylpentacosane	2535	1.95±0.24	ND	1.32±0.76
5	2-Methylhexacosane	2662	3.84±0.95	8.71±0.62	5.31±1.83
6	Heptacosene[1]	2668	2.88±0.29	ND	1.61±1.31
7	11+13-Methylheptacosane	2730	2.33±0.47	1.37±0.67	1.54±0.65
8	3-Methylheptacosane	2773	4.80±1.48	2.37±0.66	2.13±0.67
9	2-Methyloctacosane	2873	6.36±0.54	22.69±10.44	17.21±5.93
10	Nonacosene[1]	2877	2.20±0.10	1.17±0.39	1.13±0.35
11	Nonacosene[1]	2882	ND	0.69±0.30	1.31±0.37
12	2,6-Dimethyloctacosane	2906	ND	1.40±0.64	ND
13	11+13-Methylnonacosane	2938	21.44±6.10	12.08±0.48	10.73±3.49
14	9-Methylnonacosane	2943	7.72±2.24	2.77±1.08	2.60±0.58
15	7-Methylnonacosane	2950	9.74±2.97	5.74±1.74	5.26±1.72
16	5-Methylnonacosane	2958	1.88±0.61	2.41±0.51	2.82±0.97
17	9,17-Dimethylnonacosane	2971	2.34±0.54	ND	ND
18	3-Methylnonacosane	2981	3.36±1.01	4.63±1.44	3.68±1.22
19	5,x-Dimethylnonacosane	2989	ND	1.32±0.67	1.75±0.62
20	14+16-Methyltricontane	3041	ND	1.12±0.55	1.48±0.51
21	3-Methyltricontane	3041	3.70±0.28	6.54±1.73	5.64±2.16
22	Hentriacontene[1]	3076	1.61±0.01	ND	1.59±0.45
23	2,14-Dimethyltriacontane	3106	ND	1.62±0.77	1.99±0.70
24	2,6/2,8/2,10-Dimethyltriacontane	3111	ND	3.68±0.95	4.53±1.72
25	11-Methylhentriacontane	3144	12.29±3.20	6.11±2.44	7.53±2.93
26	11,19-Dimethylhentriacontane	3143	8.81±2.13	ND	ND
27	7,x-Dimethylhentriacontane[2]	3147	ND	ND	1.65±0.51
28	9,21-Dimethylhentriacontane[2]	3174	ND	2.01±1.04	2.46±0.58
29	17-Methyltritriacontane+4,8/4,10-Dimethylhentriacontane[2]	*N/A	ND	1.93±0.67	1.70±0.02
30	2,10/2,12-Dimethylhentriacontane[2]	3339	ND	1.96±0.79	2.12±0.58

[1]Double bond positions determined for adult flies only

[2]Tentative identification based on Kovats Index values and a match with NIST08 Library database

*Kovats not available due to co-eluting peak

The higher end of the chromatogram in all species also includes a large number of mono and di-methyl branched alkanes, with a dominating group of mono-methyl compounds (peak number 13-16, Table 4.2). These compounds are 11+13-MeC29:H, 9-MeC29:H, 7-MeC29:H and 5-MeC29:H. The most abundant branched methyl compound in the two Calliphora species was 2-MeC28:H (peak 9, Table 4.2) while 11+13-MeC29:H dominated in the *L. sericata* chromatogram (peak 13, Table 4.2).

Figure 4.3 shows the stacked GC chromatograms of the eggs extracted from the three blowfly species. Although superficially they may all look relatively similar, when full profile identification is established, there are some key differences between the three species. The ratios in which compounds are present also vary within the species. For example the first shaded bar in Figure 4.4 shows a group of three compounds, 2-MeC24:H and two C25:1 isomers. In the *L. sericata* profile only one C25:1 isomer is present whilst in the two Calliphora species, both are observed, but in different concentrations and the 2-MeC24:H is much more abundant in *C. vicina* (Figure 4.4).
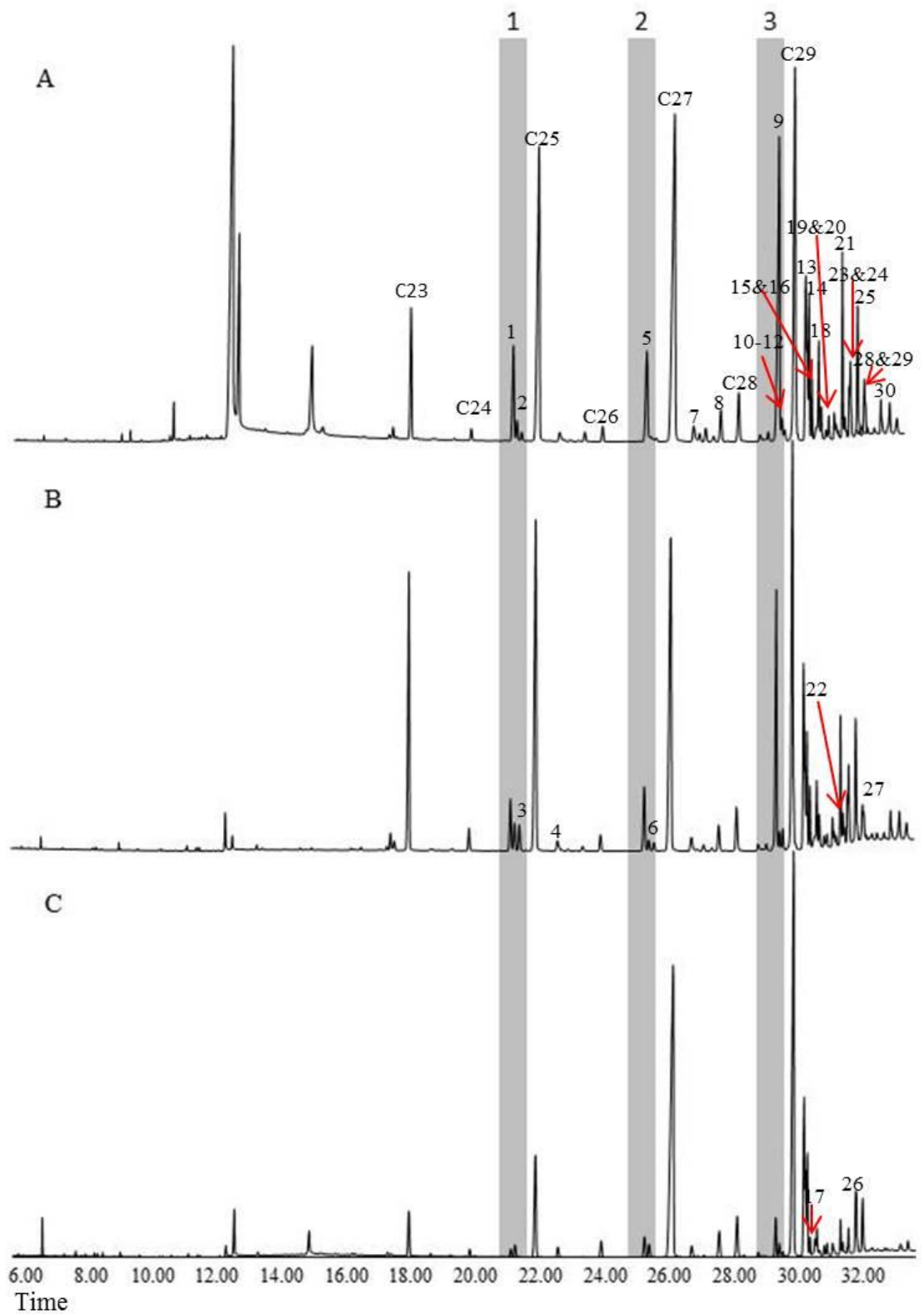
Figure 4.3: GC chromatograms showing the egg case hydrocarbon profiles of three blowfly species, A: *C. vicina*, B: *C. vomitoria*, C: *L. sericata*. Shaded bars illustrate key species-specific regions within the hydrocarbon profiles.
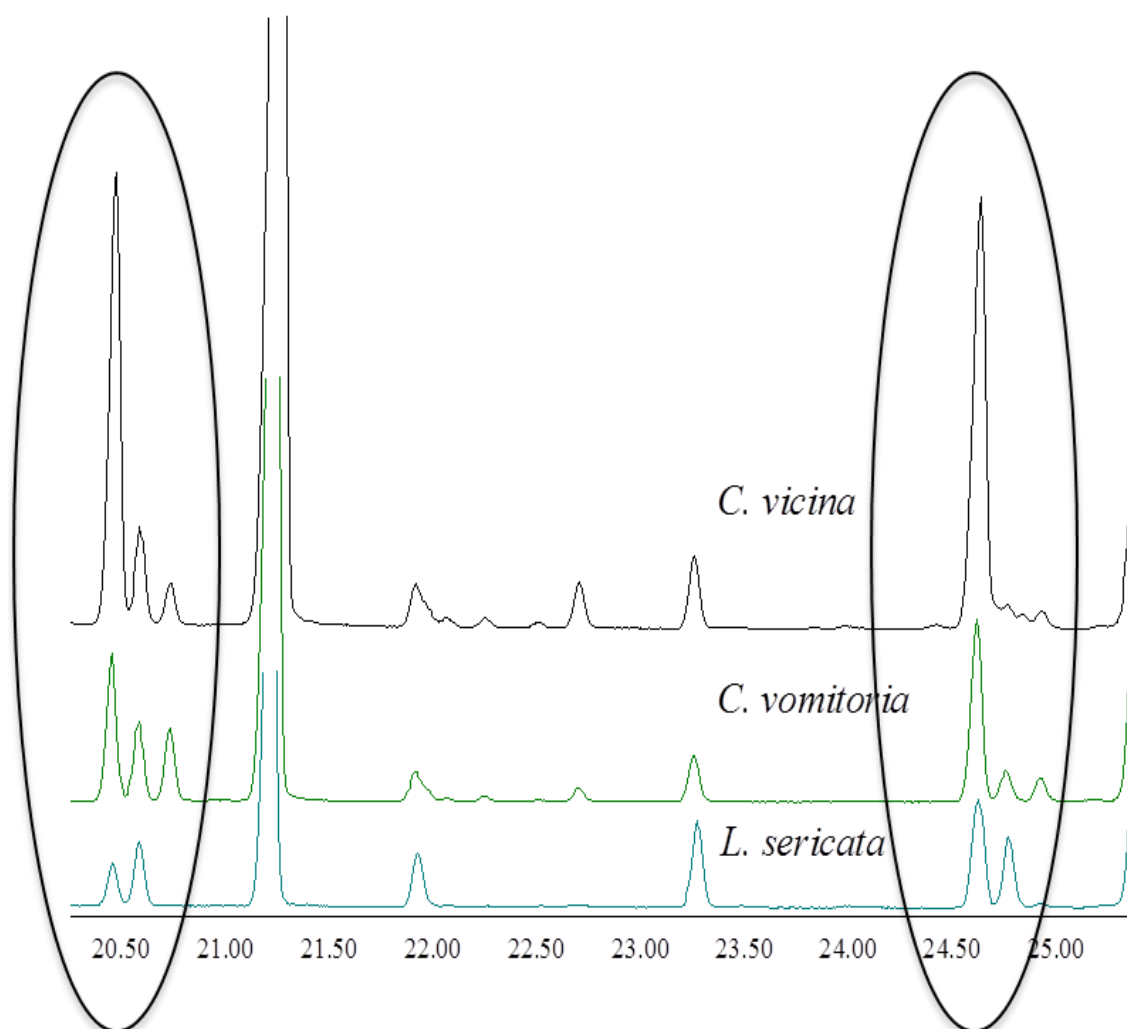
Figure 4.4: Zoomed in region of the stacked chromatograms (Figure 4.3) highlighting the varying peak rations for the 2-MeC24/C26:H and C25/C27:1 hydrocarbons.

Similarly, the second and third shaded bar shows a single mono methyl hydrocarbon in *C. vicina*, (2-MeC26:H and 2-MeC28:H) and two C29:1 isomers proceeding 2MeC28:H, whereas *C. vomitoria* exhibits the same mono methyl's and the two C29:1 isomers plus an additional of C27:1, which proceeds 2-MeC26:H. *L. sericata* displays both mono methyl's along with single alkene peaks of C27:1 and C29:1 respectively.

PCA:

To confirm the results and finalise species identification, statistical analysis is required. Statistical analysis using PCA was undertaken (see chapter 3, section 3.6) to determine the significance of the GC-MS results obtained. In the interpretation of PCA, the loadings for pairs of components may be shown as scatter plots. Each sample is represented by one data point in the plot. Peak areas were used when running the PCA and PC3 and PC2 were used over the other principal components because they most clearly display the variation in comparison with species. PC2 and PC3, comprised of 7.1% and 1.4% and the five principal components combined describing 99.9% of the variation.

The PCA plot in Figure 4.5 was derived from data containing all three classes of hydrocarbons (*n*-alkanes, alkenes and methyl branched alkanes) and used a combined dataset for all three species.
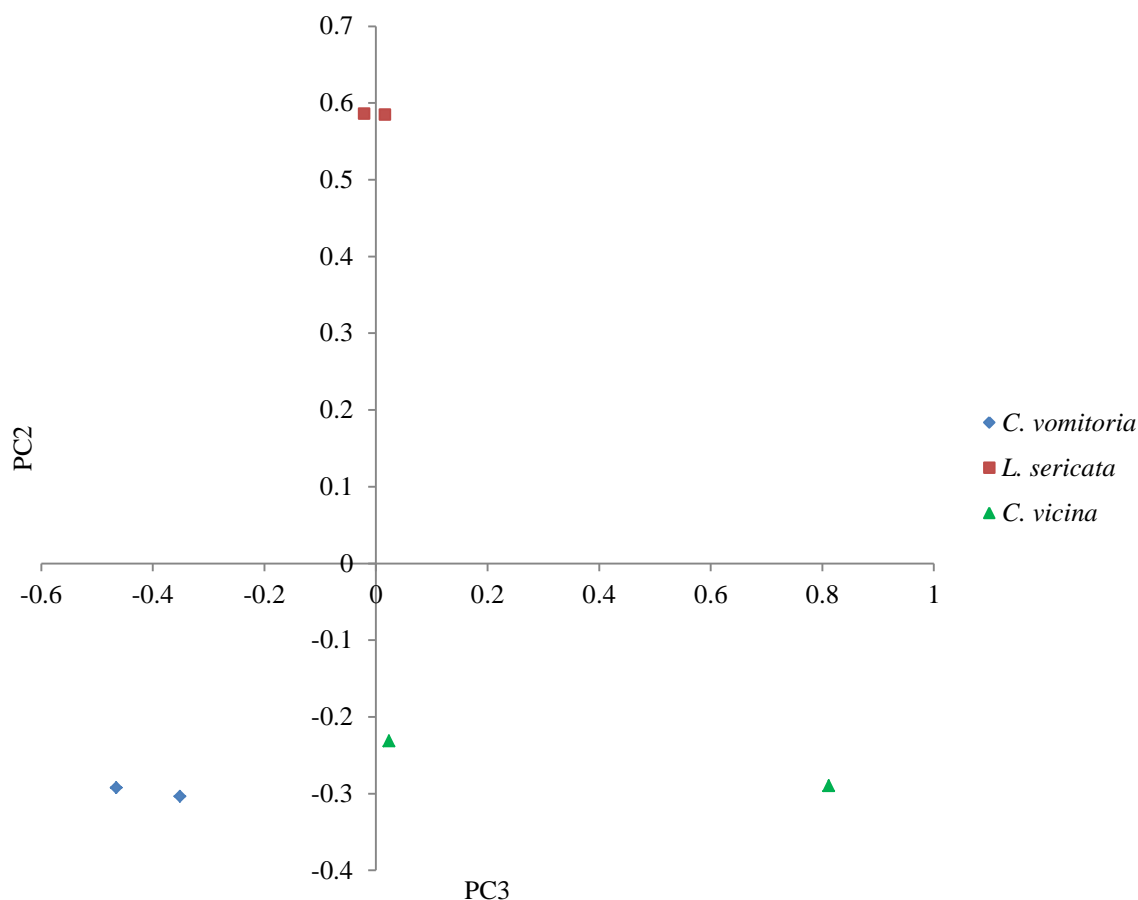
Figure 4.5: PCA plot of PC3 vs PC2 for the egg shells from *C. vomitoria*, *L. sericata* and *C. vicina* with all *n*-alkanes, alkenes and methyl branched hydrocarbons included in the PCA

The PCA plot (Figure 4.5) shows three distinct areas which correlate to the two repeats taken for each species. However, there is scatter within the two *C. vicina* repeats. Further PCA was subsequently applied to a dataset containing just the methyl branched alkanes and alkenes (Figure 4.6) and this yielded much tighter clustering for *C. vicina*, and the other two species remained in distinct spatial positions on the PCA plot.

PCA was carried out using five principal components, describing 99.9% of the variation within the dataset with the first three (PC1, PC2 and PC3) comprising 78.2%,

19.4% and 1.6% respectively. PC2 and PC3 were used to plot the relevant scores (see appendix 10 for PCA eigenvalues).
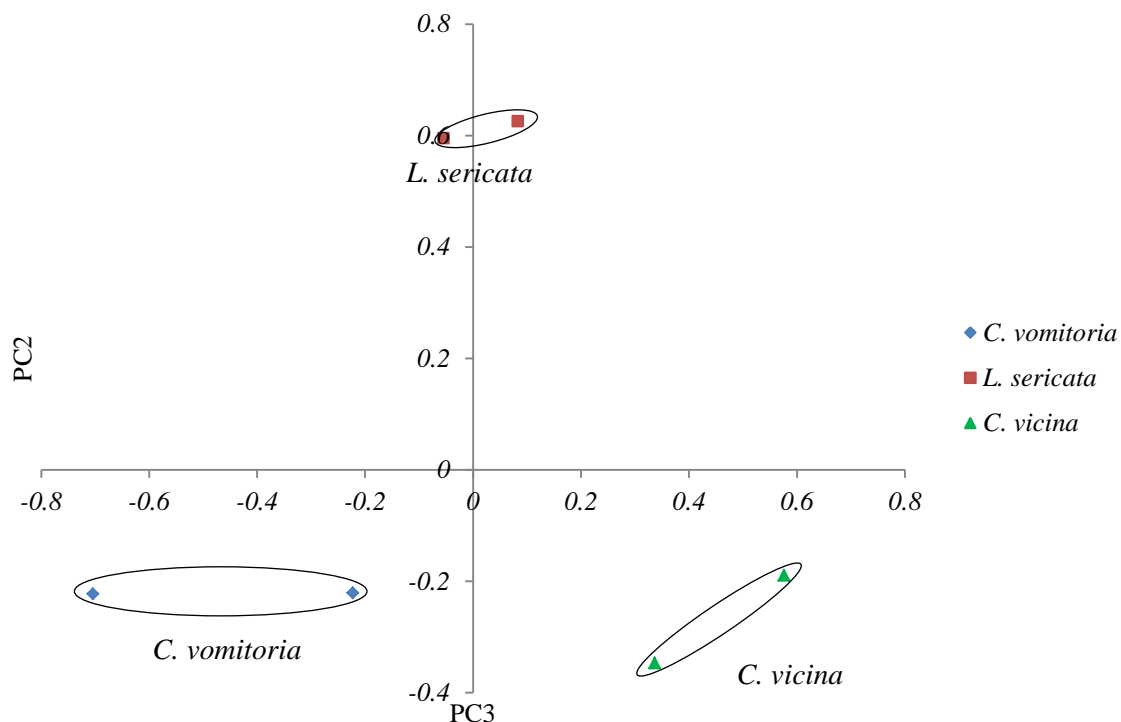
Figure 4.6: PCA plot of PC3 vs PC2 for the egg shells from *C. vomitoria, L. sericata* and *C. vicina* with just alkenes and methyl branched hydrocarbons included

Compounds that exhibit large scores will be the most significant in the changes seen in the PCA plot. The main compounds which have substantially large scores are the first C29:1 isomer (peak 10) and 9-MeC29:H (peak 14).

By combining GC-MS analysis with PCA, the identification of empty egg case can be distinguished from three forensically important blowflies. Tight clustering of repeats within PCA plots indicates little variation, signifying good experimental reliability has

been established. However, the two replicates for *C. vicina* did not group as well as the other two species, which could signify chemical changes occurring, but this is unexpected when dealing with identification extractions taken at the same age. The scatter was greatly reduced when a second PCA was carried out using only the alkenes and methyl branched alkanes, indicating that *n*-alkanes contain the most variation within the profile of *C. vicina*, and the variation is reduced when this class of hydrocarbons is excluded from analysis. Cuticular hydrocarbon studies carried out on ants have shown the *n*-alkanes are a function of environmental protection and vary within the ant profiles of the same nest-mates [13]. This demonstrated that although they are abundantly present on the cuticles, they had no role in nest-mate discrimination studies, as the *n*-alkane ratios could vary substantially within individuals from a single colony [14]. This could explain why the results are enhanced when the *n*-alkanes are removed from the PCA dataset, as the variation is removed. However, the removal of the *n*-alkanes from subsequent PCA still shows that chemical distinctions are present between the three species. The scatter seen could also be due to the small number of replicates used for this particular experiment. More replicates are required to ensure the results are accurate and conclusive.

When applying this technique to a crime scene, the analyst would perform PCA analysis on two dataset models, one with *n*-alkanes, alkenes and methyl branched alkanes and another with just methyl branched alkanes and alkenes. The results from both sets of statistical analysis could confirm the identification of *C. vicina* and distinguish between all three species but the latter would give the best results, with the tighter clustering. PCA analysis takes a matter of minutes to execute so performing PCA on two different datasets would lose little time in a criminal investigation.

Hydrocarbon analysis in combination with PCA allows results on species identity to be obtained within a short space of time once a model has been established and therefore has the potential to be a beneficial tool in the first step to aiding early PMI estimations. Current identification techniques require the use of a SEM for egg analysis, which involves a complex morphological examination by an experienced forensic entomologist or taxonomist. For empty egg cases, a SEM would also be required but it would be extremely difficult if not impossible to determine the species.

However, further work is still required to assess the robustness of the inter-specific variation in the compounds listed and this particular experiment needs to be repeated using more egg case samples to see if the scatter remains in the PCA plot for *C. vicina* using *n*-alkanes, alkenes and methyl branched alkanes. However, these preliminary results presented in this part of the chapter demonstrate that hydrocarbon analysis for species determination of egg cases is a technique that offers a promising alternative to current morphological methods currently used in the field.

4.3 Larvae

Larvae are the life stage which is most likely to be found at a crime scene and provide the most useful information in the estimation of the PMI. Therefore it is essential that the larvae are correctly identified. Many taxonomic keys have been published to allow for their identification [15].

Identification of blowfly larvae using morphological techniques is possible if done by an experienced entomologist, and if a suitable key is followed. The morphological traits used for larval identification are the mouthpiece (cephaloskeleton), spines and

anterior and posterior spiracles (Figure 4.7). However, mistakes can sometimes be made leading to misidentifications, which in turn can affect the timings for PMI estimations. These morphological traits are most visible in 3rd instar larvae and therefore this particular larval life stage are commonly used when applying morphological techniques and using one of the most detailed keys developed by Szpila [15]. However, early stage larvae in particular can be difficult to identify and in some cases DNA-based analysis [16–20] are the only techniques that can be successfully applied. Hence, currently rearing the larvae to adult flies to confirm the species identification is essential [15].
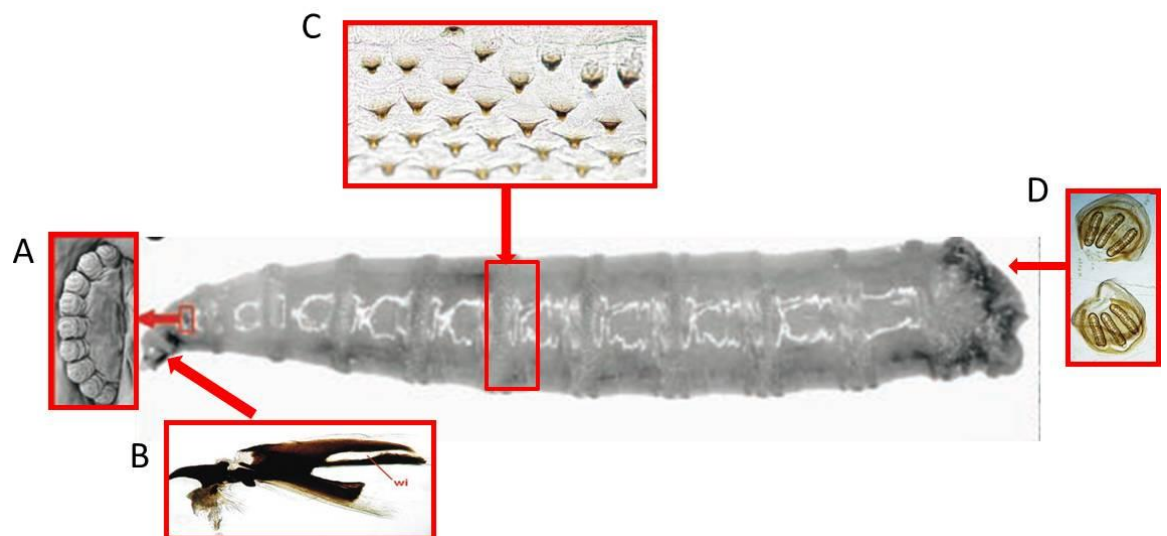
Figure 4.7: Larva of Calliphoridae showing areas of the anatomy used to identify the species in this life stage - A: Anterior spiracles, B: Mouthpiece (cephaloskeleton), C: Spines and D: Posterior spiracles). Image taken and adapted with kind permission from Springer Science and Business Media [21]

Hydrocarbon analysis is regarded as having an advantage over morphological identification techniques as it does not require larvae to be 3rd instar. It can be applied to 1st and 2nd instar larvae and still provide accurate results.

The 1st instar larvae are particularly difficult to identify morphologically due to their size. Therefore only results from this life stage shall be presented in the form of chromatograms and PCA.

4.3.1. Results and Discussion for larvae

GC-MS analysis:

The table below (Table 4.3) summarises the compounds used for PCA analysis for the three species, showing the number of hydrocarbons present according to the class of the compound for day 1 larvae only (Table 4.3).

Table 4.3: Hydrocarbon composition showing the number and percentage of *n*-alkanes, alkenes and methyl branched alkanes of each species for day 1 (1st instar) larvae only

	L. sericata	*%*	*C. vicina*	*%*	*C. vomitoria*	*%*
Alkanes	12	71	12	34	13	45
Alkenes	2	12	3	9	6	21
Methyl branched HC	3	18	20	57	10	34
Total HCs	**17**	**100**	**35**	**100**	**29**	**100**

The information given in Table 4.3 indicates that all three species hold chemically distinctive profiles once full peak identification has been established, especially when

looking at the number of methyl branched alkanes, which differs greatly between them all (18%. 57% and 34%).

Due to the life cycle timings differing for each species (all three species reared at the same temperature but develop at different rates) it is difficult to compile and align the data for PCA, but it can be done for the 1st instar larvae (Day 1- reared at 22 ˚C).

The three species of larvae exhibit low to high boiling point compounds which are a mixture of straight chain *n*-alkanes, alkenes, mono methyl and dimethyl branched alkanes (see Table 4.4 and Figure 4.8). The *n*-alkanes range from C18:H to C33:H. Although all three species exhibit a similar number of *n*-alkanes in the 1st instar larvae (day 1), the specific *n*-alkanes that are present differ. For example, C18:H is only present in quantifiable amounts in *L. sericata*. C31:H is only present in the two Calliphora species and C33:H is detectable in an adequate concentration only for *C. vomitoria*. C25:H was present for all three species but it was not included in subsequent analysis because it was co-eluting with a phthalate impurity (probably from the dishes the larvae were kept in) and therefore it was not possible to do a representative manual integration which could have led to misleading results.

One of the most noticeable differences in 1st instar larvae between the three species is the differing number of methyl branched alkanes and alkenes. *L. sericata* contains only three methyl branched alkanes and consequently exhibits a simple profile mainly consisting of *n*-alkanes. This species also has only two alkenes present in its profile; C25:1 (1.45%) and C31:1 (11.65%). The profile of *C. vomitoria* contain a higher number of methyl branched alkanes (ten) in comparison to *L. sericata*. The profile of *C. vomitoria* also displays the highest number of alkenes. The two C23:1 isomers observed are specific to this species. The profile of *C. vicina* contains a substantially

high number of methyl branched hydrocarbons, which dominate its chemical profile. There are also two alkenes specific to this species (C27:1 isomers, although only present in low percentages).

Table 4.4: List of the compounds extracted from day 1 (1st instar) larvae of *L. sericata*, *C. vomitoria* and *C. vicina,* along with the total percentage of each compound present, the percentage standard deviation and the Kovats Index to aid identification.

Peak number	Peak Identification	Kovats iu	*L. sericata* n=10 %	*C. vicina* n=10 %	*C. vomitoria* n=10 %
1	Octadecane	1800	4.53±0.84	0.00±0.00	0.00±0.00
2	Eicosene	1990	0.00±0.00	1.21±0.46	0.00±0.00
3	Eicosane	2000	7.84±1.71	0.75±0.31	1.93±0.79
4	Heneicosane	2100	0.00±0.00	0.92±0.42	1.76±0.67
5	Docosane	2200	7.91±1.86	1.33±0.65	1.67±0.59
6	2-Methyldocosane	2264	0.00±0.00	0.00±0.00	1.82±0.96
7	Tricosene	2271	0.00±0.00	0.00±0.00	3.66±1.04
8	Tricosene	2278	0.00±0.00	0.00±0.00	1.61±0.63
9	Tricosane	2300	4.61±2.37	2.07±0.95	8.80±2.93
10	9+11-Methyltricosane	2339	0.00±0.00	0.00±0.00	1.78±1.64
11	7-Methyltricosane	2342	0.00±0.00	0.00±0.00	0.85±0.38
12	Tetracosane	2400	7.79±2.01	1.88±0.87	1.78±0.70
13	2-Methyltetracosane	2464	0.00±0.00	8.51±3.27	7.45±8.29
14	Pentacosene	2471	1.45±0.87	0.00±0.00	2.17±0.91
15	Pentacosene	2479	0.00±0.00	0.00±0.00	1.67±0.44
16	9+11-Methylpentacosane	2536	1.91±1.32	6.71±2.66	10.59±15.03
17	9-Methylpentacosane	2538	0.00±0.00	1.69±0.73	0.00±0.00
18	7-Methylpentacosane	2544	2.19±0.78	1.01±0.52	0.00±0.00
19	5-Methylpentacosane	2552	0.00±0.00	0.78±0.40	0.00±0.00
20	3-Methylpentacosane	2574	0.00±0.00	1.79±0.79	1.82±2.32
21	Hexacosane	2600	8.07±2.20	2.51±1.02	2.39±1.29
22	12+14-Methylhexacosane	2636	0.00±0.00	1.04±0.44	0.00±0.00
23	2-Methylhexacosane	2665	0.00±0.00	0.00±0.00	5.50±5.31
24	*12, 22-diMethylhexacosane/12, 20-diMethylhexacosane	2666	3.74±1.79	25.70±18.29	0.00±0.00
25	Heptacosene	2676	0.00±0.00	1.34±0.60	0.00±0.00
26	Heptacosene	2679	0.00±0.00	0.39±0.24	0.00±0.00
27	Heptacosane	2700	7.81±4.77	9.93±7.65	10.78±8.93
28	11+13-Methylheptacosane	2735	0.00±0.00	5.62±2.47	5.10±7.55

|					
29	7-Methylheptacosane	2743	0.00±0.00	1.00±0.58	0.00±0.00
30	5-Methylheptacosane	2753	0.00±0.00	0.93±0.57	0.00±0.00
31	3-Methylheptacosane	2775	0.00±0.00	0.70±0.58	0.00±0.00
32	Octacosane	2800	7.36±2.10	1.61±0.84	1.36±1.05
33	2-Methyloctocosane	2871	1.21±0.58	5.79±4.77	2.00±1.61
34	Nonacosane	2900	5.70±2.70	3.39±2.40	5.62±3.64
35	11+13-Methylnonacosane	2936	0.00±0.00	1.86±1.94	2.01±1.80
36	9-Methylnonacosane	2941	0.00±0.00	0.69±0.66	0.00±0.00
37	7-Methylnonacosane	2947	0.00±0.00	0.85±0.83	0.00±0.00
38	5-Methylnonacosane	2956	0.00±0.00	0.25±0.16	0.00±0.00
39	3-Methylnonacosane	2977	0.00±0.00	0.62±0.78	0.00±0.00
40	Triacontane	3000	4.58±2.66	0.86±0.39	2.49±1.85
41	2-Methyltricontane	3067	0.00±0.00	0.99±0.78	0.00±0.00
42	Cholesterol + Hentriacontene	3070	0.00±0.00	0.00±0.00	2.50±1.28
43	Hentriacontene	3084	11.65±7.17	0.00±0.00	2.11±0.93
44	2,6/2,8/2,10-diMethyltriacontane	3097	0.00±0.00	0.55±0.63	0.00±0.00
45	Hentriacontane	3100	5.10±2.23	1.86±1.08	4.13±2.39
46	Dotriacontane	3200	6.53±2.34	2.89±1.41	2.80±1.52
47	Tritriacontane	3300	0.00±0.00	0.00±0.00	1.87±1.32

[1]Double bond positions determined for adult flies only

[2]Tentative identification based on Kovats Index values and match with NIST08 Library database

*Co-eluted with Heptacosene in immature larval stage of *C. vicina*

ND Not Detected

For a table of all compounds extracted from the larvae of *L. sericata*, *C. vicina* and *C. vomitoria* over all instars, see chapter 5, section 5.3.1.

The first shaded area in Figure 4.8 highlights 2-MeC24:H (peak 13, Table 4.4) which is present in a substantial concentration for the two Calliphora species (8.60% for *C. vicina* and 7.37% for *C. vomitoria*) but it is not observed in the profile of *L. sericata*.

The second highlighted area shows that 9+11-MeC25:H (peak 16, Table 4.4) peak which is present in the profile of all three species but at varying concentrations, with *C.*

vomitoria yielding the highest concentration and *L. sericata* displaying a significantly low concentration for this particular peak.

The third shaded region in Figure 4.8 focuses on a group of branched methyl hexacosane peaks which differ for the three species. The compound 12+14-MeC26:H (peak 22, Table 4.4) are specific to the profile of *C. vicina* but in a low concentration (1.45%). This compound could therefore be used to distinguish between these three species in this immature larval stage. The second peak highlighted in this shaded area are two co-eluting compounds; 12,20+12,22-DimeC26:H (peak 23, Table 4.4), which are observed in the profile of *L. sericata* (3.74%) but in a considerably lower concentration than *C. vicina* (25.97%). This compound is not observed in the profile of *C. vomitoria,* but in contrast, 2-MeC26:H (peak 23, Table 4.4) is specific to this species (5.04%).

The final shaded area in Figure 4.8 highlights 11+13-MeC27H (peak 27, Table 4.4) in the profiles of the two Calliphora species in similar percentages, but this peak is not present in the profile of *L. sericata*.

Since *C. vicina* and *C. vomitoria* are members of the same genus (Calliphora), it would be expected that they share more chemical similarities in comparison to the hydrocarbon profile of *L. sericata*. Figure 4.8 confirms this, with *L. sericata* displaying the most chemically different profile of the three species. *L. sericata* has a relatively simple hydrocarbon profile, dominated by *n*-alkanes, with only a small amount of alkenes and methyl branched hydrocarbons observed. *C. vicina* and *C. vomitoria* share similar hydrocarbon profiles but there are distinctive features allowing for the two to be differentiated. Firstly, the peak ratios vary considerably (e.g. for peak number 23, 25% vs 5%) which is a substantial difference when trying to identify the two species using

GC-MS analysis alone and secondly, the hydrocarbon compositions within the two species differ greatly, as previously discussed.

Therefore all three larvae species exhibit distinctive hydrocarbon profiles as seen in the GC chromatograms (Figure 4.8), with several prominent features making identification relatively simple.
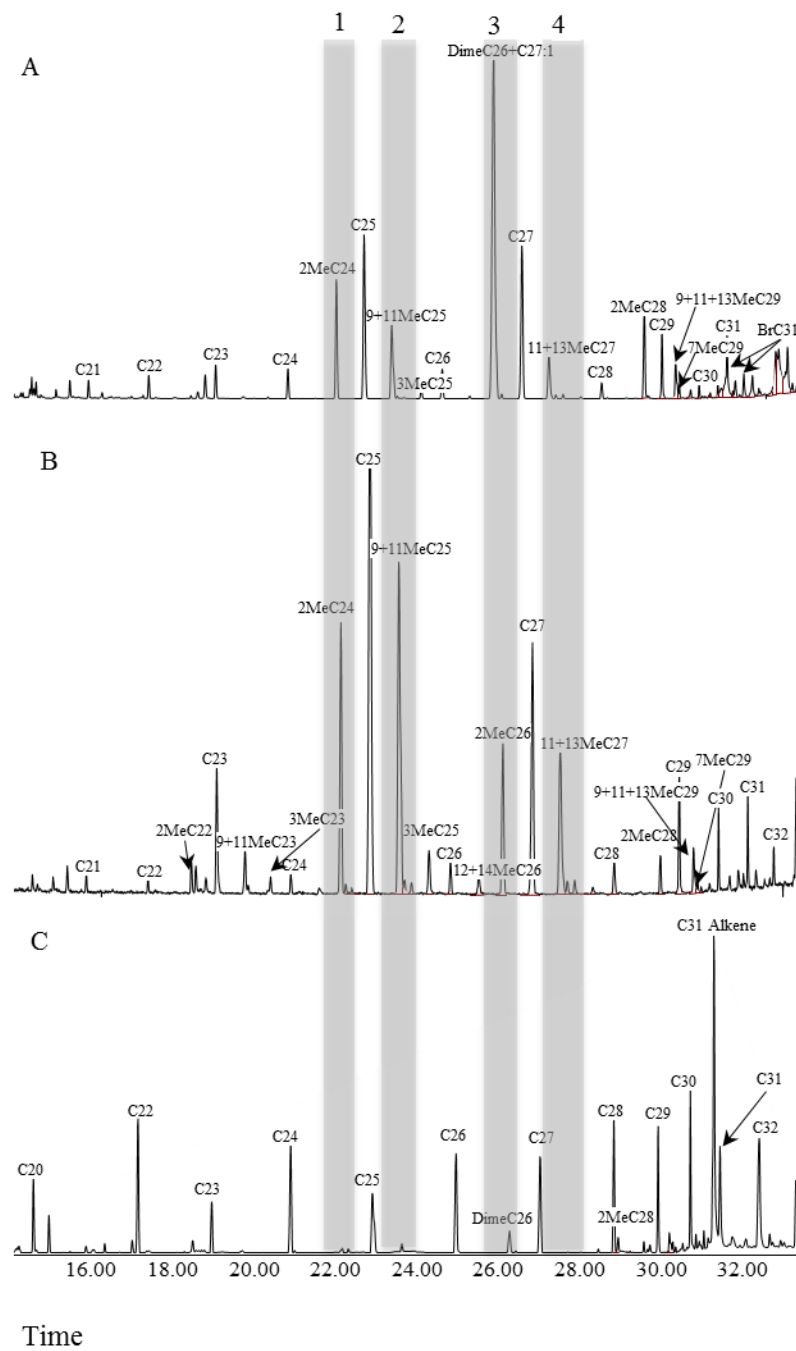
Figure 4.8: GC chromatograms showing the Day1 larvae hydrocarbon profiles of three blowfly species,

A: *C. vicina*, B: *C. vomitoria*, C: *L. sericata*. Shaded bars illustrate specific areas of interest

PCA:

Although the hydrocarbon profiles of the larvae appears to hold more individual characteristics than the egg shell cases, statistical analysis is still required to provide further quantitative identification. PCA was applied to the dataset, using all three classes of hydrocarbons. Chain lengths ranging from C18:H to C33:H were used and all three species contained a similar number of *n*-alkanes. PCA was carried out using six principal components, describing 97.8% of the variation within the dataset with the first three principal components comprising 46.9%, 26.1% and 19.8% respectively. PC2 and PC3 were used to plot the relevant scores (see appendix 11 for PCA eigenvalues).

As illustrated in Figure 4.9, there were significant differences in the *n*-alkane concentrations as well as the methyl branched compounds that each species exhibited, resulting in a PCA plot showing three distinct clusters which represent the three blowfly species.

.
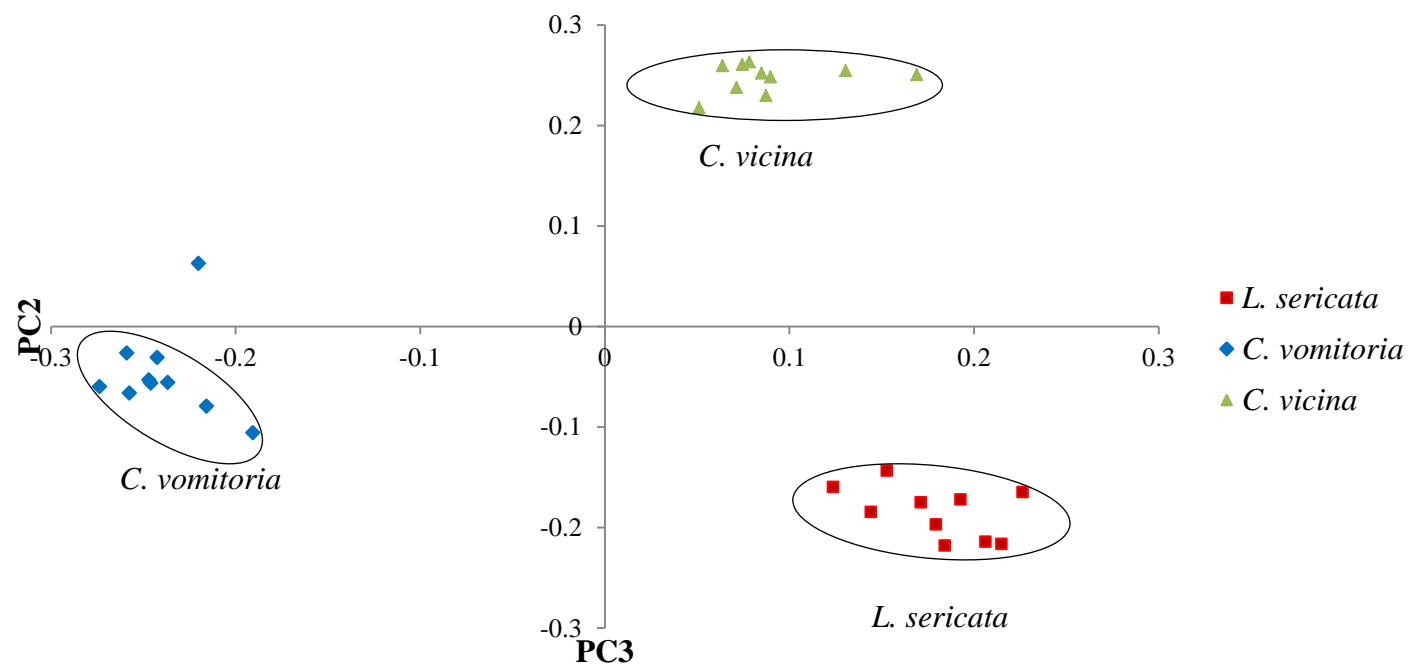
Figure 4.9: PCA plot of PC2 vs PC3 loadings for Day 1 (1st instar) larvae from *C. vomitoria, L. sericata* and *C. vicina* using *n*-alkanes and methyl branched hydrocarbons

The main compounds which have substantial scores are the isomers 12,22-DimeC26:H/12,20-DimeC26:H and C31:1. The two DimeC26:H isomers are present in a considerably large percentage in the profile of *C. vicina* (25.97%, see chromatogram A, Figure 4.7) but this could be due to the co-elution of C27:1 in a small percentage during the early stages of larvae. C31:1 is present in a much higher percentage for *L. sericata* (11.65%) in comparison the two Calliphora species (not observed for *C. vicina* and only 2.01% in the profile of *C. vomitoria*.)

The larvae results presented in this chapter only presented hydrocarbons used for PCA analysis. The whole larvae profile displayed a greater number of compounds. However, many of the volatile low boiling point hydrocarbons were excluded due to being more variable and fluctuating throughout the larvae developmental period.

Results presented for the identification of larvae were taken from Day 1 extractions. The reasoning for only focusing the research on this age was due to difficulty compiling the datasets when running PCA analysis because the three species developed at different rates at the experimental temperature of 22 ˚C. However, this age is known to be the most difficult life stage when using current morphological identification techniques and the results clearly show that species identification can be obtained from 1st instar larvae using hydrocarbon analysis when combined with GC-MS and PCA. Another advantage to this technique is the speed in which identification can be achieved, as it does not require the larvae to be reared to third instar or adult flies, therefore greatly reducing the time required to confirm identification.

Results presented in this section of the chapter show hydrocarbon analysis to be a promising identification tool which could be utilised in the field of forensic entomology. Although it is possible for blowfly larvae to be correctly identified by an expert in taxonomy, this technique not only complements the current morphological identifications, but it shows potential to be applied to species such as Sarcophagidae. It is still not possible to gain confident identification as to species in the larval stage of this family without conformation of rearing them to adults, which cause delays in criminal investigations [1,22].

4.4 Puparia

The presence of fly puparia at a crime scene can also be used to give PMI estimations as well as give toxicological information [23]. Since this life stage represent the longest developmental life stage of the life cycle (approximetaly 50% [24]), accurately ageing them would be beneficial, but as with the other life stages, in order to do this the identity of any collected puparia must first be established [25]. The appearance of blowfly puparia is morphologically very similar from species to species [23]. To establish a correct identification, current techniques used are microscopy to enable the morphological features to be visualised [23,25–28] or more recently DNA based methods [1,20]. The case of the puparium is the hardened cuticle of the third instar larvae, in which the pupa is formed, hence it consists of the anterior and posterior spiracles, spines (Figure 4.10) and the mouthpart, which can be removed from the anterior region of the case.
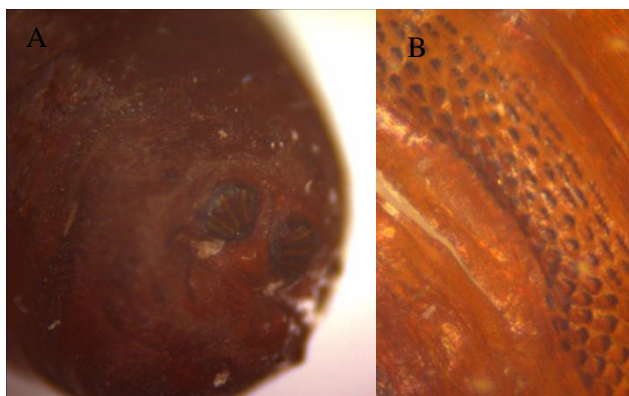
Figure 4.10: Image taken at x4.7 magnification showing the posterior spiracles (A) and spines (B) of a *C. vomitoria* puparium.

However, all these remaining features can be more difficult to use for indentification purposes due to the nature of the case and require an experienced entomologist to establish identification down to species level using SEM. New developments in DNA techniques are being utilised [23], but both techniques ideally require the insect to be reared to adult flies to confirm species identification. Hydrocarbon analysis could offer a rapid and complementary method to the current identification techniques used in the field.

4.4.1 Results and Discussion for Puparia

GC-MS analysis:

Results presented in this thesis on this life stage were obtained from two blowfly species, *L. sericata* and *C. vicina*. Straight chain *n*-alkanes made up the majority of the hydrocarbons present (*C. vicina*, 63% and *L. sericata*, 62%) in both species.

Pentacosane was again found to be co-eluting with a phthalate impurity and therefore it had to be excluded from the final PCA for the results.

Table 4.5 summarises the number of hydrocarbons present according to the class of the hydrocarbon for the puparia of *C. vicina* and *L. sericata*.

Table 4.5: Hydrocarbon composition of puparia, showing the number and percentage of *n*-alkanes, alkenes and methyl branched hydrocarbons each species has within its profile for day 1 pupae only

	L. sericata	*%*	*C. vicina*	*%*
Alkanes	16	62	15	63
Alkenes	6	23	6	25
Methyl branched HC	4	15	3	13
Total HCs	**26**	**100**	**24**	**100**

The chain length for the *n*-alkanes in both species ranges from C16:H to C31:H. Both species have the same number of alkenes while *L. sericata* has one more methyl branched alkane in its chemical profile. Although the two species produce a very similar hydrocarbon profile, the relative abundance of different *n*-alkanes alone varies considerably (Table 4.6).

Table 4.6: List of the compounds extracted and used for subsequent PCA analysis from the puparia of *L. sericata* and *C. vicina,* along with the total percentage of each compound present and the percentage standard deviation, and significant *t*-test result (Peak numbers relate to peaks in Figure 4.11)

Peak no.	Peak Identification	*L. sericata* n=10 %	*C. vicina* n=10 %	*t*-**test**
1	Octadecane	1.83±0.63	8.59±1.85	*
2	Nonadecane	ND	0.79±0.51	Not tested
3	Eicosane	1.62±0.62	4.63±0.96	*
4	Heneicosane	1.35±0.30	2.65±0.80	*
5	Docosane	2.04±0.47	3.66±1.09	*
6	Tricosane	2.56±0.54	2.83±1.22	
7	Tetracosane	2.97±0.54	2.56±0.80	
8	Hexacosane	5.11±1.10	3.97±1.84	*
9	Heptacosane	7.07±3.33	34.09±15.08	*
10	Octacosane	4.89±1.59	5.76±2.38	
11	Nonacosane	39.51±13.07	24.53±10.79	
12	Triacontane	6.67±2.01	ND	Not tested
13	Hentriacontane	24.37±5.71	5.94±2.19	*

*Significant at p < 0.05

For a table of all compounds extracted from the puparia of *L. sericata* and *C. vicina*, see chapter 6, section 6.2.1.

C. vicina yields a higher percentage for the shorter chain length *n*-alkanes (C18:H to C22:H). For example, Peak 1 in Table 4.6 shows the percentage of C18:H is more than three times higher in *C. vicina*. The percentages are similar for C23:H and C24:H, with *L. sericata* displaying a higher value for C26:H. C27:H yields a substantially large percentage in *C. vicina* and is the most dominant hydrocarbon present in its profile (34.09%). The statistical analysis of a *t*-test indicates a large number of the hydrocarbons are significantly different between the two species.

C. vicina exhibits C28:H in a higher percentage than *L. sericata*. However, there is then a noticeable change in the high boiling point *n*-alkanes as *L. sericata* produces these compounds in a substantially higher concentration. The dominating hydrocarbon in the profile of *L. sericata* is C29:H (39.51%).

As discussed, the hydrocarbons present are very similar between the two species, however, when the two chromatograms are directly compared (Figure 4.11), some significant quantitative differences can be observed. Figure 4.11 highlights a few specific areas of interest within the two profiles. The first shaded bar shows a group of three compounds: C26:H, a 3MeC26:H and C27:H. These occur in *L. sericata* in equal proportions, however C27:H is observed in a substantially higher quantity in *C. vicina* puparia in contrast to *L. sericata* puparia.

The second area highlighted shows a group of non-hydrocarbons followed by two peaks in *C. vicina*, which are C31:1 and C31:H, with C31:1 being the most abundant. *L. sericata* shows a C30:H, followed by a group of peaks, which consist of a non-hydrocarbon, C31:1 and C31:H, with C31:H being the most abundant. *C. vicina* does not exhibit C30:H in its profile above a peak area of 0.5%.
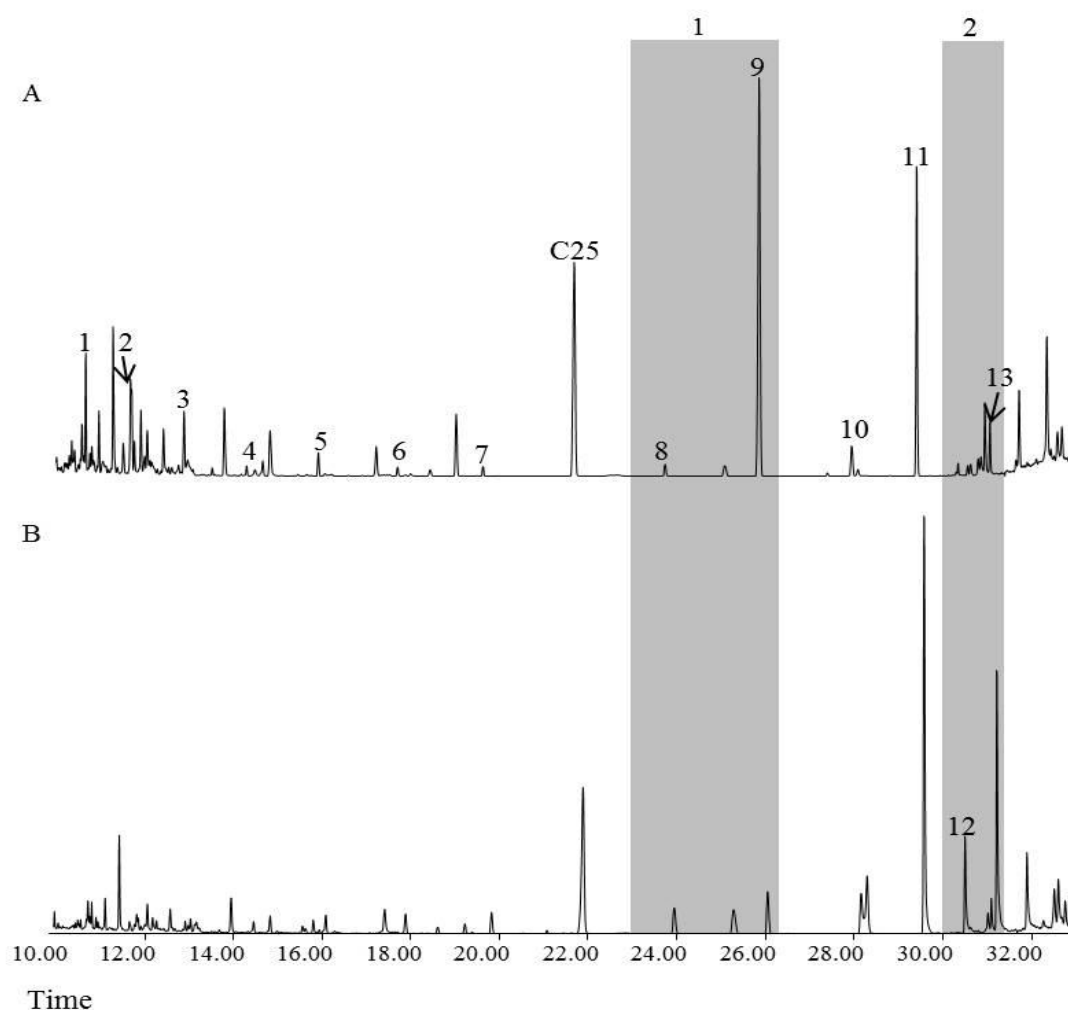
Figure 4.11: GC chromatograms showing the Day1 puparia hydrocarbon profiles of two blowfly species, *C. vicina* (A) and *L. sericata* (B). The shaded bars illustrate specific areas of interest

Although the case of the puparia is the hardened skin of the 3rd instar larvae, the hydrocarbon profile does not match that of a 3rd instar larvae, as is highlighted by the chromatogram overlay in Figure 4.12. The circled areas of the chromatogram (one of which has been enlarged) (Figure 4.12) represents the absence of several methyl branched hydrocarbons (11+13-, 7-, 5- and 3-MeC27:H) as the larvae enters the puparial life stage.
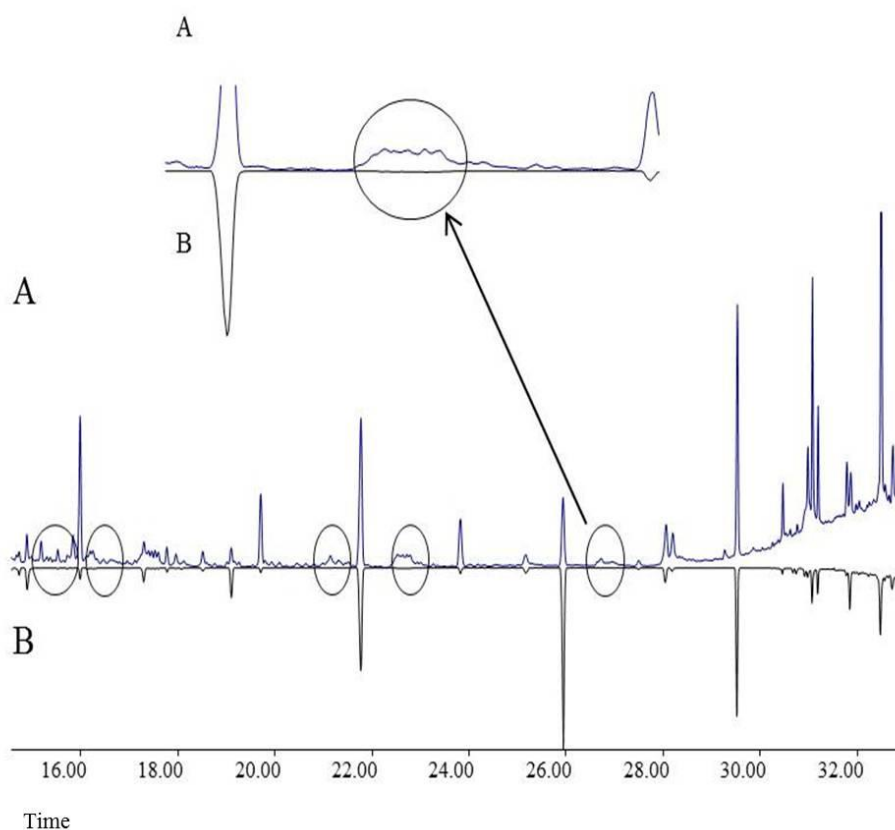
Figure 4.12: GC chromatogram overlay of *C. vicina* 3rd instar larvae (A) and Day 1 puparium (B), with the circled areas highlighting peaks that are observed in larvae but not pupae

PCA:

The two species show some substantial differences when looking at their chemical profile so it is expected that they would be highly distinguishable when statistical analysis is applied, as is displayed in Figure 4.13. PCA was applied to a dataset containing the *n*-alkanes only from the two species as the chromatograms contain a lot of background noise relative to the peak intensity and the methyl branched alkanes and alkenes were difficult to identify using the mass spectra.

The PCA was carried out using six principal components, describing 99.9% of the variation within the dataset with the first three components comprising 73.3%, 25.5% and 0.5%. PC1 and PC2 were used to plot the relevant scores (see appendix 12 for PCA eigenvalues).
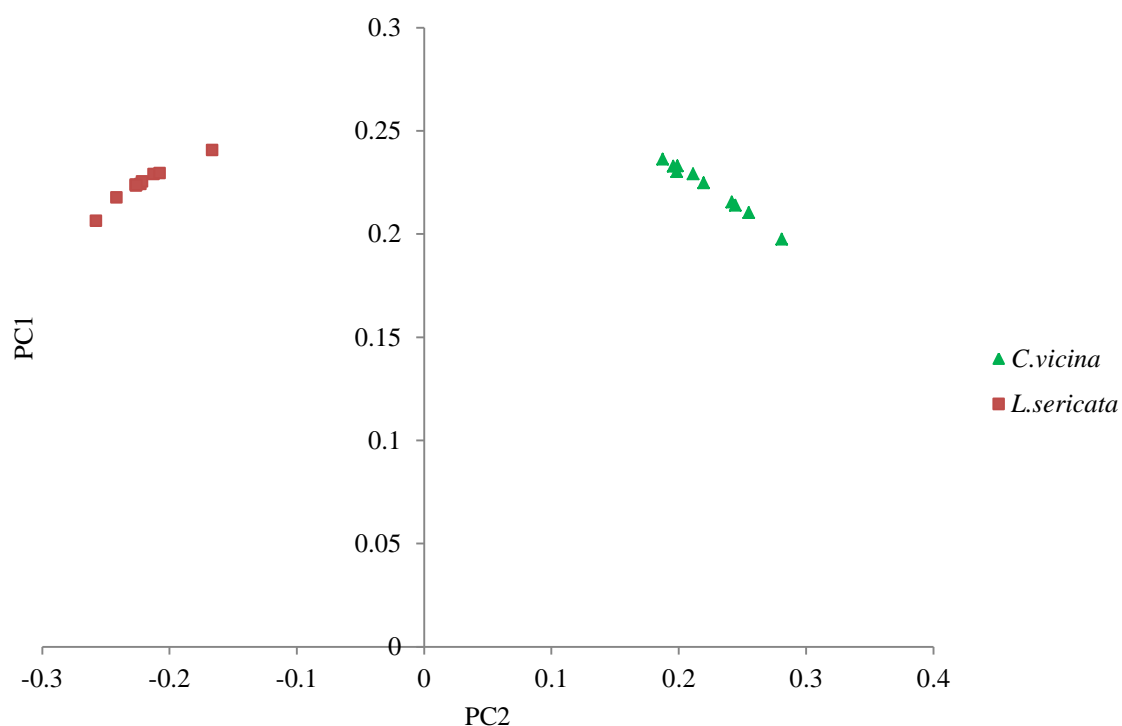
Figure 4.13: PCA plot of PC2 vs PC1 Day 1 puparia from *L. sericata* and *C. vicina* using *n*-alkanes

L. sericata and *C. vicina* display very different spatial positioning on the scatter plot, allowing for confident species identification. The compounds exhibiting the highest loading values are C27:H and C31:H.

Ye and co-workers [29] carried out a cuticular hydrocarbon study on the pupal exuviae of six necrophagous flies for taxonomic differentiation. GC-MS analysis was used to analyse the extracted hydrocarbons and one of the species used was *L. sericata*. In general the methyl branched compounds they detected in this species agreed with those presented in this chapter. However, not all were used for subsequent PCA due to peak areas dropping below the threshold of 0.5%. Ye and colleagues noted that no alkenes were present in the profile of *L. sericata* which was not consistent with results presented in section 4.4.1 where three alkenes were detected. However, the *n*-alkanes gave enough information to distinguish between the two species presented in this chapter using PCA.

Puparia yield significantly fewer hydrocarbons in their profile than when they are in the larval stage. Notably fewer methyl branched alkanes are present and the majority of the profile comprises *n*-alkanes, with the heavier molecular weight hydrocarbons (in particular C27:H, C29:H and C31:H) significantly dominating over the lower molecular weight *n*-alkanes. Methyl branched hydrocarbons (and alkenes) are believed to reduce the overall melting point and they are therefore required to keep the cutiucular surface flexible [30]. If the abundance of long chain *n*-alkanes is observed, it is likely the number of methyl branched alkanes/alkenes will also increase. However, puparia are rigid and do not require the need for a soft or flexible cuticle, which could explain why a simple profile made up of mainly straight chain *n*-alkanes are observed.

The scores from the PCA revealed large values for C27:H and C31:H which coincides with the data presented in Table 4.6. The *t*-test was applied to all of the compounds (with exception to C19:H and C30:H) and the results showed them to all be significantly different between the two species apart from C27:H dominates the profile

of *C. vicina*, whilst C31:H is present in a substantially higher percentage in the profile of *L. sericata*.

Results presented on this life stage show a relatively simple means of species identification. This technique may therefore also be highly advantageous with Sarcophagidae species which are notoriously difficult to identify in the larval stage, making them even more challenging to identify as puparia.

4.5 Puparial cases

Puparial cases are often the only entomological evidence remaining in criminal investigations involving highly decomposed remains [31]. Many studies have been published using larvae and pupal stages for PMI estimations [18,32–35], but much less research is published on puparial cases and currently they are rarely used with any great significance in criminal investigations, due to the difficulty in identifying and ageing them. However, in the past decade studies have suggested that invaluable information could be extracted from these puparial cases and hence new identification methods are being developed [29,31].

Puparial cases are the empty shells of the last layer of the larval stage (post-feeding). When an adult fly emerges from the case it will emerge from the mouth end, usually leaving the rest of the case intact. Figure 4.14 shows the image of the puparial cases for *L. sericata*, *C. vomitoria* and *C. vicina*. To correctly identify them, the same morphological features used for the pupae are examined (posterior spiracles, spines – see section 4.4). However, with empty cases, these morphological features are often destroyed during emergence of the adult fly.
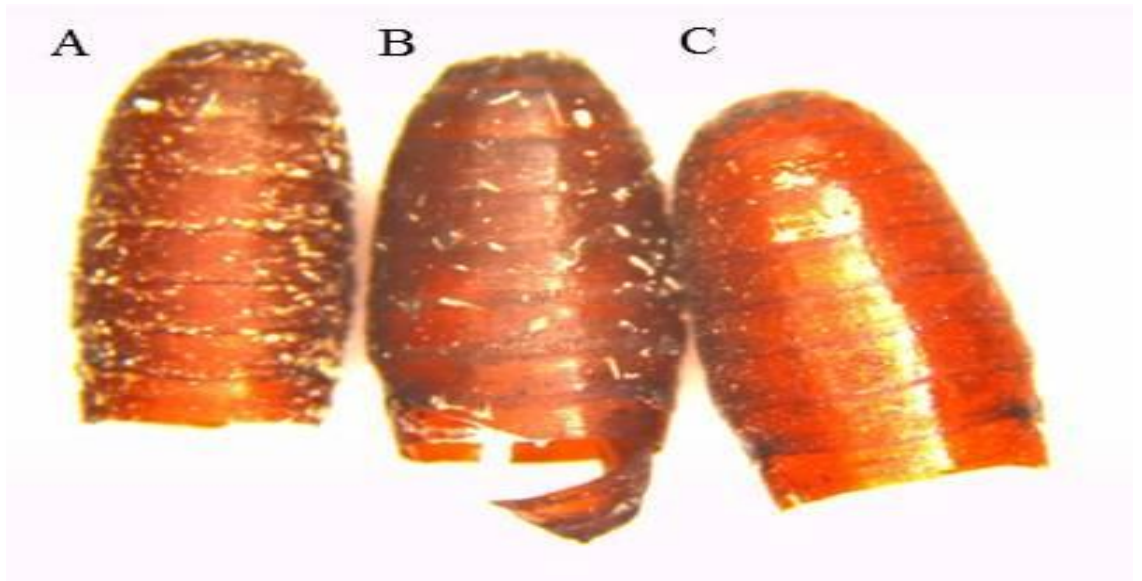
Figure 4.14: Image of *L. sericata* (A), *C. vomitoria* (B) and *C vicina* (C) puparial cases

The mouth piece (Figure 4.15) can also be found in some cases and can be used for identification in the same manner as it is used for larval identification.

Figure 4.15: Image of *C. vomitoria* mouth pieces inside the puparial case.

Hydrocarbon analysis can offer an accurate identification of puparial cases with the main advantage that species identification can not only be established on young puparial cases, but also on old cases (due to the stability of hydrocarbons) that have been crushed or have deteriorated due to weathering, making the usual morphological characteristics difficult or impossible to visualise under a microscope.

3.5.1 Results and Discussion for puparial cases

GC-MS analysis:

All three species yield very distinctive hydrocarbon profiles. The table below shows the number of hydrocarbons present (within the three classes) for each species:

Table 4.7: Hydrocarbon composition of puparial cases, showing the number and percentage of *n*-alkanes, alkenes and methyl branched hydrocarbons each species has within its profile for day 1 puparial cases only

	L. sericata	*%*	*C. vicina*	*%*	*C. vomitoria*	*%*
Alkanes	9	45	6	21	8	24
Alkenes	3	15	2	7	2	6
Methyl branched HC	8	40	21	72	24	71
Total HC's	**20**	**100**	**29**	**100**	**34**	**100**

C. vicina and *C. vomitoria* are more chemically similar in relation to their hydrocarbon compositions but they can still be easily distinguished when looking at their GC profiles. *L. sericata* contains the fewest compounds in its profile and displays a relatively simple hydrocarbon composition when compared to the other two species.

All three species exhibit mainly high boiling point hydrocarbons, closely resembling the profile of an adult fly. They contain a mixture of straight chain *n*-alkanes, alkenes and mono-, di- and tri-methyl branched alkanes. The *n*-alkane chain lengths range from C23:H to C33:H. The compound yielding the highest concentration is C27:H for all three species, closely followed by C29:H. *C. vomitoria* is the only species with a high concentration (9.40%) of C23:H, which is absent from the other two species, and could be a good identification trait. C25:H is present in a substantially higher concentration in

the profile of *C. vomitoria* (19.45%) when compared to *L. sericata* (4.43%) and *C. vicina* (4.02%). C31:H is produced in a large concentration for *L. sericata* (10.23%) compared to the two Calliphora species, where it is displayed in trace amounts (less than 0.5% for *C. vomitoria*), which could be used as an identification characteristic to distinguish *L. sericata* from *C. vicina* and *C. vomitoria*.

Figure 4.16 shows the GC comparison of the hydrocarbon profiles for the three species. It clearly shows three fingerprint profiles, which can be distinguished even just by observing the different composition of the peaks, without knowing the identity of them.

The shaded bars show areas of contrast within the GC traces. Bar 1 highlights two peaks in *C. vomitoria*, identified as being a 2-MeC26:H and C27:1. These compounds are both present for *C. vicina* but in a much lower concentration (peak area less than 0.5%) and the compounds are not present at all for *L. sericata*.

Bar 2 shows a group of methyl branched hydrocarbons for *C. vicina* (co-eluting 13+9-MeC27:H and 7-MeC27:H), both of which are present in *L. sericata* and *C. vomitoria* but in significantly lower percentages.

Bar 3 shows a large group of peaks for the three species. These peaks are identified as 2-MeC28:H, C29:1, C29:H, 9+11-MeC29:H, 7-MeC29:H, 5-MeC29:H and 3-MeC29:H. All these peaks are present in all three species but in varying percentages. The only distinction in the peaks between the species is a 3,7-DimeC29:H that co-elutes with C29:H for *C. vomitoria*. *C. vomitoria* shows a higher concentration of C29:1 than 2-MeC28:H, whereas *C. vicina* displays a relatively even concentration between the two compounds, with *L. sericata* yielding a significantly lower concentration of both compounds. For the *L. sericata* and *C. vicina* species, C29:H is

observed in a very high concentration whereas it is substantially lower in the profile of *C. vomitoria*. *C. vicina* has a higher concentration of the co-eluting 9+11-MeC29:H peak when compared to the 7-MeC29:H and the following 5-MeC29:H and 3-MeC29:H compounds. However, *C. vomitoria* exhibits a higher concentration of the 7-MeC29:H compared to the other methyl branched compounds. *L. sericata* has a much lower concentration overall in this group of methyl branched compounds when compared to the two Calliphora species with the 11+9-MeC29:H the most prominent alkane of the group.
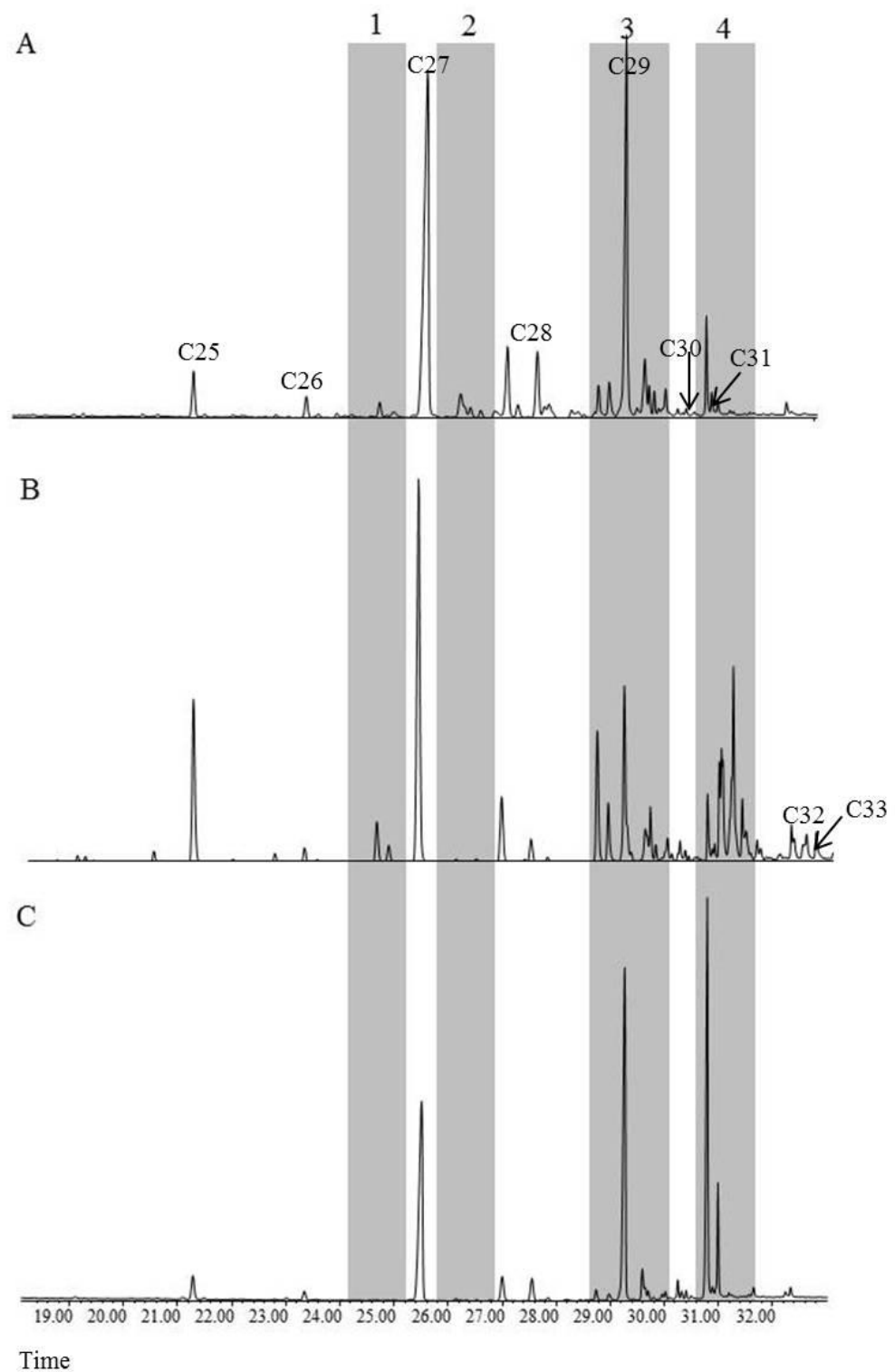
Figure 4.16: GC chromatograms showing week 1 puparial case hydrocarbon profiles of three blowfly

species, A: *C. vicina*, B: *C. vomitoria*, C: *L. sericata*. Shaded bars illustrate specific areas of contrast

Finally, bar 4 focuses on another group of peaks at the end of the chromatogram. It can clearly be seen that this group of compounds differ greatly within the three species, especially in the profile of *C. vomitoria*. *C. vicina* and *L. sericata* contain the same three compounds in this particular highlighted region of the chromatogram, consisting of a non-hydrocarbon which is the most prominent peak in both species. This compound is then followed by C31:1 and C31:H. In the profile of *C. vicina*, the alkene is present in a greater concentration that the *n*-alkane. The peak ratio of *n*-alkane vs alkene for *L. sericata* however is the opposite of this and the alkene is barely visible. The puparial cases of *C. vomitoria* contains a very different group of hydrocarbons in this region, consisting of 2-MeC30:H, 13+15-MeC31:H, 7+9-MeC31:H, a co-eluting peak consisting of four complex methyl branched compounds (11,15-DimeC31:H, 9,15-DimeC31:H, 7,15-MeC31:H and 4,6,19-TrimeC30:H - the most prominent peak in the group highlighted) and two subsequent unknown co-eluting methyl branch hydrocarbons.

PCA:

The characteristic profiles that all three species exhibit in the hydrocarbon composition and peak area ratios reveal distinguishable results when statistical analysis is applied, as shown in Figure 4.17

Table 4.8 lists the *n*-alkanes used for PCA along with the total percentage of each compound and the percentage standard deviation.

Table 4.8: List of the compounds extracted and used for subsequent PCA analysis from the empty puparial cases of *L. sericata* and *C. vicina,* along with the total percentage of each compound present, the percentage standard deviation

Peak Identification	*L. sericata* *n*=10 %	*C. vicina* *n*=10 %	*C. vomitoria* *n*=10 %
Tricosane	ND	ND	9.40±3.20
Pentacosane	4.43±2.13	4.02±0.63	19.45±6.20
Hexacosane	1.59±0.80	2.04±0.36	2.26±0.61
Heptacosane	38.48±18.57	53.64±7.98	44.55±13.73
Octacosane	3.39±1.47	6.23±0.84	3.77±1.09
Nonacosane	38.13±14.24	32.51±5.12	16.32±4.42
Triacontane	1.50±0.58	0.52±0.13	ND
Hentriacontane	10.23±4.12	0.69±0.19	ND
Dotriacontane	1.19±0.47	0.25±0.07	2.25±0.43
Tritriacontane	1.06±0.45	0.11±0.04	2.01±0.88

For a table of all compounds extracted from the empty puparial cases of *L. sericata*, *C. vicina* and *C. vomitoria*, see chapter 6, section 6.3.1.

PCA was carried out using six principal components, describing 99.99% of the variation within the dataset with the first three principal components comprising 89.8%, 8.8% and 1.2%. PC2 and PC3 were used to plot the relevant scores (see appendix 13 for PCA eigenvalues). All three species display different spatial positioning on the scatter plot, allowing for accurate species identification from the puparial cases.
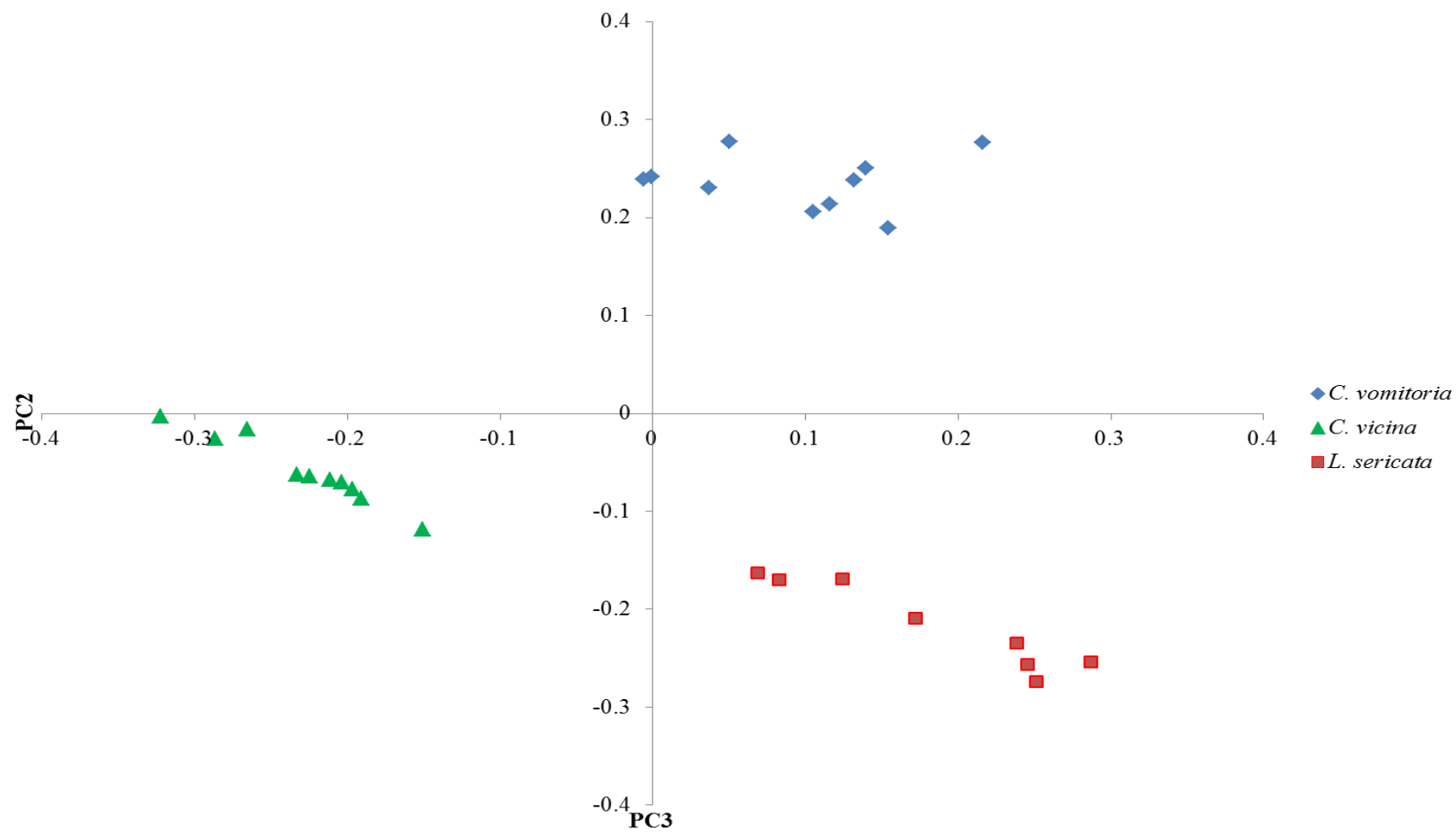
Figure 4.17: PCA plot of PC3 vs PC2 week 1 puparial cases from *L. sericata*, *C. vicina* and *C. vomitoria* using *n*-alkanes

Two samples were removed from the dataset of *L. sericata*. One replicate was removed because of instrumentation error (removed before PCA was run) and another was an outlier (removed after initial PCA was obtained).

Due to the complex methyl branched compounds present in the profiles of the three species puparial cases, only *n*-alkanes were used for PCA. The PCA plot in Figure 4.17 clearly shows sufficient clustering without the need of methyl branched or alkenes to be included in the dataset.

The highest score values belong to C25:H (most abundant in *C. vomitoria*) and C31:H (most abundant in *L. sericata*), showing that these two *n*-alkanes are the most influential when distinguishing between the three species.

4.5.2 Blind Puparial Cases Results and Discussion

Blind samples were analysed which had been extracted by a colleague (chapter 3, section 3.2.1: *Puparial cases*). This experiment was designed to test the methodology and establish if indeed the profile of the case can be distinguished between *L. sericata*, *C. vicina* and *C. vomitoria*, using hydrocarbon analysis.

Initial examination involved going through the blind samples individually (24 samples) and noting down what species their profiles matched with. From examination of the GC profiles alone, all blind samples were correctly identified as being either *C. vomitoria* or *C. vicina*. Full peak identification was then carried out on the blind samples and matched with the chemical profiles of either *C. vicina* or *C. vomitoria* (it was quickly established that none of the blind samples were *L. sericata*). Figure 4.18

and Figure 4.19 shows the GC traces of two different blind samples mirrored with the expected species profile.
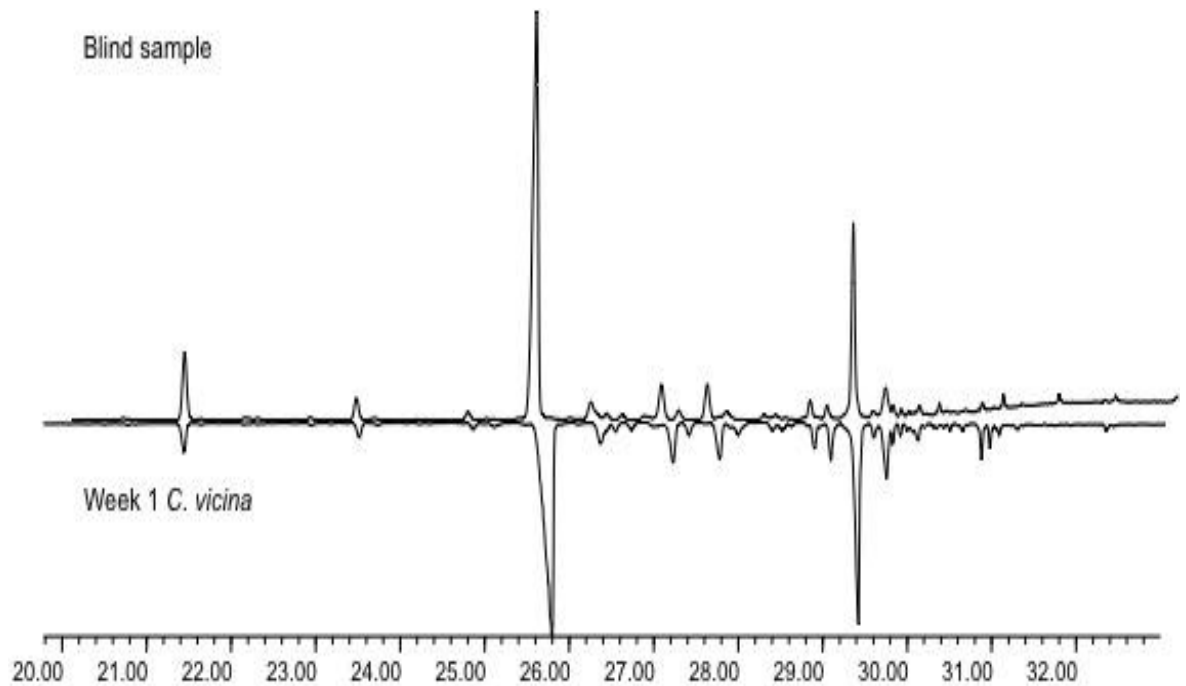
Figure 4.18: Mirrored GC chromatograms of the blind puparial case (A) and a known *C. vicina* week 1 puparial case (B)

Figure 4.18 shows a species match with *C. vicina* when the two profiles are mirrored for comparison. There are a few dissimilarities within the two chromatograms, but age must also be taken into consideration (see chapter 6, section 6.3).

The GC chromatograms in Figure 4.19 shows a species match when a blind puparial case sample is mirrored with a known *C. vomitoria* puparial case sample.
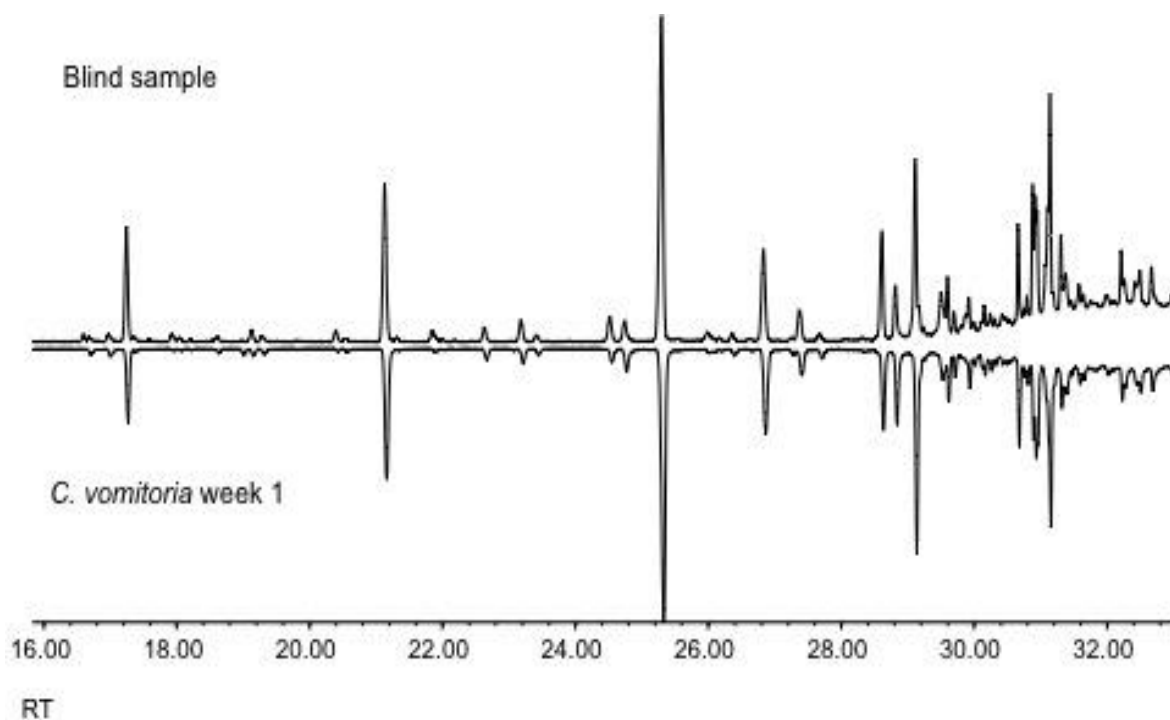
Figure 4.19: GC overlay of the blind puparial case (A) and a known *C. vomitoria* week 1 puparial case (B)

Only the *n*-alkanes were used for PCA due to the variety of methyl branched compounds each species possessed. As the species can be distinguished using the *n*-alkanes alone, it is not necessary to carry out full profile identification. This allows a non-expert in analytical chemistry to determine the species using this technique, whereas an experienced forensic entomologist/taxonomist would be required if using morphological criteria alone.

The blind samples proved the methodology is sound and enabled identification to be established from the unique fingerprint profiles that each species holds. It was very apparent when going through the blind samples that none matched the profile of *L. sericata*, as this species has the most distinguishable profile of the three (Figure 4.15).

The profile of *C. vomitoria* contains considerably more compounds in the higher retention time region of its profile (between 30 and 32 minutes) whereas *C. vicina* has no compounds exceeding a peak area of 0.5% above 31 minutes. This made it relatively simple to determine whether the blind samples were *C. vicina* or *C. vomitoria* and all of the estimated identifications were correct.

As mentioned, the profiles of the empty puparial cases closely resemble that of an adult fly. The puparia extractions only extract from the surface of the cuticle, whereas empty puparial case extractions will remove compounds residing within the case, which could be left from the cuticle of the adult fly. This is believed to be the case as compounds extracted from the surface of the empty puparial case should be identical to those extracted from the surface of the puparia. However, with an increase in the number of methyl branched alkanes observed for the empty puparial cases, it is assumed these hydrocarbons are from the cuticle of the adult fly.

Results presented in this section of the chapter offer accurate species identification of empty puparial cases for the three blowfly species studied. The technique of GC-MS and PCA to analyse hydrocarbons has shown to be a reliable means of insect identification from the puparial cases, which are becoming increasingly significant in criminal investigations where a body has reached a later stage of decomposition.

Hydrocarbon analysis, although not yet tested, could also provide information about the species from just a small fragment of the case, providing a sufficient concentration can be obtained, which would normally be impossible to determine identification down to the species using morphological features alone. Further results on puparial case identification shall be presented in chapter 7 using the new ionisation technique, Direct

Analysis in Real Time (DART) coupled to a Time of Flight Mass Spectrometer (TOFMS). This technique provided rapid analysis on the cases.

4.6 Adult flies

Although the three species chosen for this thesis are easily distinguishable in the adult stage using morphological traits (see Figure 4.20), it is important to elucidate their hydrocarbon profiles as a proof of concept.
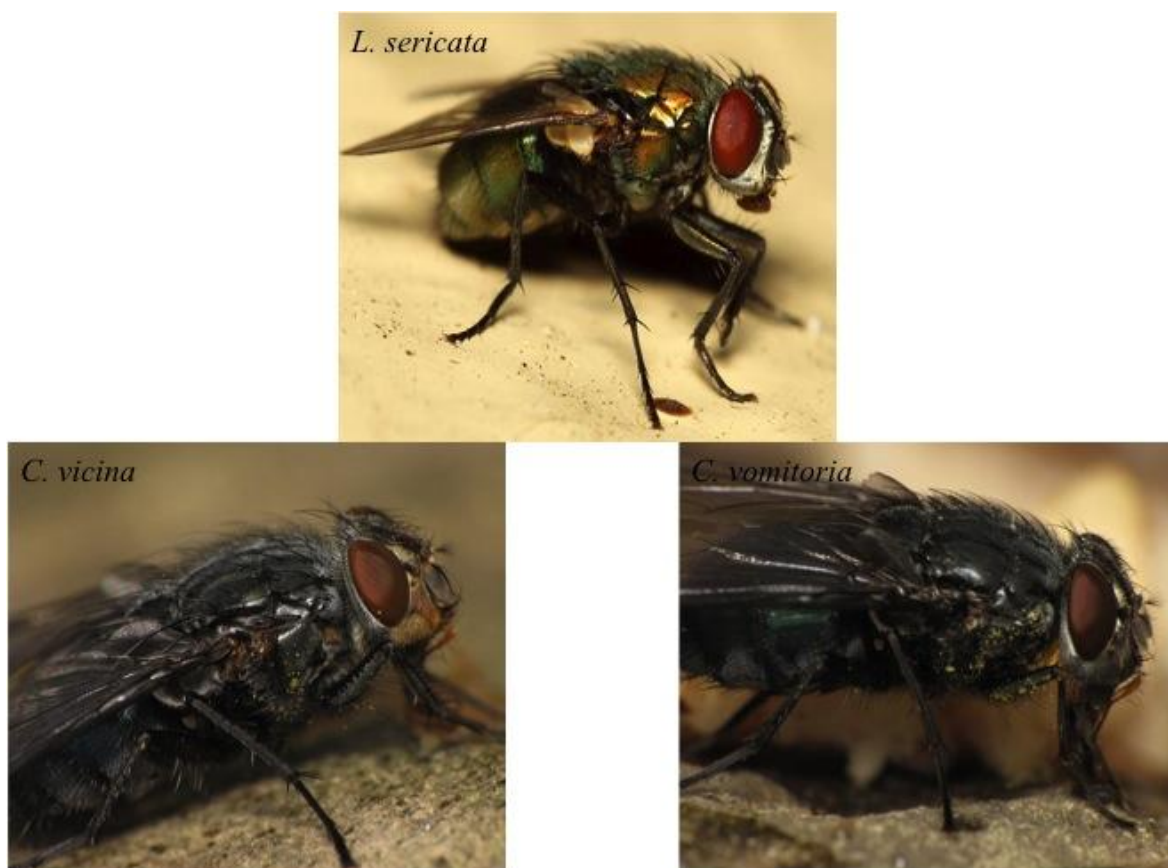
Figure 4.20: Image of *L. sericata*, *C. vicina* and *C .vomitoria* adult flies, showing that all three are morphologically distinct from each other [36].

Hydrocarbon analysis may not be used as an identification method for commonly found blowfly species but if results are as promising as for the empty egg cases, larvae, pupae and puparial cases, it shows potential for other Diptera that are more difficult to identify morphologically. For example the Sarcophagidae family, some of which can only be identified using the genitals of the male fly. Hydrocarbon analysis has the potential to offer a straightforward means of identification using GC-MS and PCA.

Lucilia sericata is highly distinguishable from *C. vicina* and *C. vomitoria* since the Lucilia genus have a metallic green body and Calliphora have metallic blue bodies. *C. vicina* and *C. vomitoria* are slightly more difficult to distinguish on first sight but *C. vomitoria* has two very characteristic features allowing for identification. Firstly, the genal dilation of C. *vomitoria* is dark in colour, whereas C. *vicina* is light and secondly, *C. vomitoria* possess orange hairs under the head (Figure 4.21).
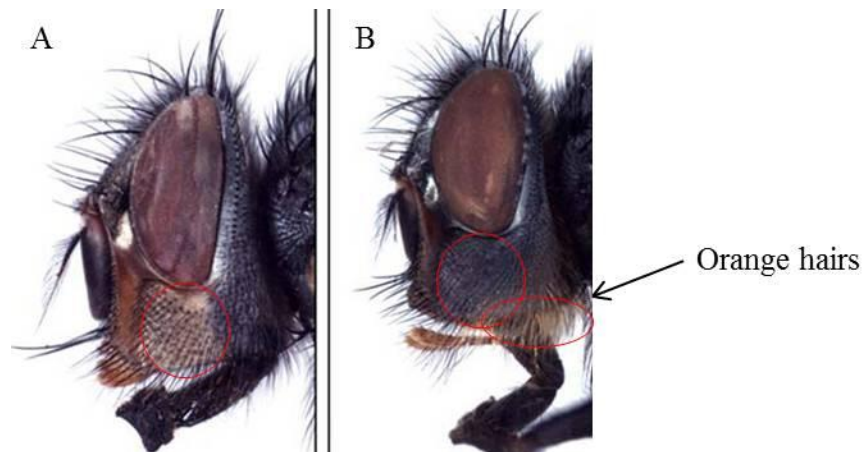
Figure 4.21: Image of A: *C. vicina* head and B: *C. vomitoria* head, illustrating the different colour of the genal dilation. Taken with permission from Szpila (personal key)

All three species will be discussed in relation to GC-MS analysis in this section of the chapter but only results for *C. vicina* and *C. vomitoria* will be presented for PCA, as there would never be a need to distinguish *L. sericata* from these two species using this technique as they are morphologically very different.

4.6.1 *Results and Discussion for adult flies*

GC-MS analysis:

The table below shows the number of hydrocarbons present (within the three hydrocarbon classes) for each species:

Table 4.9: Hydrocarbon composition of adult flies (for day 5), showing the number and percentage of *n*-alkanes, alkenes and methyl branched hydrocarbons each species has within its profile

	L. sericata	*%*	*C. vicina*	*%*	*C. vomitoria*	*%*
Alkanes	7	23	7	24	6	30
Alkenes	8	26	10	34	4	20
Methyl branched HC	16	52	12	41	10	50
Total HC's	**31**	**100**	**29**	**100**	**20**	**100**

The number of *n*-alkanes is similar between the three species. *L. sericata* has the highest number of compounds in its profile, with the largest quantity of methyl branched alkanes. The profile of *C. vicina* contains the most alkenes and *C. vomitoria* has a relatively simple profile with the lowest number of compounds present.

In the profile of the adult flies, C23:H is present in all three species but the percentage is considerably larger in *C. vomitoria* than it is for *C. vicina* and *L. sericata*, which

could be a useful identification characteristic. *C. vomitoria* was the only species to display C23:H in an adequate concentration (above 0.5% peak area).

Figure 4.22 shows the GC chromatograms of the three species at Day 5. It can clearly be seen that each exhibits very different hydrocarbon profiles. The shaded bars highlight specific areas of interest.

The first, second, fourth and fifth shaded bar show even chain length $2MeC_x$:H hydrocarbon followed by one or two odd chain length C_y:1 isomers and in the first and fourth bar, an odd chain length *n*-alkane. The ratios at which these peaks are observed differ for the three species, which could be a useful feature to distinguish between them (see Figure 4.23).

The third bar highlights a group of MeC25:H hydrocarbons as well as C26:H for *C. vicina*. The methyl branched hydrocarbons were identified as 11+9-MeC25:H, 7-MeC25:H and 3-MeC25:H. *C. vomitoria* has only 11+9-MeC25:H in an adequate concentration seen on the chromatograms in Figure 4.22, with the subsequent MeC25:H compounds (7-MeC25:H and 3-MeC25:H) and C26:H not been observed in a peak area concentration above 0.5%. *L. sericata* has 11+9-MeC25:H present as well as C26:H but the 7-MeC25:H and 3-MeC25:H are again not present in a peak area corresponding to a relative abundance above 0.5%.
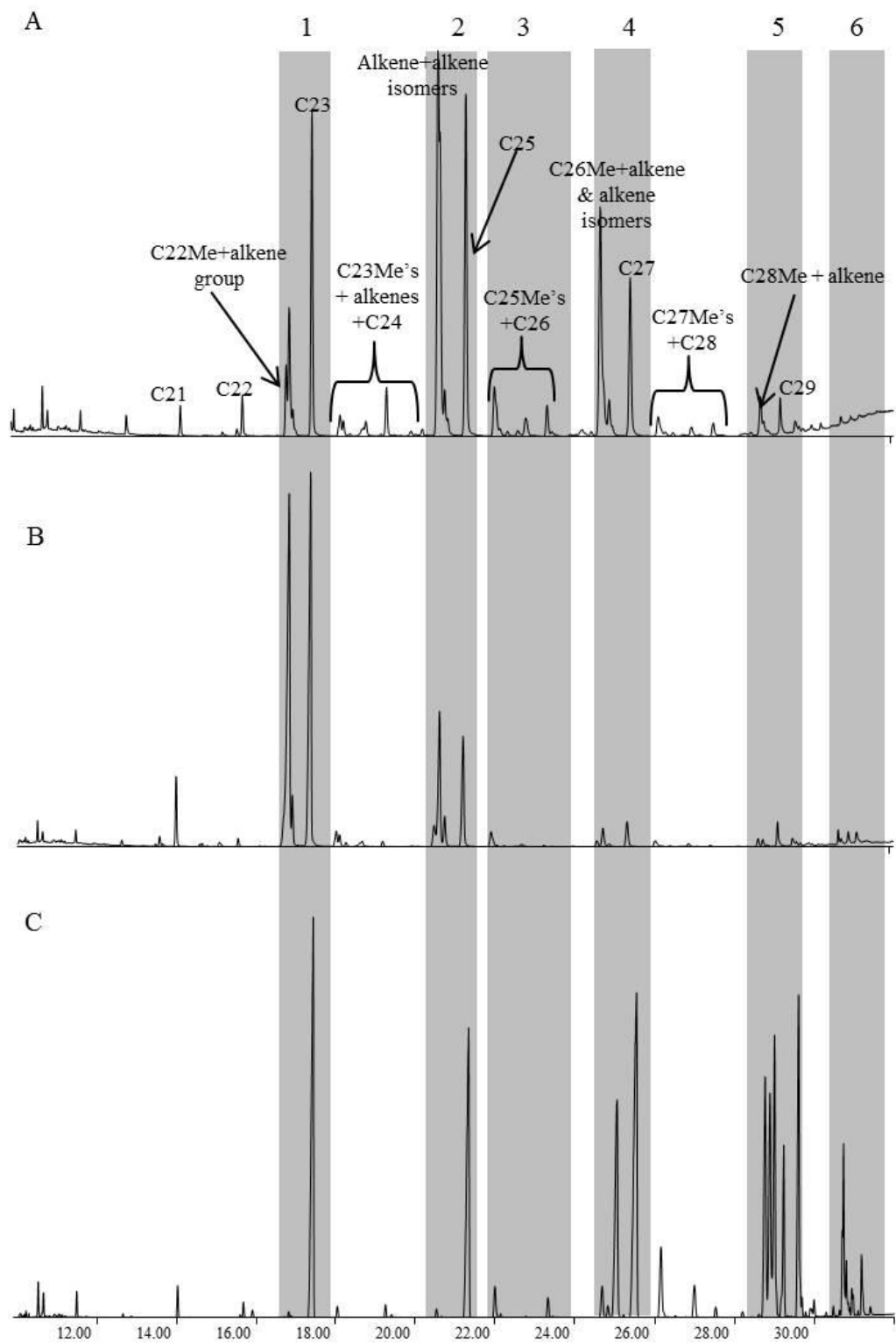
Figure 4.22: GC chromatograms of A: *C. vicina*, B: *C. vomitoria* and C: *L. sericata* taken at 5 day old

adult flies. Shaded bars illustrate specific areas of contrast

Finally bar 6 show some differences in the higher molecular weight hydrocarbons. *L. sericata* again shows the most distinguishable group of peaks, consisting of alkenes (C31:1 and C33:1) and complex methyl branched alkanes (2,8-DimeC30:H, 11+13+15-MeC31:H, 9-MeC31:H and 11,19-DimeC31:H). Only two of these compounds mentioned are observed in the two Calliphora species (2,8-DimeC30 present in the profile of *C. vomitoria* and 11+13+15-MeC31:H present in the profile of *C. vicina*) indicating this group of compounds is a useful identification feature.

There is a trend observed within the profiles of the three species which can be seen in Figure 4.23.
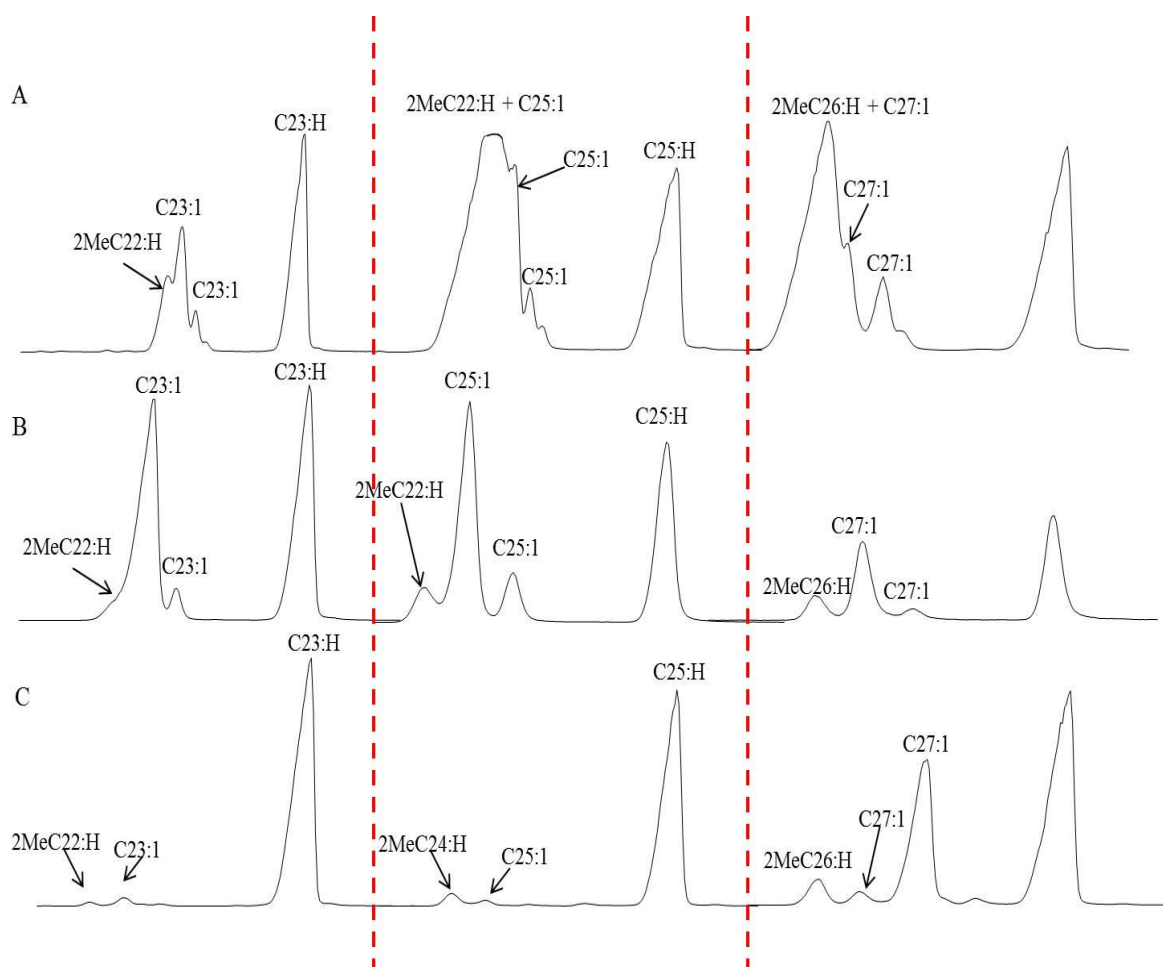
Figure 4.23: Zoomed in areas of the 2-Methyls and proceeding alkenes and *n*-alkanes showing the characteristic ratios across the three species in the profiles of the adult flies. A: *C. vicina*, B: *C. vomitoria* and C: *L. sericata*

A methylthiolation reaction with DMDS was carried out (chapter 3, section 3.5) on the adult flies to establish the double bond position of the alkenes. The table below shows the identified double bond positions but they have not be assigned to specific peaks.

Table 4.10: List of the identified alkenes established from methylthiolation reactions (double bond positions not known for alkadienes) *The *Z* configuration of the alkenes presented in table 4.11 are assumed [37].

˚C

L. sericata	C. vicina	C. vomitoria
*Z9C23:1		Z10C23:1
Z9C25:1	Z7,Z8,Z9,Z10,Z12C25:1	Z7,Z10,Z11,Z12C25:1
Z7,	Z7,Z8, Z9,	
Z9C27:1	Z10,Z11,Z12,Z13C27:1	Z7,Z8,Z10,Z11,Z12,Z13C27:1
Z9C29:1	Z7,Z8,Z9,Z10C29:1	Z7,Z8,Z,/Z10,Z11,Z12,Z13,Z14C29:1
Z9C31:1	Z8,Z9,Z10C31:1	Z9/Z10C31:1
	Z8,Z9C32	
Z9C33:1		

As Table 4.10 shows, each species holds unique alkenes, further allowing for distinctions to be made between the three species. There is also currently no published data on the alkenes of the three flies analysed, which could be a key tool used in taxonomy for closely related species which are morphologically similar, to further aid identification.

The reader is referred to appendices 14 to 16 for example mass spectra of alkenes following methylthiolation reactions, allowing for the double bond positions to be determined due to diagnostic ions. .

PCA:

It was expected that *L. sericata* would differ the most in its hydrocarbon profile from the other species due to it being a different genus, however examination of the GC trace alone is even enough to distinguish between *C. vicina* and *C. vomitoria*. For

completion, PCA was carried out on the two *Calliphora* species (Figure 4.24) using the *n*-alkanes only (Table 4.11).

Table 4.11: List of the compounds used for subsequent PCA analysis from the adult flies of *L. sericata*, *C. vicina* and *C. vomitoria,* along with the total percentage of each compound present and the percentage standard deviation

Peak no.	Peak Identification	*L. sericata* n=10 %	*C. vicina* n=10 %	*C. vomitoria* n=10 %
1	Tricosane	3.61±1.04	2.83±0.73	15.37±11.42
2	Pentacosane	13.17±2.57	12.59±2.04	14.40±7.13
3	Hexacosane	4.01±0.73	4.06±1.58	ND
4	Heptacosane	49.70±8.14	53.99±9.72	27.63±13.32
5	Octacosane	5.92±0.98	6.99±1.64	3.94±1.86
6	Nonacosane	23.59±5.14	19.54±4.63	38.66±20.12

For a table of all compounds extracted from the adult flies of *L. sericata*, *C. vicina* and *C. vomitoria*, see chapter 6, section 6.4.1.

PCA was carried out using six principal components, describing 100% of the variation within the dataset with the first three principal components comprising 83.8%, 15.3% and 0.8% respectively. PC2 and PC3 were used to plot the relevant scores (see appendix 17 for PCA eigenvalues).
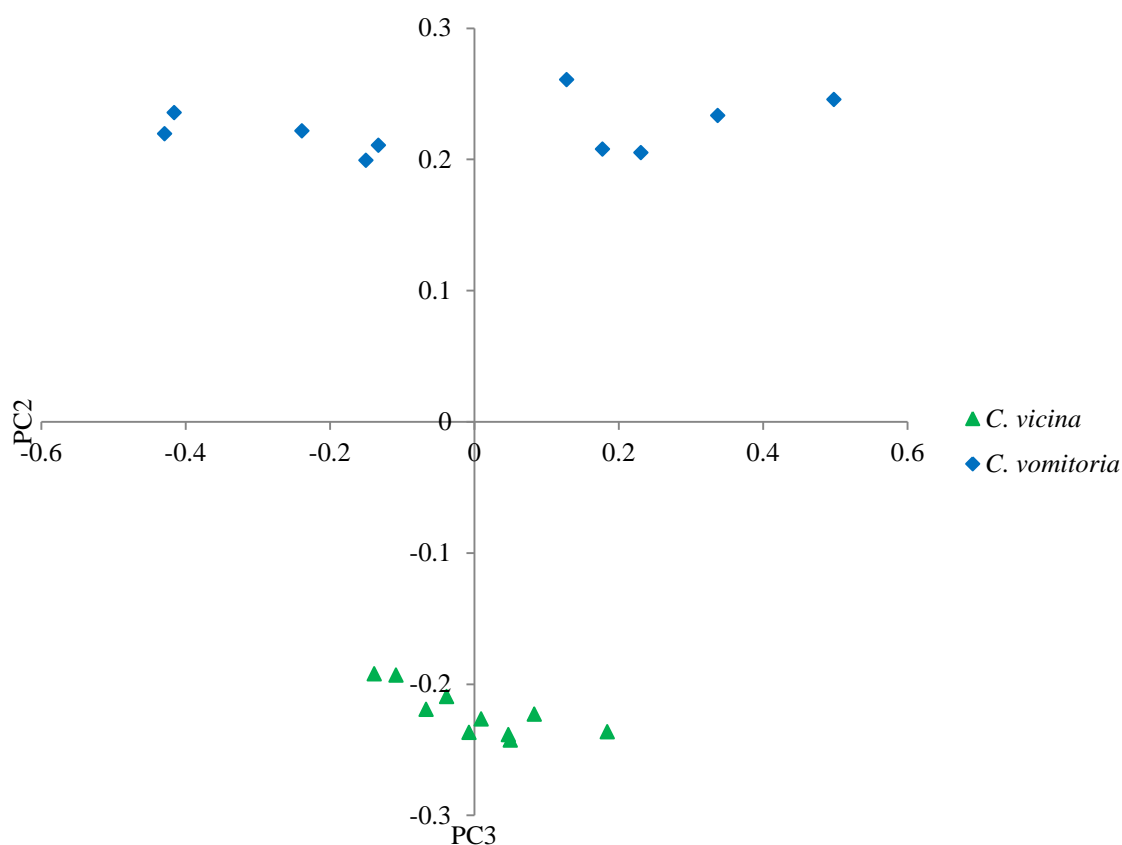
Figure 4.24: PCA plot of PC3 vs PC2 adult flies from *C. vicina* and *C. vomitoria* using *n*-alkanes only

Both species display very different spatial positioning on the scatter plot, allowing for positive species identification. The scatter for both species is linear, indicating there is little variation within PC3. The two compounds presenting the highest scores were C27:H and C29:H.

Although studies have been carried out on the cuticular hydrocarbons of adult flies [38–40], few have been published on the hydrocarbons of forensically important blowflies for taxonomy purposes [29,41]. More recently, studies have been applying DNA techniques [17,20] to identify forensically important blowflies and even flesh flies [42], which offers a good alternative to compliment morphological identification.

However, obtained results show that hydrocarbon analysis has the advantage of a single chromatogram, providing not only the identity, but also an indication of the fly's age (see chapter 6, section 6.4).

Figure 4.22 shows distinct differences between all three species when the chromatograms are analysed and compared. The profiles of *C. vicina* and *C. vomitoria* appear relatively similar between the retention times of 12 and 22 minutes with peaks in this region comprising of *n*-alkanes and methyl branched alkanes. The peak ratios and concentrations vary considerably though making them distinctive. However, the higher end of the chromatogram provides fingerprint characteristics with *C. vomitoria* containing peaks at higher retention times (>31minutes). *L. sericata* also shows a very unique profile when compared to the two Calliphora species. The lower end of the chromatogram contains a predominance of *n*-alkanes. However, the higher end of the chromatogram contains mainly methyl branched hydrocarbons in a high percentage making the profile very distinct in comparison to the profiles of *C. vicina* and *C. vomitoria*.

Two closely related species from the same genus (*C. vicina* and *C. vomitoria*) have been further examined in this section of the chapter using PCA and they both have distinctly different hydrocarbon profiles, further illustrating that these cuticular hydrocarbons are species-specific.

The double bond position within the alkenes adds further confirmation of species identification as they are very characteristic for each species of blowfly presented in this chapter. Martin and colleagues [43] presented results taken from 14 species of bumblebees, each possessing species-specific alkene positional isomers. They therefore show great potential within the field of taxonomy.

Although adult fly identification was not a main priority of this research, preliminary results have shown potential for this technique to be a useful identification tool which could now be applied to more taxonomically challenging species such as Sarcophagidae, as well as closely related species such as *Lucilia illustris* and *Lucilia cuprina* [44], which would be of great use in criminal investigations.

3.7 Overall Conclusion

The main aim of this study was to show how hydrocarbons are species-specific. Since the larval growth rate is very much dependant on the species, identification is an essential tool needed before ageing methods can be carried out. The technique of hydrocarbon analysis has the potential to drastically cut time in criminal investigations, as it could eliminate the need to rear the larvae to adult flies to confirm the species identification.

The empty egg shells, larvae, puparia, puparial cases and adult flies of *L. sericata*, *C. vicina* and *C. vomitoria* have all been examined and compared, and by using a simple extraction technique, the obtained hydrocarbon profiles of each species were unique, allowing them to be distinguished from each other in all life stages. Therefore, this technique shows great potential to be applied in the field of forensic entomology allowing for accurate, inexpensive and rapid taxonomy information, which is the first crucial step for PMI estimations.

The results presented for the empty egg shell experiment were preliminary and the experiment should be repeated using more replicates to establish if this technique can accurately be used to distinguish between the three species. The larvae results show a

huge amount of potential since they were carried out on 1-day old (1st instar) larvae which would usually be impossible to try and determine the identity to species level due to their very small size. A full profile of the empty puparial cases can be extracted from a section of the case, meaning partially intact cases can potentially still be identified to species level. The blind samples proved this technique to be sound for the three species examined, giving promising validation of the methodology.

All of the results presented clearly show the capabilities of this technique to be applied to morphologically similar species such as the flesh fly as well as other forensically important insects such as beetles.

More research on a wider range of forensically important flies now needs to be carried out to enable a hydrocarbon data base to be established, which has the potential to become a highly advantageous identification tool in forensic entomology casework.

References

[1]   J. Amendt, R. Krettek, and R. Zehner, Forensic entomology, Naturwissenschaften 91 (2004) 51–65.

[2]   R.M. Guillem, F.P. Drijfhout, and S.J. Martin, Using chemo-taxonomy of host ants to help conserve the large blue butterfly, Biological Conservation 148 (2012) 39–43.

[3]   W.V. Brown, H.A. Rose, M.J. Lacey, and K. Wright, The cuticular hydrocarbons of the giant soil-burrowing cockroach *Macropanesthia rhinoceros* saussure (Blattodea: Blaberidae: Geoscapheinae): analysis with respect to age, sex and location, Comparative Biochemistry and Physiology. Part B, Biochemistry and molecular biology 127 (2000) 261–77.

[4]   F.P. Drijfhout, Cuticular Hydrocarbons: A New Tool in Forensic Entomology?, in: Current Concepts in Forensic Entomology, eds., J. Amendt, C.P. Campobasso, M.L. Goff, and M. Grassberger, Springer (2010) 179–204.

[5]   M.I. Haverty, M.S. Collins, L.J. Nelson, and B.L. Thorne, Cuticular hydrocarbons of termites of the British Virgin Islands, Journal of Chemical Ecology 23 (1997) 927–964.

[6]   M. Page, L.J. Nelson, G.J. Blomquist, and S.J. Seybold, Cuticular hydrocarbons as chemotaxonomic characters of pine engraver beetles (*Ips* spp.) in the *grandicollis* Subgeneric Group, Journal of Chemical Ecology 23 (1997) 1053–1099.

[7]   B.K. Lavine and M.N. Vora, Identification of Africanized honeybees, Journal of Chromatography. A 1096 (2005) 69–75.

[8]   P.M. Mendonça, J.R. dos Santos-Mallet, R.P. de Mello, L. Gomes, and M.M. de Carvalho Queiroz, Identification of fly eggs using scanning electron microscopy for forensic investigations, Micron 39 (2008) 802–807.

[9]   M. Benecke, A brief history of forensic entomology, Forensic Science International 120 (2001) 2–14.

[10]   K.L. Sukontason, N. Bunchu, T. Chaiwong, B. Kuntalue, and K. Sukontason, Fine structure of the eggshell of the blow fly, *Lucilia cuprina*, Journal of Insect Science 7 (2007) 1–8.

[11]   P.J. Thyssen, Keys for identification of immature Insects, in: Current Concepts in Forensic Entomology, eds., J. Amendt, C.P. Campobasso, M.L. Goff, and M. Grassberger, Springer (2010) 25-42.

[12]   K. Sukontason, K.L. Sukontason, S. Piangjai, N. Boonchu, H. Kurahashi, M. Hope, and J.K. Olson, Identification of forensically important fly eggs using a potassium permanganate staining technique, Micron 35 (2004) 391–395.

[13]   S.J. Martin, H. Helanterä, and F.P. Drijfhout, Colony-specific hydrocarbons identify nest mates in two species of Formica ant, Journal of Chemical Ecology 34 (2008) 1072–80.

[14]   S. Martin, E. Vitikainen, H. Helanterä, and F. Drijfhout, Chemical basis of nest-mate discrimination in the ant *Formica exsecta*, Proceedings of the Royal Soceity B: Biological Sciences (2008) 1271–1278.

[15]   K. Szpila, Key for the Identification of Third Instars of European Blowflies (Diptera: Calliphoridae) of Forensic Importance, in: Current Concepts in Forensic Entomology, eds., J. Amendt, C.P. Campobasso, M. Goff, and M. Grassberger, Springer (2010) 43–56.

[16]   M. Mazzanti, F. Alessandrini, A. Tagliabracci, J.D. Wells, and C.P. Campobasso, DNA degradation and genetic analysis of empty puparia: Genetic identification limits in forensic entomology, Forensic Science International 195 (2010) 99–102.

[17]   S. Reibe, J. Schmitz, and B. Madea, Molecular identification of forensically important blowfly species (Diptera: Calliphoridae) from Germany, Parasitology research 106 (2009) 257–61.

[18]   C. Ames, B. Turner, and B. Daniel, Estimating the post-mortem interval (I): The use of genetic markers to aid in identification of Dipteran species and subpopulations, International Congress Series 1288 (2006) 795–797.

[19]   C. Ames, B. Turner, and B. Daniel, The use of mitochondrial cytochrome oxidase I gene (COI) to differentiate two UK blowfly species - *Calliphora vicina* and *Calliphora vomitoria*, Forensic Science International 164 (2006) 179–82.

[20]   J.D. Wells and J.R. Stevens, Application of DNA-based methods in forensic entomology, Annual Review of Entomology 53 (2008) 103–20.

[21]   K. Szpila, Key for the Identification of Third Instars of European Blowflies (Diptera: Calliphoridae) of Forensic Importance, in: Current Concepts in Forensic Entomology, eds., J. Amendt, C.P. Campobasso, M.L. Goff, and M. Grassberger, Springer (2010), pp. 47.

[22]   K. Saigusa, M. Takamiya, and Y. Aoki, Species identification of the forensically important flies in Iwate prefecture , Japan based on mitochondrial cytochrome oxidase gene subunit I *(COI)* sequences, Legal Medicine 7 (2005) 175–178.

[23]   S. Siriwattanarungsee, K.L. Sukontason, B. Kuntalue, S. Piangjai, J.K. Olson, and K. Sukontason, Morphology of the puparia of the housefly, *Musca domestica* (Diptera: Muscidae) and blowfly, *Chrysomya megacephala* (Diptera: Calliphoridae), Parasitology Research 96 (2005) 166–70.

[24]   R. Zehner, S. Mösch, and J. Amendt, Estimating the postmortem interval by determining the age of fly pupae: Are there any molecular tools? International Congress Series 1288 (2006) 619–621.

[25]   K.L. Sukontason, R. Ngern-Klun, D. Sripakdee, and K. Sukontason, Identifying fly puparia by clearing technique: application to forensic entomology, Parasitology Research 101 (2007) 1407–16.

[26]   K.L. Sukontason, P. Narongchai, C. Kanchai, K. Vichairat, S. Piangjai, W. Boonsriwong, N. Bunchu, D. Sripakdee, T. Chaiwong, B. Kuntalue, S. Siriwattanarungsee, and K. Sukontason, Morphological comparison between *Chrysomya rufifacies* (Macquart) and

Chrysomya villeneuvi Patton (Diptera: Calliphoridae) puparia, forensically important blow flies, Forensic Science International 164 (2006) 230–4.

[27]   K.L. Sukontason, C. Kanchai, S. Piangjai, W. Boonsriwong, N. Bunchu, D. Sripakdee, T. Chaiwong, B. Kuntalue, S. Siriwattanarungsee, and K. Sukontason, Morphological observation of puparia of *Chrysomya nigripes* (Diptera: Calliphoridae) from human corpse, Forensic Science International 161 (2006) 15–9.

[28]   J.A. Amorim and O.B. Ribeiro, Distinction among the puparia of three blowfly species (Diptera: Calliphoridae) frequently found on unburied corpses, Memórias do Instituto Oswaldo Cruz 96 (2001) 781–4.

[29]   G. Ye, K. Li, J. Zhu, G. Zhu, and C. Hu, Cuticular hydrocarbon composition in pupal exuviae for taxonomic differentiation of six necrophagous flies, Journal of Medical Entomology 44 (2007) 450–6.

[30]   D. Morgan, *Biosynthesis in Insects*, The Royal Society of Chemistry, UK (2010).

[31]   G.H. Zhu, X.H. Xu, X.J. Yu, Y. Zhang, and J.F. Wang, Puparial case hydrocarbons of *Chrysomya megacephala* as an indicator of the postmortem interval, Forensic Science International 169 (2007) 1–5.

[32]   B. Greenberg, Flies as Forensic Indicators, Journal of Medical Entomology 28 (1991) 565–577.

[33]   S.E. Donovan, M.J.R. Hall, B.D. Turner, and C.B. Moncrieff, Larval growth rates of the blowfly, Calliphora vicina, over a range of temperatures, Medical and Veterinary Entomology 20 (2006) 106–14.

[34]   J. Wang, Z. Li, Y. Chen, Q. Chen, and X. Yin, The succession and development of insects on pig carcasses and their significances in estimating PMI in South China, Forensic Science International 179 (2008) 11–8.

[35]   Z. Adams and M.J.R. Hall, Methods used for the killing and preservation of blowfly larvae, and their effect on post-mortem larval length, Forensic Science International 138 (2003) 50–61.

[36]   Identification, images and information for insects, spiders and their kin for the United States & Canada, http://bugguide.net/node/view/15740.

[37]   G.J. Blomquist and A.G. Bagnères, *Insect Hydrocarbons: Biology, Biochemistry, and Chemical Ecology*, Cambridge University Press (2010).

[38]   M. Trabalon, M. Campan, J.L. Clement, C. Lange, and M.T. Miquel, Cuticular hydrocarbons of *Calliphora vomitoria* (Diptera): Relation to age and sex, General and Comparative Endocrinology 85 (1992) 208–216.

[39]   R. Urech, G.W. Brown, C.J. Moore, and P.E. Green, Cuticular hydrocarbons of buffalo fly, *Haematobia exigua*, and chemotaxonomic differentiation from horn fly, *H. irritans*, Journal of Chemical Ecology 31 (2005) 2451–61.

[40] W.V. Brown, R. Morton, and J.P. Spradbery, Cuticular hydrocarbons of the old world screw-worm fly, *Chrysomya bezziana* Villeneuve (Diptera: Calliphoridae). Chemical characterization and quantification by age and sex, Comparative Biochemistry and Physiology Part B: Comparative Biochemistry 101 (1992) 665–671.

[41] O. Roux, C. Gers, and L. Legal, Ontogenetic study of three Calliphoridae of forensic importance through cuticular hydrocarbon analysis, Medical and Veterinary Entomology 22 (2008) 309–17.

[42] S. Hwa, M. Rizman-idid, E. Mohd-aris, H. Kurahashi, and Z. Mohamed, DNA-based characterisation and classification of forensically important flesh flies (Diptera : Sarcophagidae) in Malaysia, Forensic Science International 199 (2010) 43–49.

[43] S.J. Martin, J.M. Carruthers, P.H. Williams, and F.P. Drijfhout, Host Specific Social Parasites (*Psithyrus*) Indicate Chemical Recognition System in Bumblebees, Journal of Chemical Ecology 36 (2010) 855–863.

[44] J.D. Wells, R. Wall, and J.R. Stevens, Phylogenetic analysis of forensically important *Lucilia* flies based on cytochrome oxidase I sequence : a cautionary tale for forensic species determination, International Journal of Legal Medicine 121 (2007) 229–233.

Chapter 5

Age Determination of Immature Life Stages Using Cuticular Hydrocarbons*

5. Introduction

When presented with a crime scene, a forensic entomologist will collect and preserve insect samples from the corpse and the surrounding area and rear them to adulthood in the laboratory [1–4]. Once the identity of the insect to species level has been established, the next stage in determining the PMI_{min} is to establish the age of the insects present. This process of insect rearing (at the same temperature and humidity of the crime scene) can be quite time consuming. A method that removes the necessity for this procedure but is still able to determine the age of the oldest colonising species of forensically important blowflies would be highly advantageous in a criminal investigation.

Methods currently used in the field to estimate the post-mortem interval include two main steps:

1) For the early post-mortem interval, the oldest insect specimens that have developed on the body must be identified and aged.

2) For late post-mortem estimations, the succession patterns of arthropods present on the body must also be examined [3].

An indication of age for the larvae is usually estimated using temperature data and growth charts [5] for the identified species as well as looking at morphological traits which serve as larval stage indicators [3]. An example of a growth chart is presented in Grassberger and Reiter [5] in reference to isomegalen- and isomorphen-diagrams for *L. sericata*. These diagrams illustrate the morphological changes that occur during the development of the fly, which is dependent on time and temperature. For an indoor environment where the temperature remains roughly constant, the age of the larvae can be read off instantly from the larval length. However, if the temperature varies such as it would for an outdoor environment, an age range can be estimated [5].

Another method of calculating the larval age is using Accumulated Degree Days (ADD) or Accumulated Degree Hours (ADH).

$$ADD = (T - T_L) \text{ x days}$$

$$ADH = (T - T_L) \text{ x hours}$$

T = Temperature/mean temperature

T_L = Lower threshold temperature (at which the larvae cease to develop) [6].

Larvae require a certain amount of heat in order to develop from egg to the time of eclosion. The time taken for this to occur can be calculated in units of degree days or hours [4]. By using the simple equations shown above, the calculated degree days and hours are accumulated as a product of temperature and time from the development thresholds for each day [4]. Although there are many ADH/ADD values and thresholds published [6–13], a reliable PMI will also be dependent on the data used and other critical factors such as whether maggot mass temperature was taken into consideration, the minimum temperature threshold used, (some use 0 ˚C, others use 6 ˚C or 10 ˚C [9]) and how the larvae were killed and preserved [14]. It is also preferable to use data from species of the same region as developmental data from different geographical regions may vary [4,5,15]

In addition to the above methods mentioned, the number of posterior spiracles will give information regarding the instar whilst the absence of the crop will indicate the larvae have moved into the post-feeding stage of its life cycle.

However, recent studies on Diptera have shown that hydrocarbons have the potential not only to be used for taxonomic purposes [16–18] but also as a possible ageing tool [19,20]. Therefore, potentially, hydrocarbons could be used to establish the age of forensically important blowflies. If the hydrocarbon profile differs at distinguishable ages, a reliable method complementary to the current methods used for ageing the six stages of the blowfly's life cycle could be developed.

5.1 Aims and Objectives

This chapter examines the hydrocarbon profiles of the forensically important blowflies *Lucilia sericata, Calliphora vicina* and *Calliphora vomitoria* extracted from the early life stages, which include the empty egg cases and larvae. Chapter 6 will discuss the hydrocarbon profiles of the later life stages, including puparia, puparial cases and adult flies. Many succession rate studies have been carried out (for examples see references [21–23]) and these three species are known to be amongst the first wave of Calliphoridae to inhabit decomposing remains, hence they are of forensic importance when establishing the PMI.

The aims of the experiments presented in this chapter are to extract and analyse the compounds on the cuticle of the three aforementioned blowfly species using GC-MS, focusing on the non-polar hydrocarbon compounds. With the aid of statistical analysis, the chromatograms have been closely examined in order to determine if there are any systematic chemical changes within the hydrocarbon profiles over time, giving the potential for using these compounds as an indication of the age of the immature life stages.

5.2 Egg cases

Estimating the age of empty egg cases is extremely difficult and there are currently no techniques capable of accomplishing this. Hydrocarbon analysis could hold advantages over DNA analysis if distinguishable changes can be detected over time. The two species used for the preliminary investigation of ageing egg cases were *C. vomitoria*

and *C. vicina*. There is currently no published work for ageing the egg cases of these two species.

5.2.1 Results and Discussion for egg cases

C. vomitoria:

The empty egg cases of *C. vomitoria* extracted at 5 and 12 days after hatching, yield a profile consisting of 43 different identifiable compounds with some co-eluting for a total of 34 resolvable peaks (Table 5.1). The compounds from day 5 consisted of *n*-alkanes (21%), alkenes (18%) and methyl-branched hydrocarbons (62%). The compounds from day 12 consisted of *n*-alkanes (23%) and methyl-branched hydrocarbons (77%), with the chain lengths of the *n*-alkanes ranging from C17 to C33. Table 5.1 lists the identified compounds extracted from the egg shell cuticle along with the Kovats Index values, the total percentage of each compound present and the percentage standard deviation for each of the two days.

Table 5.1 shows that the peak area concentrations generally increased with age for most of the compounds present but this is due to all of the alkenes being present below the 0.5% peak area threshold, and therefore they are excluded from further analysis, which will have the overall effect of increasing the total percentage for each compound.

Table 5.1: List of the compounds extracted and used for subsequent PCA analysis from the egg cases of *C. vomitoria,* with the total percentage of each compound present, the percentage standard deviation for each day and the Kovats Indices to aid identification

Peak number	Peak Identification	Kovats iu	Day 5 n=2 %	Day 12 n=2 %
1	Tricosane	2300	9.19±2.47	9.60±0.39
2	Tetracosane	2400	0.69±0.18	0.79±0.22
3	2-Methyltetracosane	2463	1.64±0.39	1.78±0.46
4	Pentacosene[1]	2469	2.58±0.53	tr
5	Pentacosene[1]	2476	2.27±0.40	tr
6	Pentacosane	2500	14.42±3.68	14.74±2.69
7	9+11-Methylpentacosane	2534	0.77±0.13	tr
8	Hexacosane	2600	0.59±0.22	tr
9	2-Methylhexacosane	2663	2.41±0.94	2.72±0.89
10	Heptacosene[1]	2669	1.01±0.24	tr
11	Heptacosane	2700	14.03±5.76	15.75±3.35
12	11+13-Methylheptacosane	2731	0.80±0.19	0.79±0.24
13	3-Methylheptacosane	2773	0.93±0.40	1.08±0.25
14	Octacosane	2800	1.59±0.75	1.67±0.51
15	2-Methyloctacosane	2872	7.60±3.34	8.77±2.28
16	Nonacosene[1]	2877	0.53±0.16	tr
17	Nonacosene[2]	2882	0.61±0.17	tr
18	Nonacosane	2900	13.29±8.30	14.58±5.27
19	11+13-Methylnonacosane	2935	4.97±1.65	5.50±1.91
20	9-Methylnonacosane	2939	1.05±0.49	1.47±0.43
21	7-Methylnonacosane	2946	2.29±1.02	2.74±0.74
22	5-Methylnonacosane	2955	1.23±0.57	1.44±0.43
23	3-Methylnonacosane	2977	1.59±0.74	1.80±0.48
24	5,x-Dimethylnonacosane[1]	2985	0.77±0.35	0.83±0.26
25	14+16-Methyltriacontane	3035	0.65±0.29	0.71±0.26
26	2-Methyltriacontane	3076	2.44±1.26	2.54±0.69
27	Hentriacontene[1]	3084	0.67±0.30	tr
28	2,14-Dimethyltriacontane	3098	0.87±0.41	0.94±0.26
29	2,6/2,8/2,10-Dimethyltriacontane[2]	3101	1.99±0.97	2.10±0.46
30	11-Methylhentriacontane	3123	3.30±1.65	3.49±1.16
31	9,21-Dimethylhentriacontane	3143	1.03±0.43	1.18±0.27
32	7,x-Dimethylhentriacontane[2]	3147	0.71±0.32	0.76±0.18
33	17-Metritriacontane+4,8/4,10-Dimethylhentriacontane[2]	3241	0.55±0.33	1.06±0.23
34	2,10/2,12-Dimethylhentriacontane[2]	3281	0.92±0.35	1.16±0.07

[1] Double bond positions assumed but not assigned to specific peaks

[2] Tentative identification based on Kovats Index values and match with NIST08 Library database

tr = Detected in trace amounts (<0.5%)

The chromatogram in Figure 5.1 shows two mirrored samples taken from day 5. It clearly illustrates the repeatability within the samples, indicating a sound methodology was established.
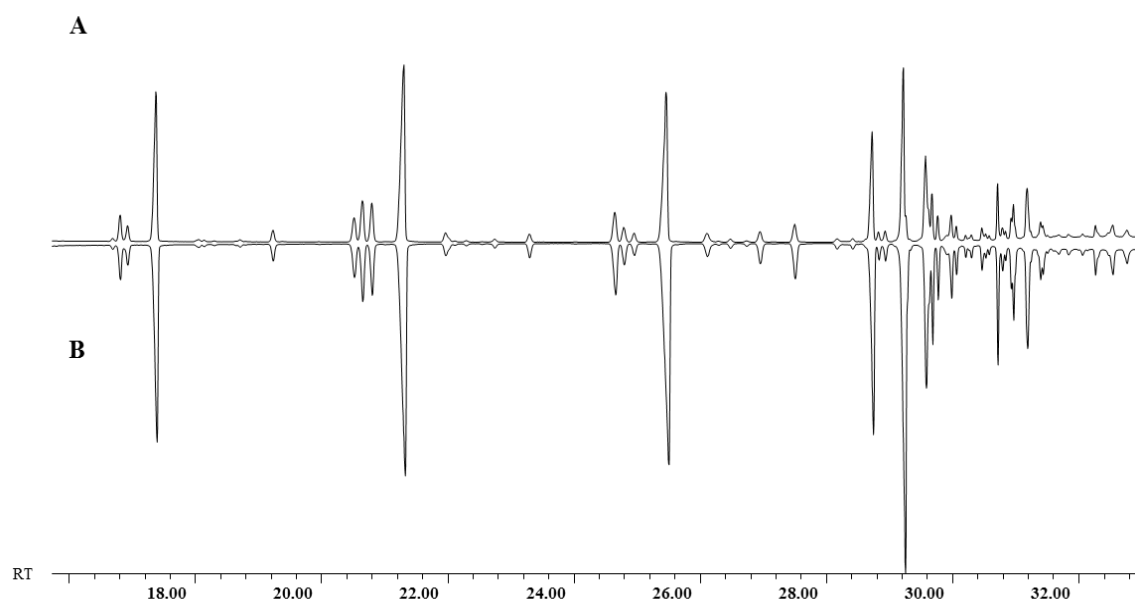
Figure 5.1: GC trace overlay of two samples from Day 5 *C. vomitoria* egg cases, illustrating the small variation between the daily extractions

In contrast, Figure 5.2 shows the GC chromatograms of a single sample from day 5 and day 12 egg cases. Here, chemical distinctions can be made between the different ages of the cases.

143
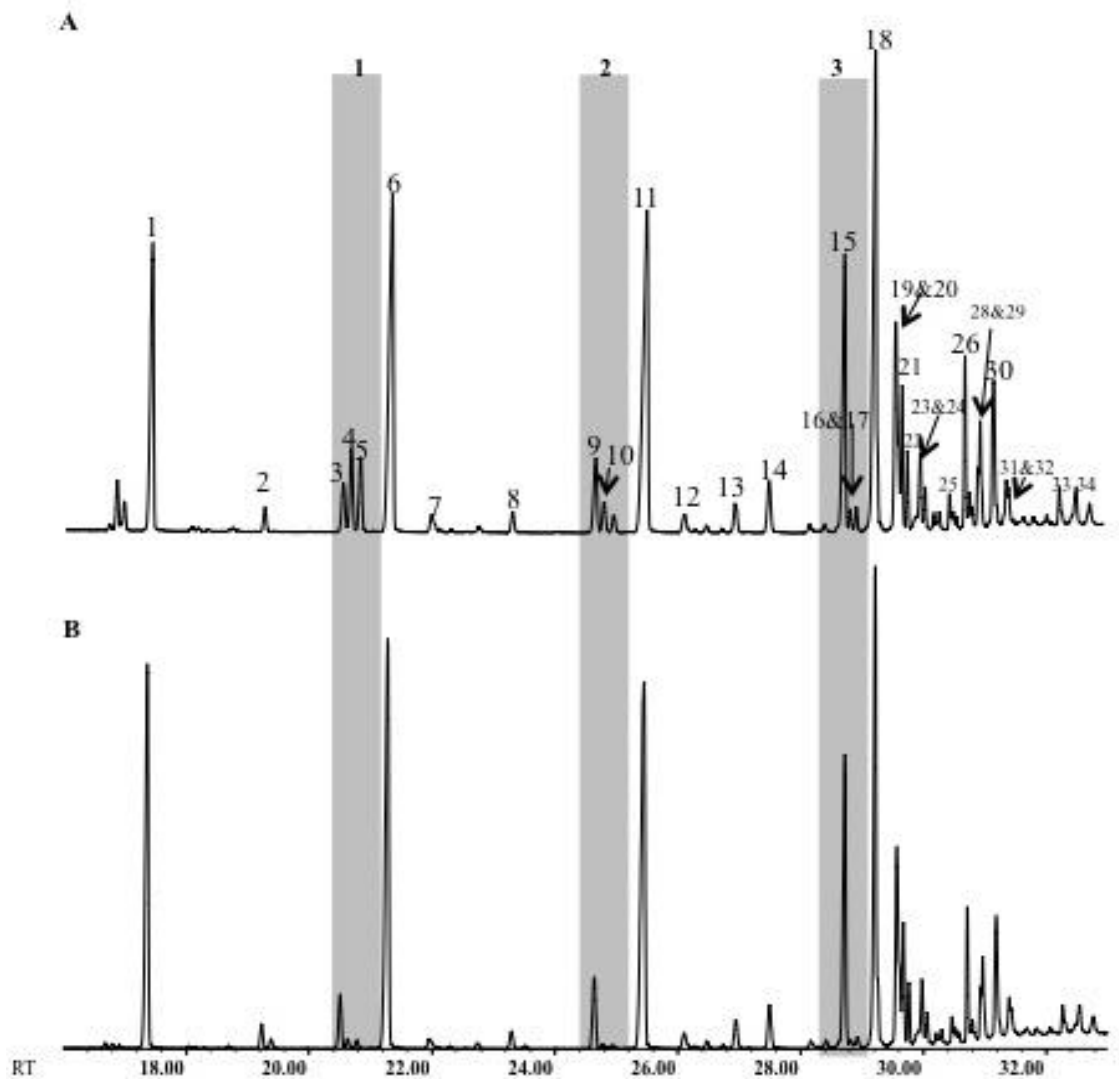
Figure 5.2: GC chromatograms of *C. vomitoria* empty egg cases at two different ages, A: Day 5 and B: Day 12. Shaded bars illustrate distinctive changes over time indicating specific areas of interest

As shown in Table 5.1, the alkenes are present in day 12 in trace amounts which fall below the 0.5% peak area threshold and are therefore excluded. This in contrast to day 5, whereby 18% of the total hydrocarbons present are alkenes.

The GC chromatograms in Figure 5.2 clearly show a potential for the empty egg shells to be aged due to the distinguishing changes over time. The shaded bars show some

areas of contrast within the profiles at the two different ages and a definite trend can be observed. The shaded bars all highlight small clusters of peaks which are even chain length methyl branched hydrocarbons, 2-MeC$_x$:H (x=C24/C26/C28) and odd chain length alkene isomers, C$_x$:1(X=C25/C27/C29). As seen in the profile of the day 12 empty egg shells, the 2Methyl alkanes remain relatively stable over the two ages but the alkenes all decrease below the 0.5% peak area threshold.

All of the 34 resolvable peaks used for PCA analysis were hydrocarbons, of which 62% were branched, 21% were *n*-alkanes and 18% of the hydrocarbons were alkenes.

Although the chain lengths ranged from C17:H to C33:H, there were only trace amounts of the low molecular weight (C17:H to C22:H) and high molecular weight (C30:H to C33:H) *n*-alkanes present in the profile and these were therefore not included in PCA.

The PCA was carried out using four principal components, describing 99.95% of the variation within the dataset with the first three principal components comprising 83.5% and 15.2% and 1.1% respectively. PCA was carried out on a dataset including all three classes of hydrocarbons. PC1 and PC2 were used to plot the relevant scores (see appendix 18 for PCA eigenvalues).
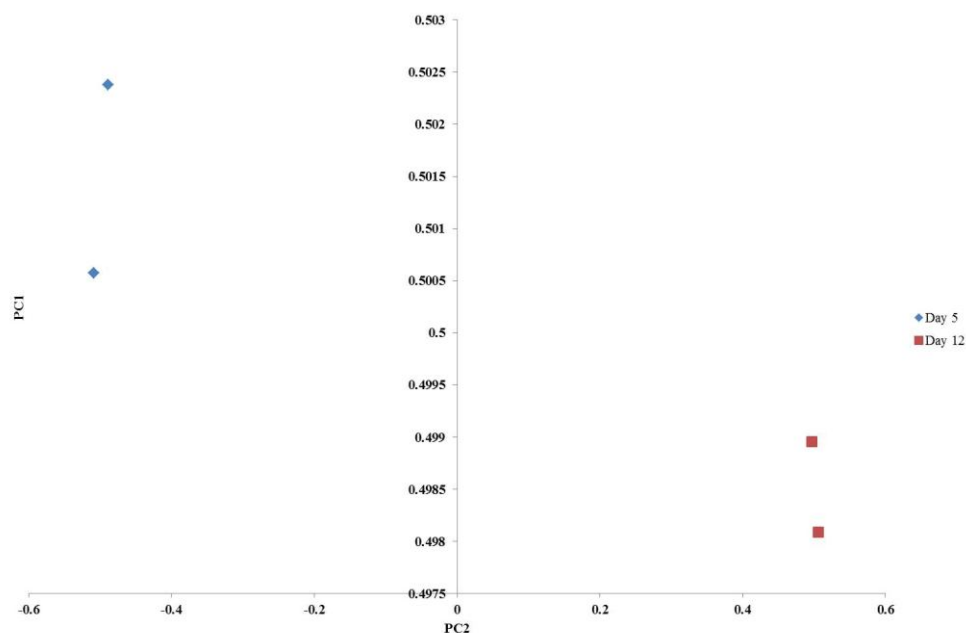
Figure 5.3: PCA plot showing PC2 vs PC1 for *C. vomitoria* empty egg cases using data extracted from day 5 and day 12

The PCA plot potentially shows two distinct areas of clustering. However, with only two replicates used in the dataset, the PCA cannot be used to give a confident age of the empty egg case.

The alkenes also act as a fundamental age indicator as they are not observed in the profiles of day 12 egg cases. In general, all of the total hydrocarbon percentages appear to increase with age but this is most likely due to the alkenes decreasing (below 0.5% peak area) in day 12 and hence reflecting in other compounds being present in higher percentages.

The slight differences seen in the overlaid chromatograms in Figure 5.2, mainly associated with alkenes being more prominent in the younger age of the empty egg

cases, could be enough to be able to distinguish between the two ages.

C. vicina:

The chemical profiles were analysed from the empty egg shells of *C. vicina* extracted at 2 and 8 days after the larvae hatched. There were 35 identifiable compounds with some co-eluting for a total of 27 resolvable peaks (Table 5.2), consisting of *n*-alkanes (19%), alkenes (7%) and branched methyl hydrocarbons (74%) for day 2. The chain lengths range from C20:H to C33:H but as with *C. vomitoria*, the lower and higher molecular weight *n*-alkanes were not present in a sufficient concentration (<0.5%) and hence only *n*-alkanes ranging from C23:H to C29:H were applied for subsequent analysis.

Table 5.2 shows the identified compounds extracted from the egg case cuticle along with their Kovats Indices, the total percentage of each compound present and the percentage standard deviation for each of the two days.

Table 5.2: List of the compounds extracted and used for subsequent PCA analysis from the egg cases of *C. vicina,* along with the total percentage of each compound present, the percentage standard deviation for each day and the Kovats Indices to aid identification

Peak number	Peak Identification	Kovats iu	Day 2 n=2 %	Day 8 n=2 %
1	Tricosene[1]	2269	0.45±0.09	0.81±0.35
2	Tricosane	2300	4.49±0.19	10.01±0.12
3	2-Methyltetracosane	2463	2.99±1.26	2.97±0.93
4	Pentacosene[1]	2468	0.79±0.03	1.80±1.20
5	Pentacosane	2500	13.56±3.76	16.58±1.66
6	2-Methylhexacosane	2662	4.28±0.30	3.13±1.53
7	Heptacosane	2700	17.23±7.32	13.61±1.11
8	11+13-Methylheptacosane	2730	0.67±0.33	0.77±0.27
9	3-Methylheptacosane	2773	1.17±0.33	0.95±0.12
10	Octacosane	2800	1.81±0.57	1.66±0.14
11	2-Methyloctacosane	2873	11.16±5.13	8.82±1.07
12	Nonacosane	2900	14.21±0.02	14.62±1.31
13	2,6-Dimethyloctacosane[2]	2906	0.69±0.32	0.46±0.51
14	11+13-Methylnonacosane	2938	5.94±0.24	3.88±0.20
15	9-Methylnonacosane	2943	1.36±0.53	0.99±0.06
16	7-Methylnonacosane	2950	2.82±0.86	2.58±0.35
17	5-Methylnonacosane	2958	1.18±0.25	1.34±0.21
18	3-Methylnonacosane	2981	2.28±0.71	1.95±0.32
19	5,x-Dimethylnonacosane[2]	2989	0.65±0.33	0.61±0.11
20	14+16-Methyltricontane	3041	0.55±0.27	tr
21	2-Methyltriacontane	3041	3.22±0.85	3.72±0.52
22	2,14-Dimethyltriacontane[2]	3106	0.80±0.38	0.74±0.28
23	2,6/2,8/2,10-Dimethyltriacontane[2]	3111	1.81±0.47	1.99±0.05
24	11-Methylhentriacontane	3144	3.01±1.20	2.85±0.57
25	9,21-Dimethylhentriacontane[2]	3174	0.99±0.51	1.00±0.16
26	17-Methyltritriacontane+4,8/4,10-Dimethylhentriacontane[2]	[3]N/A	0.95±0.33	1.07±0.22
27	2,10/2,12-Dimethylhentriacontane[2]	3339	0.96±0.39	1.11±0.03

[1]Double bond positions assumed but not assigned to specific peaks

[2]Tentative identification based on Kovats Index values and match with NIST08 Library database

[3]Kovats Index value not available due to co-eluting compound

tr = Detected in trace amount (<0.5%)

Generally, the percentage in which the shorter chain length *n*-alkanes and alkenes (C23:H to C25:H) are present increase with time. However, the longer chain length *n*-alkanes and alkenes (C27:H and C29:H) decrease with time, with the exception of C29:H. The majority of the methyl branched alkanes present also decrease with time, with the exception of a few (compounds 8, 21, 23, 25, 26 and 27).

Figure 5.4 shows the GC chromatograms of a single egg case from day 2 and day 8. Unlike *C. vomitoria*, significant chemical differences are not as clear between the two ages of the cases, but some distinctions can be made by looking at the differing concentrations of the compounds present.
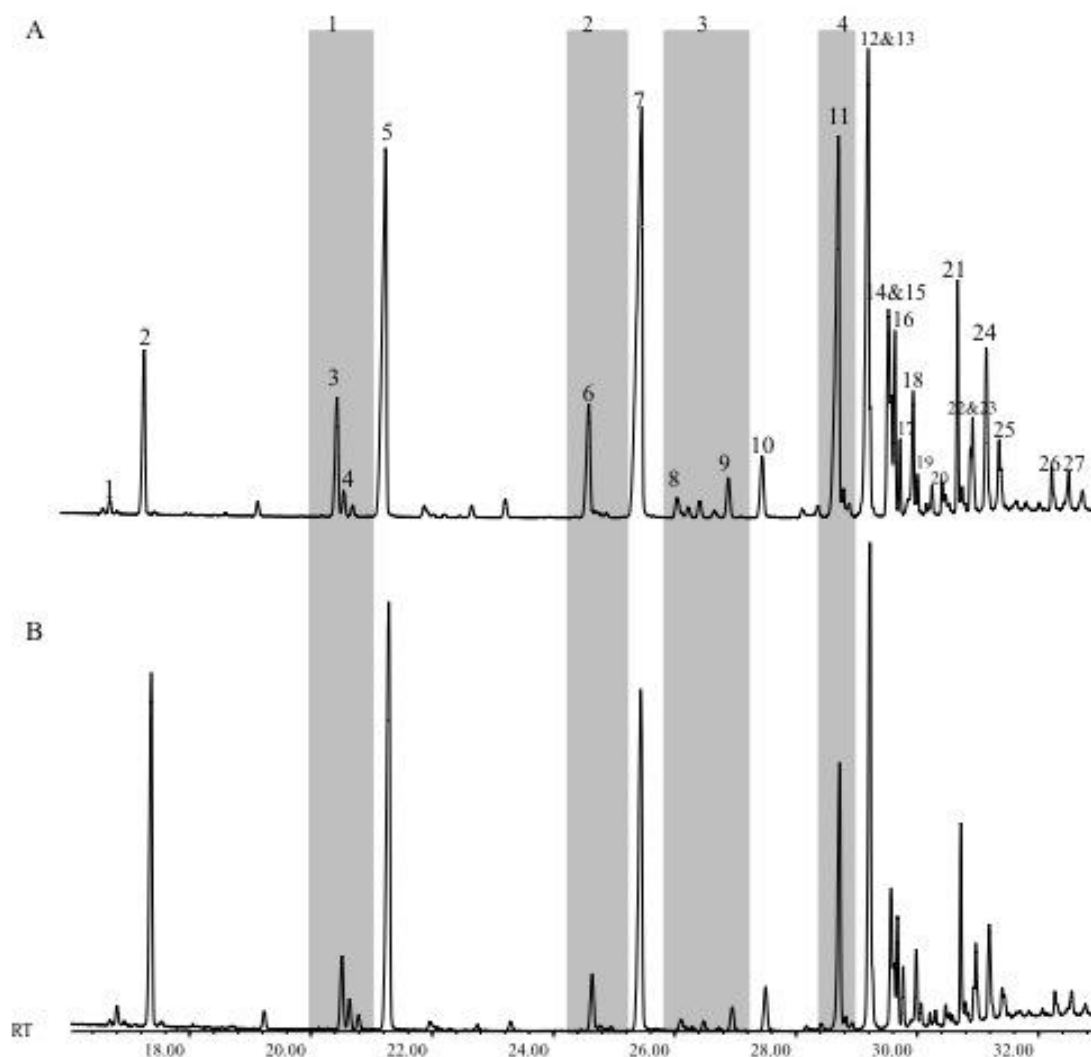
Figure 5.4: GC chromatograms of *C. vicina* egg cases at two different ages, A: Day 2 and B: Day 8. Highlighted areas illustrate distinctive changes over time indicating specific areas of interest

The shaded areas highlight some contrasting chemical distinctions within the concentrations of certain compounds. The alkenes remain present in both ages of the egg cases for *C. vicina*, but the concentration for most of the mono-methyl compounds decreases with time, in particular for compounds 11 and 14. However, definite age cannot be determined from the GC chromatogram alone. PCA can be an extremely effective technique as it can extract subtle variations within the peak area

concentrations allowing for distinctions to be made between the ages.

Of the 27 resolvable peaks used for PCA analysis, 69% were branched, 17% were *n*-alkanes and 14% of the hydrocarbons were alkenes. PCA was carried out using five principal components, describing 99.9% of the variation within the dataset with the first three principal components comprising 95.9%, 2.9% and 1.1% respectively. PC1 and PC2 were used to plot the relevant scores (see appendix 19 for PCA eigenvalues). Figure 5.5 shows the PCA plot of PC2 vs PC1 for data obtained from day 2 and day 8.
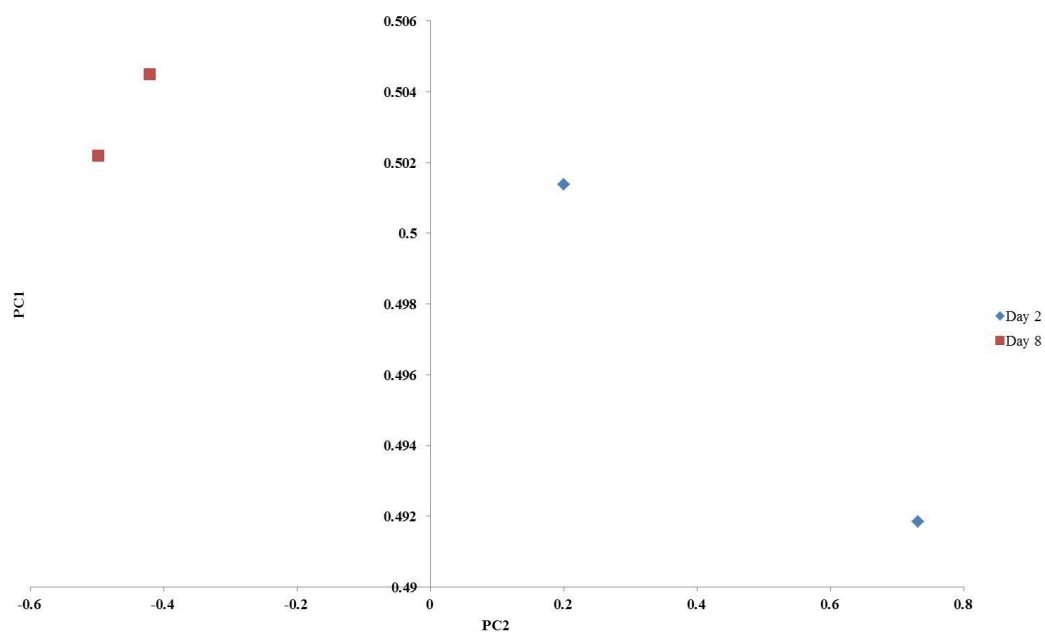
Figure 5.5: PCA plot showing PC2 against PC1 for *C. vicina* egg cases using data extracted from day 2 and day 8

The PCA plot (Figure 5.5) shows a lot of scatter within the day 2 repeats and as with *L. sericata* egg cases, accurate ageing cannot be achieved when only two replicates were examined.

The main compounds which have substantial score values for *C. vicina* empty egg cases are C25:H and C27:H, indicating they are highly significant within the PCA when ageing this particular Calliphora species. The relative percentage C25:H increases with age whilst the relative percentage for C27:H decreases with age.

The high loading values for the two *n*-alkanes (C25:H and C27:H) indicates that the odd chain length *n*-alkanes hold some influence when ageing the empty egg shells. This is not the case for the older life stages, as discussed in chapter 3, *C. vicina* usually displays more discriminating PCA results when the *n*-alkanes are removed. Enhanced PCA plots are seen in results presented later in this chapter and chapter 6, for the larvae, puparial cases and adult flies, when *n*-alkanes are removed for this particular species.

The preliminary results show potential for the empty egg cases to be aged, which is valuable information that is currently unobtainable by any other techniques used in the field of forensic entomology.

5.2.2 General Discussion and Conclusion for ageing egg cases

The profile of *C. vomitoria* reveals alkenes as the main age indicators, as they are absent in the older egg cases. *C. vicina* has fewer characteristics when looking at its hydrocarbon profile over time, so for this species, there is a greater reliance on PCA to

establish the age of the empty egg cases.

As there were only 2 samples available for each of the two extraction days for both species, this experiment needs to be carried out again using more repeats to determine more accurate variability within the samples. All data presented on the empty egg cases in this chapter are preliminary results, however they provide an indication of the potential use of hydrocarbon analysis for ageing.

Very little experimental work has been carried out for age determination of empty egg cases in blowflies, because ageing is very difficult to achieve, which is due to the shell no longer holding its shape once the larvae has hatched and characteristic features becoming difficult to visualise. Therefore, the results presented here offer potential of ageing the empty egg cases once the technique is developed further, because at present this seems to be the only means of providing an age indication for the empty egg cases.

5.3 Larvae

A common issue forensic entomologist are often faced with when presented with a crime scene is the dominance of third instar larvae, leading to a large time window corresponding to larval age at discovery.

Being able to age larvae is vital for accurate post mortem estimations to be established. The larvae can be aged according to their body size and weight, which increases with age [7,14]. Since larval development is directly related to temperature, it is therefore essential to take the temperature of the larvae feeding on the body as well as the ambient temperature at the crime scene. The length and weight of the larvae is then

compared against the temperature data and an estimate of the age can be established [5].

Other morphological characteristics are also examined such as the posterior spiracles, which determine the instar (Figure 5.6) as well as the mouthparts and the presence of the crop (Figure 5.7), which can establish whether larvae has progressed into the post-feeding stage of the life cycle.
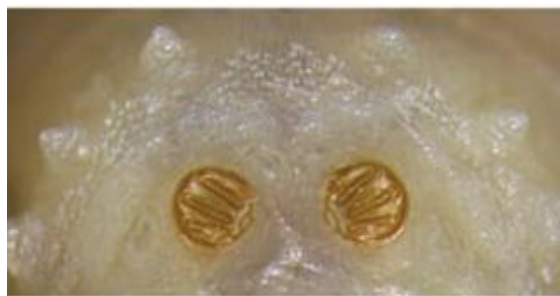
Figure 5.6: Posterior spiracles of the third instar larvae from *L. sericata* [24]
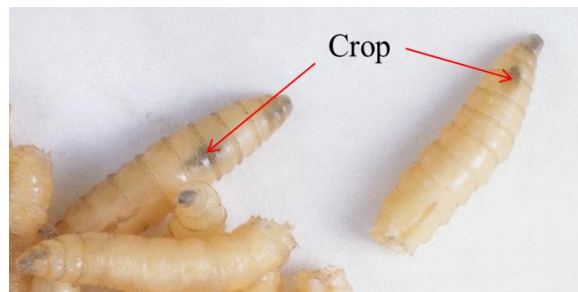
Figure 5.7: The crop of the third instar larvae

L. sericata is abundantly present at the early stages of decomposition [24,25]. However, currently only developmental charts exist to aid with the ageing of this species [5,11,12]. More work has been published on *C. vicina* in comparison to *L. sericata* [7,26–28]. The main area of research for *C. vicina* is in its developmental rates

at varying temperatures [7,11,26]. A few papers have examined the cuticular hydrocarbons to try to age this species [19,29] and the results presented showed great potential for using this technique to distinguish between and within larval life stages. Previous work published on *C. vomitoria* is mainly in the area of its development and it is known to have a longer life cycle than the closely related *C. vicina* [30]. As with *C. vicina*, there are some studies that have been carried out on the cuticular hydrocarbons of the species [19,29,31]. Recent papers have suggested that hydrocarbons could be used to establish the age of forensically important blowfly larvae as their profiles change over time [19,20]. Hydrocarbon analysis could potentially complement the current ageing techniques by presenting a more objective and reliable means of ageing the larvae of forensically important blowflies, allowing for a more accurate PMI estimation.

The data in this part of the chapter was extracted from the whole larval life span of *L. sericata*, *C. vicina* and *C. vomitoria*. Results from GC-MS analysis and subsequent results from PCA will be discussed in detail for each species.

5.3.1 Results and Discussion for larvae

C. vomitoria:

C. vomitoria exhibited a profile of 57 identifiable compounds with some co-eluting giving a total of 51 resolvable peaks (Table 5.3). Of these 51 resolvable peaks, 96% were hydrocarbons, with day 1 consisting of *n*-alkanes (28%), alkenes (29%) and mono-methyl alkanes (43%). The chain length of all hydrocarbons range from C16 to C33.

Table 5.3: List of all compounds from C20:H extracted from the larvae of *C. vomitoria* and their Kovats Indices to aid identification. Compounds in bold were used for subsequent PCA (peak numbers refer to numbers in Figure 5.8)

Peak Number*	Peak Identification	Kovats iu
1	Eicosane	2000
2	Heneicosene[1]	2066
3	Heneicosene[1]	2074
4	Henicosane	2100
5	**3-Methylhenicosane**	2172
6	Docosane	2200
7	**2-Methyldocosane**	2264
8	Tricosene[1]	2271
9	Tricosene[1]	2278
10	Tricosane	2300
11	**9+11-Methyltricosane**	2339
12	**7-Methyltricosane**	2343
13	**5-Methyltricosane**	2348
14	**3-Methyltricosane**	2374
15	Tetracosane	2400
16	**2-Methyltetracosane**	2464
17	Pentacosene[1]	2471
18	Pentacosene[1]	2478
19	Pentacosane	2500
20	**9+11-Methylpentacosane**	2536
21	**7-Methylpentacosane**	2539
22	**5-Methylpentacosane**	2549
23	**3-Methylpentacosane**	2574
24	Hexacosane	2600
25	**2-Methylhexacosane**	2665
26	Heptacosene[1]	2669
27	Heptacosene[1]	2679
28	Heptacosane	2700
29	**9+11-Methylheptacosane**	2735
30	**3-Methylheptacosane**	2774
31	Octacosane	2800
32	**2-Methyloctacosane**	2871
33	Nonacosene[1]	2879
34	Nonacosene[1]	2886
35	Nonacosane	2900
36	**11+13-Methylnonacosane**	2937
37	**7-Methylnonacosane**	2948

38	**5-Methylnonacosane**	2957
39	**Dimethylnonacosane**	2966
40	**3-Methylnonacosane**	2978
41	Tricontane	3000
42	Cholesterol + Hentriacontene[1]	3070
43	Hentriacontene[1]	3077
44	Hentriacontene[1]	3085
45	Hentriacontane	3100
46	**11+15-Methylhentriacontane**	3131
47	**3-Methylhentriacontane**	3175
48	Dotriacontane	3200
49	Tritriacontene[1]	3263
50	Tritriacontene[1]	3276
51	Tritriacontane	3300

[1] Double bond position assumed but not assigned to specific peaks

Figure 5.8 shows the chromatograms of a single sample from days 1, 4, 8 and 13. Chemical distinctions can be made between the different larvae ages from the chromatogram comparison because of the distinguishing changes over time. The shaded bars highlight some regions of contrast within the profiles of the different ages.

The lower retention time compounds of the profile are mainly made up of volatile compounds which are less stable and therefore excluded from PCA datasets. The middle section of the chromatogram consists of *n*-alkanes, alkenes and methyl branched alkanes (ranging from C23:H to C27:H). The higher end of the chromatogram is dominated by high molecular weight *n*-alkanes (ranging from C29:H to C33:H) and methyl branched alkanes which are at their most abundant in the 3rd instar larvae (Figure 5.10).

There are no compounds specific to the profile of day 1 larvae (1st instar). However,

there are a few compounds specific to (specific means >0.5% which depends on the amount extracted) certain larval ages, such as 3-MeC29:H and 3-MeC31:H, which are only seen with a relative peak area percentage greater than 0.5% in day 4. 3-MeC27:H and an unidentified DimeC29:H are specific to day 9 larvae (in a peak area exceeding 0.5%). These compounds are therefore good age indicators for these two larval ages.

2-MeC22:H is only present in the early larval life stages (days 1 to 3) and significantly decreases with age so the presence of this compound could be used to determine the early larval life age (1st and 2nd instar).

7-MeC23:H and 3-MeC23:H are present in a large concentration in day 3. 2-MeC24:H is present in substantial concentrations in days 1 and 2 then decrease with age, before an increase is seen in the late post-feeding stage. 9+11-MeC25:H and 2-MeC26:H also appear in a very high concentration in the immature larvae stages (days 1 and 2). Three peaks are absent (below the peak area threshold of 0.5%) from the 1st and 2nd instar larvae (3-MeC21:H, 9+11-MeC27:H and 11+15-MeC31:H) and three compounds are absent from the 1st instar larvae alone (compounds 5-MeC23:H, 3-MeC23:H and 7-MeC25:H). The absence of these compounds from the immature life stages makes them good age indicators.

A group of MeC23:H compounds (9+11-MeC23:H, 5-MeC23:H and 3-MeC23:H) increases significantly in the post-feeding stage (days 10 to 14), implying that they could act as a good post-feeding stage indicator. 7-MeC23:H is not present in a sufficient concentration in the late post-feeding stage (days 10 and 11), which again could potentially be a useful age indicator for this life stage. 11+15-MeC31:H is relatively stable over the first three instars after which a considerable increase in the

peak area concentration is observed in the post-feeding stage.

Figure 5.9 shows the methyl branched hydrocarbons plotted against the peak areas (total peak area percentage), allowing for patterns to be seen regarding the concentrations of individual compounds over time (see appendix 20 for the same graph as presented in Figure 5.9, but in relation to instars rather than the individual days).
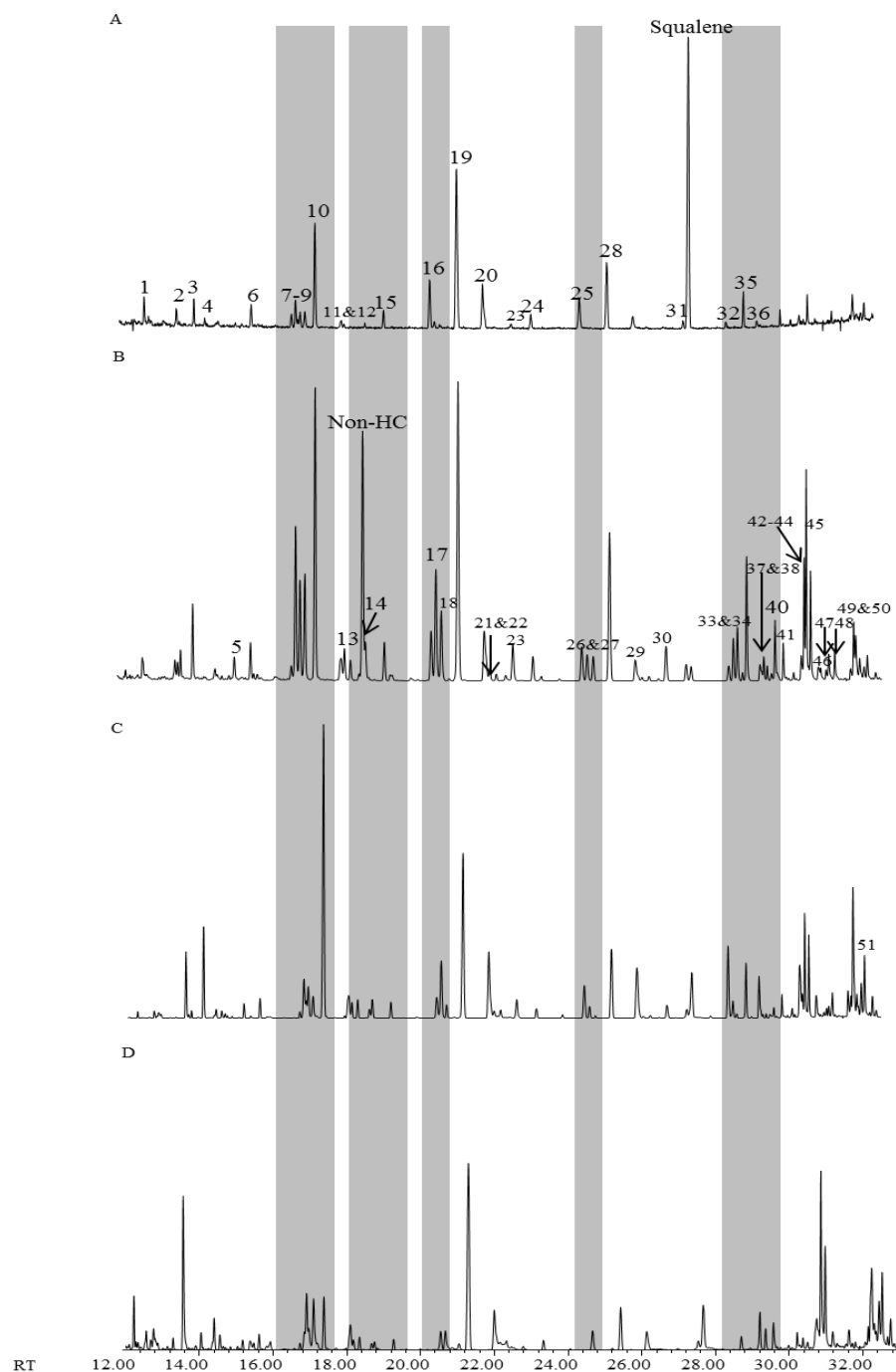
Figure 5.8: GC chromatograms of *C. vomitoria* larvae at four different ages, A: Day 1, B: Day 4, C: Day 8

and D: Day 13. Shaded bars illustrate distinctive changes over time indicating specific areas of interest
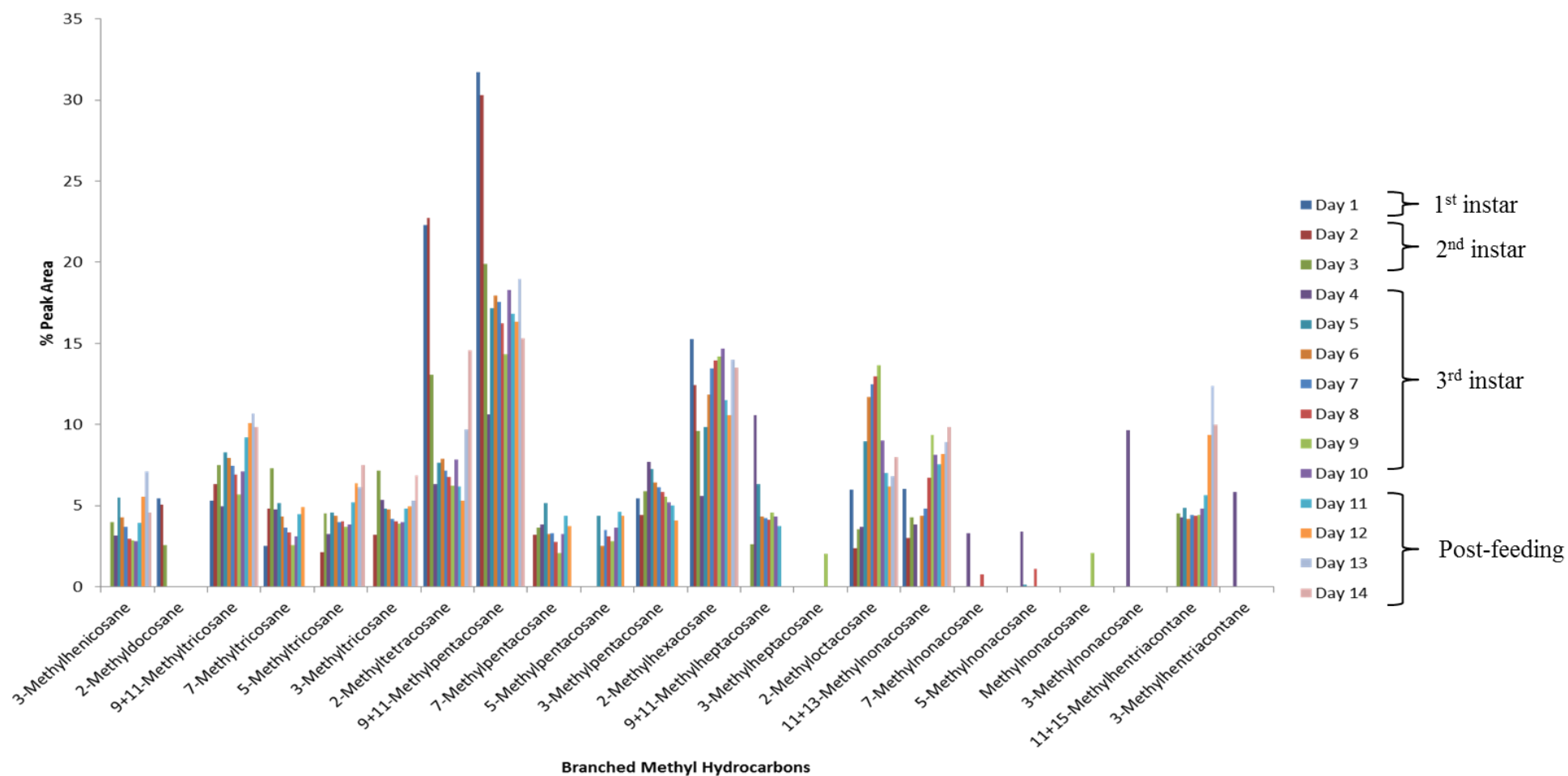
Figure 5.9: Graph of the average percentage peak area of each methyl branched hydrocarbon over the larvae extraction period for *C. vomitoria*
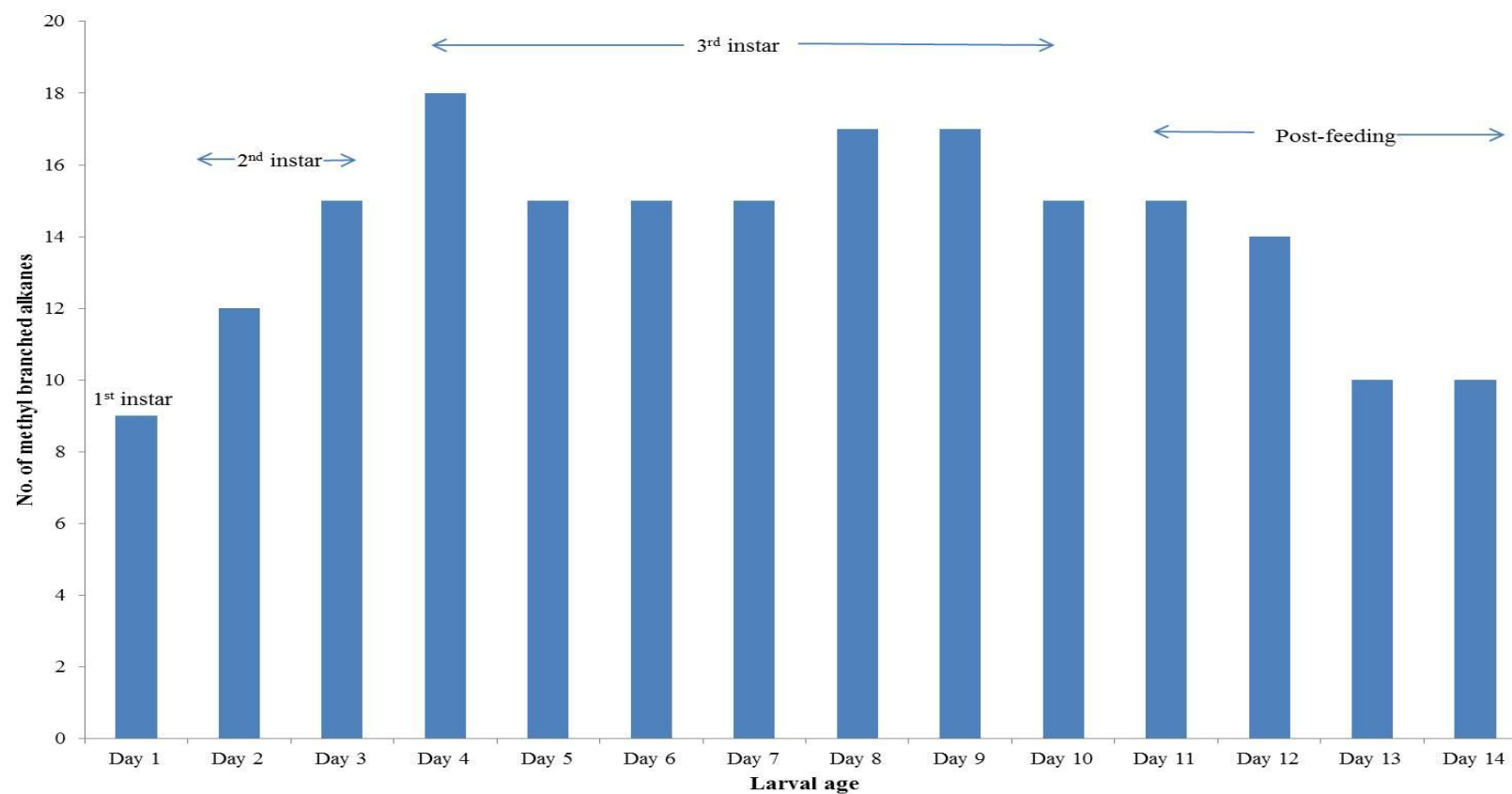
Figure 5.10: Graph showing the total number of methyl branched hydrocarbons present over the larvae life cycle for *C. vomitoria*

Figure 5.10 shows the total number of methyl branched alkanes present over the full larval life span.

Of the 51 resolvable peaks extracted from the cuticle of *C. vomitoria*, 29 of them were used for subsequent PCA (see chapter 3, section 3.2.4: *Larvae*). The *n*-alkanes were removed and the relative percentage was re-calculated based on the 29 compounds. Table 5.4 shows the compounds used along with the total percentage of each compound present, the percentage standard deviation for each day and the Kovats Index value for each compound.

Table 5.4: List of the compounds extracted and used for subsequent PCA analysis from the larvae of *C. vomitoria,* with the total percentage of each compound present, the percentage standard deviation for each day and the Kovats Index to aid identification

			Day 1	Day 2	Day 3	Day 4	Day 5	Day 6	Day 7
Peak	Peak	Kovats	*n*=10	*n*=10	*n*=10	*n*=10	*n*=10	*n*=10	*n*=10
no.	Identification	iu	%	%	%	%	%	%	%
5	3-Methylhenicosane	2172	tr	tr	3.97±0.68	3.16±0.61	5.47±2.49	4.27±0.51	3.70±1.00
7	2-Methyldocosane	2264	5.44±2.86	5.06±1.56	2.58±1.05	tr	tr	tr	tr
11	9+11-Methyltricosane	2339	5.32±4.90	6.31±2.67	7.47±2.17	4.96±1.65	8.30±3.96	7.93±1.13	7.47±2.21
12	7-Methyltricosane	2343	2.53±1.13	4.83±1.72	7.31±1.51	4.78±0.89	5.15±2.20	4.33±0.48	3.66±0.84
13	5-Methyltricosane	2348	tr	2.11±0.72	4.53±0.93	3.24±0.70	4.58±1.95	4.37±0.58	3.98±0.90
14	3-Methyltricosane	2374	tr	3.19±1.08	7.15±1.76	5.36±1.26	4.81±2.19	4.77±1.08	4.18±1.03
16	2-Methyltetracosane	2464	22.30±24.82	22.76±11.56	13.06±9.31	6.34±1.38	7.65±4.12	7.87±1.46	7.17±2.01
20	9+11-Methylpentacosane	2536	31.70±44.99	30.31±18.40	19.89±13.24	10.63±1.90	17.14±7.75	17.94±2.32	17.56±4.49
21	7-Methylpentacosane	2539	tr	3.19±1.47	3.63±0.91	3.82±1.77	5.14±2.78	3.24±0.91	3.28±1.04
22	5-Methylpentacosane	2549	tr	tr	tr	tr	4.35±2.52	2.49±0.96	3.48±1.03
23	3-Methylpentacosane	2574	5.45±6.96	4.44±2.04	5.87±1.99	7.69±1.25	7.27±3.24	6.41±0.79	6.14±1.57
25	12,22-Dimethylhexacosane[1], 12,20-Dimethylhexacosane[1]	2665	15.26±22.60	12.44±6.84	9.61±6.20	5.58±1.39	9.86±4.40	11.84±1.56	13.45±2.92
29	9+11-Methylheptacosane	2735	tr	tr	2.61±0.96	10.56±2.76	6.31±2.72	4.31±0.63	4.22±1.18
30	3-Methylheptacosane	2774	tr	tr	tr	tr	tr	tr	tr
32	2-Methyloctacosane	2871	5.98±4.83	2.36±0.86	3.56±2.47	3.67±0.99	8.98±3.96	11.69±1.06	12.46±2.63
36	11+13-Methylnonacosane	2937	6.02±5.39	2.99±1.35	4.27±2.98	3.82±1.08	tr	4.38±0.51	4.81±2.14
37	7-Methylnonacosane	2948	tr	tr	tr	3.31±1.80	tr	tr	tr
38	5-Methylnonacosane	2957	tr	tr	tr	3.39±1.12	0.10±0.32	tr	tr
39	Dimethylnonacosane	2966	tr	tr	tr	tr	tr	tr	tr

40	3-Methylnonacosane	2978	tr	tr	tr	9.62±2.57	tr	tr	tr
46	11+15-Methylhentriacontane	3131	tr	tr	4.50±5.66	4.26±1.97	4.88±2.35	4.16±0.49	4.44±1.28
47	3-Methylhentriacontane	3175	tr	tr	tr	5.82±1.96	tr	tr	tr

Peak no.	Peak Identification	Kovats iu	Day 8 n=10 %	Day 9 n=10 %	Day 10 n=10 %	Day 11 n=10 %	Day 12 n=10 %	Day 13 n=10 %	Day 14 n=10 %
5	3-Methylhenicosane	2172	2.97±1.13	2.87±1.03	2.83±0.43	3.92±0.89	5.54±1.93	7.10±2.82	4.55±1.97
7	2-Methyldocosane	2264	tr	tr	tr	tr	tr	tr	tr
11	9+11-Methyltricosane	2339	6.93±1.36	5.67±2.14	7.12±2.12	9.19±1.14	10.11±4.36	10.66±7.84	9.86±10.06
12	7-Methyltricosane	2343	3.33±0.62	2.57±0.92	3.11±0.67	4.48±0.77	4.89±1.95	tr	tr
13	5-Methyltricosane	2348	4.01±0.83	3.68±1.19	3.82±0.88	5.21±0.84	6.37±2.18	6.12±3.13	7.51±10.51
14	3-Methyltricosane	2374	4.05±1.03	3.90±1.41	4.00±1.00	4.83±0.86	4.97±2.17	5.32±2.00	6.88±10.70
16	2-Methyltetracosane	2464	6.76±1.48	6.25±2.17	7.86±6.63	6.19±1.05	5.32±2.40	9.71±6.52	14.59±9.64
20	9+11-Methylpentacosane	2536	16.23±2.94	14.32±5.08	18.29±12.81	16.82±1.87	16.33±7.39	18.98±13.12	15.29±9.74
21	7-Methylpentacosane	2539	2.78±0.36	2.08±0.85	3.22±1.22	4.37±1.14	3.75±2.88	tr	tr
22	5-Methylpentacosane	2549	3.12±0.37	2.81±1.04	3.66±1.12	4.60±1.20	4.39±3.29	tr	tr
23	3-Methylpentacosane	2574	5.86±0.74	5.55±1.81	5.21±2.07	5.01±0.95	4.09±1.22	tr	tr
25	12,22-Dimethylhexacosane[1], 12,20-Dimethylhexacosane[1]	2665	13.96±2.49	14.18±4.56	14.66±7.08	11.48±1.12	10.57±4.14	14.00±8.26	13.51±9.57
29	9+11-Methylheptacosane	2735	4.13±0.64	4.58±1.12	4.32±0.96	3.71±0.60	tr	tr	tr
30	3-Methylheptacosane	2774	tr	2.05±0.63	tr	tr	tr	tr	tr
32	2-Methyloctacosane	2871	12.95±2.97	13.66±3.43	9.00±1.24	7.00±0.79	6.17±2.60	6.81±4.27	7.98±10.56
36	11+13-Methylnonacosane	2937	6.71±1.19	9.36±2.47	8.13±2.00	7.53±0.90	8.16±2.94	8.91±5.54	9.83±10.14
37	7-Methylnonacosane	2948	0.77±0.31	tr	tr	tr	tr	tr	tr
38	5-Methylnonacosane	2957	1.09±0.49	tr	tr	tr	tr	tr	tr
39	Dimethylnonacosane	2966	tr	2.05±0.79	tr	tr	tr	tr	tr
40	3-Methylnonacosane	2978	tr	tr	tr	tr	tr	tr	tr
46	11+15-Methylhentriacontane	3131	4.37±1.81	4.42±1.86	4.80±0.90	5.65±0.73	9.36±3.59	12.38±5.99	10.00±10.05

| 47 | 3-Methylhentriacontane | 3175 | tr | tr | tr | tr | tr | tr | tr |

[1]Tentative identification based on Kovats Index values and match with NIST08 Library database

tr = Trace amount detected (<0.5%)

Statistical analysis was preliminary carried out on all three classes of hydrocarbons (*n*-alkanes, alkenes and methyl branched alkanes), shown in Figure 5.11.
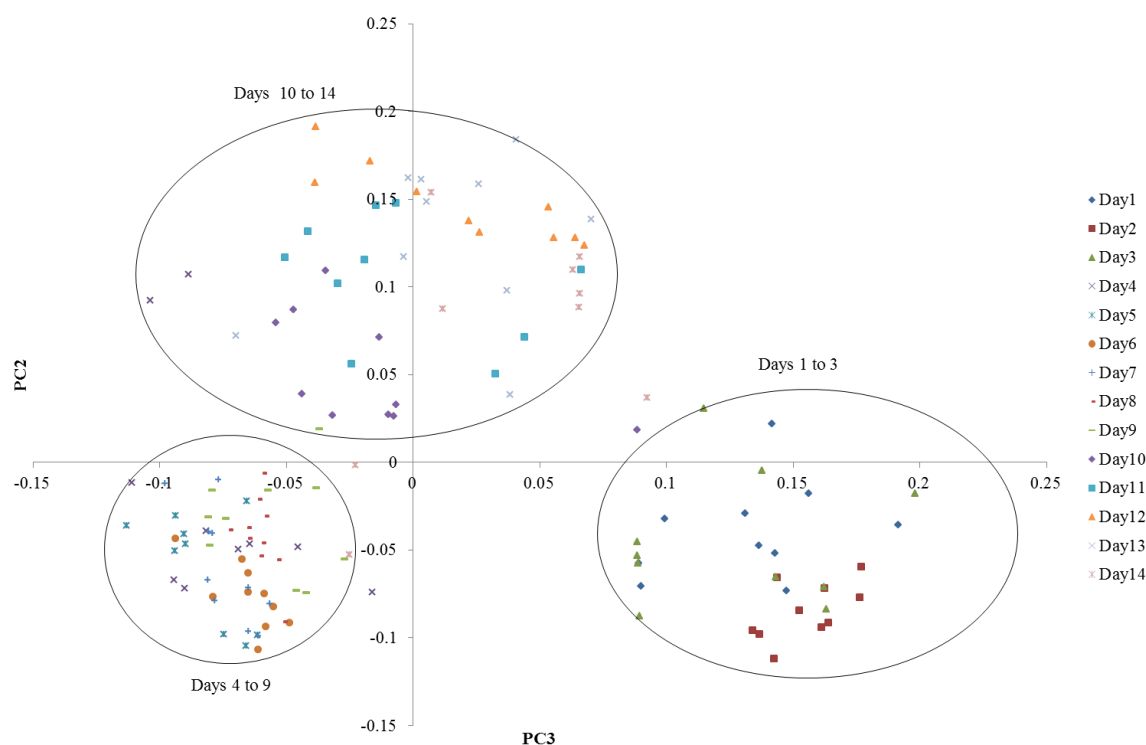
Figure 5.11: PCA plot showing PC3 against PC2 for *C. vomitoria* larvae using *n*-alkanes, alkenes and methyl branched alkanes, with clustering days circled

The initial PCA plot in Figure 5.11 shows three groups where samples are clustering. The group on the bottom right of the plot shows the principal components from days 1 to 3. The second group on the bottom left clusters days 4 to 9 and the final group clusters days 10 to 14. Only the post-feeding stage can be established by using this particular analysis. There is substantial scatter and although an age indication is possible it is impossible to age the other days accurately. Hereafter, analysis was

carried out on a second dataset that excluded the *n*-alkanes, shown in Figure 5.12.
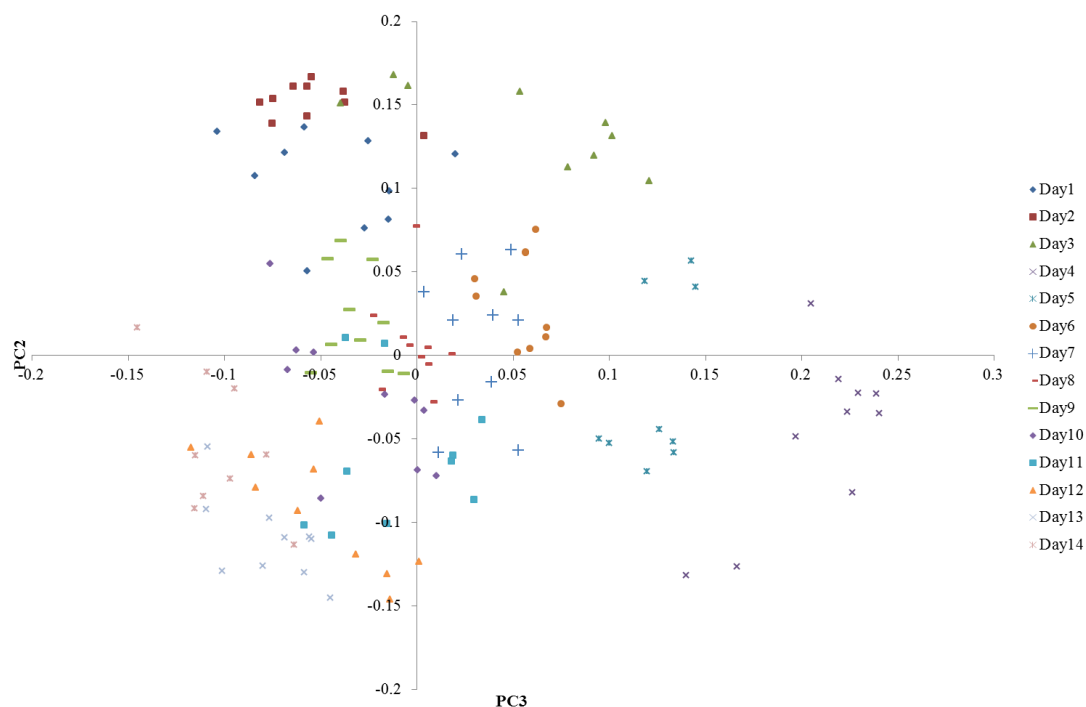
Figure 5.12: PCA plot showing PC3 against PC2 for *C. vomitoria* larvae using alkenes and methyl branched alkanes

The PCA plot in Figure 5.12 shows significantly more scatter when the *n*-alkanes are removed and cannot be used to classify the age of any of the extraction days. However, there is still a systematic direction within the days, which move clockwise around the plot.

PCA was then applied to a third dataset which included just the *n*-alkanes and the methyl branched alkanes (Figure 5.13).
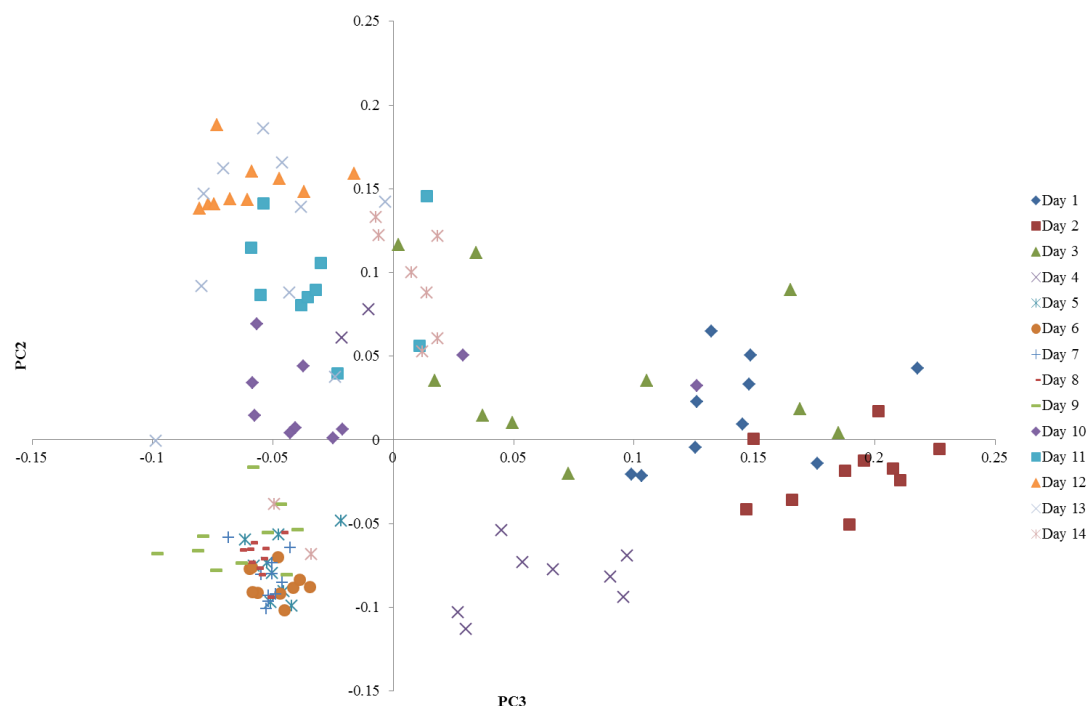
Figure 5.13: PCA plot showing PC3 against PC2 for *C. vomitoria* larvae using *n*-alkanes and methyl branched alkanes

The PCA plot in Figure 5.13 shows better clustering compared to Figure 5.12, with days 5 to 9 forming a group on the bottom left of the plot, but this is still not sufficient when trying to accurately age the larvae to the day. Hence, a final dataset (data presented in Table 5.4) was analysed consisting of just methyl branched alkanes shown in Figure 5.14. PCA was carried out using six principal components, describing 97.2% of the variation within the dataset, with the first four principal components comprising 73.3%, 8.6%, 6.6% and 4.1% respectively. PC3 and PC4 were used to plot the relevant scores (see appendix 21 for PCA eigenvalues).
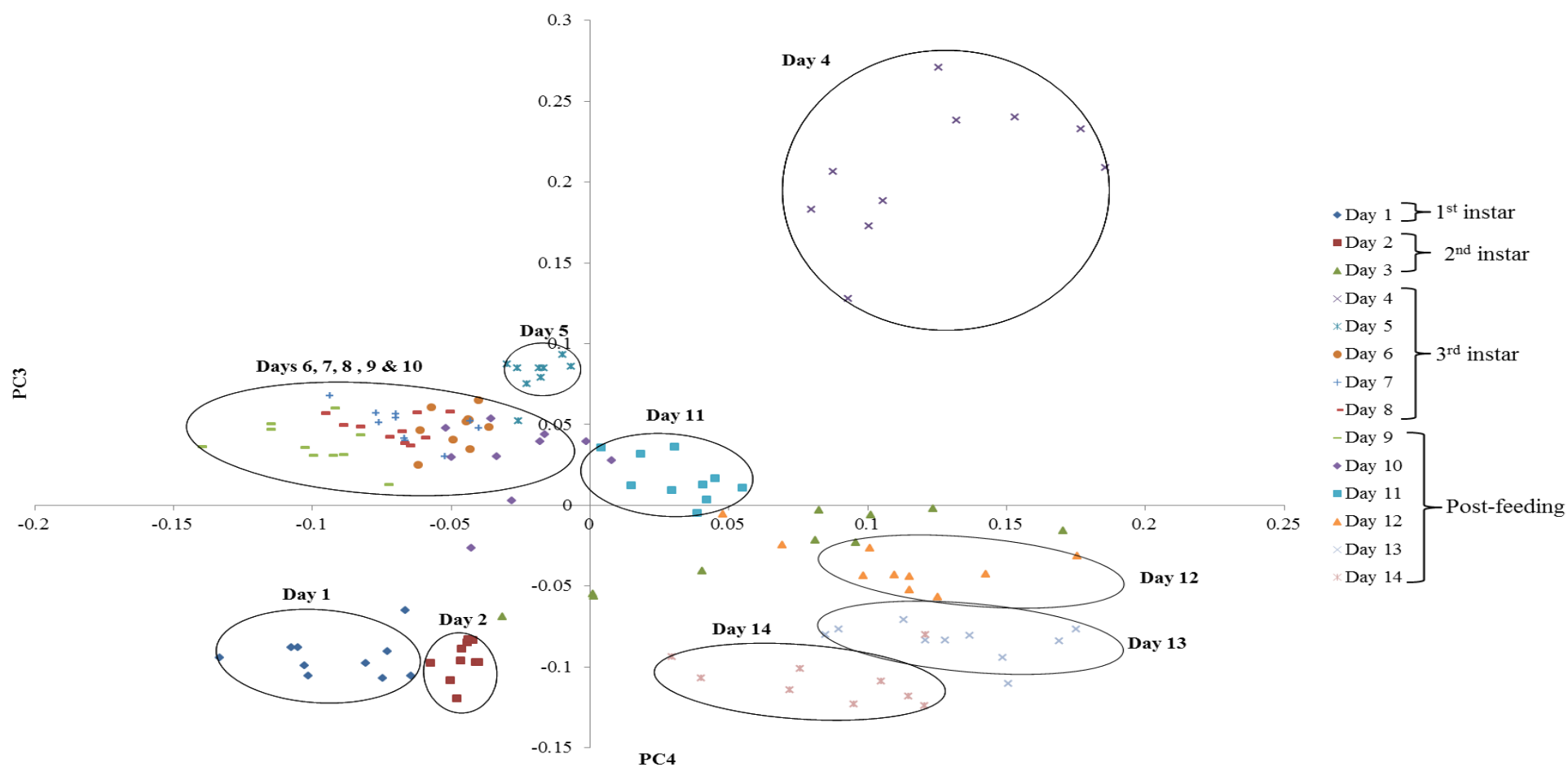
Figure 5.14: PCA plot showing PC4 against PC3 for *C. vomitoria* larvae using methyl branched alkanes only, with clustering days circled

This final PCA plot (Figure 5.14) gives significantly enhanced clustering within the PCA plot, allowing for ageing to be established to a much higher degree of accuracy, with the exception of day 3 which is extremely scattered and days 6 to 10 are all clustered within the same group. All of the other extracts can be aged to the individual days, even the post-feeding stage which is highly advantageous and a novel result.

The scatter seen in the PCA plot for day 3 indicates chemical changes associated with this age. There is a change in PC loadings between day 2 (2nd instar) to day 4 (3rd instar) and this scatter observed in day 3 indicates larvae going through the transition between these two instars and the PCA plots indicate substantial chemical changes are occurring within their profiles.

The Euclidean distances were calculated between the loadings for the data, taken in pairs, from each day of the experiment. This confirms that the greatest similarity is between days 1 and 2 ($d = 0.0842$) and days 6, 7 and 8 (3rd instar). The largest sequential differences in composition, for example between days 3 and 4 ($d = 0.3490$), are also reflected in this analysis (see appendix 22).

The PCA plot in Figure 5.14 allows ageing to be determined down to the day, with the exception of the third instar larvae. However, the post-feeding stage is often extremely difficult to age and there are no publications able to age this life stage accurately. This species therefore shows very promising results for ageing the post-feeding stage to the day.

C. vicina:

In total, *C. vicina* yielded a profile of 46 different identifiable compounds with some co-eluting resulting in a total of 40 resolvable peaks from day 1 to 11 (Table 5.5). All compounds were hydrocarbons consisting of *n*-alkanes (33%), alkenes (18%), and branched methyl hydrocarbons (50%) for day 1. The chain lengths ranged from C20:H to C33:H.

The lower molecular weight compounds in the profile are mainly made up of volatile compounds which are chemically less stable and therefore not used for subsequent PCA analysis as they show little significance in ageing the larvae. The middle region of the chromatogram consists of straight chain *n*-alkanes, alkenes and methyl branched alkanes (ranging from C23:H to C27:H). The higher end of the chromatogram is dominated by high boiling point *n*-alkanes (ranging from C29:H to C33:H) and methyl branched alkanes which are at their most abundant in the 1st and 2nd instar larvae.

Table 5.5: List of all compounds extracted from the larvae of *C. vicina* and their Kovats Indices to aid identification. Compounds in bold were used for subsequent PCA analysis (peak numbers refer to numbers in Figure 5.15)

Peak number	Peak Identification	Kovats iu
1	**Eicosene[1]**	1990
2	Eicosane	2000
3	Heneicosane	2100
4	**Docosene[1]**	2190
5	Docosane	2200
6	Tricosane	2300
7	**7-Methyltricosane**	2342
8	**5-Methyltricosane**	2351
9	**3-Methyltricosane**	2373
10	Tetracosane	2400
11	**2-Methyltetracosane**	2465
12	**Pentacosene[1]**	2471
13	**Pentacosene[1]**	2479
14	Pentacosane+Phthalate	2500
15	**11-Methylpentacosane**	2536
16	**9-Methylpentacosane**	2538
17	**7-Methylpentacosane**	2544
18	**5-Methylpentacosane**	2552
19	**3-Methylpentacosane**	2574
20	Hexacosane	2600
21	**x,12-Dimethylhexacosane[2] + Heptacosene[1]**	2666
22	**Heptacosene[1]**	2676
23	**Heptacosene[1]**	2679
24	Heptacosane	2700
25	**11+13-Methylheptacosane**	2735
26	**7-Methylheptacosane**	2743
27	**5-Methylheptacosane**	2753
28	**3-Methylheptacosane**	2775
29	Octacosane	2800
30	**2-Methyloctacosane**	2871
31	Nonacosane	2900
32	**11+13-Methylnonacosane**	2936
33	**9-Methylnonacosane**	2941
34	**7-Methylnonacosane**	2947
35	**3-Methylnonacosane**	2977
36	Triacontane	3000

37	**2-Methyltricontane**	3067
38	**2,6/2,8/2,10-Dimethyltriacontane[2]**	3097
39	Hentriacontane	3100
40	Tritriacontane	3200

[1]Double bond position assumed but not assigned to specific peaks

[2]Tentative Identification based on Kovats Index values and match with NIST08 Library database

Figure 5.15 shows the stacked GC chromatograms of a single sample from larvae extracted at days 1, 5, 7 and 11. The shaded bars highlight areas of contrast within the profiles showing potential for ageing the larvae of *C. vicina* because of the distinguishable chemical changes occurring with time.

The profile of the 1st instar (day 1) possesses no peaks specific to this stage. The 2nd instar, represented in day 2 also reveals no age specific compounds but there are eight peaks specific to both the 1st and 2nd instar stage, identified as 7-MeC27:H, 5-MeC27:H, 11+13-MeC29:H, 9-MeC29:H, 7-MeC29:H, 5-MeC29:H, 2-MeC30:H and 2,6/2,8/2,10-DimeC30:H. The number of methyl branched compounds is greatly reduced from the immature larvae stages (1st and 2nd) to the 3rd instar. This can be seen in Figure 5.15 in the highlighted areas on the two chromatograms of A (day 1-1st instar) and B (day 5 – 3rd instar).
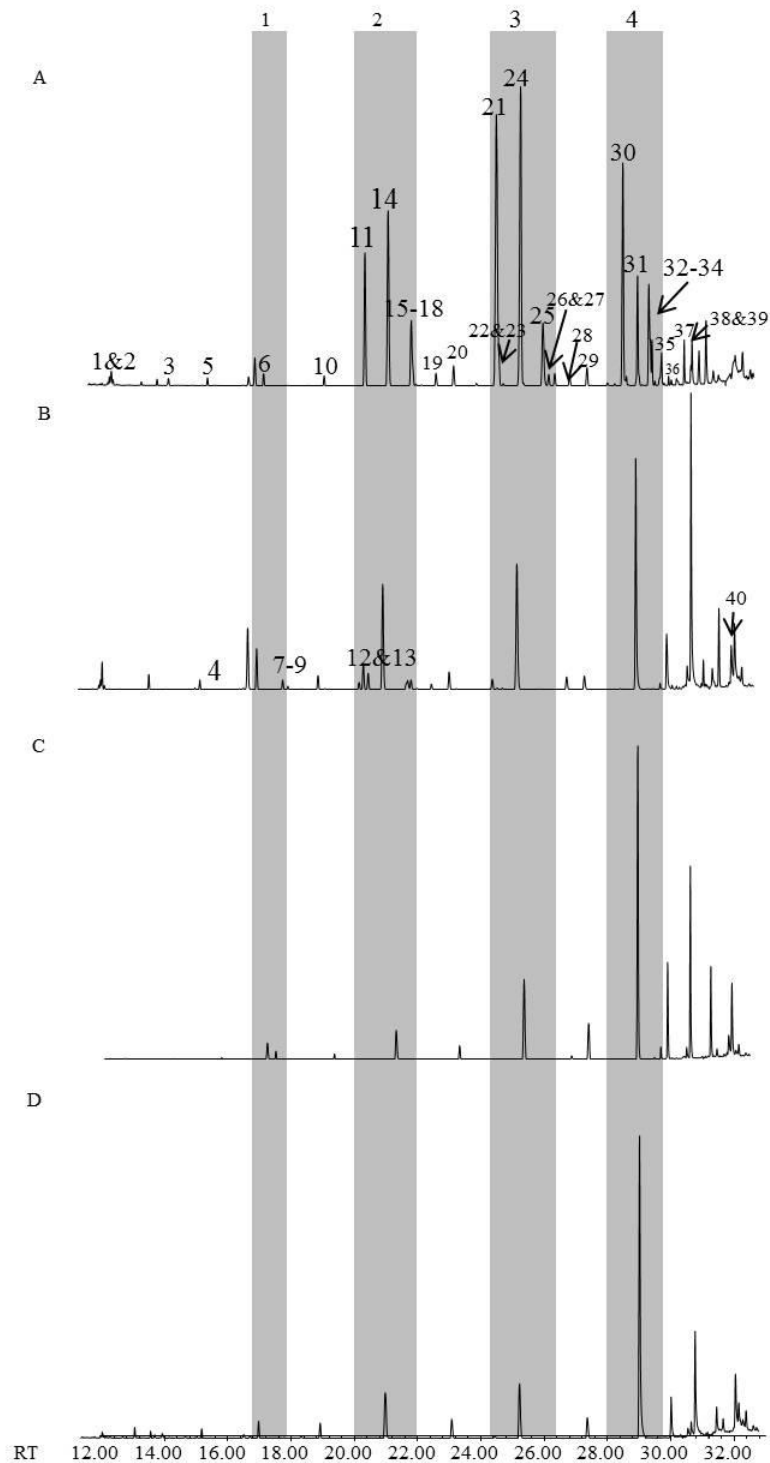
Figure 5.15: GC chromatograms of *C. vicina* larvae at four different ages, A: Day 1, B: Day 5, C: Day 7

and D: Day 11. Shaded bars illustrate distinctive changes over time indicating specific areas of interest

176

Peak 25 (mixture of 11+13-MeC27:H) is only detectable in an adequate concentration in days 1, 2 and 3, with the concentration decreasing with time.

Day 3 to day 5 reveal very similar chromatograms but with PCA they can be aged to the day rather than to the instar (3rd instar) because of the varying peak area ratios (Table 5.6). This instar has three compounds that are specific to this phase, 7-MeC23:H, 5-MeC23:H and 3-MeC23:H. This group of MeC23:H isomers (peak 7 to 9 in Figure 5.15) could be a very good age indicator for the 3rd instar stage, with the 7-MeC23:H (compound 7) also increasing further with age during the 3rd instar (Figure 5.16). Compound 17 is present in the larvae profiles until day 7 (early post-feeding).

The percentage abundance of this compound gradually increases with age, peaking at day 5 before rapidly decreasing and by day 8 its abundance is reduced to less than 0.5%. Compound 18, another MeC25:H, is also present up to day 7 and follows the same trend as compound 17, progressively increasing with time but this compounds percentage peaks at day 6, then decreases in day 7, and it is not observed in a sufficient concentration in day 8. Peak 21 (x,12-DimeC26:H) co-elutes with C27:1 in the younger larvae (up to day 2), making it a good age indicator. C21:1 and C22:1 (compounds 1 & 4) both increase gradually as the larvae age (up to 23% and 16% respectively), before decreasing in concentration in the late post-feeding stage at day 11. As the late post-feeding stage consists primarily of *n*-alkanes and a few methyl branched alkanes and alkenes, the relative percentage of the latter are very high in Table 5.6 as the *n*-alkanes were excluded from further analysis.

All of the branched methyl hydrocarbons and alkenes data are summarised in Figure 5.16 which shows the branched methyl hydrocarbons and alkenes against the average percentage peak area for each day (see appendix 23 for the same graph as presented in Figure 5.16, but in relation to instars rather than the individual days).

Figure 5.16: Graph of the average percentage peak area of the branched methyl alkane and alkene compounds over the extraction period of *C. vicina* larvae

179

Figure 5.17 displays the three classes of hydrocarbons found in the profile of *C. vicina* plotted against the number of compounds present for each group. Again, the number of *n*-alkanes remain the most consistent throughout the larvae life cycle with very little fluctuation observed. The only difference seen over time is the absence of C33:H in the 1st and 2nd instar. The number of alkenes reached their maximum in the 3rd instar stage. They steadily increase until they reach day 5 before decreasing and becoming consistent in the early post-feeding stage of days 6 and 7. There is a further loss of two alkenes (relative percentage dropping below 0.5%) before stabilising once again in the late post-feeding stage. This decrease of three alkenes (peak area falling below 0.5%) between the late 3rd instar and early post-feeding stage could be a good age indicator, as well as the second stabilisation observed in the late post-feeding stage.
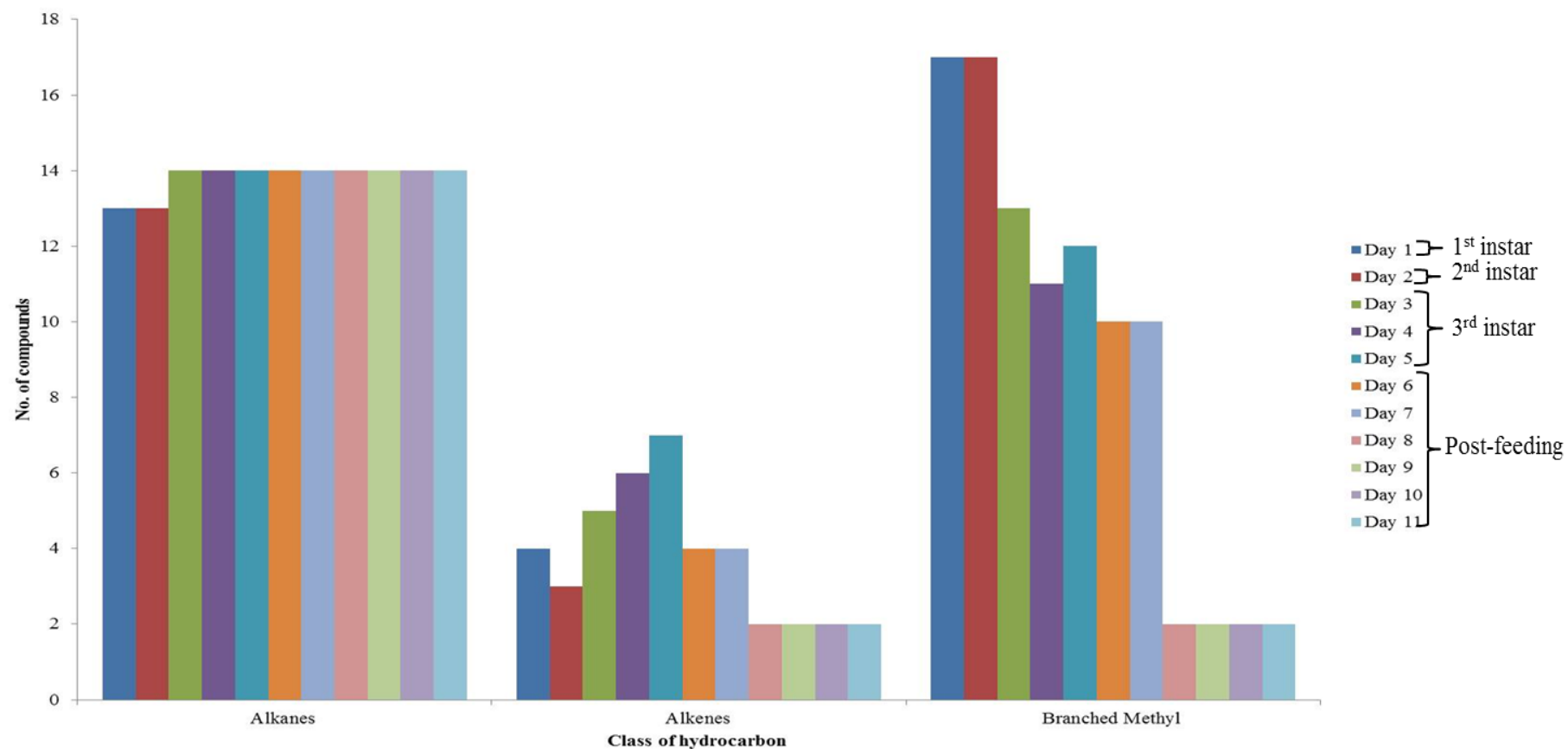
Figure 5.17: Graph showing the total number of alkanes, alkenes and methyl branched hydrocarbons present over the larvae life cycle for *C. vicina*

The branched methyl alkanes are most dominant in the 1st and 2nd instar stage. There is a gradual decrease before following the same pattern as the alkenes which remain constant in the early post-feeding stage before substantially decreasing when entering the late post-feeding (due to the loss of eight compounds), where they remain stable with just two branched methyl compounds remaining in the profile. The abundance of methyl branched hydrocarbons present in days 1 and 2 could act as another good age indicator as well as the decrease seen with time, followed by the significant loss of compounds between days 7 and 8.

All *n*-alkanes were removed for the final statistical analysis and the reasoning for this will be presented below. Of the 40 resolvable peaks extracted from the cuticle of *C. vicina* larvae, 27 were used for PCA analysis, of which 76% were branched and 24% of the hydrocarbons were alkenes. Table 5.6 shows the compounds used for PCA analysis, along with the total percentage of each compound present, the percentage standard deviation for each day and the Kovats Indices.

Table 5.6: List of the compounds extracted and used for subsequent PCA analysis from the larvae of *C. vicina,* with the total percentage of each compound present, the percentage standard deviation for each day and the Kovats Indices to aid identification.

Peak number	Peak Identification	Kovats iu	Day 1 n=10 %	Day 2 n=10 %	Day 3 n=10 %	Day 4 n=10 %	Day 5 n=10 %	Day 6 n=10 %	Day 7 n=10 %	Day 8 n=10 %	Day 9 n=10 %	Day 10 n=10 %	Day 11 n=10 %
1	Eicosene[1]	1990	1.79±0.68	3.52±1.54	5.48±2.47	3.55±0.64	4.55±2.12	7.19±3.07	6.61±1.36	9.62±2.60	23.23±17.18	23.77±5.38	14.59±12.54
4	Docosene[1]	2190	tr	tr	tr	tr	3.26±1.51	5.52±1.35	5.79±1.24	8.59±2.47	17.03±10.91	16.43±4.43	11.93±9.49
7	7-Methyltricosane	2342	tr	tr	4.43±2.13	4.76±1.49	5.60±3.23	tr	tr	tr	tr	tr	tr
8	5-Methyltricosane	2351	tr	tr	2.44±1.23	2.21±0.76	2.92±1.77	tr	tr	tr	tr	tr	tr
9	3-Methyltricosane	2373	tr	tr	2.48±1.25	tr	2.79±1.55	tr	tr	tr	tr	tr	tr
11	2-Methyltetracosane	2465	12.55±4.83	8.12±5.46	5.07±3.02	4.40±1.40	5.05±3.13	4.75±1.16	8.14±2.93	13.23±9.07	20.76±13.98	15.78±5.01	18.20±15.51
12	Pentacosene[1]	2471	tr	tr	13.88±7.34	14.89±5.04	12.35±6.91	13.06±5.15	tr	tr	tr	tr	tr
13	Pentacosene[1]	2479	tr	tr	11.24±6.25	11.79±4.36	8.94±5.27	8.99±4.20	tr	tr	tr	tr	tr
15	11-Methylpentacosane	2536	9.90±3.93	5.34±1.26	4.59±2.93	4.17±1.37	4.53±2.49	4.63±1.63	6.78±1.62	8.87±2.63	tr	tr	tr
16	9-Methylpentacosane	2538	2.49±1.08	2.13±0.44	3.74±2.15	4.42±1.69	5.62±3.04	5.33±2.03	4.88±0.78	5.78±1.78	tr	tr	tr
17	7-Methylpentacosane	2544	1.48±0.76	2.66±0.46	4.80±3.12	6.15±2.70	8.43±4.54	7.25±2.50	6.21±1.73	tr	tr	tr	tr
18	5-Methylpentacosane	2552	1.16±0.60	1.63±0.68	2.09±1.47	2.49±1.55	3.80±2.98	4.42±1.98	3.38±1.73	tr	tr	tr	tr
19	3-Methylpentacosane	2574	2.19±1.21	2.41±0.87	4.06±2.68	4.97±1.97	4.92±2.66	4.90±1.78	5.24±1.21	5.76±1.95	tr	tr	tr
21	x,12-Dimethylhexacosane[2] + Heptacosene	2666	37.91±26.98	38.39±25.62	17.51±11.18	14.61±4.73	8.87±4.84	9.41±2.44	16.12±5.84	29.33±15.37	38.97±22.46	44.02±15.38	55.28±39.23
22	Heptacosene[1]	2676	1.97±0.88	tr	tr	4.79±1.70	4.30±2.50	tr	tr	tr	tr	tr	tr
23	Heptacosene[1]	2679	0.58±0.35	1.95±0.31	4.32±2.31	4.56±1.96	3.12±1.73	tr	tr	tr	tr	tr	tr
25	11+13-Methylheptacosane	2735	8.29±3.64	6.45±4.78	3.98±2.00	tr	tr	tr	tr	tr	tr	tr	tr
26	7-Methylheptacosane	2743	1.47±0.86	1.67±1.59	tr	tr	tr	tr	tr	tr	tr	tr	tr

183

#	Compound	KI											
27	5-Methylheptacosane	2753	1.37±0.84	1.63±1.52	tr	tr	tr	tr	tr	tr	tr	tr	tr
28	3-Methylheptacosane	2775	1.03±0.86	2.08±1.44	6.15±3.65	8.10±3.06	8.04±4.85	11.47±4.61	17.47±1.83	8.76±3.51	tr	tr	tr
30	2-Methyloctacosane	2871	8.53±7.04	11.28±16.23	3.74±2.65	4.14±2.32	2.91±1.67	4.46±1.21	4.95±1.35	tr	tr	tr	tr
32	11+13-Methylnonacosane	2936	2.75±2.87	3.78±5.39	tr	tr	tr	tr	tr	tr	tr	tr	tr
33	9-Methylnonacosane	2941	1.01±0.97	1.48±1.97	tr	tr	tr	tr	tr	tr	tr	tr	tr
34	7-Methylnonacosane	2947	1.25±1.22	1.85±2.58	tr	tr	tr	tr	tr	tr	tr	tr	tr
35	3-Methylnonacosane	2977	tr	tr	tr	tr	tr	8.63±4.57	14.44±3.31	10.05±7.41	tr	tr	tr
37	2-Methyltricontane	3067	1.46±1.15	2.77±2.34	tr	tr	tr	tr	tr	tr	tr	tr	tr
38	2,6/2,8/2,10-Dimethyltriacontane[2]	3097	0.81±0.92	0.88±0.63	tr	tr	tr	tr	tr	tr	tr	tr	tr

[1]Double bond position assumed but not assigned to specific peaks

[2]Tentative identification based on Kovats Index values and match with NIST08 Library database

tr = Trace amounts detected <0.5%

Statistical analysis was initially carried out on all three classes of hydrocarbons (*n*-alkanes, alkenes and methyl branched alkanes), shown in Figure 5.18
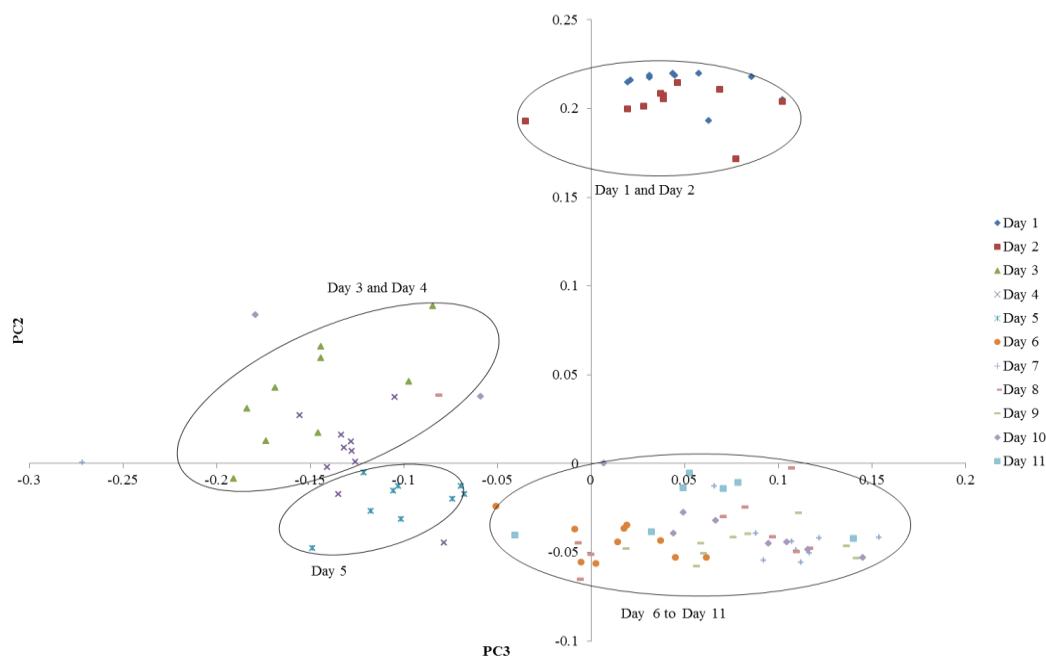
Figure 5.18: PCA plot showing PC3 against PC2 for *C. vicina* larvae using *n*-alkanes, alkenes and methyl branched alkanes, with clustering days circled

Figure 5.18 shows four areas of clustering within the plot, however, a fair amount of scatter is observed within the groups and it cannot be used to accurately age the larvae. Therefore, PCA was applied to an alternative dataset consisting of just alkenes and methyl branched alkanes (Figure 5.19). PCA was carried out on this adjusted dataset using 6 principal components describing 96.9% of the variation within the dataset with the first three comprising 60.5%, 20.3% and 8.9% respectively (for Figure 5.16). PC2 and PC3 were used to plot the relevant scores (see appendix 24 for PCA eigenvalues).
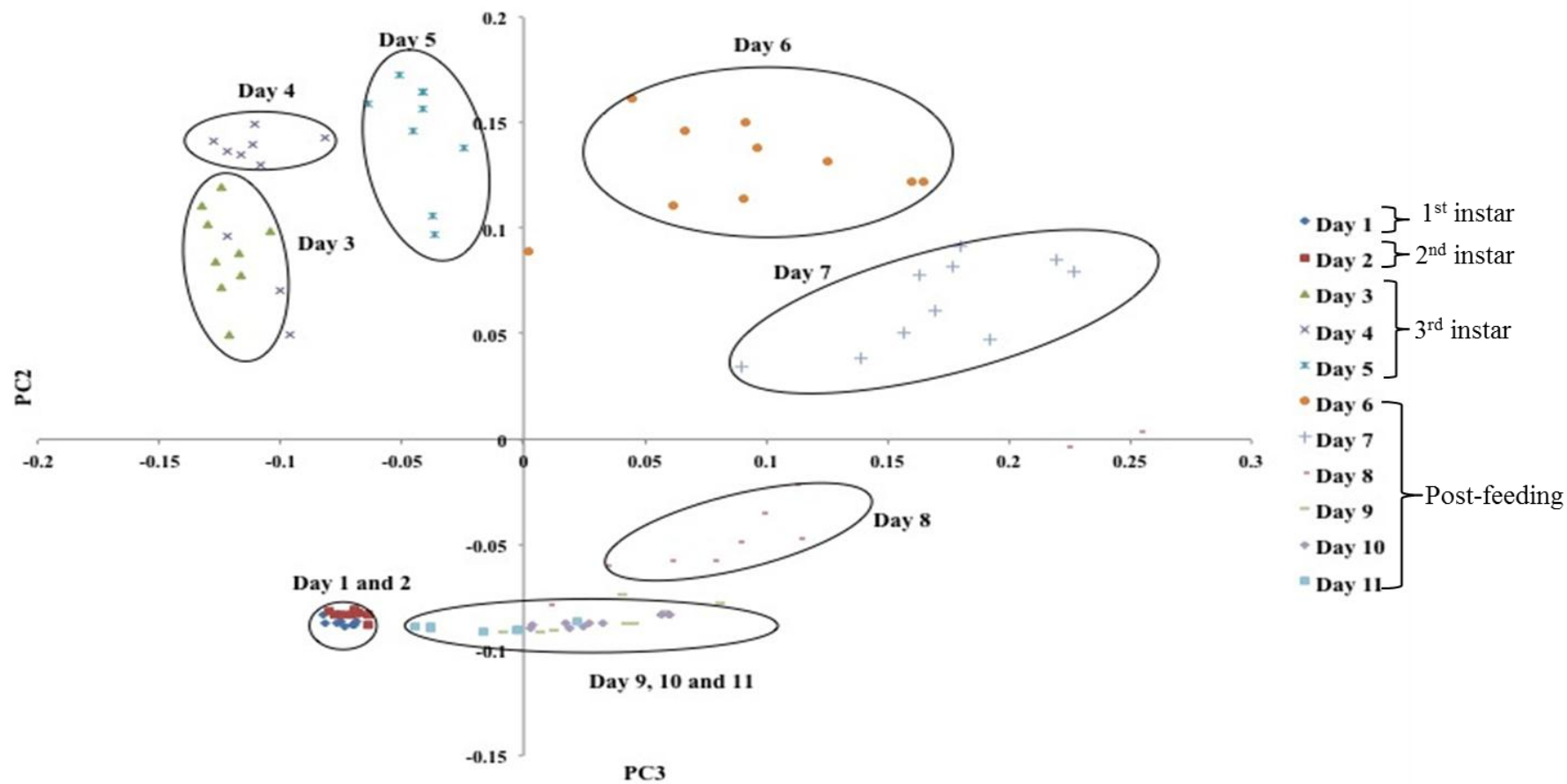
Figure 5.19: PCA plot showing PC3 against PC2 for *C. vicina* larvae using alkenes and methyl branched alkanes only, with clustering days circled

186

Figure 5.19 shows the PCA plot of PC3 vs PC2 for data gathered from day 1 to day 11 of larvae extractions of *C. vicina*. There are now eight clusters within the plot allowing for the larvae to be aged down to the day with the compromise of days 1 and 2 the late post-feeding stage (days 9 to 11).

Although day 1 has a single compound specific to that day, day 1 and day 2 have eight compounds detectable only in those two instars (1st and 2nd instar), hence the likely reasoning for these two instars clustering together in the PCA plot in Figure 5.19. There is a substantial change within the PCA plot from day 2 to day 3, which represents the transition between the 2nd and 3rd instar.

The main compounds which have substantial score values are x,12-DimeC26:H which co-elutes with C27:1 in the early larval stages. Another compound exhibiting a high score is 2-MeC24:H. Both methyl branched hydrocarbons are present throughout the larval life cycle for *C. vicina*.

The Euclidean distances were calculated between the loadings for the data, taken in pairs, from each day of the experiment. This confirms that the greatest similarity is between days 9, 10 and 11 ($d = 0.098$, $d=0.1017$), which relates to the late post-feeding stage. The largest sequential differences in composition, for example between days 5 and 6 ($d = 0.3218$), are also reflected in this analysis (see appendix 25).

From the results presented in this section of the chapter, it has been shown that age related changes can be seen over time, showing potential for ageing the larval stages of the life cycle of *C. vicina*.

The PCA plot in Figure 5.19 shows the potential to age the larvae down to the day, with the exception of the 1st and 2nd instar larvae (days 1 and 2) and late post-feeding larvae (days 9 to 11). The very tight clustering observed in days 1 and 2 maybe due to the eight methyl branched compounds, which are specific to these two days.

Day 3 has a few principal components within its clustering region from day 4, indicating some of the extracted larvae were developing at a slightly faster rate than others.

The clusters seen in the PCA plot form a systematic sequence that tracks the chemical changes. Starting from days 1 and 2 on the bottom left, the changes can be followed in a large clockwise direction. The large jump from days 1 and 2 to day 3 corresponds to the chemical change going from the 1st and 2nd instar to the 3rd instar.

L. sericata:

In total, *L. sericata* yielded a profile of 60 different compounds (of which 57 were identifiable) with some co-eluting giving a total of 56 resolvable peaks from day 1 (day of emergence) to day 9 (Table 5.7) (for extraction methodology refer to chapter 3, section 3.2.4: *Larvae*). The hydrocarbons present made up 64% of the total number of compounds in the profile and consisted of *n*-alkanes, alkenes and mono- and di-methyl alkanes. The chain lengths ranged from C16:H to C33:H. Other compounds present consisted of steroids (11%), acids (7%), alcohols (5%), amides (4%) and other compounds belonging to various other classes (9%).

Table 5.7: List of all compounds extracted from the larvae of *L. sericata* and their Kovats Indices to aid identification. Compounds in bold were used for subsequent PCA (peak numbers refer to numbers in Figure 5.20)

Peak number	Peak ID	Kovats i.u
1	Hexadecane	1600
2	Heptadecane	1700
3	Tetramethylheptadecane	1754
4	**Octadecene[1]**	1790
5	**Octadecane**	1800
6	Unknown	1854
7	Tetramethyloctadecene	1864
8	Hexadecanol	1886
9	Hexadecenoic acid[1]	1944
10	Hexadecenoic acid[1]	1949
11	Unknown	1969
12	Dimethylnonadecane	1983
13	Dimethylnonadecane	1988
14	**Eicosane**	2000
15	**Octadecanol[2]**	2052
16	**Octadecanol[2]**	2088
17	Octadecenoic acid[2]	2130
18	Ethylhexylcinnamate[2]	2138
19	Hexadecanamide[2]	2147
20	Octadecanoic acid[2]	2148
21	Dimethylhenicosane	2193
22	**Docosane**	2200
23	Unknown	2275
24	**Tricosane**	2300
25	**Octadecenamide[2] + 11-Methyltricosane**	2311
26	5-Methyltricosane	2350
27	Hexanedioic acid, ethylhexyl ester[1]	2377
28	**Tetracosane**	2400
29	**Pentacosene[1]**	2469
30	Pentacosane + Phthalate[3]	2500
31	**9+11-Methylpentacosane**	2537
32	**7-Methylpentacosane**	2544

33	**5-Methylpentacosane**	2551
34	**3-Methylpentacosane**	2574
35	**Hexacosane**	2600
36	**12,22+12,20diMethylhexacosane**	2675
37	**Heptacosene[1]**	2680
38	**Heptacosene[1]**	2687
39	**Heptacosane**	2700
40	**11-Methylheptacosane**	2734
41	3-Methylheptacosane	2775
42	**Octacosane**	2800
43	Squalene	2809
44	**2-Methyloctacosane**	2868
45	**Nonacosane**	2900
46	**Tricontane**	3000
47	Steroid[3]	3073
48	**Hentriacontene[4]**	3084
49	**Hentriacontane**	3100
50	Steroid[4]	3191
51	**Dotriacontane**	3200
52	Steroid[4]	3254
53	Steroid[4]	3295
54	**Tritriacontane**	3300
55	Steroid[4]	N/A
56	Steroid[4]	N/A

[1]Double bond position determined but not assigned to specific peaks

[2]Tentative identification based on Kovats Index values and match with NIST08 Library database

[3]Co-eluting compounds, hence not used in PCA analysis

[4]Only identified as a compound belonging to the class of steroids

The lower section of the GC trace is made up of volatile compounds as well as *n*-alkanes, alkenes and alcohols but many of the smaller less dominant peaks are complex branched compounds that are difficult to interpret and fully identify. The middle

section of the GC trace is principally made up of straight chain *n*-alkanes, C23:H (peak 24), C24:H (compound 28), C25:H (compound 30), C26:H (compound 35), C27:H (compound 39), and a group of branched alkanes (peaks 31- 34) that are only present in younger larvae (day 1 to day 5). The higher end of the chromatogram is dominated by long chain *n*-alkanes (C29:H to C32:H) and a few alkenes, of which C31:1 (compound 48) is present in substantial amounts. The longest chain length detectable for this species is C33:H (compound 54) but as previous papers have suggested, there may be much longer chain lengths present if samples were analysed using a different high temperature column [32].

Figure 5.20 shows the GC chromatograms of a single larvae sample from days 3, 5, 7 and 9. When observing the chromatograms, chemical distinctions can be made between the different larval ages clearly showing a potential for ageing the larvae. The shaded bars show some areas of contrast within the profiles of the different days. The 1st instar (day 1) has a compound specific for that day, 2-MeC28:H (Table 5.8, peak 44). Although this compound is present in larvae up to three days old, it is only present in very small amounts. The 2nd instar, represented in day 2 and day 3 are chemically very similar in relation to the compounds present but the ratios of the peak areas alter between the two ages. However, this was not enough to be able to distinguish between these two days.
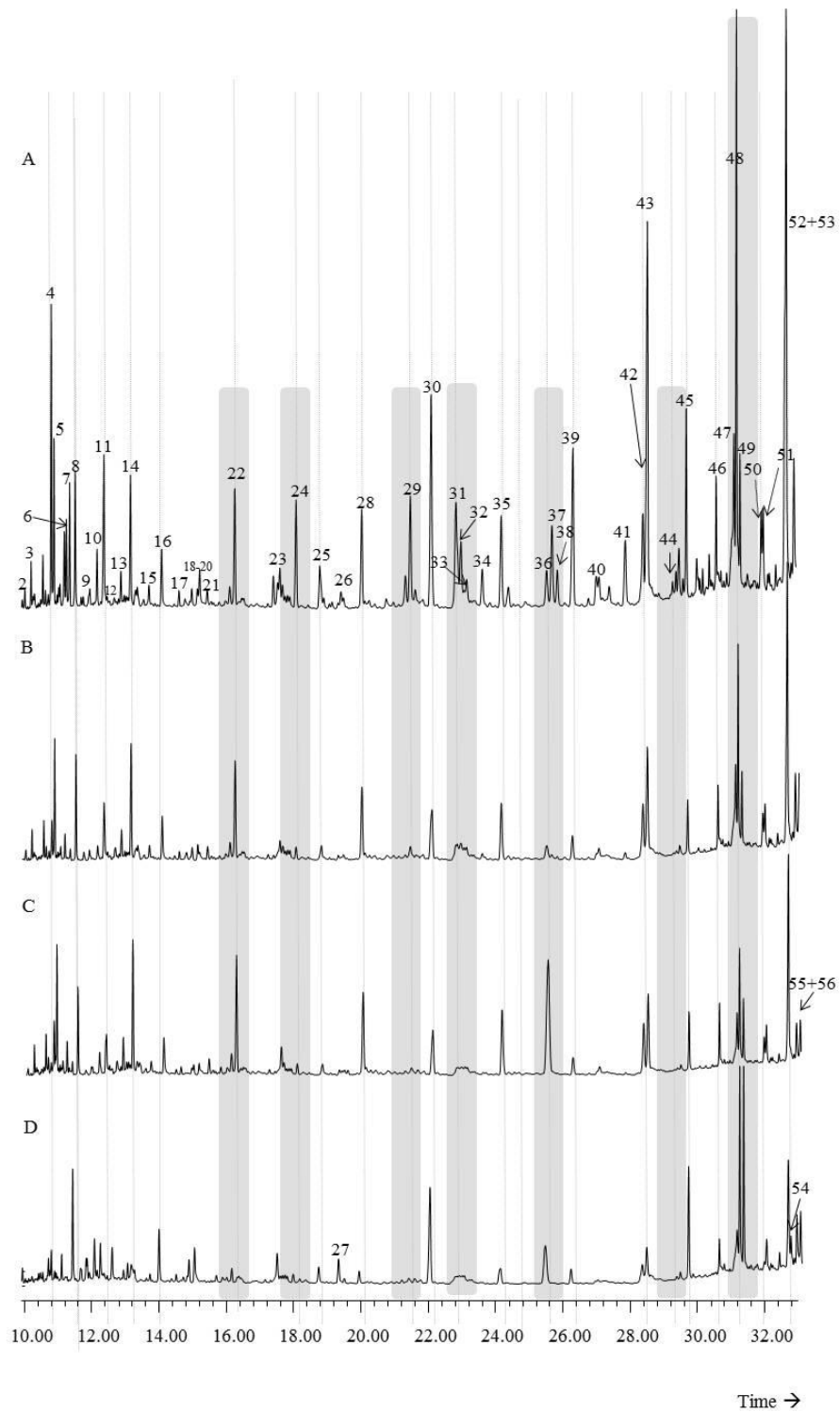
Figure 5.20: GC chromatograms of *L. sericata* larvae at four different ages, A: Day 3, B: Day 5, C: Day

7 and D: Day 9. Shaded bars illustrate distinctive changes over time indicating specific areas of interest

192

The 1st and 2nd instar larvae in general had a number of branched hydrocarbons present that were significantly reduced from day 5 onwards. This can clearly be seen in Figure 5.20 in the highlighted areas. As seen with the 2nd instar, the 3rd instar (day 4 and day 5) gives very similar chromatograms but the peak area ratios vary considerably more, enabling them to be aged to the day, rather than just to the instar. Day 6 is characterised by the start of an increase in the amounts present for peak 36, a mixture of two DimeC26:H, present in substantial quantities in days 7 to 9. As the larvae reach the post-feeding stage this coincides with C31:1 (peak 48) and C31:H (peak 49) being present in almost equal amounts in contrast to earlier days where C31:1 is the more abundant of the two.

11-MeC23:H (peak 25) is present from day 2 to day 5 as a co-eluting peak with octadecenamide. However, from day 6 onwards its presence decreases to a concentration lower than 0.5%, which could be another good age indicator for the post feeding stage.

Day 7 yields a chromatogram similar to day 6. The late post-feeding stage, day 8 and day 9, are the only two days to have C33:H (compound 54) present in quantifiable amounts. Figure 5.21 shows the total number of compounds plotted against the class of hydrocarbons, which can be split into three groups, *n*-alkanes, alkenes and methyl branched alkanes.
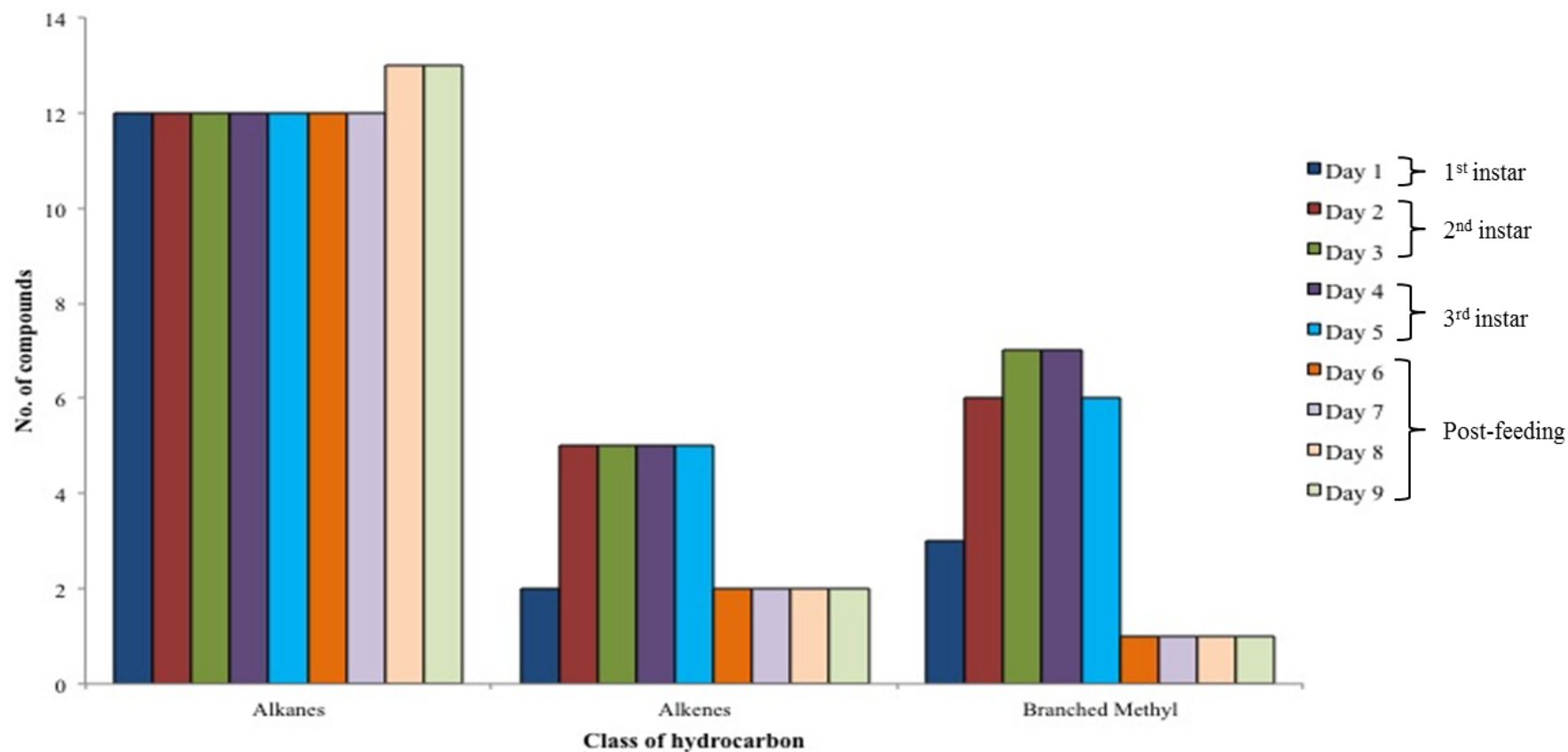
Figure 5.21: Graph showing the total number of *n*-alkanes, alkenes and methyl branched hydrocarbons present over the larvae life cycle for *L. sericata*

It is clear to see that the number of *n*-alkanes remains the most consistent throughout the life cycle. The only change seen over time is C33:H which appears in a significant concentration (3.5% vs <0.5% in days 1 to 7) in the late post-feeding stage of day 8 and 9. The number of alkenes and methyl branched alkanes present are higher in the 2nd and 3rd instar stage of the life cycle (days 2 to 5). The decrease of these latter two classes of hydrocarbons from day 6 onwards could be a good age indicator as the larvae progress into the post-feeding stage.

Although the number of *n*-alkanes remains fairly consistent throughout the larval life cycle, there is variation within the percentage of each *n*-alkane, as is clearly seen in Figure 5.22, which shows that the relative percentage of the high molecular weight odd numbered *n*-alkanes (C29:H, C31:H and C33:H) increase with age whilst the lower molecular weight mid-chain length *n*-alkanes (e.g. C22:H) gradually increase with time before sharply decreasing in the late post-feeding stage (see appendix 26 for the same graph as presented in Figure 5.22, but in relation to instars rather than the individual days).
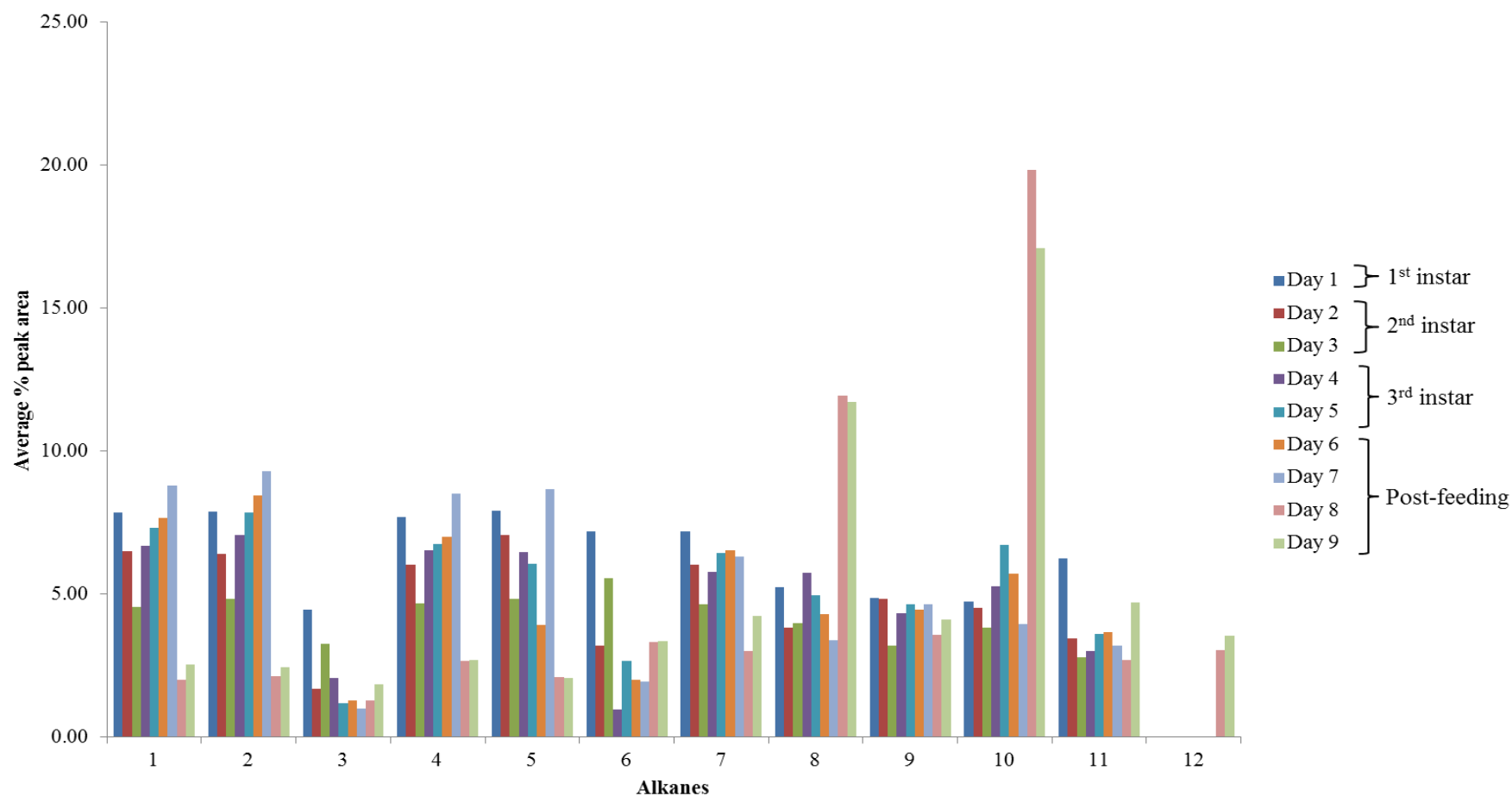
Figure 5.22: Graph of the average percentage peak area with error bars for selected *n*-alkanes over the larvae extraction period for *L. sericata*

In the previous analysis, polar compounds were excluded from the larvae analysis of all three species since the focus in this research was on hydrocarbon changes in ageing. Any steroid compounds were also removed from the dataset, as they are believed to originate internally and hence are less relevant to this study of cuticular chemistry. However, compounds which yielded consistent relative peak areas greater than 1% were always included in the analysis (e.g. peaks 15 and 16). C25:H was not included in the final PCA results for any of the larvae species presented in this chapter because unfortunately it was co-eluting with a phthalate impurity (probably from the dishes the larvae were kept in) and therefore it was not possible to do a representative manual integration as this could have led to misleading results.

Of the 56 resolvable peaks detected 28 were used in the subsequent analysis. Table 5.8 gives the average total percentage of these compounds for day 1 up to day 9.

Table 5.8: List of the compounds extracted and used for subsequent PCA analysis from the larvae of *L. sericata,* with the Kovats Indices to aid identification

Peak number	Peak Identification	Kovats iu	Day 1 n=10 %	Day 2 n=10 %	Day 3 n=10 %	Day 4 n=10 %	Day 5 n=10 %	Day 6 n=10 %	Day 7 n=10 %	Day 8 n=10 %	Day 9 n=10 %
4	Octadecene[1]	1790	tr	1.46±0.46	5.05±0.69	4.65±0.76	2.79±0.44	2.36±0.54	2.82±1.01	3.20±0.66	3.19±0.96
5	Octadecane	1800	4.58±0.89	3.82±0.60	3.99±0.59	5.23±0.68	5.52±0.68	5.43±0.85	5.48±0.98	2.93±0.52	3.21±0.93
14	Eicosane	2000	7.86±1.55	6.51±0.99	4.54±0.65	6.69±1.20	7.31±1.24	7.66±1.38	8.80±1.14	2.01±0.40	2.54±0.47
15	Octadecenol[1]	2053	2.94±1.58	3.64±1.06	1.08±0.68	1.73±0.78	2.77±1.24	7.53±2.52	2.34±1.76	0.95±0.34	1.23±0.37
16	Octadecanol	2083	2.88±1.54	2.91±0.88	2.01±1.94	1.81±1.07	1.40±1.21	6.25±1.42	0.83±0.70	2.02±0.74	3.82±1.60
22	Docosane	2200	7.88±1.39	6.41±2.48	4.84±0.63	7.07±0.91	7.86±1.26	8.47±1.15	9.29±1.18	2.13±0.31	2.43±0.35
24	tricosane	2300	4.46±1.83	1.69±0.49	3.27±0.45	2.05±0.35	1.20±0.16	1.29±0.37	0.98±0.17	1.27±0.47	1.85±0.40
25	11-Methyltricosane + Octadecanamide	2311	tr	1.27±0.37	2.45±0.34	1.54±0.26	0.90±0.12	tr	tr	tr	tr
28	Tetracosane	2400	7.69±1.08	6.04±2.25	4.67±0.47	6.54±0.86	6.76±1.35	7.02±1.32	8.52±1.28	2.65±0.30	2.69±0.54
29	Pentacosene[1]	2469	1.30±0.49	6.71±0.77	4.46±0.48	2.58±0.45	2.22±0.39	tr	tr	tr	tr
31	11+9-Methylpentacosane	2536	2.08±0.29	2.65±0.44	6.38±0.82	3.99±0.60	3.86±1.60	tr	tr	tr	tr
32	7-Methylpentacosane	2544	tr	1.89±0.40	3.42±0.42	2.48±0.38	3.01±1.23	tr	tr	tr	tr
33	5-Methylpentacosane	2555	tr	1.18±0.29	1.59±0.20	1.23±0.29	1.90±0.69	tr	tr	tr	tr
34	3-Methylpentacosane	2574	tr	0.66±0.13	2.01±0.29	0.98±0.25	0.73±0.44	tr	tr	tr	tr
35	Hexacosane	2600	7.92±1.04	7.06±0.73	4.85±0.50	6.47±1.10	6.07±1.07	3.91±0.70	8.68±1.49	2.09±0.56	2.07±0.48
36	12,22-Dimethylhexacosane, 12,20-Dimethylhexacosane[2]	2675	3.64±1.29	5.73±3.27	3.23±1.52	2.74±1.20	1.91±0.57	5.10±1.54	19.52±4.90	22.56±9.88	16.71±5.02
37	Heptacosene[1]	2680	tr	1.08±0.25	3.26±0.42	1.59±0.31	0.68±0.28	tr	tr	tr	tr
38	Heptacosene[1]	2687	tr	0.61±0.12	1.51±0.22	4.47±0.80	0.29±0.11	tr	tr	tr	tr
39	Heptacosane	2700	7.18±2.84	3.19±0.79	5.56±1.00	0.97±0.38	2.65±0.30	2.01±0.52	1.92±0.32	3.31±0.44	3.36±0.70
40	11-Methylheptacosane	2734	tr	ND	1.33±0.12	0.79±0.08	tr	tr	tr	tr	tr
42	Octacosane	2800	7.18±0.63	6.01±0.46	4.65±0.33	5.76±0.45	6.44±0.52	6.52±0.60	6.31±0.98	3.02±0.88	4.25±2.26

44	2-Methyloctacosane	2868	1.11±0.25	tr	tr	tr	tr	tr	tr	tr	tr
45	Nonacosane	2900	5.24±1.03	3.82±0.38	3.99±0.48	5.74±0.66	4.96±0.90	4.29±1.13	3.40±0.76	11.96±2.21	11.73±1.54
46	Tricontane	3000	4.87±2.71	4.83±0.69	3.20±0.29	4.32±0.49	4.64±0.65	4.46±0.53	4.64±0.71	3.56±0.61	4.10±0.80
48	Hentriacontene1	3084	10.19±4.22	12.87±3.60	12.03±3.30	10.31±3.49	13.76±2.36	18.31±4.16	9.31±3.57	10.79±3.07	11.47±4.23
49	Hentriacontane	3100	4.75±1.28	4.51±0.52	3.83±1.51	5.26±0.46	6.72±1.26	5.70±1.25	3.95±1.61	19.83±3.87	17.09±2.04
51	Dotriacontane	3200	6.24±0.98	3.45±0.27	2.80±0.39	3.02±0.35	3.62±0.32	3.68±0.34	3.21±0.41	2.68±0.38	4.72±1.34
54	Tritriacontane	3300	tr	tr	tr	tr	tr	tr	tr	3.03±0.70	3.55±0.72

[1] Double bond positions assumed but not assigned to specific peaks

[2] Tentative identification based on Kovats Index values and match with NIST08 Library database

tr = Trace amount detected (<0.5%)

The total percentage of hydrocarbons present of the 28 resolvable peaks used for PCA is 93%, of which 29% were branched alkanes, 46% *n*-alkanes and 18% of the hydrocarbons were alkenes. PCA was carried out using six principal components, describing 96.1% of the variation within the dataset with the first three principal components comprising 62.9%, 16.4% and 6.9% respectively. PC2 and PC6 (2.5%) were used to plot the relevant scores (see appendix 27 for PCA eigenvalues). Figure 5.23 shows the PCA plot of PC6 vs PC2 for data gathered from day 1 to day 9 larvae extractions of *L. sericata*.
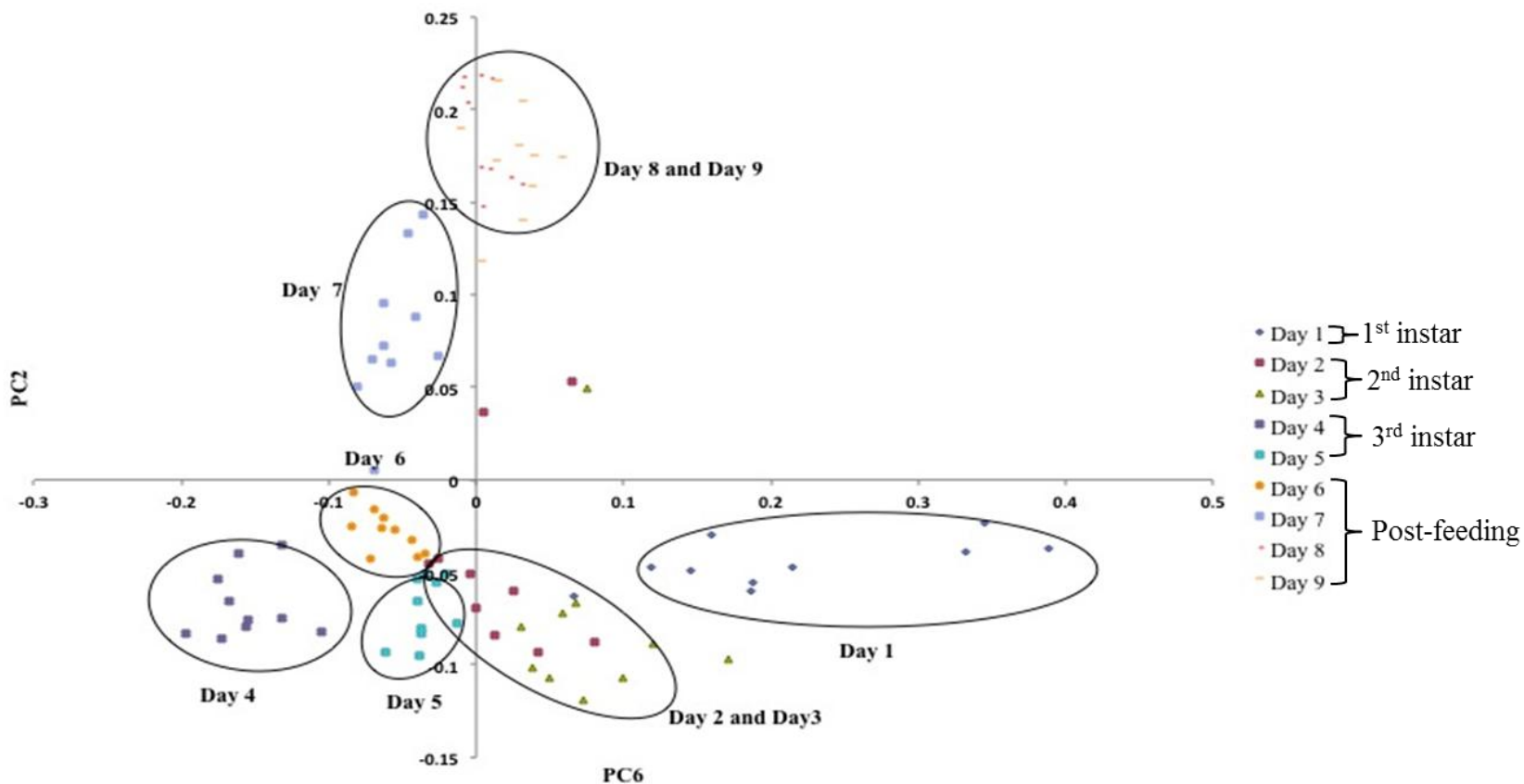
Figure 5.23: PCA plot showing PC2 against PC6 for *L. sericata* larvae with clustering days circled

Discrimination between the chromatograms following PCA may also be tested by calculating the Euclidean distances between the loadings for the data, taken in pairs, from each day of the experiment [33]. This allows comparison based on all principal components calculated, not just those chosen for a graphical representation. This analysis confirmed that by far the greatest similarity is between days 8 and 9 (d=0.0592), which relate to the late post-feeding stage. All other sets have distances at least an order of magnitude greater than this. The largest sequential differences in composition, for example between days 3 and 4 ($d = 0.3474$), are also reflected in this analysis which relates to the jump seen between these two days on the PCA plot (Figure 5.23) (see appendix 28).

The volatile hydrocarbons appear to have little significance on the PCA results and they are excluded from analysis as the main focus of this study is to examine cuticular hydrocarbons, which usually start from a chain length of 20 carbons. In addition, studies carried out on ants have indicated the volatile compounds are primarily coming from the internal glands [34].

The PCA facilitates the quantification of variability in the overall hydrocarbon profile of the cuticle both within each day and from day to day across the whole time-span of the experiment. Although the loading plot (Figure 5.23) does not relate directly to any particular compound, the output of the calculation does allow the key compounds that are involved in changes to be identified. In this case, two DimeC26:H hydrocarbons, C27:H, and C31:H have the largest values in the PCA results.

There are two principal conclusions from Figure 5.23. Firstly the clustering of samples allows data from most days to be clearly discriminated. Some of the clusters, such as those for days 5 and 6, form fairly tight groups indicating little variation in the chemical composition across the 10 samples and good reproducibility in the experimental methodology. Others such as on days 1 and 7 are more spread out suggesting there is more variation within the samples, which may be due to on-going chemical changes during that particular time-span. For instance no two larvae will enter the next life cycle stage at the exact same time period. For two consecutive days (days 8 and 9) the two clusters overlap showing much smaller chemical changes across all 20 samples over these two days. The scatter observed in day 1 may also be due to the low concentration detected from the GC-MS, which ranged over all 10 replicates making some compounds difficult to quantify accurately.

The second conclusion from Figure 5.23 is that the clusters form a systematic sequence that tracks the chemical changes across the PCA plot. Starting from day 1 at the bottom right, the changes can be followed chronologically, moving to day 4 at the bottom left then up the centre and finally ending up at the top with days 8/9. The first stages are characterised by the loadings for PC6 moving from positive to negative whilst from day 5 the main change is that PC2 becomes increasingly positive. These jumps between clusters also relate to the instar status of the larvae. For instance the large shift from day 1 to 2 corresponds to the 2nd instar formation whilst going from day 6 to 7 the large increase in the PC2 loading relates to larvae entering the post-feeding stage.

These changes can also be related to specific chemical changes in the samples. For example, days 8 and 9 are grouped together as the late post-feeding stage of the life cycle and these two days are also the only period across the larvae life cycle where C33:H is clearly present, which may provide a good age indicator for this species, i.e. in late post-feeding stages. The post-feeding period is very difficult to age and there is currently nothing in the literature besides growth charts that can accurately age this stage. By using hydrocarbon analysis with GC-MS and PCA, the results have shown a distinction can be made between early and late post-feeding for this particular species.

As larvae age, the higher molecular weight compounds become more abundant. The heavier long chain hydrocarbons are believed to be involved in waterproofing [35–37] which could explain why *L. sericata* exhibit an increase in these compounds at a later age. When the larvae become older and gradually move into the post-feeding stage of the life cycle they move away from the source of food and seek a site for pupation, exposing them to a drier environment. Therefore they have a greater need for extra waterproofing compared to their younger age where they are usually submerged within their food source which is warm and moist. The display of higher molecular weight *n*-alkanes mixed in with alkenes and methyl hydrocarbons has also been linked to flexibility of the cuticle [38].

The changes in the hydrocarbons over time are primarily linked to the whole profile rather than specific compounds. For example the percentage of high mass odd chain length *n*-alkanes (C29:H, C31:H and C33:H) significantly increased with age. Hence the method of relating peak areas to a reference compound (e.g. C29:H) [20] was not

suitable for the study of this species and PCA was applied to the dataset instead. Furthermore, the stability of C28:H and/or C30:H would suggest that they would be more suited as reference peaks for this particular set of data. As it is not known beforehand which molecules are likely to be most indicative of the ageing process, PCA has the advantage of not focusing on specific compounds. However, there are a few peaks that do stand out because of their significant PCA score, indicating that they are influential within the dataset, especially the C31:1 (compound 48). Other compounds with notably large scores are C22:H (compound 22), 2-MeC28:H (compound 44) which is specific to day 1 larvae, C32:H (compound 51) and C33:H (compound 54). This suggests the larger alkanes and methyl branched hydrocarbons appear to be the most significant as age markers.

Results presented show that the larvae of *L. sericata* can be aged down to the day in most cases (with the exception of days 2 and 3 and the late post-feeding represented by days 8 and 9) by using hydrocarbons analysed by GC-MS and the statistical processing of PCA. More work needs to be carried out in the field to see how stable the *L. sericata* hydrocarbon profiles are when exposed to the environment and to test the practicalities of this technique.

5.3.2 General Discussion and Conclusion for ageing larvae

Roux and co-workers [19] examined the cuticular hydrocarbons of three forensically important blowflies (*C. vicina, C. vomitoria* and *P. terraenovae*). They examined the

ontogenetic study of these three species from egg through to 8 day old adult flies. Similar observations were noted in comparison to the larvae results presented in this chapter. Short-chain hydrocarbons present in the profiles of larvae and post-feeding evolved into long-chain compounds for the pupae and adult flies. The methyl branched alkanes were also seen to be more abundant in the immature stages of the larvae, with a substantial decrease as they became post-feeding.

The two main factors believed to be influential for the composition of hydrocarbon pools are development/genetic factors and physiological state /environmental conditions [19,39,40]. The changes observed during the blowflies development may be affected by the environment they are exposed to. Larvae develop in warm, humid conditions (decomposing remains) and in this stage of their life cycle (pre-post-feeding), they yield profiles consisting of a mixture of low and high molecular weight hydrocarbons. From the larvae results presented in this chapter, the higher molecular weight hydrocarbons become more abundant as the larvae age. When the larvae become older and gradually move into the post-feeding stage of the life cycle they move away from the source of food and seek a site for pupation, exposing them to a drier environment. Therefore they have a greater need for extra water proofing when they are at a younger age where they are usually submerged within their food source which is warm and moist [35–37]. The display of higher boiling point n-alkanes mixed in with alkenes and methyl branched hydrocarbons has also been linked to flexibility of the cuticle [38]. To help flexibility in the larvae's cuticle it will need a composition of methyl branched alkanes and alkenes, which have lower melting points compared to the straight chain alkanes.

These results show great potential to utilise this technique and enough evidence was obtained from all three species to support developing this method into a highly useful ageing tool. One GC trace could facilitate not only the ageing of the blowfly but also provide confirmation of the species (Chapter 4).

Results presented in this chapter were executed in a controlled laboratory environment; however experiments need to be carried out in the field to look at the effects that weathering may have on the stability of the hydrocarbons. On-going method development will test if practical implications will be an issue for hydrocarbon analysis, for example, pooled samples of young and old larvae collected from the crime scene.

References

[1]   R. Hart, A, J., Whitaker, A, P., Hall, M, J, The use of forensic entomology in criminal investigations: How it can be of benefit to SIOs, The Journal of Homicide and Major Incident Investigation 4 (2008) 37–48.

[2]   J. Amendt, R. Krettek, C. Niess, R. Zehner, and H. Bratzke, Forensic entomology in Germany, Forensic Science International 113 (2000) 309–14.

[3]   J. Amendt, C.P. Campobasso, E. Gaudry, C. Reiter, H.N. LeBlanc, and M.J.R. Hall, Best practice in forensic entomology-standards and guidelines, International Journal of Legal Medicine 121 (2007) 90–104.

[4]   J. Amendt, R. Krettek, and R. Zehner, Forensic entomology, Naturwissenschaften 91 (2004) 51–65.

[5]   M. Grassberger and C. Reiter, Effect of temperature on *Lucilia sericata* (Diptera: Calliphoridae) development with special reference to the isomegalen- and isomorphen-diagram, Forensic Science International 120 (2001) 32–6.

[6]   S. Niederegger, J. Pastuschek, and G. Mall, Preliminary studies of the influence of fluctuating temperatures on the development of various forensically relevant flies, Forensic Science International 199 (2010) 72–78.

[7]   S.E. Donovan, M.J.R. Hall, B.D. Turner, and C.B. Moncrieff, Larval growth rates of the blowfly, Calliphora vicina, over a range of temperatures, Medical and Veterinary Entomology 20 (2006) 106–14.

[8]   M.I. Marchenko, Medicolegal relevance of cadaver entomofauna for the determination of the time of death, Forensic Science International 120 (2001) 89–109.

[9]   S.L. VanLaerhoven, Blind validation of postmortem interval estimates using developmental rates of blow flies, Forensic Science International 180 (2008) 76–80.

[10]   A.S. Kamal, Comparative study of thirteen species of sarcosaprophagous Calliphridae and Sarcophagidae (Diptera). I Bionomics, Annals of the Entomological Society of America 51 (1958) 261–270.

[11]   G.S. Anderson, Minimum and maximum development rates of some forensically important Calliphoridae (Diptera), Journal of Forensic Sciences 45 (2000) 824–32.

[12]   M. Grassberger and C. Reiter, Effect of temperature on development of the forensically important holarctic blow fly *Protophormia terraenovae* (Robineau-Desvoidy) (Diptera: Calliphoridae), Forensic Science International 128 (2002) 177–82.

[13]   J.H. Byrd and J.C. Allen, The development of the black blow fly, *Phormia regina* (Meigen), Forensic Science International 120 (2001) 79–88.

[14]   Z. Adams and M.J.R. Hall, Methods used for the killing and preservation of blowfly larvae, and their effect on post-mortem larval length, Forensic Science International 138 (2003) 50–61.

[15]   B. Greenberg, Flies as Forensic Indicators, Journal of Medical Entomology 28 (1991) 565–577.

[16]   R. Urech, G.W. Brown, C.J. Moore, and P.E. Green, Cuticular hydrocarbons of buffalo fly, *Haematobia exigua*, and chemotaxonomic differentiation from horn fly, *H. irritans*, Journal of Chemical Ecology 31 (2005) 2451–61.

[17]   W.V. Brown, R. Morton, and J.P. Spradbery, Cuticular hydrocarbons of the Old World screw-worm fly, *Chrysomya bezziana* Villeneuve (Diptera: Calliphoridae). Chemical characterization and quantification by age and sex, Comparative Biochemistry and Physiology Part B: Comparative Biochemistry 101 (1992) 665–671.

[18]   G. Ye, K. Li, J. Zhu, G. Zhu, and C. Hu, Cuticular hydrocarbon composition in pupal exuviae for taxonomic differentiation of six necrophagous flies, Journal of Medical Entomology 44 (2007) 450–6.

[19]   O. Roux, C. Gers, and L. Legal, Ontogenetic study of three Calliphoridae of forensic importance through cuticular hydrocarbon analysis, Medical and Veterinary Entomology 22 (2008) 309–17.

[20]   G.H. Zhu, G.Y. Ye, C. Hu, X.H. Xu, and K. Li, Development changes of cuticular hydrocarbons in *Chrysomya rufifacies* larvae: potential for determining larval age, Medical and Veterinary Entomology 20 (2006) 438–44.

[21]   J. Wang, Z. Li, Y. Chen, Q. Chen, and X. Yin, The succession and development of insects on pig carcasses and their significances in estimating PMI in South China, Forensic Science International 179 (2008) 11–8.

[22]   M.A. O'Flynn, The succession and rate of development of blowflies in carrion in Southern Queensland and the application of these data to forensic entomology, Journal of the Australian Entomological Society 22 (1983) 137–148.

[23]   S.C. Voss, H. Spafford, and I.R. Dadour, Annual and seasonal patterns of insect succession on decomposing remains at two locations in Western Australia, Forensic Science International 193 (2009) 26–36.

[24]   K. Szpila, Key for the identification of third instars of European blowflies (Diptera: Calliphoridae) of forensic importance, in: Current Concepts in Forensic Entomology, eds., J. Amendt, C.P. Campobasso, M. Goff, and M. Grassberger, Springer (2010) 43–56.

[25]   K. Clark, L. Evans, and R. Wall, Growth rates of the blowfly, *Lucilia sericata*, on different body tissues, Forensic Science International 156 (2006) 145–9.

[26]   S. Arnott and B. Turner, Post-feeding larval behaviour in the blowfly, *Calliphora vicina*: effects on post-mortem interval estimates, Forensic Science International 177 (2008) 162–7.

[27]   C. Ames, B. Turner, and B. Daniel, Estimating the post-mortem interval (I): The use of genetic markers to aid in identification of Dipteran species and subpopulations, International Congress Series 1288 (2006) 795–797.

[28]   M.I. Arnaldos, M.D. García, E. Romera, J.J. Presa, and A. Luna, Estimation of postmortem interval in real cases based on experimentally obtained entomological evidence, Forensic Science International 149 (2005) 57–65.

[29]   O. Roux, C. Gers, and L. Legal, When, during ontogeny, waxes in the blowfly (Calliphoridae) cuticle can act as phylogenetic markers, Biochemical Systematics and Ecology 34 (2006) 406–416.

[30]   S. Ireland and B. Turner, The effects of larval crowding and food type on the size and development of the blowfly, *Calliphora vomitoria*, Forensic Science International 159 (2006) 175–81.

[31]   M. Trabalon, M. Campan, J.L. Clement, C. Lange, and M.T. Miquel, Cuticular hydrocarbons of *Calliphora vomitoria* (Diptera): Relation to age and sex, General and Comparative Endocrinology 85 (1992) 208–216.

[32]   T. Akino, Cuticular hydrocarbons of *Formica truncorum* (Hymenoptera: Formicidae): Description of new very long chained hydrocarbon components, Applied Entomology and Zoology 41 (2006) 667–677.

[33]   R.G. Brereton, *Chemometrics: Data Analysis for the Laboratory and Chemical Plant*, Wiley, UK (2003).

[34]   T. Akino, K. Yamamura, S. Wakamura, and R. Yamaoka, Direct behavioral evidence for hydrocarbons as nestmate recognition cues in *Formica japonica* (Hymenoptera: Formicidae), Applied Entomology and Zoology 39 (2004) 381–387.

[35]   R. Toolson, E. C., Kuper-Simbron, Laboratory evolution of epicuticular hydrocarbon composition and cuticular permeability in *Drosophila pseudoobscura*: effects on sexual dimorphism and thermal- acclimation ability, Evolution 43 (1989) 468–473.

[36]   T. Tregenza, S.H. Buckley, V.L. Pritchard, and R.K. Butlin, Inter- and intra-population effects of sex and age on epicuticular composition of meadow grasshopper, *Chorthippus parallelus*, Journal of Chemical Ecology 26 (2000) 257–278.

[37]   J.F. Ferveur, Cuticular hydrocarbons: their evolution and roles in *Drosophila* pheromonal communication, Behavior Genetics 35 (2005) 279–95.

[38]   D. Morgan, *Biosynthesis in Insects*, The Royal Society of Chemistry, UK (2010).

[39]   G.J. Blomquist, D.R. Nelson, and M. De Renobales, Chemistry, biochemistry, and physiology of insect cuticular lipids, Archives of Insect Biochemistry and Physiology 6 (1987) 227–265.

[40]   J.A. Espelie, K.E., Payne, Characterization of the cuticular lipids of the larvae and adults of the pecan weevil, *Curculio caryae*, Biochemical Systematics and Ecology 19 (1991) 127–132.

Chapter 6

Age Determination of the Later Life Stages Using Cuticular Hydrocarbons

6. Introduction

In the previous chapter the hydrocarbon profiles of the immature life stages i.e. eggs and larvae, were discussed. This chapter focuses on the potential of using hydrocarbon analysis to age the mature life stages (puparia, puparial cases and adult flies) of the three forensically important blowflies.

The later life stages are all very difficult to age although a rough estimation can be achieved by using temperature data as well as succession patterns and looking at the presence of other insects feeding on the cadaver. An experienced entomologist can establish the identification of insects that were present using the empty puparial cases if they are in good enough condition but there are currently no means of ageing the empty cases. In scenarios where all other entomological evidence is no longer present, puparial cases can often be all that remains and therefore being able to establish the age

could give an indication of the PMI. However, this could give rise to very long PMI calculations being estimated due to the absence of means for accurately ageing the puparial cases. In addition, the age of a mature adult fly cannot be established. However, as with the puparia and puparial cases, looking at succession patterns, along with the presence of other insects, can provide a rough indication.

The fact that there are currently no means of ageing puparial cases and adult flies, suggests there is a need for more techniques to be developed in the area of ageing the mature life stages of forensically important blowflies [1]. Techniques such as DNA are being applied to puparia [1,2] which looks like a promising alternative to current methods. On-going research using hydrocarbon analysis to age the puparial cases [3,4] and adult flies [5,6] show great potential for this technique to be applied within the field of forensic entomology. This chapter will examine the hydrocarbon profiles of *L. sericata*, *C. vicina* and *C. vomitoria* in their later life stages.

6.1 Aims and Objectives

The three species examined were *Lucilia sericata, Calliphora vicina* and *Calliphora vomitoria* with the overall aim of ageing the life stages mentioned for these three forensically important species. The main focus will once again be on the non-polar hydrocarbons extracted from the insect's cuticle to establish if distinguishable changes within the profiles occur over time. The results from the GC chromatograms and PCA plots are discussed to determine any trends observed within the profiles.

6.2 Puparia

Less work has been carried out on ageing forensically important puparia in comparison to larvae, but this is of great importance since they comprise of 50% of the immature developmental cycle [2]. Therefore, this life stage may give invaluable information when determining PMI estimations.

It is extremely difficult to age puparia using morphological changes, hence DNA techniques are being developed to look into ageing this life stage using gene expression [2,7] with a good degree of success. There is also on going work using low energy X-rays to image developing flies through the outer case (Martin Hall and co-workers Natural History Museum, London, pers comm). This technique enabled pupae to be imaged multiple times during their development with no adverse effects.

There are currently very few studies on hydrocarbon profiles of puparia and it has not yet been utilised for ageing this life stage. This section of the chapter presents preliminary results of hydrocarbon analysis from two species, *Lucilia sericata* and *Calliphora vicina.* There was limited success and neither of the two species could be accurately aged hence the decision was taken not to focus on this life stage for the thesis. However, the results will still be presented, showing the GC chromatograms of their extracted cuticular profiles and corresponding PCA plots.

6.2.1 Results and Discussion for puparia

L. sericata:

The puparia were extracted daily until they metamorphosed into adult flies, which took five days (hatched on the fifth day, therefore four days of extractions). The extracted profile of *L. sericata* puparium contained 22 different hydrocarbons with one co-eluting for a total of 21 resolvable peaks. The *n*-alkanes dominated the profiles, consisting of 76% of the total number of hydrocarbons present with chain lengths ranging from C16:H to C31:H. Of the 22 hydrocarbons extracted, three were alkenes (14%), while only 2 methyl branched alkanes (10%) were present. Table 6.1 shows the identified hydrocarbons extracted from the puparium of *L. sericata*.

Figure 6.1 shows the chromatogram from day 1 extracted *L. sericata* puparium. Many of the volatile low boiling point compounds eluting between 10 and 13 minutes comprised of acids, alcohols and other non-polar compounds that were therefore excluded from any further analysis. The bulk of the profile consisted of *n*-alkanes. C29:H and C31:H were the dominating *n*-alkanes for this species. C27:H could potentially be useful as an age indicator because it decreases slightly over time (Table 6.2).

Table 6.1: List of all hydrocarbon compounds extracted from the puparium of *L. sericata* and the Kovats Indices to aid identification (peak numbers refer to Figure 6.1)

Peak number	Peak identification	Kovats iu
1	Hexadecane	1600
2	Heptadecane	1700
3	Octadecene[1]	1787
4	Octadecene[1]	1791
5	Octadecane	1800
6	Methyloctadecane	1896
7	Nonadecane	1900
8	Eicosane	2000
9	Heneicosane	2100
10	Docosane	2200
11	Tricosane	2300
12	Tetracosane	2400
13	Pentacosane	2500
14	Hexacosane	2600
15	12,22+12,20-Dimethylhexacosane[2]	2665
16	Heptacosane	2700
17	Octacosane	2800
18	Nonacosane	2900
19	Triacontane	3000
20	Hentriacontene[1]	3083
21	Hentriacontane	3100

[1]Double bond positions only determined in adult flies

[2]Tentative identification based on Kovats Index
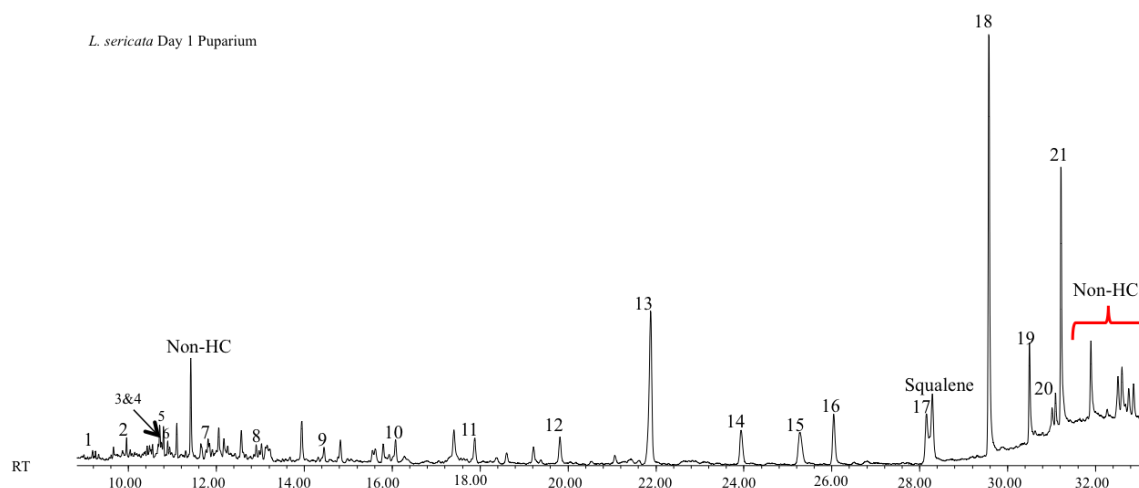
Figure 6.1: GC chromatogram of *L. sericata* puparium extracted on day 1 of pupation

To try to establish the age of the puparia and to see if any chemical changes had occurred with time, PCA was applied. The dataset consisted of the peak areas of the hydrocarbons present between days 1 and 4. All compounds from C20:H onwards were included in the PCA dataset (Table 6.2). As with the larvae, C25:H was found to be co-eluting with phthalate and was therefore excluded from the analysis.

Table 6.2: List of the compounds used for subsequent PCA analysis from the puparia of *L. sericata*, with the total percentage of each compound, the percentage standard deviation for each day and the Kovats Indices to aid identification

Peak number	Peak Identification	Kovats iu	Day 1 n=10 %	Day 2 n=10 %	Day 3 n=10 %	Day 4 n=10 %
8	Eicosane	2000	1.34±0.56	1.10±0.46	1.10±0.26	1.29±0.50
9	Heneicosane	2100	1.19±0.27	0.99±0.37	1.00±0.40	0.90±0.16
10	Docosane	2200	1.79±0.41	1.35±0.53	1.42±0.58	1.21±0.20
11	Tricosane	2300	2.25±0.48	1.56±0.62	1.89±1.32	1.35±0.25
12	Tetracosane	2400	2.60±0.48	1.88±0.96	2.17±1.19	1.52±0.29
14	Hexacosane	2600	4.49±0.96	3.36±2.35	3.59±1.89	3.01±0.95
15	12,22+12,20-Dimethylhexacosane[1]	2665	7.54±2.29	6.75±7.19	8.96±4.38	8.15±3.31
16	Heptacosane	2700	6.21±2.92	4.99±3.10	4.30±1.95	4.23±2.06
17	Octacosane	2800	4.29±1.39	3.30±1.68	3.72±2.02	3.37±2.13
18	Nonacosane	2900	34.69±11.47	32.74±18.29	32.64±13.39	34.11±16.08
19	Triacontane	3000	5.86±1.77	5.58±2.58	5.81±3.12	4.18±1.22
20	Hentriacontene[2]	3083	6.35±4.58	11.19±4.00	10.77±3.10	13.94±6.69
21	Hentriacontane	3100	21.40±5.02	25.22±12.44	22.64±5.47	22.74±7.45

[1] Tentative identification based on Kovats Index   [2]Double bond positions only determined in adult flies

218

PCA was carried out using six principal components, describing 99.9% of the variation within the dataset with the first three principal components comprising 94.8%, 3.4%, and 0.78% respectively. PC1 and PC2 were used to plot the relevant scores (see appendix 29 for PCA eigenvalues).
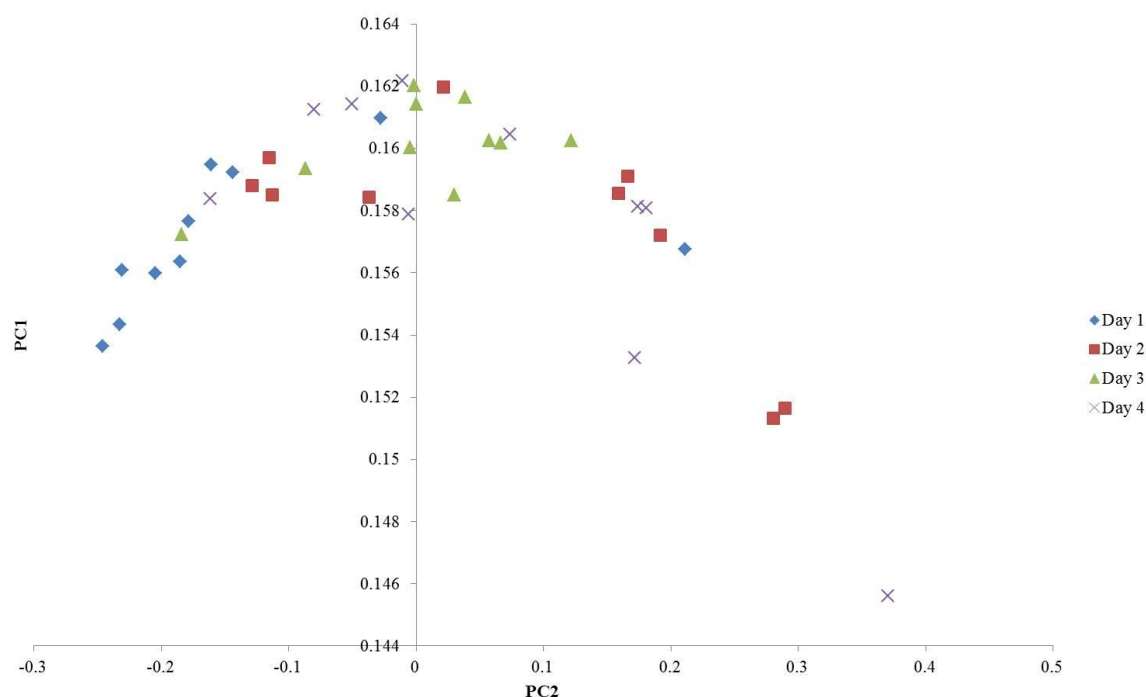
Figure 6.2: PCA plot showing PC2 against PC1 for *L. sericata* pupria from days 1 to 4

The PCA plot in Figure 6.2 shows considerable scatter within the extraction days, indicating that there is considerable variation within the hydrocarbon profiles. Therefore the age could not be established using the results obtained for *L. sericata* puparia. The usual combination of PC3 and PC2 (as well as all other possible combinations) gave a similar results as the plot presented in Figure 6.2.

C. vicina:

The puparia were extracted daily from days 1 to 13. Under closer examination and after dissecting a quarter of the samples at day 13, it was clear that the pupae had not developed and had died under the conditions they were reared at. It is not known at what age they died but it is expected to be in the early stages of pupation. Table 6.3 shows the identified hydrocarbons extracted from the puparium of *C. vicina*.

The chromatogram in Figure 6.3 shows the chemical profile extracted from the puparia of *C. vicina* (day 1). Many of the more volatile compounds eluting between 10 and 13 minutes comprised again of acids, alcohols and other non-polar compounds which were therefore excluded from any further analysis. The bulk of the profile consisted of *n*-alkanes, with C27:H and C29:H dominating the profile.

The profile of *C. vicina* puparia contained 23 identifiable compounds with one co-eluting for a total of 22 resolvable peaks, consisting mainly of *n*-alkanes (68%) with chain lengths ranging from C16:H to C31:H. The four alkenes made up 18% of the profile and 14% were methyl branched alkanes (three in total).

Table 6.3: List of all hydrocarbon compounds extracted from the puparia of *C. vicina* and the Kovats

Indices to aid identification (peak numbers refer to Figure 6.3)

Peak number	Peak Identification	Kovats iu
1	Hexadecene[1]	N/A
2	Hexadecane	1600
3	Heptadecene[1]	1663
4	Heptadecane	1700
5	Octadecene[1]	1791
6	Octadecane	1800
7	Dimethyloctadecane[2]	1814
8	Nonadecane	1900
9	Eicosane	2000
10	Heneicosane	2100
11	Docosane	2200
12	Tricosane	2300
13	Tetracosane	2400
14	Pentacosane	2500
15	Hexacosane	2600
16	x,12-Dimethylhexacosane[2]	2664
17	Heptacosane	2700
18	9+11-Methylheptacosane	2733
19	Octacosane	2800
20	Nonacosane	2900
21	Hentriacontene[1]	3084
22	Hentriacontane	3100

[1]Double bond positions only determined in adult flies

[2]Methyl position not determined
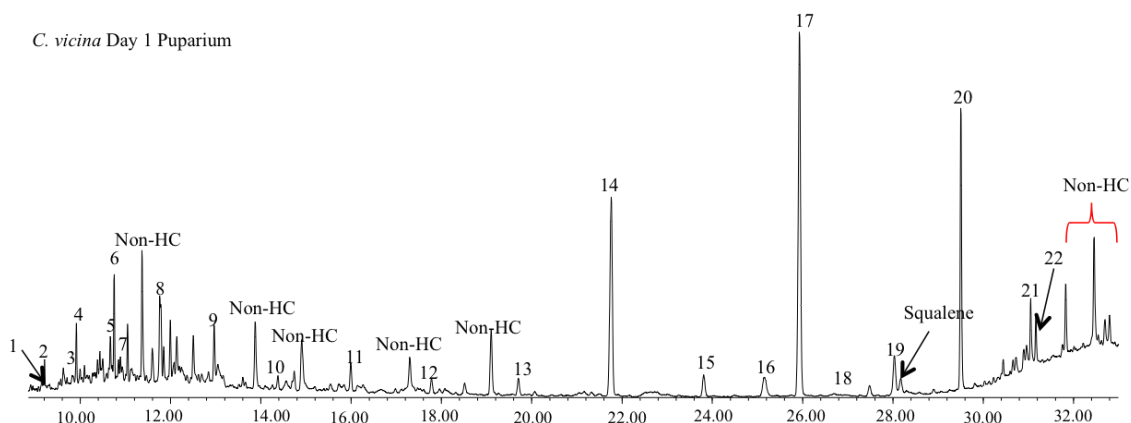
Figure 6.3: GC chromatogram of *C. vicina* puparium extracted on day 1 of pupation

PCA analysis was applied to the data gathered between days 1 and 13 to see if any chemical changes could be identified, even though the specimens died at an unknown age. All compounds (*n*-alkanes, alkenes and methyl branched) from C20:H onwards were used (Table 6.4) for subsequent PCA as there was such a low number of methyl branched compounds (best statistical results for this species usually occur when only the branched methyl alkanes and alkenes are applied – see pages 181 to 186, chapter 5). The results presented in Table 6.4 are for day 1 only as it is not known at what stage the pupae died. PCA was applied to a dataset but the data is not shown as no clustering groups were observed and therefore little information could be gathered from the plot.

Table 6.4: List of the compounds used for subsequent PCA analysis from the puparia of *C. vicina*, with the total percentage of each compound, the percentage standard deviation and the Kovats Indices to aid identification.

Peak number	Peak Identification	Kovats iu	Day 1 n=10 %
1	Hexadecene[1]	N/A	3.33±1.95
2	Hexadecane	1600	1.84±1.39
3	Heptadecene[1]	N/A	1.84±1.22
4	Heptadecane	1700	3.86±1.18
5	Octadecene[1]	1791	2.39±1.22
6	Octadecane	1800	4.72±1.02
7	Dimethyloctadecane[2]	1814	1.62±0.63
8	Nonadecane	1900	0.43±0.28
9	Eicosane	2000	2.55±0.53
10	Heneicosane	2100	1.46±0.44
11	Docosane	2200	2.01±0.60
12	Tricosane	2300	1.56±0.67
13	Tetracosane	2400	1.41±0.44
15	Hexacosane	2600	2.18±1.01
16	3-Methylhexacosane	2664	5.16±2.69
17	Heptacosane	2700	18.74±8.29
18	9+11-Methylheptacosane	2733	tr
19	Octacosane	2800	3.17±1.31
20	Nonacosane	2900	13.48±5.93
21	Hentriacontene[2]	3084	6.82±2.50
22	Hentriacontane	3100	3.26±1.20

[1]Double bond positions only determined in adult flies

[2] Methyl position not determined

6.2.2 General Discussion and Conclusion for ageing puparia

Roux and colleagues [5] carried out a complete ontogenetic study on three forensically important blowflies using cuticular hydrocarbon analysis. One of the species examined was *C. vicina* and they reported that they had difficulty in detecting hydrocarbons for this species in the puparia life stage. They therefore had to extract hydrocarbons from the nymph's membrane after the puparium was opened. The results for *C. vicina* puparia presented here appeared to be in agreement that very few hydrocarbons were present in comparison to the other life stages but *n*-alkanes were detectable and although it was not possible to establish the age of the puparia, enough compounds were extracted from the profile using the technique stated (chapter 3, section 3.2.1: Pupae) at least for identification to be established between *C. vicina* and *L. sericata* (chapter 4, section 4.4.1).

As mentioned before (see section 6.2), the results were relatively unsuccessful and hydrocarbon analysis combined with PCA was unable to effectively determine the age of *L. sericata* and *C. vicina* puparia.

Given the developments in DNA analysis and the results it gives on the potential for ageing puparia, hydrocarbon analysis may be better applied to other life stages, where other ageing techniques fall short. Ageing results for this life stage using hydrocarbon analysis proved to be less successful. However, this procedure needs to be repeated, especially for *C. vicina* as they died during the extraction period hence this provided an unresolved dataset.

6.3 Puparial Cases

The presence of empty puparial cases is often associated with an older corpses and can often give vital information in relation to PMI estimations as well as indicating the presence of drugs that the larvae were exposed to, which can remain in the case once the adult has emerged [8]. At present, several papers have been published looking at using the larvae and pupae of forensically important blowflies to calculate the PMI estimations [2,5,7,9–11] however few papers have looked into the possibility of using puparial cases and its potential has not yet been fully realised [12]. Although DNA can be used to identify empty puparial cases [8], there are no such techniques that can age them. One research group from China analysed the cuticular hydrocarbons and the effects of weathering of *Chrysomya megacephala* to establish the age of the cases, but only preliminary observations were presented [3].

The use of morphology as an identification tool of empty puparial cases is discussed in chapter 4 (section 4.5) and results presented within that chapter showed the potential that hydrocarbon analysis has for identification of broken cases as well as fully intact ones. The same applies for ageing, as a hydrocarbon profile can be obtained from a small portion of the case, which can provide taxonomic identification as well as an indication of age, giving invaluable information for criminal investigations.

This section of the chapter presents preliminary results for ageing the empty puparial cases of two species of blowflies, *C. vicina* and *L. sericata* using their cuticular hydrocarbons and PCA analysis, over a period of nine months

6.3.1 Results and Discussion for puparial cases

L. sericata:

The empty puparial cases were extracted weekly for the first 8 weeks then monthly until month 9 (see chapter 3, section 3.2.1: *Puparial cases*).

In total, *L. sericata* yielded a profile of 24 identifiable compounds (with a peak area exceeding 0.5%) with some co-eluting for a total of 20 resolvable peaks from week 1 to month 9 (Table 6.5). The hydrocarbons (from week 1) consisted of *n*-alkanes (45%), alkenes (5%) and methyl branched hydrocarbons (50%). The chain lengths range from C25:H to C33:H. As mentioned in section 6.1, the main compounds found in the mature life stages presented in this chapter were cuticular hydrocarbons and there were far fewer polar contaminants in comparison to larvae (due to larvae being immersed in decomposing remains during their active feeding stage of the life cycle). Therefore, C25:H was included in the analysis of the puparial cases and adult flies.

Figure 6.4 shows the GC chromatogram of a sample from Week 1. In comparison to the larvae profiles, there are far fewer compounds present, and they are all high molecular weight hydrocarbons, resembling the profile of the adult fly (section 6.4).
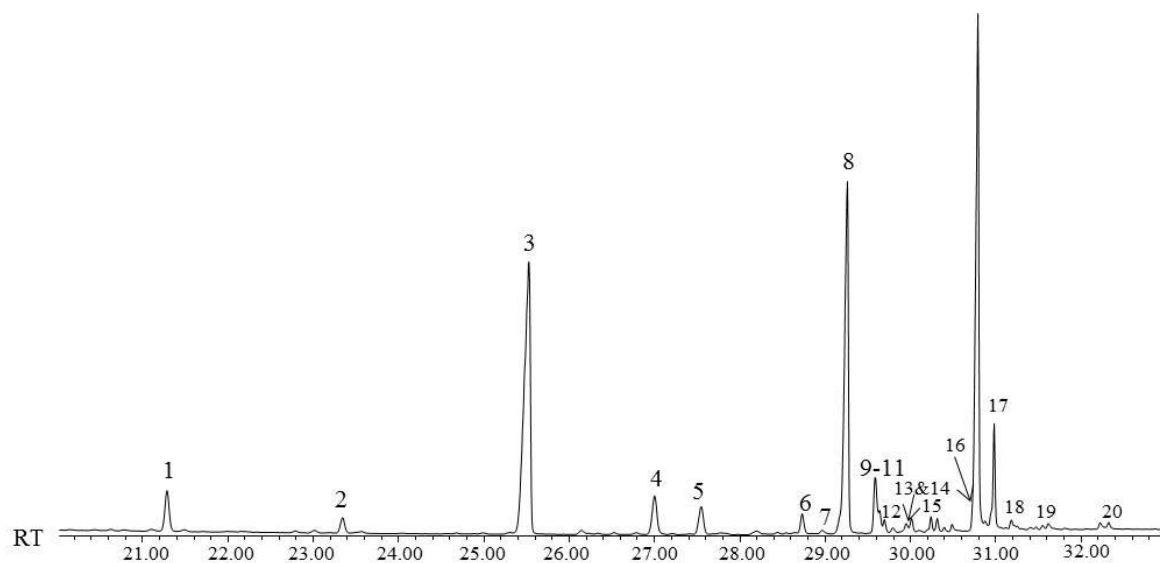
Figure 6.4: GC chromatogram of *L. sericata* puparial case extracted at week 1

In general, the odd *n*-alkanes exhibit much larger peak areas than the even *n*-alkanes, methyl branched and alkene compounds.

Table 6.5 lists the identified compounds extracted from the cuticle of the puparial case along with the total percentage of each compound present, the percentage standard deviation and the Kovats Indices.

227

Table 6.5: List of the compounds extracted from the puparial case and used for subsequent PCA analysis of *L. sericata,* with the total percentage of each compound present, the percentage standard deviation for each week/month and the Kovats Indices to aid identification (peak numbers refer to Figure 6.4)

Peak number	Peak identification	Kovats iu	Week 1 n=10 %	Week 2 n=10 %	Week 3 n=10 %	Week 4 n=10 %	Week 5 n=10 %	Week 6 n=10 %	Week 7 n=10 %
1	Pentacosane	2500	3.88±1.00	8.14±1.80	7.12±1.19	7.48±1.32	5.85±4.54	5.60±1.84	6.68±2.34
2	Hexacosane	2600	1.41±0.36	1.25±0.29	1.28±0.34	1.36±0.36	1.54±0.23	1.92±0.63	1.70±0.43
3	Heptacosane	2700	34.05±7.75	34.33±8.72	34.72±8.08	34.48±9.62	34.31±5.40	47.82±10.55	46.77±11.26
4	3-Methylheptacosane	2774	4.26±1.08	5.08±1.39	4.89±1.44	4.44±1.15	4.99±1.10	7.36±1.72	7.45±1.93
5	Octacosane	2800	2.96±0.53	4.03±1.07	4.19±1.10	4.23±1.21	4.55±0.68	2.70±1.00	2.55±0.75
6	2-Methyloctacosane	2869	1.62±0.59	2.51±0.96	2.17±0.56	2.63±1.02	2.48±0.52	2.35±0.77	2.38±0.66
7	Nonacosene[2]	2883	0.90±0.42	tr	tr	tr	tr	tr	tr
8	Nonacosane	2900	31.99±3.68	30.19±6.98	32.48±8.04	32.78±7.24	32.99±5.88	18.63±5.23	17.92±4.86
9	11+15-Methylnonacosane	2935	3.23±0.92	4.66±2.34	2.80±0.55	3.59±1.12	2.76±1.20	4.56±1.49	4.52±2.28
10	9-Methylnonacosane	2940	1.12±0.30	0.97±0.71	0.34±0.29	0.33±0.28	0.55±0.55	1.76±0.60	2.04±0.77
11	7-Methylnonacosane	2946	0.71±0.19	1.53±0.61	1.57±0.40	1.54±0.46	1.55±0.33	1.65±0.55	1.85±0.61
12	5-Methylnonacosane	2955	tr	0.70±0.27	0.75±0.25	0.70±0.24	0.83±0.18	0.48±0.24	0.63±0.17
13	9,17-Dimethylnonacosane[1]	2971	0.64±0.14	0.13±0.06	1.43±0.41	0.15±0.15	0.72±0.13	1.11±0.46	1.35±0.41
14	3-Methylnonacosane	2977	0.83±0.19	1.39±0.43	1.39±0.41	1.13±0.49	1.43±0.24	1.29±0.46	1.49±0.42
15	Triacontane	3000	1.26±0.19	0.65±0.15	0.63±0.21	0.67±0.19	0.93±0.22	0.26±0.14	0.26±0.07
16	2-Methyltriacontane	3067	tr	1.13±0.47	1.00±0.30	1.15±0.49	1.03±0.17	0.81±0.34	0.97±0.27
17	Hentriacontane	3100	8.32±1.65	2.34±0.75	2.14±1.00	2.15±0.79	2.25±0.74	0.90±0.34	0.57±0.47
18	9+11+13+15-Methylhentriacontane	3132	0.95±0.31	0.40±0.30	0.35±0.18	0.41±0.21	0.43±0.15	0.35±0.14	0.47±0.17
19	Dotriacontane	3200	1.00±0.17	0.24±0.03	0.40±0.14	0.37±0.19	0.41±0.18	0.31±0.06	0.25±0.04
20	Tritriacontane	3300	0.88±0.21	0.34±0.05	0.36±0.09	0.40±0.09	0.39±0.09	0.16±0.05	0.15±0.06

Peak number	Peak identification	Kovats iu	Week 8 n=10 %	Month 3 n=10 %	Month 4 n=10 %	Month 5 n=10 %	Month 6 n=10 %	Month 7 n=10 %	Month 8 n=10 %	Month 9 n=10 %
1	Pentacosane	2500	5.41±1.03	1.02±0.36	0.63±0.29	0.67±0.26	0.97±0.33	2.61±1.06	1.25±0.37	0.94±0.69
2	Hexacosane	2600	1.73±0.40	1.61±0.50	1.12±0.49	1.42±0.19	1.33±0.31	1.38±0.20	1.47±0.55	1.30±0.70
3	Heptacosane	2700	49.51±11.44	43.34±14.03	34.15±17.00	39.16±6.63	37.27±7.66	33.08±6.69	34.81±12.70	33.79±18.92
4	3-Methylheptacosane	2774	7.24±1.14	4.57±1.71	4.31±1.49	4.20±0.65	4.05±1.25	3.80±0.57	3.80±1.22	4.12±2.65
5	Octacosane	2800	2.10±1.25	4.39±1.60	4.56±1.39	4.20±0.76	4.10±0.77	3.49±0.75	3.67±1.40	3.91±2.25
6	2-Methyloctacosane	2869	2.31±0.50	2.23±0.93	2.72±0.91	2.60±0.58	2.07±0.31	2.07±0.33	2.26±0.83	2.27±1.08
7	Nonacosene[2]	2883	tr	tr	tr	tr	tr	tr	tr	tr
8	Nonacosane	2900	18.18±4.03	30.39±11.24	34.46±11.13	30.73±6.17	33.35±7.05	30.55±6.94	32.60±12.19	32.38±16.50
9	11+15-Methylnonacosane	2935	4.31±0.90	3.93±1.62	5.47±2.64	4.89±0.85	4.08±1.78	5.19±1.42	4.21±1.10	4.63±1.46
10	9-Methylnonacosane	2940	1.72±0.27	1.45±0.58	1.40±0.48	1.39±0.23	1.65±0.84	2.03±0.46	1.65±0.47	1.63±0.65
11	7-Methylnonacosane	2946	1.62±0.29	1.26±0.47	1.34±0.53	1.27±0.19	1.35±0.93	1.76±0.33	1.47±0.41	1.49±0.62
12	5-Methylnonacosane	2955	0.52±0.13	0.54±0.29	0.74±0.24	0.63±0.08	0.54±0.24	0.75±0.12	0.72±0.18	0.77±0.44
13	9,17-Dimethylnonacosane[1]	2971	1.15±0.27	0.53±0.25	0.31±0.11	0.24±0.10	0.21±0.12	0.66±0.15	0.63±0.17	0.70±0.34
14	3-Methylnonacosane	2977	1.37±0.22	1.25±0.50	1.56±0.63	1.53±0.24	1.70±0.96	1.26±0.23	1.40±0.44	1.51±0.93
15	Triacontane	3000	0.23±0.09	0.49±0.25	0.83±0.31	0.69±0.15	1.14±1.08	1.00±0.28	0.89±0.32	1.03±0.45
16	2-Methyltriacontane	3067	0.91±0.22	1.09±0.61	1.76±0.96	1.96±0.57	1.53±0.53	1.05±0.26	1.31±0.47	1.45±0.81
17	Hentriacontane	3100	0.80±0.36	1.04±0.51	2.96±0.86	2.72±0.95	3.06±0.64	5.27±1.84	4.27±1.26	4.79±1.39
18	9+11+13+15-Methylhentriacontane	3132	0.47±0.09	0.25±0.16	0.81±0.35	0.78±0.20	0.65±0.24	1.64±0.74	1.53±0.38	1.12±0.45
19	Dotricontane	3200	0.25±0.06	0.39±0.12	0.31±0.18	0.31±0.09	0.28±0.08	1.13±0.40	0.95±0.37	0.95±0.41
20	Tritriacontane	3300	0.16±0.04	0.21±0.06	0.55±0.31	0.61±0.25	0.68±0.06	1.27±0.24	1.10±0.44	1.21±0.42

[1] Tentative identification based on Kovats Index   [2] Double bond position determined but not assigned to specific peaks

The PCA was carried out using six principal components, describing 99.9% of the variation within the dataset with the first three principal components comprising 95.8%, 3.0% and 0.6% respectively. PC3 and PC2 were used to plot the relevant scores (see appendix 30 for PCA eigenvalues).

Four clustering groups are apparent from the PCA plot (Figure 6.5). These groups contain extracts from week 1, which cluster as an individual group. Weeks 2 to 5 cluster together to form a second group. Weeks 6 to 8 form the third group and the final group consists of months 3 to 9.
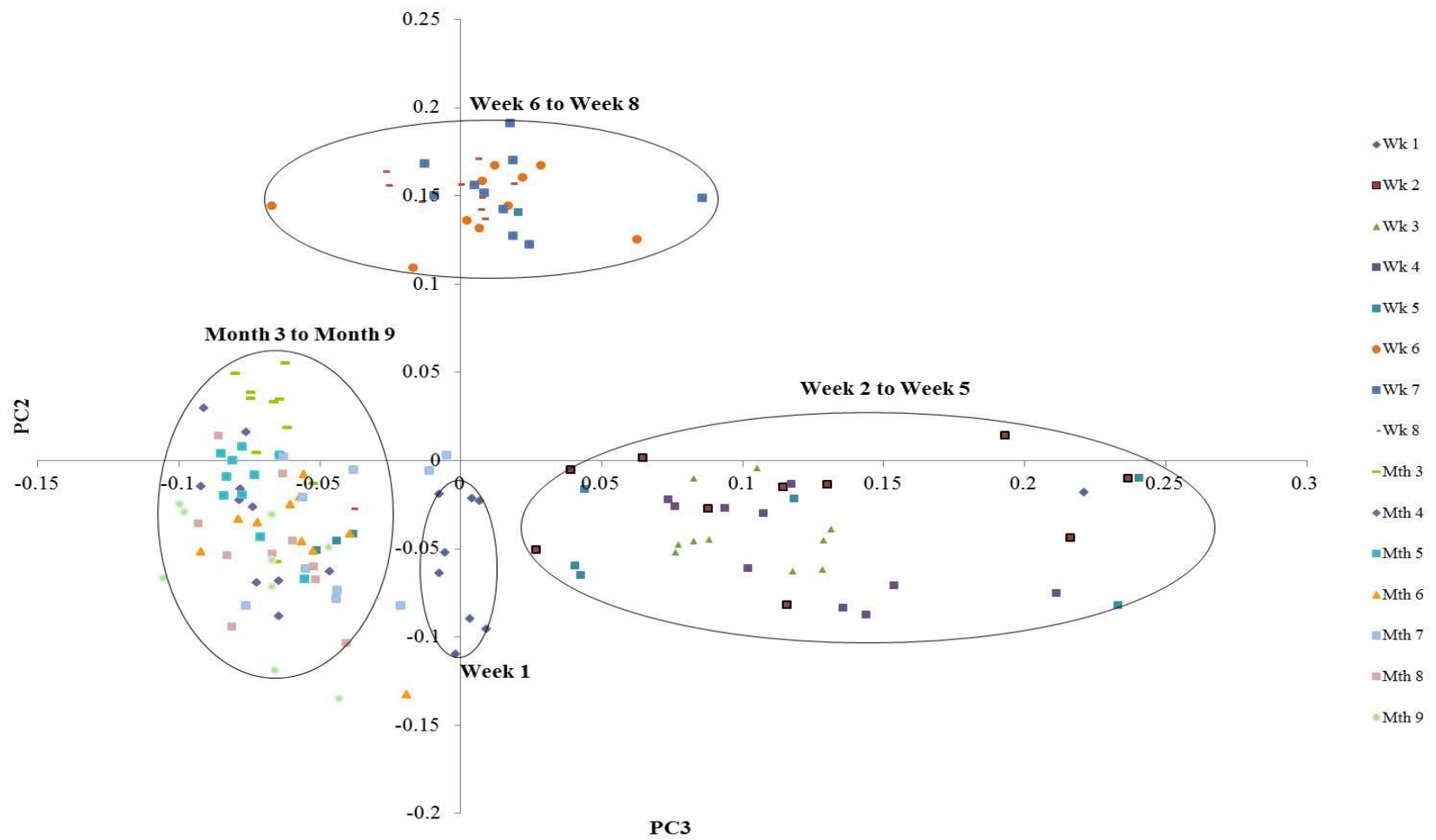
Figure 6.5: PCA plot showing PC3 against PC2 for *L. sericata* puparial cases with clustering days circled

Although it is very difficult to visualise any changes occurring within the GC chromatograms over time, small changes were present and PCA allowed for these slight variations to be visualised. Age-related changes over time were observed for the puparial cases of *L. sericata*. Therefore the results show some potential for hydrocarbon analysis to be used in PMI estimations of older cadavers, when other entomology evidence may not be present.

A useful week 1 age indicator is C29:1 (compound 7), which is specific to this age, which is likely to explain why this week is the only week to group individually in the PCA plot (Figure 6.5). The percentage for C27:H and C29:H are relatively stable with the exception of weeks 6 to 8 and month 3, where there is more variation. Week 6 to 8 are seen to group together within the PCA plot.

Results were presented up to month 9 and four age groups can be established using PCA, consisting of week 1, weeks 2 to 5, weeks 6 to 8 and finally a much larger group containing months 3 to 9. Although this last group hold a much wider time frame it is still very useful to be able to determine young puparial cases from older ones which are three months or older. Also, with the aid of other entomological evidence that maybe present (beetles, moths etc) and the state of decomposition of the carrion, all this information could be brought together to give a more accurate age of time since colonization.

C. vicina:

The hydrocarbon profile of *C. vicina* puparial cases contained 37 compounds with some co-eluting giving a total of 31 resolvable peak from week 1 to month 9 (Table

6.6). The hydrocarbons consisted of *n*-alkanes (29%), alkenes (3%) and methyl branched alkanes (68%) in the form of mono-, di- and tri-methyl alkanes. The chain lengths ranged from C25:H to C33:H.

Table 6.6: List of all compounds extracted from the puparial case of *C. vicina* and the Kovats Index to aid identification. Compounds in bold were used for subsequent PCA analysis.

Peak number	Peak Identification	Kovats iu
1	Pentacosane	2500
2	**3-Methylpentacosane**	2574
3	Hexacosane	2600
4	**2-Methylhexacosane**	2661
5	Heptacosane	2700
6	**11+13-Methylheptacosane**	2731
7	**9-Methylheptacosane**	2734
8	**7-Methylheptacosane**	2740
9	**5-Methylheptacosane**	2749
10	**11,15-Dimethylheptacosane[1]**	2762
11	**3-Methylheptacosane**	2775
12	***5,x-Dimethylheptacosane[x]**	2783
13	Octacosane	2800
14	**Trimethylpentacosane[2]**	2814
15	**12+15+16-Methyloctacosane**	2839
16	**8-Methyloctacosane**	2846
17	**2-Methyloctacosane**	2869
18	**x,10/x,12/x,14-Dimethyloctacosane[y]**	2881
19	Nonacosane	2900
20	**4,8,12-Trimethyloctacosane[1]**	2922
21	**11+13-Methylnonacosane**	2937
22	**7-Methylnonacosane**	2946
23	**5-Methylnonacosane**	2955
24	**11,15-Dimethylnonacosane[1]**	2964
25	**9,15-Dimethylnonacosane[1]**	2971
26	**3-Methylnonacosane**	2977
27	Triacontane	3000
28	**Hentriacontene[3]**	3085

29	Hentriacontane	3100
30	Dotriacontane	3200
31	Tritriacontane	3300

[1] Tentative identification based on Kovats Index

[2] Methyl branch position not determined

[3] Double bond positions only determined in adult flies

[x] x = 9,11, 15

[y] x= methyl branched position not determined
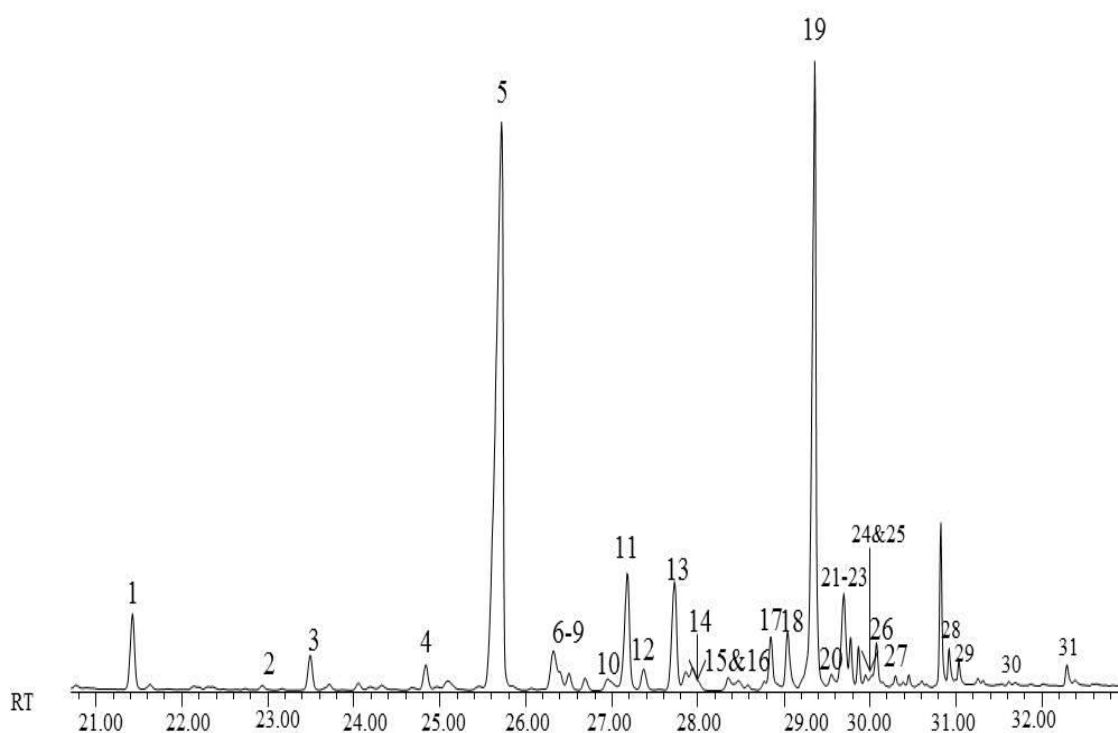
Figure 6.6: GC chromatogram of *C. vicina* puparial case extracted at week 1

Figure 6.6 shows the chemical profile extracted from a week 1 puparial case of C. vicina with all peaks numbered and identified (Table 6.6).

There is considerable fluctuation within the peak areas over time across the compounds used for PCA (Table 6.7 – *n*-alkanes removed). A group of compounds exhibiting substantially higher peak areas over others are 11+13-MeC27:H (peak 6), 3-MeC27:H (peak 11) and 11+13-MeC29:H (peak 21).

C31:1 (compound 28) is the only alkene present in the profile and is detected at its most abundant in week 5 before the concentration drops for the remainder of the extraction period.

When looking at the chromatograms of the varying ages across the extraction period, very few distinctions can be made and ageing from observing the hydrocarbon profiles alone is not possible.

Table 6.7: List of the compounds extracted and used for subsequent PCA analysis from the puparial cases of *C. vicina,* with the total percentage of each compound present, the percentage standard deviation for each week/month and the Kovats Indies to aid identification

Peak number	Peak Identification	Kovats iu	Week 1 n=10 %	Week 2 n=10 %	Week 3 n=10 %	Week 4 n=10 %	Week 5 n=10 %	Week 6 n=10 %	Week 7 n=10 %	Week 8 n=10 %
2	3-Methylpentacosane	2574	0.68±0.28	3.19±1.10	3.01±1.13	3.07±1.10	2.82±1.54	3.07±1.14	3.05±0.78	2.91±0.53
4	2-Methylhexacosane	2661	2.65±1.73	1.60±0.38	2.34±0.62	1.97±0.24	1.97±0.60	2.52±0.87	2.57±1.03	2.38±0.54
6	11+13-Methylheptacosane	2731	6.53±2.69	7.53±1.75	6.97±1.71	7.97±1.94	7.11±2.04	11.57±4.64	9.65±2.18	10.44±2.47
7	9-Methylheptacosane	2734	2.08±0.70	1.77±0.47	1.86±0.53	1.87±0.60	1.93±0.57	2.35±1.31	2.15±0.46	2.28±0.74
8	7-Methylheptacosane	2740	2.54±0.86	3.43±0.74	3.23±0.80	3.25±0.87	3.36±1.09	4.36±1.77	4.02±0.89	4.04±0.73
9	5-Methylheptacosane	2749	2.14±0.79	2.92±0.78	2.88±0.66	2.84±0.53	2.83±1.05	3.06±1.03	2.96±0.59	3.07±0.58
10	11,15-Dimethylheptacosane[1]	2762	2.19±0.57	2.33±0.54	2.40±0.50	2.58±0.58	2.27±1.00	3.05±0.55	2.90±0.53	2.95±0.73
11	3-Methylheptacosane	2775	15.39±2.47	27.58±8.66	27.55±6.60	27.38±6.90	27.27±11.50	21.78±3.82	24.51±5.05	23.29±4.87
12	*5,x-Dimethylheptacosane[1]	2783	3.80±1.21	2.78±0.71	2.71±0.74	2.72±0.70	2.68±0.92	3.49±0.87	3.22±0.70	3.47±0.86
14	Trimethylpentacosane[2]	2814	3.62±1.15	3.53±0.84	3.79±0.90	2.99±1.04	4.60±2.80	1.49±0.27	1.27±0.27	1.32±0.30
15	12+15+16-Methyloctacosane	2839	2.68±1.25	1.81±0.42	1.89±0.43	2.06±0.41	2.12±0.76	2.46±0.68	2.13±0.45	2.40±0.63
16	8-Methyloctacosane	2846	2.34±0.87	2.62±0.75	2.62±0.70	2.58±0.89	2.40±1.15	3.31±0.77	3.24±0.71	3.24±0.60
17	2-Methyloctacosane	2869	7.45±2.88	0.85±0.28	0.83±0.27	0.91±0.27	1.07±0.60	0.65±0.11	0.76±0.21	0.71±0.21
18	x,10/x,12/x,14-Dimethyloctacosane[1]	2881	9.36±2.26	3.00±0.68	3.17±0.68	3.01±0.64	2.72±1.10	5.49±0.83	5.87±1.49	5.22±1.69
20	4,8,12-Trimethyloctacosane[1]	2922	3.02±1.20	2.88±0.91	2.74±0.76	2.83±1.10	2.58±1.39	3.77±0.89	3.85±0.92	3.85±0.69
21	11+13-Methylnonacosane	2937	15.96±5.09	12.29±3.29	12.79±2.84	12.35±3.42	11.87±4.58	14.67±3.04	14.39±2.84	14.88±2.96
22	7-Methylnonacosane	2946	3.83±0.55	3.04±0.85	3.10±0.64	3.04±0.63	3.15±0.99	3.07±0.73	3.28±0.57	3.35±0.58

23	5-Methylnonacosane	2955	2.60±0.22	1.77±0.52	1.85±0.46	2.01±0.55	1.90±0.73	1.41±0.30	1.63±0.38	1.60±0.40
24	11,15-Dimethylnonacosane[1]	2964	1.55±0.46	1.51±0.58	1.37±0.43	1.41±0.61	1.23±0.66	1.41±0.29	1.56±0.34	1.47±0.26
25	9,15-Dimethylnonacosane[1]	2971	1.23±0.40	1.47±0.34	1.54±0.37	1.60±0.54	1.44±0.56	2.11±0.34	1.98±0.40	2.05±0.58
26	3-Methylnonacosane	2977	4.57±0.85	3.83±1.12	3.90±0.82	3.97±0.92	3.84±1.35	3.70±0.69	3.84±0.66	3.89±0.80
28	Hentriacontene[3]	3085	3.78±0.83	8.30±3.28	7.47±2.11	7.60±2.45	8.85±2.06	1.22±0.15	1.18±0.40	1.19±0.24

Peak number	Peak Identification	Kovats iu	Month 3 n=10 %	Month 4 n=10 %	Month 5 n=10 %	Month 6 n=10 %	Month 7 n=10 %	Month 8 n=10 %	Month 9 n=10 %
2	3-Methylpentacosane	2574	2.75±0.59	3.13±0.72	2.87±1.14	2.03±0.55	2.16±0.63	2.20±0.23	1.94±0.46
4	2-Methylhexacosane	2661	3.81±10.65	0.39±0.12	2.46±0.95	1.78±0.53	1.81±0.37	1.94±0.45	1.86±0.32
6	11+13-Methylheptacosane	2731	10.20±2.05	10.15±1.86	10.44±4.10	7.59±2.45	7.96±2.15	8.59±1.85	9.01±2.05
7	9-Methylheptacosane	2734	2.32±0.64	2.28±0.48	2.40±0.95	1.55±0.59	1.66±0.50	1.78±0.34	2.06±0.35
8	7-Methylheptacosane	2740	3.93±0.69	4.03±0.78	4.12±1.60	3.04±1.01	3.17±0.85	3.33±0.65	3.59±0.74
9	5-Methylheptacosane	2749	2.75±0.52	3.05±0.58	3.02±1.16	2.80±1.56	2.54±0.68	2.54±0.40	2.43±0.55
10	11,15-Dimethylheptacosane[1]	2762	3.00±0.63	3.03±0.60	2.98±1.17	2.44±0.77	2.53±0.63	2.59±0.51	2.35±0.47
11	3-Methylheptacosane	2775	22.80±4.06	23.68±4.45	23.26±8.94	19.43±5.57	21.13±6.07	20.20±2.46	18.71±4.53
12	5,x-Dimethylheptacosane[x]	2783	3.50±1.04	3.44±0.79	3.53±1.38	2.76±0.90	2.66±0.63	2.84±0.68	3.14±0.57
14	Trimethylpentacosane[2]	2814	1.09±0.20	1.13±0.24	1.55±0.67	3.54±1.09	3.33±0.75	3.42±0.85	4.07±0.99
15	12+15+16-Methyloctacosane	2839	3.81±0.75	3.87±0.90	4.16±1.54	1.93±0.63	1.97±0.49	2.07±0.47	2.11±0.42
16	8-Methyloctacosane	2846	3.07±0.57	3.01±0.70	3.02±1.20	3.15±1.55	2.61±0.69	2.69±0.63	2.96±0.62
17	2-Methyloctacosane	2869	0.65±0.17	0.70±0.14	0.66±0.29	7.05±2.80	6.22±1.43	6.82±1.85	6.60±1.29
18	x,10/x,12/x,14-Dimethyloctacosane[y]	2881	5.42±0.92	6.06±1.41	4.81±1.90	6.59±1.77	6.80±1.81	5.78±1.13	4.36±1.30
20	4,8,12-Trimethyloctacosane[1]	2922	3.65±0.78	3.58±0.88	3.59±1.44	4.26±1.32	3.62±0.94	3.54±0.90	3.91±0.91
21	11+13-Methylnonacosane	2937	14.15±2.25	14.58±2.62	14.34±5.55	14.04±4.02	13.95±3.61	14.62±3.31	16.48±3.33
22	7-Methylnonacosane	2946	3.11±0.52	3.40±0.58	3.27±1.25	3.18±1.01	3.25±0.95	3.26±0.60	3.66±0.83
23	5-Methylnonacosane	2955	1.62±0.49	1.67±0.28	1.63±0.65	1.84±0.62	1.92±0.62	1.73±0.26	1.64±0.46
24	11,15-Dimethylnonacosane[1]	2964	1.60±0.50	1.43±0.25	1.31±0.55	1.69±0.56	1.50±0.41	1.51±0.33	1.58±0.40
25	9,15-Dimethylnonacosane[1]	2971	1.94±0.36	2.13±0.47	2.10±0.79	2.46±0.93	2.17±0.73	2.27±0.49	2.30±0.53
26	3-Methylnonacosane	2977	3.84±0.65	3.97±0.68	3.94±1.51	4.22±1.28	4.14±1.10	4.14±0.70	4.38±1.01

| 28 | Hentriacontene[3] | 3085 | 1.01±0.23 | 1.29±0.33 | 0.53±0.26 | 2.63±0.77 | 2.89±0.89 | 2.17±0.53 | 0.87±0.36 |

[1]Tentative identification based on Kovats Index

[2]Methyl branch position not determined

[3]Double bond positions only determined for adult flies

[x]x = 9,11, 15

[y]x= methyl branched position not determined

Of the 31 resolvable peaks extracted from the cuticle of the puparial cases, 22 were used for PCA. Enhanced PCA results were obtained when the *n*-alkanes were excluded from the dataset. The methyl branched compounds consisted of 66% and the alkenes only contributed 3% to the total number of hydrocarbons present. The *n*-alkanes were removed to reduce the scatter and enhance the results.

The PCA was carried out using six principal components, describing 99.0% of the variation within the dataset with the first three principal components comprising 91.7%, 3.8% and 2.2% respectively. PC3 and PC2 were used to plot the relevant scores (see appendix 31 for PCA eigenvalues).
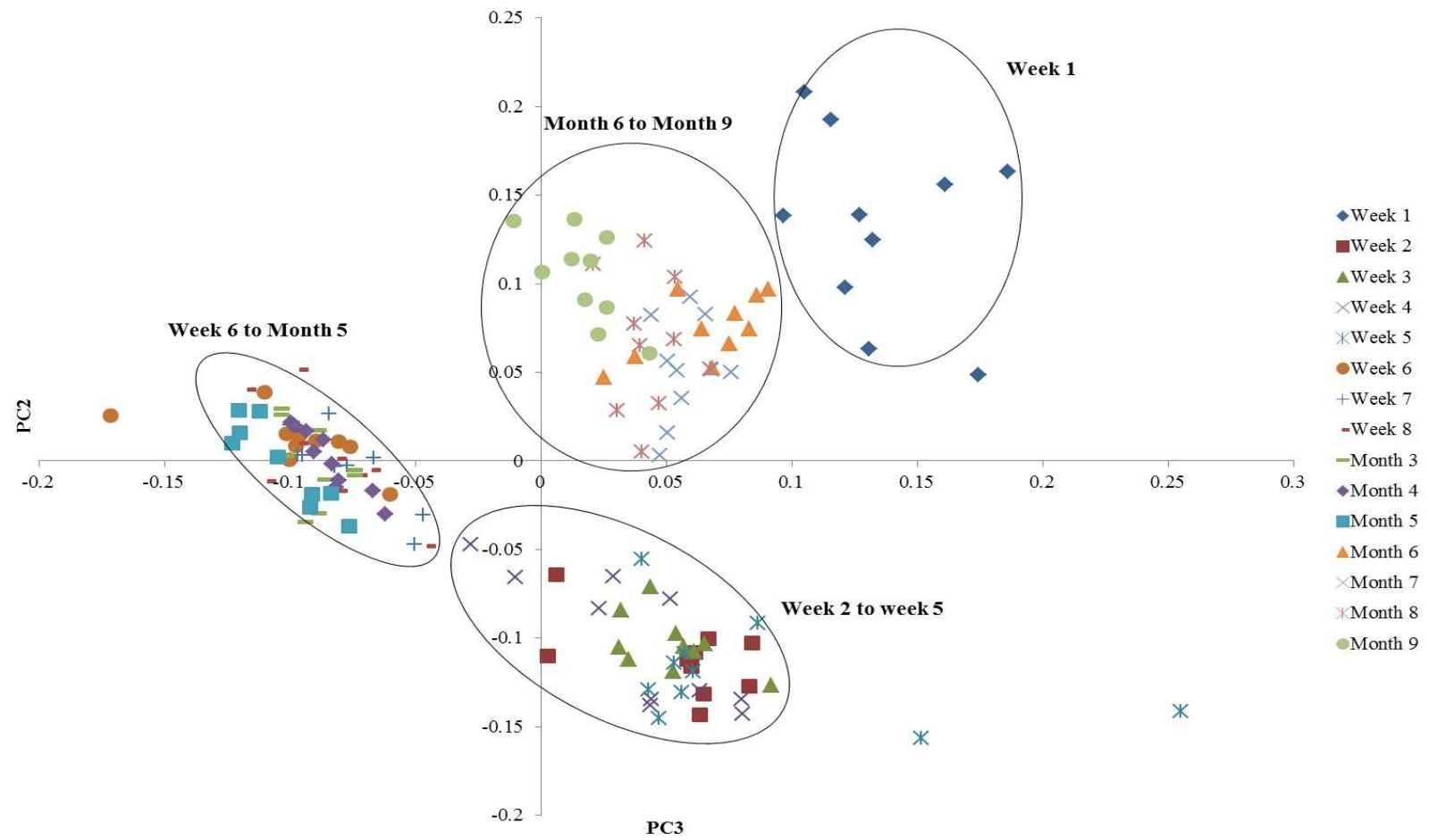
Figure 6.7: PCA plot showing PC3 against PC2 for *C. vicina* puparial cases with clustering days circled

Four groups are apparent from the PCA plot in Figure 6.7. These groups contain extracts from week 1, which clusters individually to the other extracts as one group (although more scatter is observed). Weeks 2 to 5 cluster together as does week 6 to month 5 and finally months 6 to 9. The compounds that yield substantially large scores in the PCA are 11+13-MeC29:H and C31:1.

Results were presented up to month 9 and although there are two groups within the PCA plot that clustered a number of extraction periods (i.e. months 6 to 9), this technique still demonstrates great potential and when used in conjunction with other entomological evidence that may be present, it may help to shorten the window of time in long PMI estimations.

6.3.2 General Discussion and Conclusion for ageing puparial cases

The profile of *L. sericata* consisted of fewer methyl-branched hydrocarbons (50%) in comparison to *C. vicina* (68%), which enables the profiles to be used for identification means (chapter 4) as well as for ageing.

A paper published by Zhu and co-workers [3] presented results from the puparial case of *Chrysomya megacephala* to test the effect that weathering may have on the hydrocarbons. They were able to determine a number of significant time-dependant changes within the hydrocarbon profile, therefore highlighting its potential to be used for ageing the empty puparial cases and aiding PMI estimations [3].

The results presented for *L. sericata* and *C. vicina* puparial cases show great potential for a life stage that presently cannot be aged. Puparial cases are often overlooked at

crime scenes because little information about their age can be established. However, in scenes where puparial cases are the only entomological evidence present, being able to age them or have an indication of their age would be extremely advantageous.

Both species can be aged to a similar time period, with week 1 clustering by itself, followed by another cluster of weeks 2 to 5. The cluster times then differ slightly between the two species.

Observation of the GC chromatograms alone cannot be used to determine the ages of the cases and there are very few significant trends when looking at the peak area percentages of the compounds present. The results are therefore reliant on PCA analysis to discriminate between the varying peak ratios over time and to group the ages accordingly.

However, even to be able to age the younger puparial cases in a 3 to 4 week time frame is extremely beneficial for criminal investigations since there are currently no means of ageing the empty puparial cases and their evidence can be compiled with other entomological information present at the scene to achieve a more accurate PMI estimation.

The results presented here were obtained from standardised laboratory conditions but future work would examine puparial cases that have been exposed to the outdoor environment to study the stability of hydrocarbons and to see what effect weathering may have on them.

6.4 Adult Flies

When a forensic entomologist is presented with an indoor crime scene where adult flies have accumulated e.g. by a window, it would be advantageous if the age of the flies could be established. This could determine the age of the older flies that are potentially the initial colonisers of the body or the younger flies that have developed on the body and hatched at the scene.

The only morphological changes that occur happen within the first few hours after a fly has emerged. As it emerges from the puparial case, flies have an unusual appearance (Figure 6.8). There is a protruding region of the flies head, called the ptilinum, which becomes inflated with blood and enables them to push their way out of the case. This retracts after a few hours, forming the ptilinal suture of the head. The wings of the fly are also crumpled and the body is brown/grey in colour.

Figure 6.8: Newly emerged fly, showing the inflated ptilinum, unformed wings and lack of colouring

However, once the ptilinum sinks back into the facial structure, the fly's wings are fully formed and it gains its colour (a few hours after eclosion), there are no other morphological characteristics to determine the age.

Hydrocarbon analysis on mature insects such as grasshoppers [13] and cockroaches [14] has been carried out to establish the age and sex. Hydrocarbon studies have also been carried out on several Diptera [15–18], and also more specifically on Calliphoridae [6], but few have been carried out in relation to its importance in forensic entomology [5].

The final part of this chapter presents preliminary results in an attempt to age the three species of blowflies, *L. sericata*, *C. vicina* and *C. vomitoria*. The cuticular hydrocarbons were extracted from the flies and analysed using GC-MS and PCA, over a period of thirty days (with the exception of *L. sericata* which was extracted at three time intervals up to 10 days – experiment carried out at the end of the experimental period and this particular colony did not produce enough eclosing adult flies to continue any further past this age).

6.4.1 Results and Discussion for adult flies

L. sericata:

The hydrocarbon profile of *L. sericata* yielded 59 identifiable compounds with some co-eluting for a total of 48 peaks from day 1 to day 10. They consisted of *n*-alkanes (15), alkenes (23%), and methyl hydrocarbon (63%) (for day 1). Figure 6.9 shows the GC chromatograms of a single adult fly sample from day 1, 5 and 10. Chemical distinctions can be made between the different fly ages, especially between days 1 and 5 where the chemical profiles change considerably.
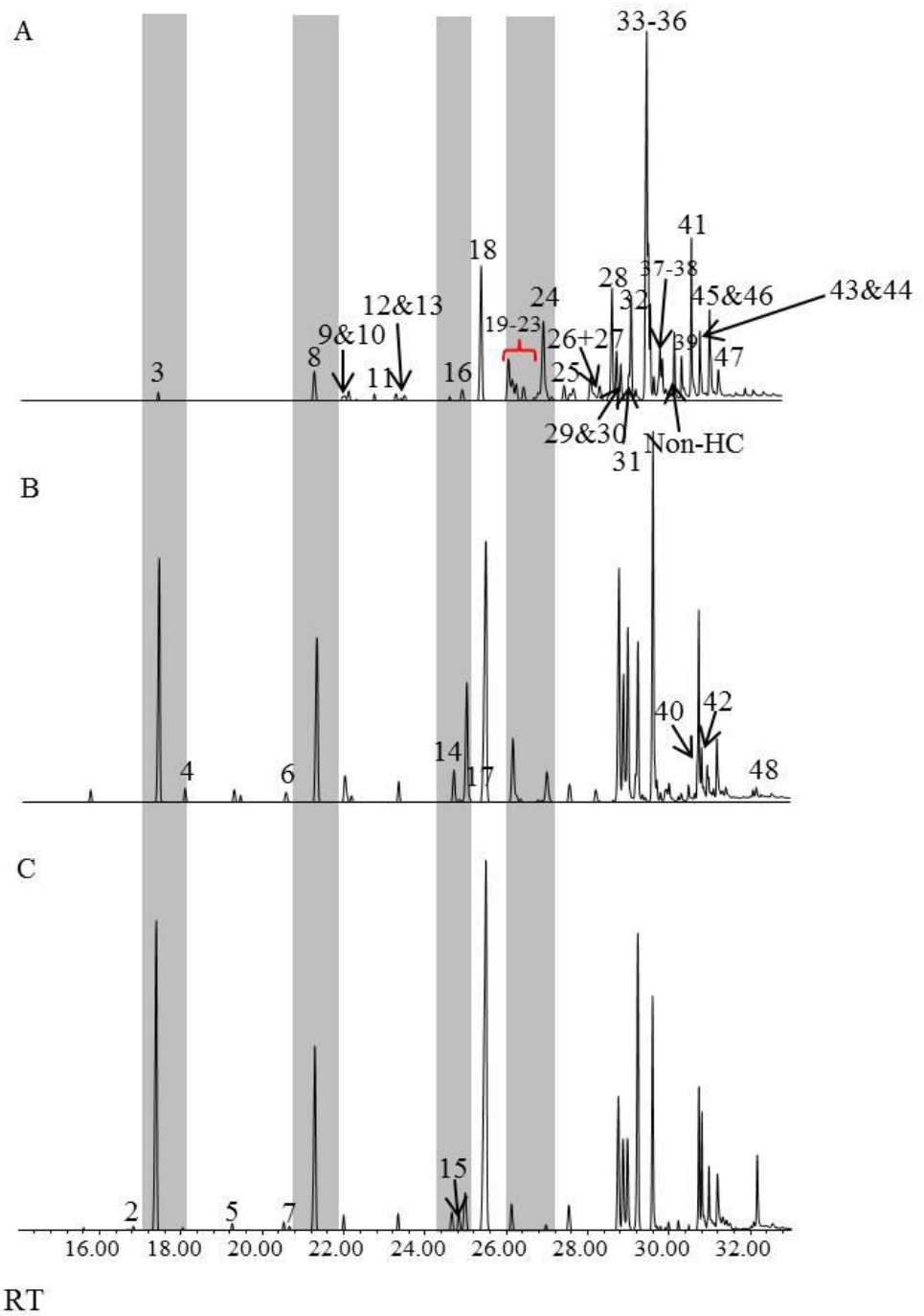
Figure 6.9: GC chromatograms of *L. sericata* adult fly at three different ages, A: Day 1, B: Day 5 and

C: Day 10. Shaded bars illustrate distinctive changes over time indicating specific areas of interest

When looking at the GC chromatograms of the extracted flies (Figure 6.9), it is more

difficult to distinguish between day 5 and day 10. However, when the peaks have been

identified, there are some characteristic compounds that are specific to the two ages.

For example, there is a C23:1 isomer (compound 2) that is only detectable in day 10 (1.23%), as well as C24:H (compound 5 – present in a low percentage 0.69%) and C25:1 (compound 7, 2.15%). The presence of these three compounds alone with a peak area of at least 0.5% indicates the fly is older than 5 days.

Figure 6.10 shows the total number of compounds plotted against the class of hydrocarbons, from days 1, 5 and 10.
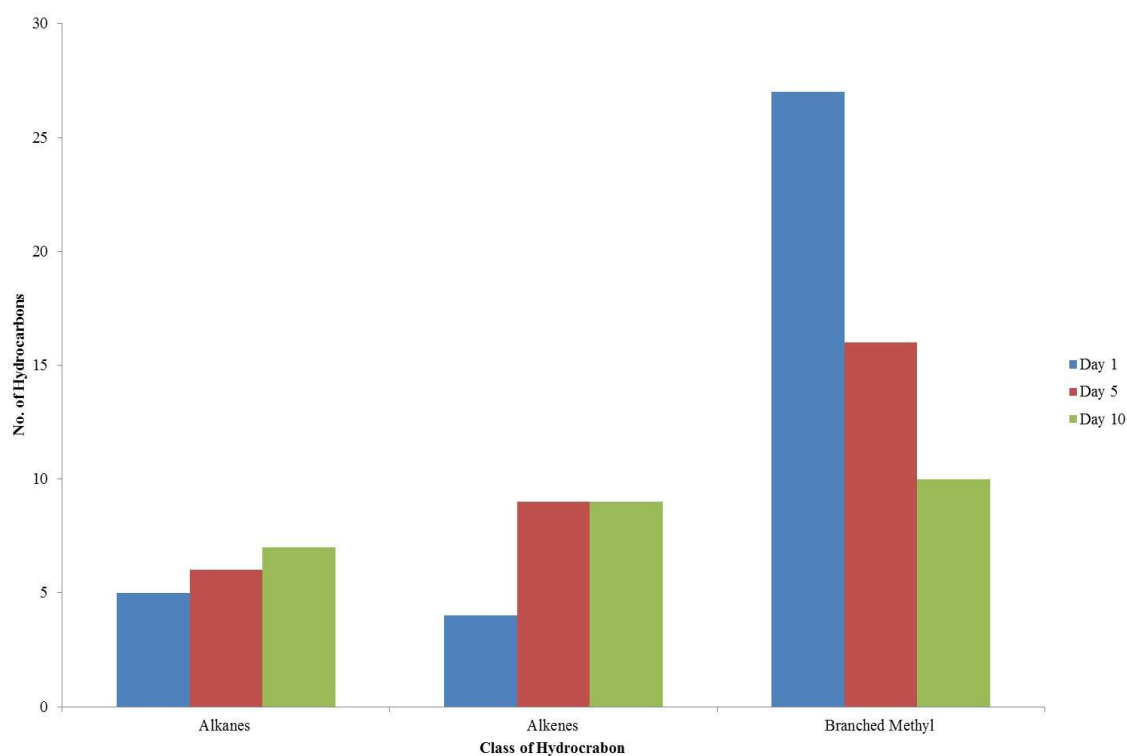
Figure 6.10: Graph showing the total number of *n*-alkanes, alkenes and methyl branched alkane hydrocarbons present up to day 10 of the adult fly of *L. sericata*

The number of *n*-alkanes increases slightly with age whilst the number of alkenes increases substantially between days 1 and 5 and then even out in day 10. However,

day 5 and 10 do not display the same alkene compounds. Day 5 contains one C23:1 peak and C25:1 is not observed in a sufficient relative percentage, whereas day 10 contains two C23:1 compounds in different amounts and C25:1. Day 10 only contains two C27:1 peaks (day 5 exhibits three) and C31:2 is specific (above the 0.5% threshold) to day 5 only. The number of methyl branched hydrocarbons decreases considerably over the extractions period and day 1 contains a large number of methyl branched hydrocarbons specific to that day, making them very good age indicators. Table 6.8 lists the compounds extracted from the fly over the 10 days.

Table 6.8: List of the compounds extracted and used for subsequent PCA from the adult flies of *L. sericata,* with the total percentage of each compound present, the percentage standard deviation for each day and the Kovats Indices to aid identification

Peak no.	Peak Identification	Kovats iu	Day 1 n=10 %	Day 5 n=10 %	Day 10 n=10 %
1	Henicosane	2100	tr	0.72±0.32	0.83±0.48
2	Tricosene[2]	2265	tr	tr	1.23±0.94
3	Tricosane	2300	0.63±0.18	11.62±6.87	19.21±17.86
4	9+11-Methyltricosane	2337	tr	0.48±0.23	tr
5	Tetracosane	2400	tr	tr	0.69±0.37
6	2-Methyltetracosane	2464	tr	0.64±0.22	0.65±0.30
7	Pentacosene[2]	2472	tr	tr	2.15±1.86
8	Pentacosane	2500	2.28±0.44	8.20±4.89	16.06±9.20
9	9+11-Methylpentacosane	2539	0.81±0.24	1.43±0.67	1.58±0.89
10	7-Methylpentacosane	2544	0.84±0.25	tr	tr
11	3-Methylpentacosane	2574	0.67±0.30	tr	tr
12	Hexacosane	2600	0.69±0.13	0.66±0.44	0.93±0.39
13	8-Methylhexacosane	2611	0.68±0.27	tr	tr
14	2-Methylhexacosane	2664	tr	1.60±0.57	1.78±0.89

15	Heptacosene[2]	2671	tr	0.49±0.46	4.71±3.88
16	Heptacosene[2]	2678	0.78±0.36	7.53±4.11	1.53±0.65
17	Heptacosene[2]	2689	tr	0.31±0.17	tr
18	Heptacosane	2700	8.60±1.41	13.27±6.15	18.36±7.22
19	13-Methylheptacosane	2734	3.57±0.68	2.08±1.40	1.51±0.54
20	9-Methylheptacosane	2738	1.46±0.32	tr	tr
21	7-Methylheptacosane	2743	1.26±0.25	tr	tr
22	5-Methylheptacosane	2752	1.35±0.29	tr	tr
23	2-Methylheptacosane	2769	0.70±0.22	tr	tr
24	3-Methylheptacosane	2775	7.66±1.40	1.85±0.75	0.62±0.24
25	Octacosane	2800	1.03±0.17	0.80±0.30	0.64±0.21
26	12+14-Methyloctacosane	2841	2.01±0.36	0.71±0.36	tr
27	8-Methyloctacosane	2845	0.55±0.12	tr	tr
28	2-Methyloctacosane	2872	5.29±0.89	8.86±3.15	5.01±1.68
29	Nonacosene[2]	2879	2.63±0.78	5.51±3.06	7.85±4.57
30	Nonacosene[2]	2885	1.57±0.45	6.61±3.32	1.55±0.31
31	2,12/2,14-Dimethyloctacosane[1]	2897	1.04±0.18	0.73±0.50	tr
32	Nonacosane	2900	4.08±0.89	4.37±1.70	4.10±1.84
33	11+15-Methylnonacosane	2939	19.23±2.94	10.88±5.31	2.88±1.02
34	9-Methylnonacosane	2943	6.25±5.02	0.54±0.24	tr
35	7-Methylnonacosane	2948	3.78±0.55	tr	tr
36	5-Methylnonacosane	2957	1.10±0.19	tr	tr
37	9,17-Dimethylnonacosane[1]	2972	2.26±0.36	tr	tr
38	3-Methylnonacosane	2978	1.80±0.28	0.65±0.28	tr
39	12+14+16+18-Methyltriacontane	3035	1.81±0.33	tr	tr
40	Hentriacontadiene[2]	3064	tr	0.97±0.66	tr
41	2-Methyltriacontane	3068	5.09±0.95	3.62±1.28	2.32±0.64
42	Hentriacontene[2]	3078	tr	1.43±0.55	1.20±0.40
43	2,12/2,14-Dimethyltricontane[1]	3096	1.88±0.56	0.73±0.32	0.60±0.17
44	2,8-Dimethyltriacontane[1]	3099	0.56±0.15	tr	tr
45	11+13+15-Methylhentriacontane	3121	3.05±0.56	1.48±0.93	1.05±0.31
46	9-Methylhentriacontane	3123	1.02±0.23	tr	tr
47	11,19-Dimethylhentriacontane[1]	3143	1.98±0.39	0.61±0.30	tr
48	Tritriacontene[2]	3217	tr	0.60±0.28	0.93±0.28

[1] Tentative identification based on Kovats Index

[2] Double bond positions determined for adult flies (see page 126)

tr = Trace amount detected (<0.5%)

Some compounds fluctuate above the 0.5% threshold in particular days. Day 1 has 14 peaks detectable above 0.5% that are observed in peak areas lower than the stated threshold in all of the other days. These 14 peaks are all methyl branched compounds (peaks 10, 11, 13, 20-23, 27, 35-37, 39, 44 and 46). In particular, the presence of two MeC27:H (peaks 20-23) and MeC29:H (peaks 35-37) classify the profile of a very immature fly that is aged between 1 and 4 days old.

Day 5 has three compounds that are present above the threshold, making them detectable in this day only. These compounds are 9+11-MeC23:H, C27:1 and C31:2. Day 10 also has three compounds specific to that day which are C23:1, C25:1 and C24:H. These small differences in the chemical composition of the profiles for the three different ages make them very distinguishable and allow for the age range (day 1, 5 or 10) to be established from the hydrocarbon profile.

Figure 6.11 shows selected hydrocarbons plotted against the average percentage peak area, highlighting trends in the concentrations of certain compounds with time.
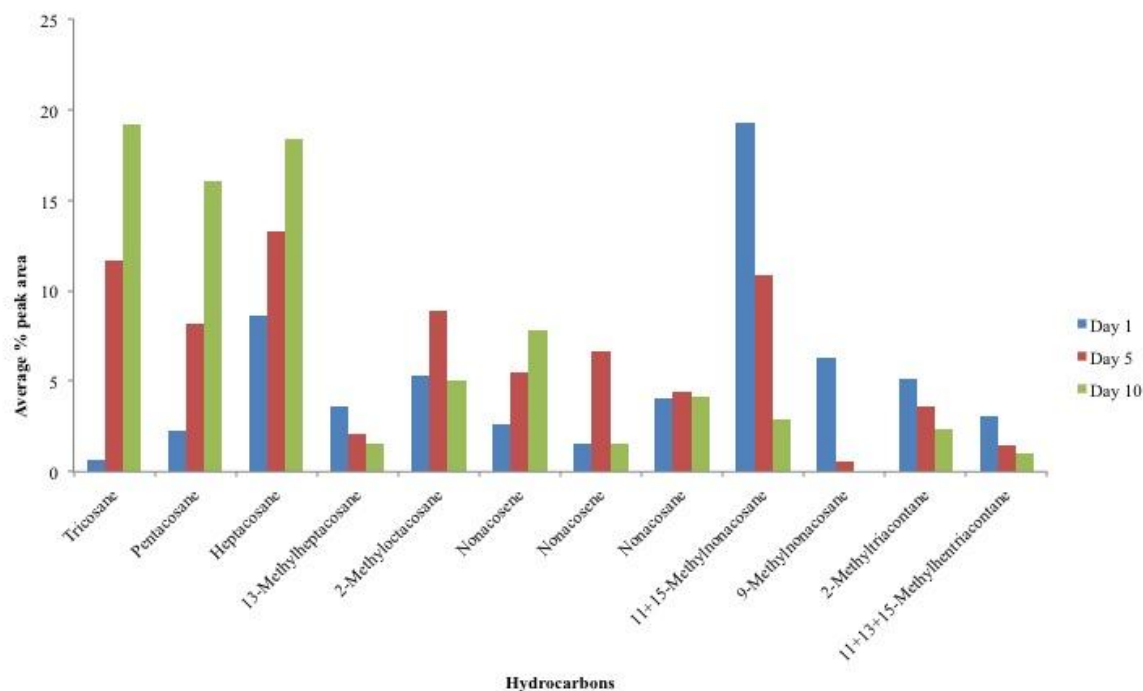
Figure 6.11: Graph of the average percentage peak area for selected hydrocarbon compounds over the 10 day extraction period for *L. sericata* adult flies

When looking at the percentages of the hydrocarbons present, more characteristic trends are observed. In general, the relative percentage of the *n*-alkanes increase with age (Figure 6.11). The alkenes and methyl hydrocarbons also make good age indicators. One isomer of C29:1 increases with age and in general the methyl hydrocarbons decrease with time.

The PCA was carried out using six principal components, describing 99.0% of the variation within the dataset with the first three principal components comprising 65.5%, 24.3% and 3.7% respectively. PC3 and PC2 were used to plot the relevant scores (see appendix 32 for PCA eigenvalues).

Figure 6.12 shows the PCA plot of PC3 vs PC2 for data gathered from day 1, 5 and 10 of adult fly extractions of *L. sericata*.

Figure 6.12: PCA plot showing PC3 against PC2 for *L. sericata* adult flies, with clustering days circled.
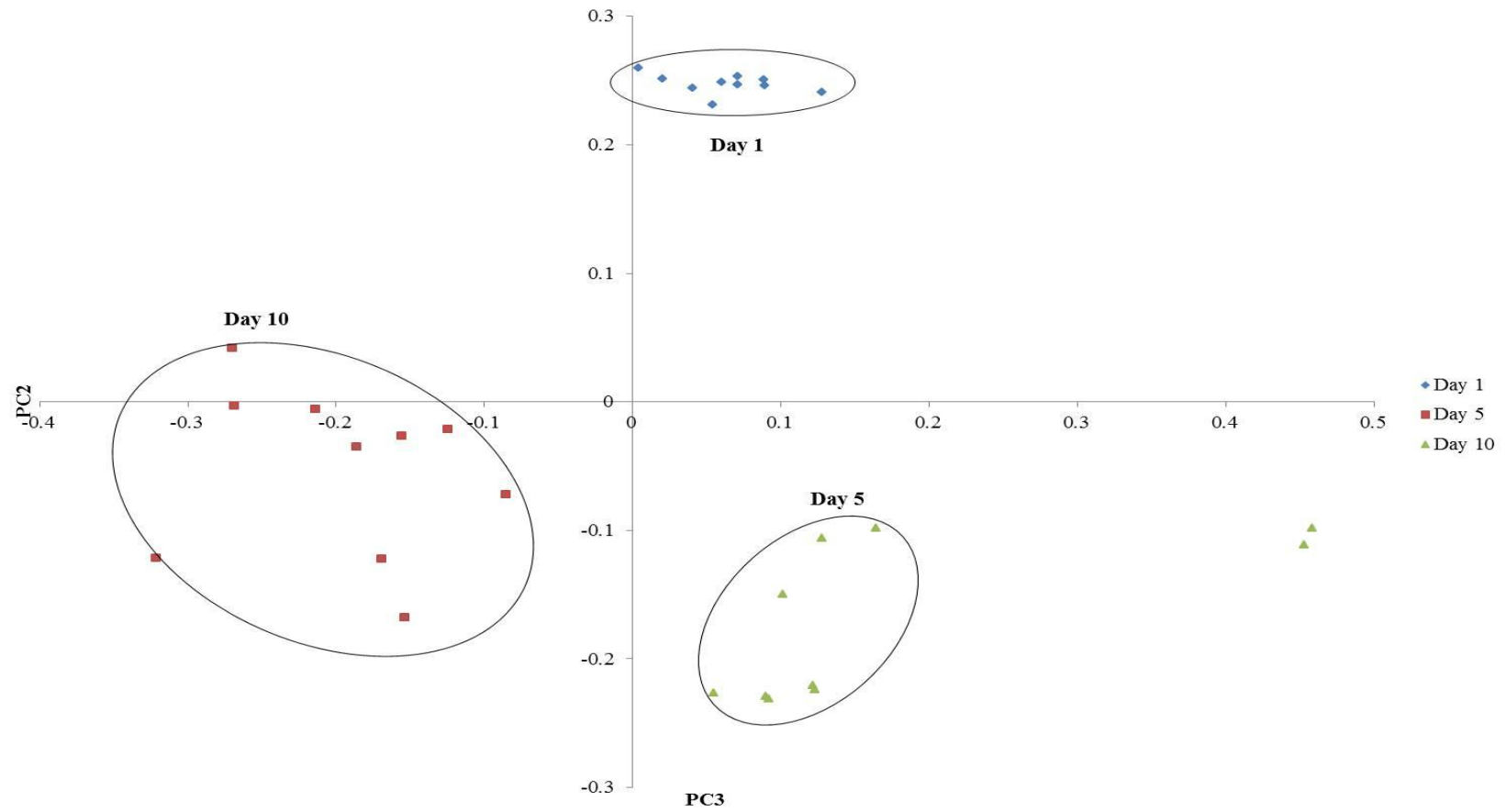
From the PCA plot, it is evident that there are three distinct groups where the principal components of each sample cluster together, representing the ages of the flies over the three extraction days. Even with the scatter observed in the older flies, the age range can still be established from the plot. The key compound which has a substantial loading value is 11+15-MeC29:H.

From the results presented for the adult fly of *L. sericata*, it is clear to see distinct chemical changes associated with the age. The increase of C25:H and C27:H and decrease of C28:H with time give potential for these three *n*-alkanes to be utilised as good age markers within the hydrocarbon profile of *L. sericata* adult flies.

As illustrated in the results section, there are a number of compounds that are specific to certain days and therefore their presence, or lack of, can give an indicator of the fly's age even before PCA analysis is applied to the correlated dataset.

The profile of Day 1 changes drastically compared to that of day 5 and day 10. This immature age is dominated by methyl branched hydrocarbons. A very simple and quick way to determine a day 1 fly from an older one would be to look for a group of MeC27:H peaks (peaks 20 to 23) and two MeC29:H and one DimeC29:H (peaks 35-37).

C. vicina:

The hydrocarbon profile of *C. vicina* exhibits 77 compounds with some co-eluting for a total of 57 resolvable peaks from day 1 to day 30, with day 1 consisting of *n*-alkanes (12%), alkenes (23%) and methyl hydrocarbons (65%). Figure 6.13 shows the stacked

GC chromatograms of a single sample from day 1, 5, 10 and 20 respectively. Clear distinctions can be made between the different ages when the chemical profile is examined.
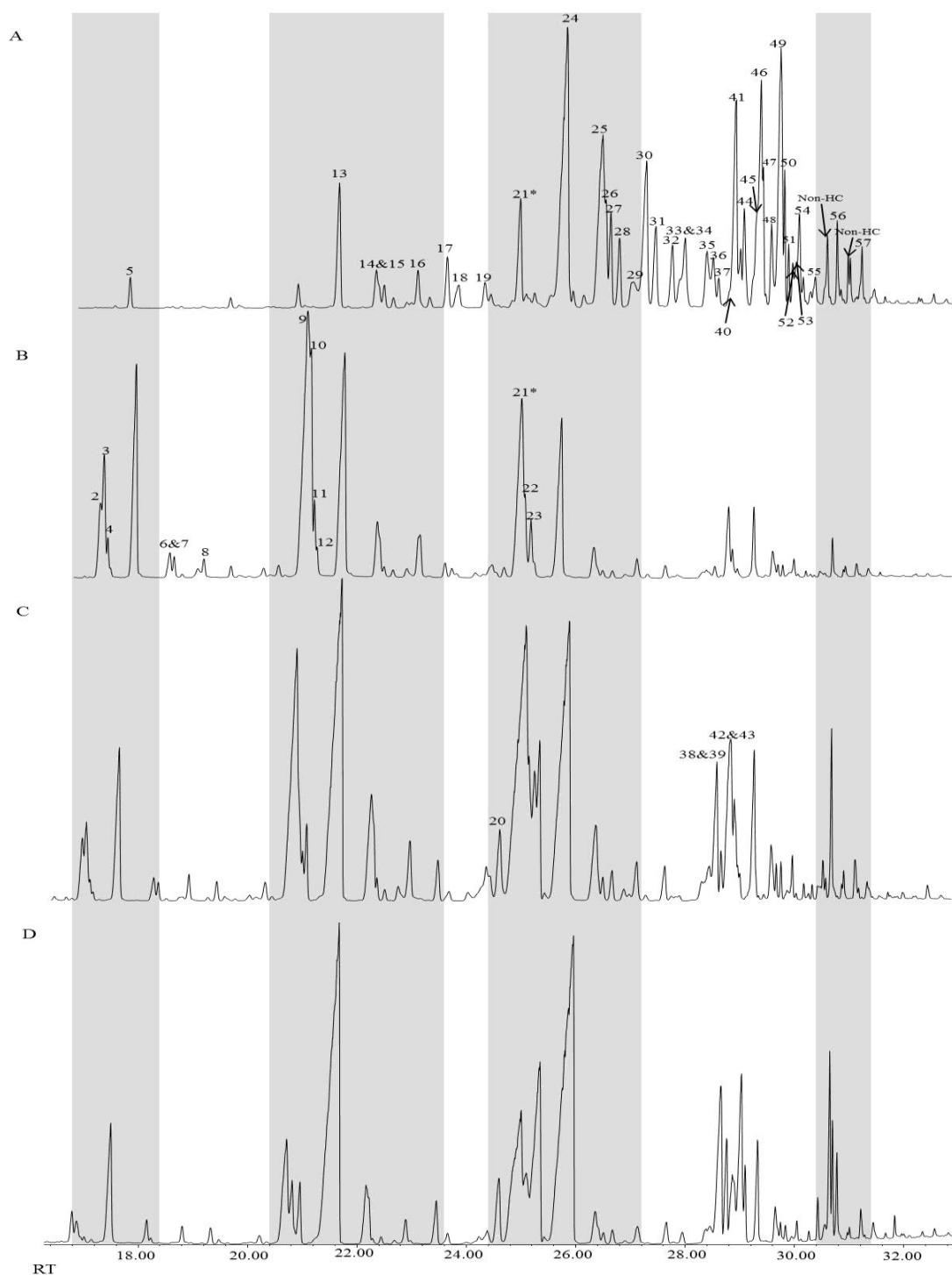
Figure 6.13: GC chromatograms of *C. vicina* adult flies at four different ages, A: Day 1, B: Day 5, C: Day 10 and D: Day 20. Shaded bars illustrate distinctive changes over time indicating specific areas of interest

It is clear to see characteristic changes in relation to the fly's age from the chromatogram comparison. The shaded bars show some areas of contrast within the profiles of the different ages. The stacked GC chromatograms in Figure 6.13 show that some peaks are overloaded. This is due to the adult flies having a much larger surface area and therefore containing a much higher concentration of hydrocarbons on their cuticles.
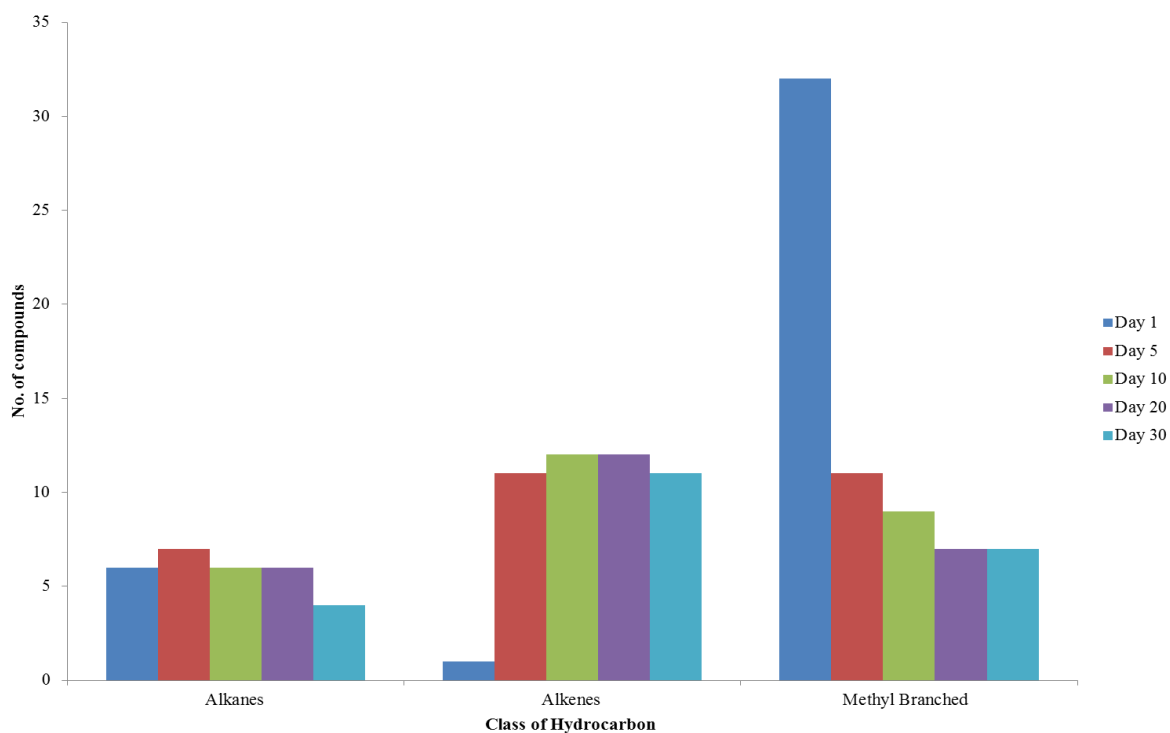
Figure 6.14: Graph showing the total number of alkanes, alkenes and methyl branched hydrocarbons present up to day 30 for the adult fly of *C. vicina*

The number of *n*-alkanes remains relatively stable across the 30 days with the exception of day 30 which decreases due to the "loss" of C28:H and C30:H (peak areas drop below 0.5%). C31:H only displays a peak area above 0.5% in day 5.

There is a considerable increase in the number of alkenes between day 1 and day 5 (Figure 6.14), as seen in the profile of *L. sericata* adult flies. However, from day 5 onwards they remain relatively stable across the extraction period. The number of methyl branched compounds decreases over the extraction period, and day 1 is dominated by methyl branched compounds specific to that day, making them effective age indicators. The total number of hydrocarbons also decreases with age.

Table 6.9 lists the compounds extracted from the fly over the 30-day period.

The reader is referred to appendices 33 and 34 for example mass spectra of tri-methyl alkanes.

Table 6.9: List of the compounds extracted and used for subsequent PCA analysis from the adult flies of *C. vicina,* with the total percentage of each compound present, the percentage standard deviation for each day and the Kovats Indices to aid identification

Peak no.	Peak Identification	Kovats iu	Day 1 n=10 %	Day 5 n=10 %	Day 10 n=10 %	Day 20 n=10 %	Day 30 n=10 %
1	Heneicosane	2100	tr	0.66±0.23	tr	tr	tr
2	2-Methyldocosane	2269	tr	3.84±3.63	1.99±0.91	0.82±0.38	1.97±1.12
3	Tricosene[1]	2273	tr	4.63±3.48	2.57±0.57	0.63±0.20	tr
4	Tricosene[1]	2275	tr	0.79±0.53	tr	tr	tr
5	Tricosane	2300	0.42±0.19	9.10±3.99	5.47±0.81	2.68±0.73	tr
6	11+9-Methyltricosane	2338	tr	1.22±0.77	0.91±0.26	tr	tr
7	7-Methyltricosane	2343	tr	0.89±0.78	tr	tr	tr
8	3-Methyltricosane	2372	tr	0.61±0.35	tr	tr	tr
9	2-Methyltetracosane + Pentacosene[1]	2446	tr	11.30±6.01	1.17±0.43	tr	tr
10	Pentacosene[1]	2475	tr	3.12±1.53	10.72±4.96	4.35±1.14	5.73±4.67
11	Pentacosene[1]	2476	tr	0.93±0.51	2.31±0.64	1.72±0.61	2.89±2.41
12	Pentacosene[1]	2484	tr	0.82±0.27	2.31±0.81	1.29±0.47	1.18±1.04
13	Pentacosane	2500	3.52±0.57	12.53±5.13	17.60±4.40	18.74±7.08	21.12±11.53
14	11+9-Methylpentacosane	2535	1.43±0.44	4.80±2.54	2.98±1.36	2.72±0.85	3.39±1.76
15	7-Methylpentacosane	2543	0.74±0.22	tr	tr	tr	tr
16	3-Methylpentacosane	2574	1.17±0.34	1.26±0.60	0.94±0.46	0.70±0.35	0.91±0.68
17	Hexacosane	2600	1.14±0.44	0.80±0.22	0.86±0.27	0.87±0.31	0.83±0.33
18	3,7-Dimethylpentacosane[2]	2610	1.09±0.35	tr	tr	tr	tr
19	12+14+16-Methylhexacosane	2633	0.83±0.30	tr	tr	tr	tr
20	Heptacosadiene	2655	tr	tr	1.81±0.72	1.54±0.42	1.15±0.69

259

21	Heptacosene[1*]	2661	3.49±0.78	12.47±5.49	11.37±8.20	15.31±16.58	17.57±16.20
22	Heptacosene[1]	2667	tr	2.25±0.76	3.46±1.48	2.49±0.70	2.38±1.34
23	Heptacosene[1]	2671	tr	2.25±0.76	4.09±2.72	5.83±3.48	4.26±3.27
24	Heptacosane	2700	15.12±2.72	10.67±4.92	14.48±3.85	22.74±9.70	21.59±8.31
25	11+13-Methylheptacosane	2734	9.32±2.27	2.68±1.86	1.18±0.84	0.95±0.38	1.18±0.49
26	9-Methylheptacosane	2737	1.95±0.43	tr	tr	tr	tr
27	7-Methylheptacosane	2742	2.15±0.47	tr	tr	tr	tr
28	5-Methylheptacosane	2750	1.89±0.41	tr	tr	tr	tr
29	9,13+9,15-Dimethylheptacosane[2]	2764	1.33±1.17	tr	tr	tr	tr
30	3-Methylheptacosane	2776	6.28±1.21	1.13±0.55	0.72±0.36	tr	tr
31	5,9+5,13-Dimethylheptacosane[2]	2784	2.53±0.57	tr	tr	tr	tr
32	Octacosane	2800	1.96±0.46	1.76±3.32	0.76±0.35	tr	tr
33	3,9+3,11-Dimethylheptacosane[1]	2811	0.90±0.29	tr	tr	tr	tr
34	Trimethylheptacosane[2]	2815	2.47±0.54	tr	tr	tr	tr
35	12+14+16-Methyloctacosane	2840	2.39±0.53	tr	tr	tr	tr
36	3,7,15+3,7,15-Trimethylheptacosane[2]	2847	1.11±0.32	tr	tr	tr	tr
37	6-Methyloctacosane	2853	0.76±0.17	tr	tr	tr	tr
38	Nonacosadiene	2860	tr	0.80±0.43	2.83±1.49	4.70±1.40	2.94±2.26
39	Nonacosadiene	2865	tr	tr	0.92±0.45	1.48±0.81	1.41±1.28
40	4-Methyloctacosane	2867	4.71±1.80	tr	tr	tr	tr
41	2-Methyloctacosane	2871	1.28±1.41	3.36±1.82	3.08±2.15	2.69±1.43	3.04±2.26
42	Nonacosene[1]	2880	tr	1.22±0.80	2.37±1.30	2.64±1.14	2.31±2.04
43	Nonacosene[1]	2887	tr	tr	tr	1.81±2.80	0.72±1.18
44	6,14-Dimethyloctacosane[2]	2882	2.53±0.57	tr	tr	tr	tr
45	2,12+2,14-Dimethyloctacosane[2]	2895	1.44±0.78	tr	tr	tr	tr
46	Nonacosane	2900	5.47±1.30	2.30±1.55	1.91±1.08	2.11±0.75	2.21±1.01
47	x,6-Dimethyloctacosane + x,10,14-Trimethyloctacosane	2904	1.13±0.31	tr	tr	tr	tr

48	4,8,12+4,8,14-trimethyloctacosane[2]	2921	1.34±0.39	tr	tr	tr	tr
49	9+11+1315-Methylnonacosane	2941	8.25±1.92	0.90±0.52	tr	tr	tr
50	7-Methylnonacosane	2949	1.98±0.47	tr	tr	tr	tr
51	5-Methylnonacosane	2957	1.16±0.42	tr	tr	tr	tr
52	11,15-Dimethylnonacosane[2]	2966	0.63±0.20	tr	tr	tr	tr
53	9,17-Dimethylnonacosane[2]	2972	0.89±0.24	tr	tr	tr	tr
54	3-Methylnonacosane +7,11-Dimethylnonacosane[2]	2979	2.45±0.54	tr	tr	tr	tr
55	trimethylnonacosane	3015	0.65±0.13	tr	tr	tr	tr
56	2-Methyltriacontane	3070	1.07±0.29	0.90±0.33	1.18±0.52	1.19±0.44	1.23±0.56
57	11+13-Methylhentriacontane	3124	1.05±0.28	tr	tr	tr	tr

[1] Double bond positions determined (see page 126) – alkadiene bond position not determined

[2] Tentative identification based on Kovats Index values and match with NIST08 Library database

[*] 2-MeC26:H in day 1 then co-elutes with C27:1 in day 5 onwards

Tr = Trace amount detected (<0.5%)

Day 1 has a substantially large number of compounds (25) observed above the 0.5% peak area threshold for that day alone, all of which are methyl branched compounds (see Table 6.9). They are mainly long chain length methyl branched compounds and act as a very good age indicator for the immature flies. Day 1 has a 2-MeC26:H hydrocarbon that is seen as a single peak for this age, but from day 5 onwards the peak is largely C27:1.

Day 5 has four compounds specifically observed above the 0.5% threshold for this day alone, one *n*-alkane (compound 1), an alkene (compound 4) and two MeC23:H compounds (peaks 7 & 8). Days 10, 20 and 30 have no compounds specific to the individual days but there are compounds only observed in the mature flies, for example compounds 20, 39 and 43 which are all alkenes and dienes. The slight differences in the hydrocarbon profiles for the five different ages make them relatively distinguishable and allow for an age of the immature flies to be established based on the hydrocarbon profile.
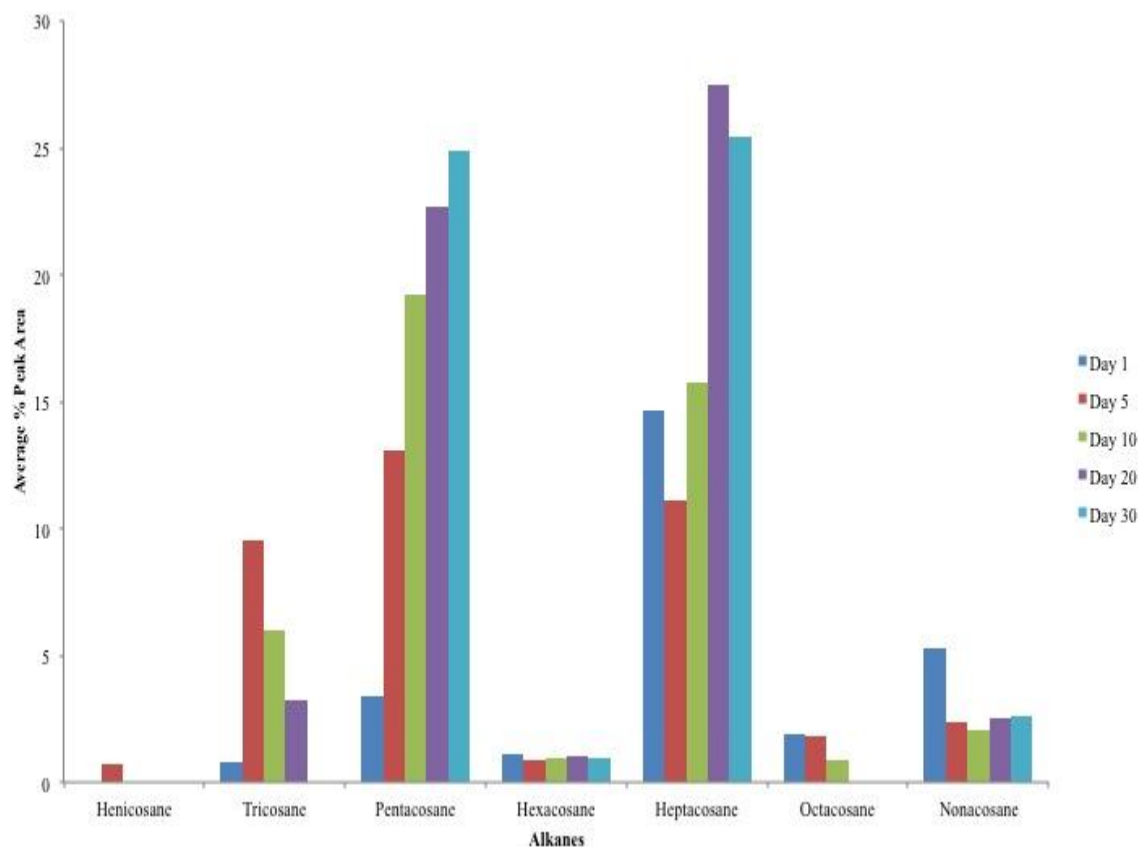
Figure 6.15: Graph of the average percentage peak area for *n*-alkanes over the 30 day extraction period for *C. vicina* adult flies

The concentrations of some of the compounds change systematically with time which can also be a good indicator of age. Figure 6.15 shows the *n*-alkanes plotted against the average peak area concentrations from day 1 to day 30. The concentration of C23:H increases significantly between days 1 and 5, then gradually decreases with time and is not observed in a concentration above 0.5% in the final day of extractions (day 30).

The PCA was carried out using six principal components, describing 97.7% of the variation within the dataset with the first three principal components comprising

71.0%, 15.3% and 6.2% respectively. PC3 and PC2 were used to plot the relevant

scores (see appendix 35 for PCA eigenvalues).
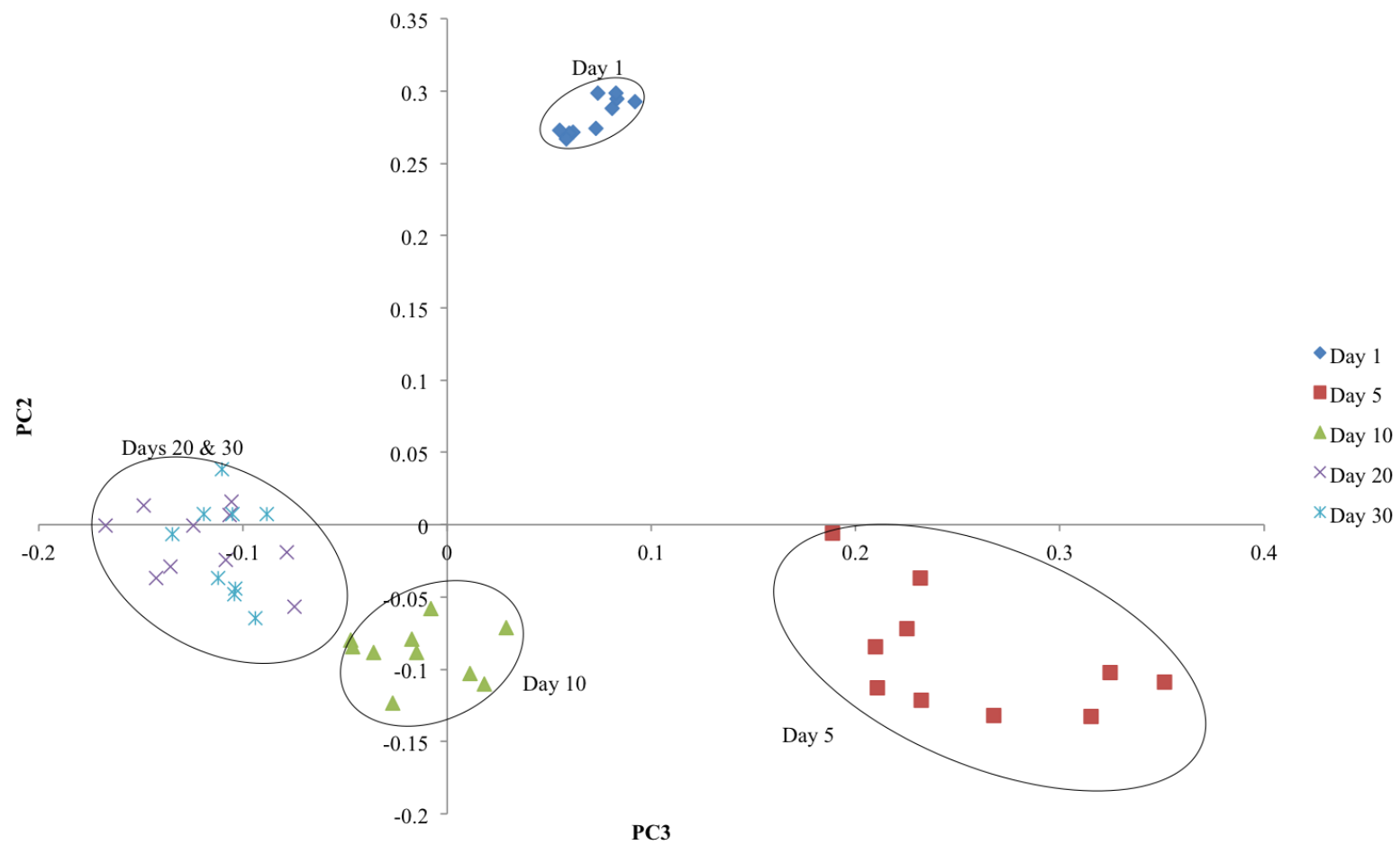
Figure 6.16: PCA plot showing PC3 against PC2 for *C. vicina* adult flies, with clustering days circled

From the PCA plot in Figure 6.16, it is clear to see four distinct groups where the principal components of the individual samples cluster together. Once again, the age of the flies follows a systematic pattern around the plot, starting with day 1 at the top, then jumping below the PC3 axis to the bottom right and moving to the left where day 10 clusters. Days 20 and 30 cannot be separated and cluster together above and below the PC3 axis on the far left of the plot. Even with the scatter observed in the extractions taken from day 5 flies, ageing can still be established from the plot.

The main compounds which have significantly large loading values are C27:H 11+13-MeC27:H and 9+11+13+15-MeC29:H. The latter two are present in 8-9% in day 1 flies but drop to values of 3% or less in older flies.

The results presented in this section of the chapter for *C. vicina* adult flies show that hydrocarbon analysis can be used to give an indication of the age, due to characteristic changes occurring over time.

As with *L. sericata*, there are a number of compounds that are specific to certain days, in particular days 1 and 5. These compounds therefore act as very good age indicators. For the more mature flies, there are no compounds specific to the individual days but there are alkenes and dienes which are only present in days 10, 20 and 30 which can give an indication that the fly is 10 days or older.

There is a noticeable absence of alkene hydrocarbons in day 1, most likely due to the flies not being sexually mature in the first 48 hours after hatching [6]. However, in the mature flies, there are an abundance of alkenes present in comparison to the profile of *L. sericata*. When the double bond positions of the alkenes were established, they

showed to be far more varied in comparison to *L. sericata*, which mainly comprised of *Z*7 alkenes (see chapter 4, section 4.6)

With the aid of GC-MS, the hydrocarbon profiles extracted from the cuticle of *C. vicina* can be utilised to establish the age of the fly. Once full profile identification has been established, and concentrations of specific age marker compounds (C25:H increasing with age) are determined, an estimation of the age can be given. To be more precise with the results, PCA confirms the age by being able to age all of the extracted samples to their individual days, with the exception of day 20 and 30, but this is still a very promising result.

C. vomitoria:

The hydrocarbon profile of *C. vomitoria* contains 72 compounds with some co-eluting for a total of 54 resolvable peaks from day 1 to day 30. They consist of *n*-alkanes (15%), alkenes (15%) and methyl hydrocarbons (70%). Figure 6.17 shows the GC chromatograms of a single sample from day 1, 5, 10 and 20 respectively. Highlighted on the chromatograms are shaded bars indicating distinct areas that change with time.
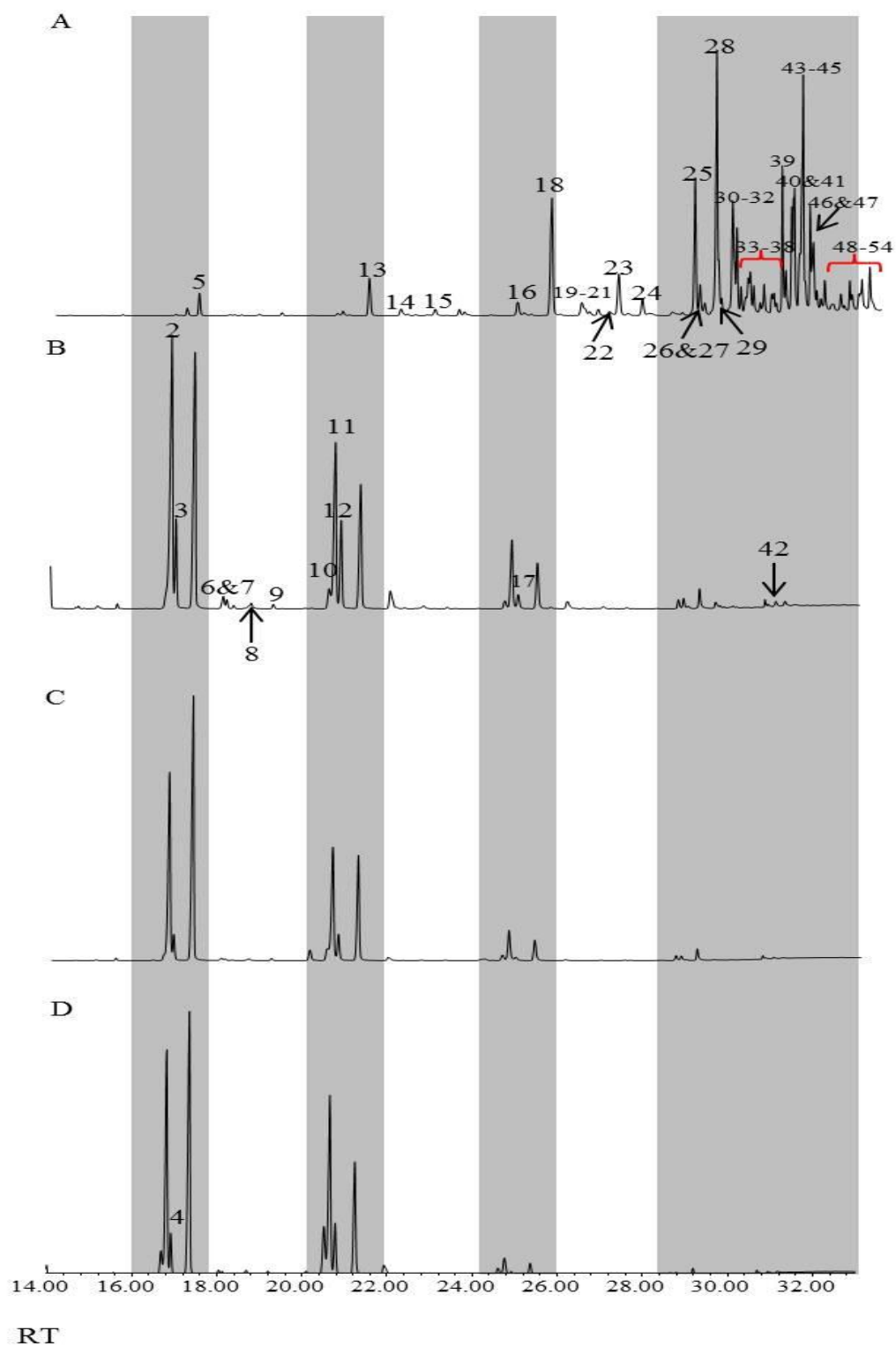
Figure 6.17: GC chromatograms of *C. vomitoria* adult flies at four different ages, A: Day 1, B: Day 5,

C: Day 10 and D: Day 20. Shaded bars illustrate distinctive changes over time indicating specific areas

of interest

The stacked chromatogram comparison in Figure 6.17 clearly shows that the profiles change with time, especially the heavy molecular weight compounds within the profiles of 1-day and 5-day old flies.

Figure 6.18 shows the total number of compounds plotted against the class of hydrocarbons, from days 1, 5, 10, 20 and 30.
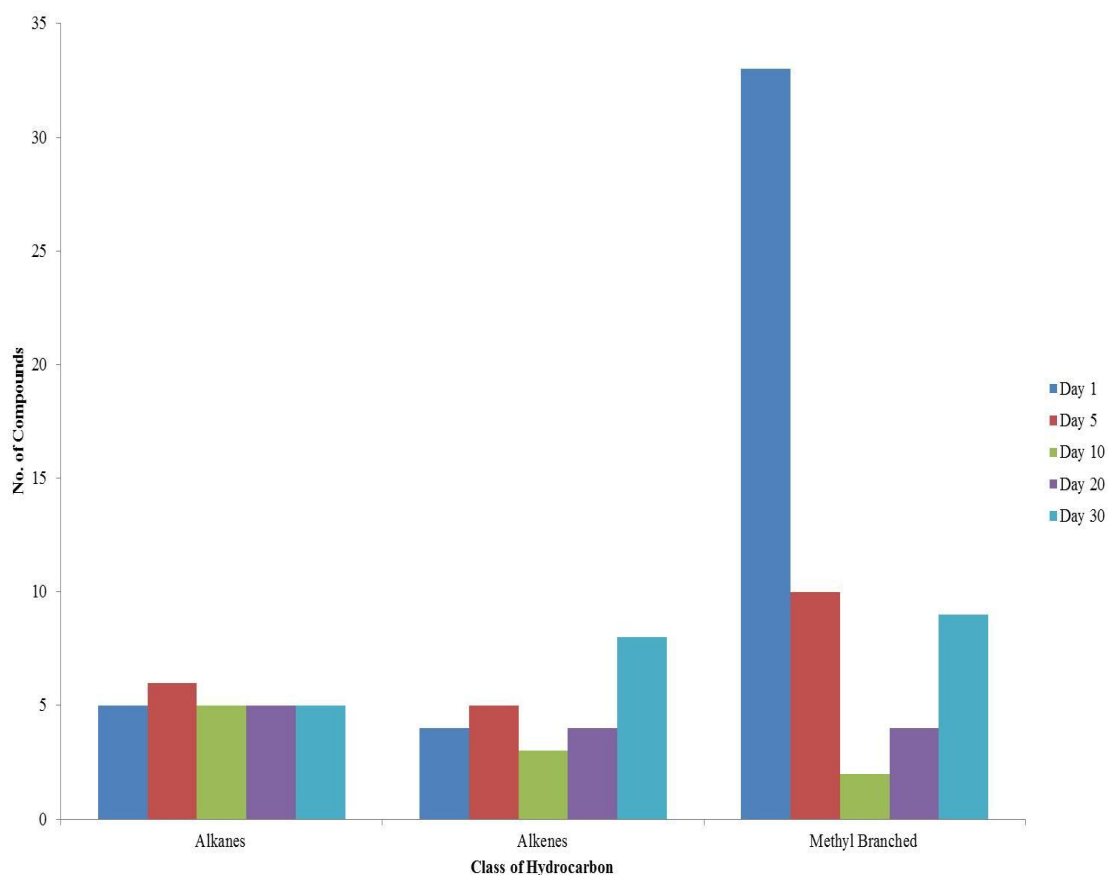
Figure 6.18: Graph showing the total number of *n*-alkanes, alkenes and methyl branched alkane hydrocarbons present up to day 30 for the adult fly of *C. vomitoria*

The number of *n*-alkanes remains reasonably stable across the 30 days. The alkenes also remain relatively stable from days 1 to 20 then increase in day 30. The methyl

branched compounds decrease significantly from day 1 to day 10 before increasing in days 20 and 30.

Figure 6.19 shows the *n*-alkanes plotted against the average percentage peak area. There are some interesting trends observed which could act as good age markers. Notably, the increase of C25:H over time. The same pattern in also observed in both Calliphora adult fly species but for C29:H.
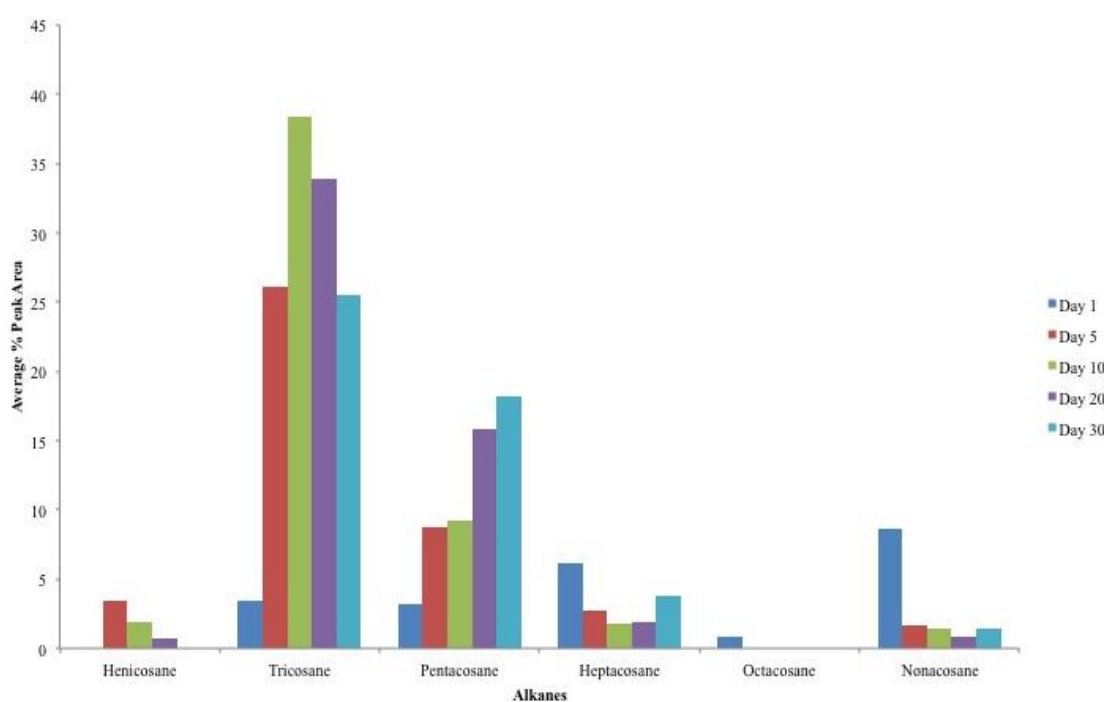
Figure 6.19: Graph of the average percentage peak area for *n*-alkanes over the 30 day extraction period for *C. vomitoria* adult flies

Table 6.10 lists the compounds extracted from the fly over the 30-day period.

Table 6.10: List of the compounds extracted and used for subsequent PCA from the adult flies of *C. vomitoria,* with the total percentage of each compound present, the percentage standard deviation for each day and the Kovats Indices to aid identification

Peak no.	Peak Identification	Kovats iu	Day 1 n=10 %	Day 5 n=10 %	Day 10 n=10 %	Day 20 n=10 %	Day 30 n=10 %
1	Heneicosane	2100	tr	3.44±1.26	1.89±1.53	0.72±0.21	tr
2	2-Methylhenicosane	2272	tr	31.64±8.45	1.01±0.44	1.37±0.68	0.95±0.62
3	Tricosene[1]	2276	tr	2.99±1.59	30.50±12.99	18.80±3.76	9.67±6.31
4	Tricosene[1]	2275	tr	tr	tr	tr	4.02±2.22
5	Tricosane	2300	3.24±2.41	26.10±7.74	38.44±18.03	33.95±9.37	25.51±10.37
6	9+11-Methyltricosane	2337	tr	1.22±0.42	tr	tr	0.77±0.23
7	7-Methyltricosane	2342	tr	0.76±0.29	tr	tr	tr
8	Tetracosene[1] + 3-Methyltricosane	2373	tr	0.75±0.26	tr	tr	0.62±0.24
9	Tetracosane	2400	tr	tr	tr	tr	0.70±0.17
10	2-Methyltetracosane	2466	0.88±0.85	2.00±1.77	2.14±1.19	3.62±1.11	2.94±1.23
11	Pentacosene[1]	2472	1.47±1.26	9.53±4.00	11.79±5.30	14.66±2.53	12.50±6.48
12	Pentacosene[1]	2476	tr	tr	tr	4.92±1.17	7.14±3.08
13	Pentacosane	2500	3.04±1.51	8.80±1.99	9.23±4.02	15.87±3.67	18.19±5.16
14	9+11-Methylpentacosane	2536	2.67±1.91	1.83±0.78	tr	1.00±0.20	2.40±0.63
15	2-Methylpentacosane	2664	2.21±1.64	0.68±0.29	tr	0.65±0.24	1.45±0.45
16	Heptacosene[1]	2671	0.86±0.54	2.61±1.74	1.72±1.09	1.68±0.64	3.61±1.87
17	Heptacosene[1]	2675	tr	tr	tr	tr	1.54±0.80
18	Heptacosane	2700	5.83±2.81	2.76±0.91	1.83±0.85	1.89±0.68	3.76±1.52
19	11+13-Methylheptacosane	2734	3.40±2.20	0.53±0.25	tr	tr	0.63±0.18
20	9-Methylheptacosane	2738	0.91±0.48	tr	tr	tr	tr
21	5-Methylheptacosane	2753	0.83±0.39	tr	tr	tr	tr

22	9,15+9,17-Dimethyheptacosane[2]	2765	0.91±0.48	tr	tr	tr	tr
23	3-Methylheptacosane	2775	3.27±1.12	tr	tr	tr	tr
24	Octacosane	2800	0.83±0.39	tr	tr	tr	tr
25	2-Methyloctacosane	2868	5.98±4.28	0.57±0.18	tr	tr	0.99±0.40
26	Nonacosene[1]	2879	2.64±0.68	0.61±0.22	tr	tr	0.65±0.34
27	Nonacosene[1]	2885	0.98±0.36	tr	tr	tr	tr
28	Nonacosane	2900	8.16±4.25	1.71±0.71	1.45±0.92	0.87±0.22	1.37±0.55
29	2, 6-Dimethyloctacosane[3]	2905	1.35±0.76	tr	tr	tr	tr
30	9+11-Methylnonacosane	2938	8.84±3.66	tr	tr	tr	tr
31	7-Methylnonacosane	2947	2.96±0.96	tr	tr	tr	tr
32	5-Methylnonacosane	2957	0.91±0.32	tr	tr	tr	tr
33	[x]9,x+[y]11,x-Dimethylnonacosane[4]	2966	0.83±0.40	tr	tr	tr	tr
34	7,x-Dimethylnonacosane[2] and 3-Methylnonacosane	2973	3.07±1.31	tr	tr	tr	tr
35	5,13+5,15+5,17-Dimethylnonacosane[2]	2986	1.07±0.61	tr	tr	tr	tr
36	3,7-Dimethylnonacosane[3]	3013	1.18±0.44	tr	tr	tr	tr
37	12+14+16-Methyltriacontane	3036	0.86±0.39	tr	tr	tr	tr
38	8-Methyltricontane	3044	0.59±0.25	tr	tr	tr	tr
39	2-Methyltriacontane	3070	3.19±1.68	tr	tr	tr	0.60±0.28
40	6,14-Dimethyltricontane[2]	3081	1.41±0.41	tr	tr	tr	tr
41	2,12+2,14-Dimethyltriacontane[3]	3099	2.55±1.26	tr	tr	tr	tr
42	Hentriacontane	3100	tr	0.77±0.54	tr	tr	tr
43	2,6+2,8-Dimethyltricontane[3]	3103	3.45±1.87	tr	tr	tr	tr
44	4,8,14-Trimethyltricontane[2]	3116	1.60±0.77	tr	tr	tr	tr
45	2,6,14-Trimethyltricontane[2]	3125	7.40±3.17	0.72±0.33	tr	tr	tr
46	2,6,10,14-Tetramethyltricontane[2]	3141	1.95±1.01	tr	tr	tr	tr
47	7,15-Dimethylhentricaontane[2]	3148	2.39±1.01	tr	tr	tr	tr

48	5,15-Dimethylhentriacontane[2]	3156	0.58±0.20	tr	tr	tr	tr
49	Unknown Hydrocarbon	3165	0.50±0.13	tr	tr	tr	tr
50	5,9,13+5,11,15-triMethylhentriacontane[2]	3174	1.06±0.38	tr	tr	tr	tr
51	Unknown Hydrocarbon	3209	0.71±0.22	tr	tr	tr	tr
52	17-Methyltritriacontane	3229	0.92±0.49	tr	tr	tr	tr
53	7,17-Dimethyltritriacontane[2]	3255	1.22±0.54	tr	tr	tr	tr
54	7,11,15-Trimethyltritriacontane[2]	3272	1.28±0.63	tr	tr	tr	tr

[1]Double bond position determined (see page 126). Bond position not determined for alkadienes

[2]Tentative identification based on Kovats Index values and match with NIST08 Library database

[3]Position of the first methyl was established by using the Kovats Index [19]

[4]x = 15, 17, 19

y = 15, 17

tr = Trace amount detected (<0.5%)

Day 1 has a substantially large number of peaks specific (above peak areas exceeding the 0.5% peak area threshold) to that day (30 in total – see Table 6.10), which mainly consist of long chain length methyl branched compounds (C27:H up to C33:H).

Day 5 has one compound specific to this day, C31:H (compound 42). Days 10 and 20 have no compounds specific to the individual days. Day 30 has three compounds that are not detectable in a sufficient concentration on any other extraction day. These compounds are a C23:1 isomer (compound 4), C24:H (compound 9) and a C27:1 isomer (compound 17).

The PCA was carried out using six principal components, describing 99.2% of the variation within the dataset with the first three principal components comprising 64.1%, 19.9% and 10.6% respectively. PC3 and PC2 were used to plot the relevant scores (see appendix 36 for PCA eigenvalues). Figure 6.20 shows the PCA plot of PC3 against PC2 for data gathered from day 1, 5, 10, 20 and 30 of adult fly extractions of *C. vomitoria*.
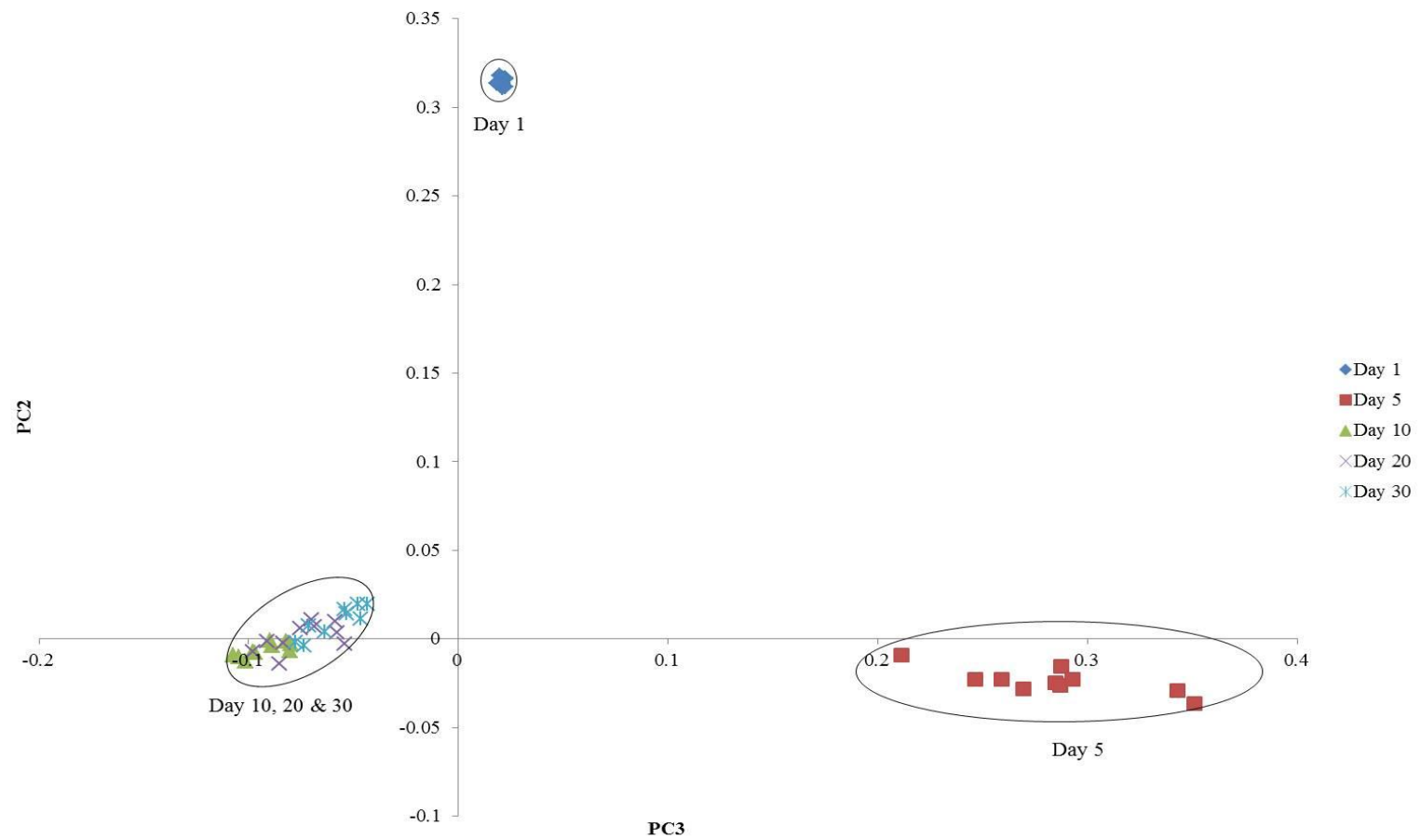
Figure 6.20: PCA plot showing PC3 against PC2 for *C. vomitoria* adult flies, with clustering days circled

The PCA plot in Figure 6.20 shows three distinct clustering groups of principal components. Day 1 is very tightly clustered at the top of the plot. There is then a jump between day 1 and day 5, with day 5 clustering just below the PC3 axis on the right hand side. As with *C. vicina*, the most scatter is observed in day 5, but the spatial positions on the plot still allows for the age to be confidently established. Unfortunately day 10, 20 and 30 cannot be separated and cluster together above and below the PC3 axis on the left hand side.

Generally, the methyl branched hydrocarbons had high loading values, but the two main compounds that yielded significantly large values were C29:H, 9+11-MeC29:H and 15-MeC31:H.

The results presented for the adult fly of *C. vomitoria* show the potential for ageing to be established over the 10-day period, using hydrocarbon analysis. Characteristic changes within the hydrocarbon profile over time allow for distinctions to be made, especially between days 1, 5 and 10, which is expected due to the substantial chemical differences seen within the profile at these two ages.

As with the other two species, C25:H increases with age, making this compound influential for ageing adult flies. The profile of the fly at day 1 is the most distinguishable due to the large number of methyl branched compounds that are not observed in the profiles of the other four ages. These methyl branched compound have chain lengths ranging from C27:H to C33:H.

6.4.2 General Discussion and Conclusion for ageing adult flies

The profiles of adult flies are dominated by an abundance of high molecular weight hydrocarbons (with very few low molecular weight compounds present). Adult flies have to be able to withstand much drier environmental conditions, therefore, the cuticles require the larger hydrocarbons which offer increased impermeability [5][20] and under less favourable conditions.

The hydrocarbon composition changes drastically with age, especially the methyl branched hydrocarbons. The fly is also not sexually mature until approximately 48 hours after it has emerged, [6] therefore no sex alkenes were present in the young adult profiles.

The profiles of day 1 flies for all three species are dominated by a considerably high number of methyl hydrocarbons, making its profile very unique and therefore easily distinguishable from the other ages.

The profiles of the three species do not display the higher boiling point n-alkanes, unlike the profiles of the larvae which display n-alkanes up to C33:H, but the overall abundance of the higher molecular weight n-alkanes is significantly larger in adult flies. For *L. sericata*, the prominent changes and the distinct differences seen between the three different ages (day 1, 5 and 10) clearly show very promising results for the ageing of relatively young *L. sericata* blowflies. The hydrocarbon extraction method remains very simple and the profiles are straightforward to analyse because they contain less polar contaminants (in comparison to larvae extracts). The results presented show that all of the three ages examined can be determined using the hydrocarbon profiles analysed by GC-MS and PCA. *C. vicina* adult flies can be

accurately aged up to day 20, with days 1, 5 and 10 all clustering into individual groups on the PCA plot. Unfortunately days 20 and 30 cannot be separated but this is still a very promising results. Although *C. vomitoria* cannot be aged as accurately as *C. vicina*, a distinction can still be made between young and old flies. Therefore, a differentiation between flies that have developed on the cadaver that are newly emerged, to older flies that have been attracted by odour can be established [5].

Adult flies from all three species aged 1-day and 5-days old can be determined from the GC chromatogram alone as the two ages display distinctly different chemical profiles, but the age is confirmed by PCA which exhibited separate clustering for these two ages in the PCA plots. Further experimental work is required to extract the flies on a daily basis to determine exactly where the systematic chemical changes occur within the hydrocarbon profiles.

6.5 Overall Conclusion for ageing all six life stages of three forensically important blowflies using CHC's

As mentioned in chapter 5, Roux et al. [5] carried out a complete ontogenetic study on three forensically important blowflies (*C. vicina*, *C. vomitoria* and *P. terraenovae*). Similar observations were observed for the larvae results presented in chapter 5 with short-chain hydrocarbons present in the profiles of larvae and post-feeding evolving into long-chain compounds for the pupae and adult flies.

The results they presented are also in agreement for the empty puparial case and adult fly profiles where the profiles were dominated by high chain-length, complex methyl branched compounds and high molecular weight *n*-alkanes and alkenes. The abundance

of the higher molecular weight compounds was also seen to increase. However, the chain lengths ranged from C20:H to C31:H for all three species whereas for *C. vomitoria* and *C. vicina* used for this thesis, *n*-alkanes up to C33:H were detected.

The main aim of this initial study was to determine whether the surface hydrocarbons of the blowfly species *L. sericata*, *C. vicina* and *C. vomitoria* could be used to determine the age of all six life stages of the blowflies life cycle. From the results presented in chapter 5 and 6 it is clear that age related changes over time were observed within the hydrocarbon profiles and therefore there is potential for their use in PMI estimations.

References

[1]   J. Amendt, R. Krettek, and R. Zehner, Forensic entomology, Naturwissenschaften 91 (2004) 51–65.

[2]   R. Zehner, S. Mösch, and J. Amendt, Estimating the postmortem interval by determining the age of fly pupae: Are there any molecular tools? International Congress Series 1288 (2006) 619–621.

[3]   G.H. Zhu, X.H. Xu, X.J. Yu, Y. Zhang, and J.F. Wang, Puparial case hydrocarbons of *Chrysomya megacephala* as an indicator of the postmortem interval, Forensic Science International 169 (2007) 1–5.

[4]   G. Ye, K. Li, J. Zhu, G. Zhu, and C. Hu, Cuticular hydrocarbon composition in pupal exuviae for taxonomic differentiation of six necrophagous flies, Journal of Medical Entomology 44 (2007) 450–6.

[5]   O. Roux, C. Gers, and L. Legal, Ontogenetic study of three Calliphoridae of forensic importance through cuticular hydrocarbon analysis, Medical and Veterinary Entomology 22 (2008) 309–17.

[6]   M. Trabalon, M. Campan, J.L. Clement, C. Lange, and M.T. Miquel, Cuticular hydrocarbons of *Calliphora vomitoria* (Diptera): Relation to age and sex, General and Comparative Endocrinology 85 (1992) 208–216.

[7]   R. Zehner, J. Amendt, and P. Boehme, Gene expression analysis as a tool for age estimation of blowfly pupae, Forensic Science International: Genetics Supplement Series 2 (2009) 292–293.

[8]   M. Mazzanti, F. Alessandrini, A. Tagliabracci, J.D. Wells, and C.P. Campobasso, DNA degradation and genetic analysis of empty puparia: genetic identification limits in forensic entomology, Forensic Science International 195 (2010) 99–102.

[9]   Z. Adams and M.J.R. Hall, Methods used for the killing and preservation of blowfly larvae, and their effect on post-mortem larval length, Forensic Science International 138 (2003) 50–61.

[10]   S.L. VanLaerhoven, Blind validation of postmortem interval estimates using developmental rates of blow flies, Forensic Science International 180 (2008) 76–80.

[11]   S. Arnott and B. Turner, Post-feeding larval behaviour in the blowfly, *Calliphora vicina*: effects on post-mortem interval estimates, Forensic Science International 177 (2008) 162–7.

[12]   F.P. Drijfhout, Cuticular hydrocarbons: A new tool in forensic entomology, in: Current Concepts in Forensic Entomology, eds., J. Amendt, C.P. Campobasso, M.L. Goff, and M. Grassberger, Springer (2010) 179–203.

[13]   T. Tregenza, S.H. Buckley, V.L. Pritchard, and R.K. Butlin, Inter- and intra-population effects of sex and age on epicuticular composition of meadow grasshopper,*Chorthippus parallelus*, Journal of Chemical Ecology 26 (2000) 257–278.

[14] W.V. Brown, H.A. Rose, M.J. Lacey, and K. Wright, The cuticular hydrocarbons of the giant soil-burrowing cockroach *Macropanesthia rhinoceros* saussure (Blattodea: Blaberidae: Geoscapheinae): analysis with respect to age, sex and location, Comparative Biochemistry and Physiology. Part B, Biochemistry and Molecular Biology 127 (2000) 261–77.

[15] R. Urech, G.W. Brown, C.J. Moore, and P.E. Green, Cuticular hydrocarbons of buffalo fly, *Haematobia exigua*, and chemotaxonomic differentiation from horn fly, *H. irritans*, Journal of Chemical Ecology 31 (2005) 2451–61.

[16] W.V. Brown, R. Morton, and J.P. Spradbery, Cuticular hydrocarbons of the Old World screw-worm fly, *Chrysomya bezziana* Villeneuve (Diptera: Calliphoridae). Chemical characterization and quantification by age and sex, Comparative Biochemistry and Physiology Part B: Comparative Biochemistry 101 (1992) 665–671.

[17] S. Mpuru, G.J. Blomquist, C. Schal, M. Roux, M. Kuenzli, G. Dusticier, J.L. Clément, and A.G. Bagnères, Effect of age and sex on the production of internal and external hydrocarbons and pheromones in the housefly, *Musca domestica*, Insect Biochemistry and Molecular Biology 31 (2001) 139–55.

[18] L.E. Hugo, B.H. Kay, G.K. Eaglesham, N. Holling, and P.A. Ryan, Investigation of cuticular hydrocarbons for determining the age and survivorship of Australasian mosquitoes, The American Journal of Tropical Medicine and Hygiene 74 (2006) 462–74.

[19] D.A. Carlson, U.R. Bernier, and B.D. Sutton, Elution patterns from capillary GC for methyl-branced alkanes, Journal of Chemical Ecology 24 (1998) 1845–1865.

[20] R. Toolson, E. C., Kuper-Simbron, Laboratory evolution of epicuticular hydrocarbon composition and cuticular permeability in *Drosophila pseudoobscura*: effects on sexual dimorphism and thermal- acclimation ability, Evolution 43 (1989) 468–473.

Chapter 7

Future Developments: Direct Analysis in Real Time (DART-MS) and Artificial Neural Networks (ANN)

7. Introduction

This chapter will cover two techniques which could show great potential for future use in the field of forensic entomology. The first technique is an alternative to GC-MS and it was explored to see if there was an analytical technique capable of producing rapid taxonomic information for the three blowfly species used. It is the recently developed ion source, Direct Analysis in Real Time (DART), which was developed in 2005 by Laramée and Cody [1]. When coupled to high resolution mass spectrometer, it allows for rapid qualitative and quantitative analysis of a wide variety of samples [2]. DART's potential is being exploited in a broad range of applications from food science [3][4] to drug analysis [5][6]. It has also been utilised for non-polar compound analysis which is of particular interest when looking at its potential to analyse insect cuticular hydrocarbons. One of the disadvantages of DART analysis is that it does not separate

components in time (like chromatography) for sample mixtures. However, when this technique is coupled with a high resolution mass spectrometer, the relatively simple mass spectra (mostly $[M+H]^+$ for positive ion, $[M-H]^-$ for negative ion) provide high mass accuracy measurements that can be used to calculate the elemental compositions for each peak observed in the DART mass spectra. Additionally, if chromatography is necessary, the DART source can be interfaced with the GC column output as was shown by Cody in which he successfully separated and analysed non-polar compounds [7]. However, this technique adds time to the overall analysis which undercut the speed that DART offers without chromatography.

Work has also been previously published on hydrocarbon analysis (without chromatography) using DART, where Yew et al [8] analysed adult fly species of the *Drosophila*. They were able to see differences in the chemical composition between male and female profiles by detecting the unsaturated hydrocarbons. Besides the rapid analysis DART offers, unlike GC-MS, it does not require the insect to be killed for hydrocarbon analysis to be undertaken, so an awake behaving fly can be analysed several times and followed through its life cycle.

Co-inventor of the DART, Dr Robert Cody, has also designed software allowing for Principal Component Analysis (PCA) and Linear Discriminant Analysis (LDA) to be applied to datasets obtained from DART spectra. This will allow for any trends to be visualised and the different species should cluster in different areas of the PCA/LDA plots. This was therefore utilised to classify the species of blowflies.

The second technique that will be presented in this chapter is a potential alternative to PCA as a data analysis method. As with DART-MS, Artificial Neural Networks (ANN) was only carried out as a small side project to look into other techniques that could be

used to analyse and interpret hydrocarbon results obtained from forensically important blowflies. Gaining a PCA plot can be a time consuming as the analyst has to plot all of the combinations of PCs in order to visualise the best possible combination. Only two or three dimensions can be plotted, meaning information that maybe important from excluded PCs are lost. The whole process of running the PCA and plotting the numerous combinations of PCs has to be rerun when new data is collected. Artificial Neural Networks (ANNs) [9] are an attractive alternative to the PCA technique used in this thesis. ANNs are modelled on the functionality of biological neurons in the brain [11]. They have been widely studied and utilised in the field of computational intelligence due to their ability to learn and recognise characteristic features within datasets that they are exposed to. Like PCA, they are capable of identifying trends within datasets, but they work on a training and learning basis. Once trained, ANNs can reduce the amount of analysis time required by clarifying novel data based on their knowledge of the domain that they have acquired during training. There are numerous characteristics that make the application of ANNs so appealing in many branches of science, but for the purpose of this study, the main advantage they hold is the ability to cope with data containing significant noise (Butcher et al) [10].

There are many types of both supervised and unsupervised ANNs [11], but the results presented in this chapter were obtained using one of the most common types of unsupervised ANNs, Self Organising Maps (SOMs) [12]. For further, detailed information on ANN, see references [9][10][13]. SOMs have been applied with a great deal of success to a broad range of applications from detecting defects in reinforced concrete [11] to DNA classifications [14]. A typical SOM consists of an input layer

which receives input data and an output layer, onto which the input data is mapped according to its underlying characteristics [10].

The huge potential ANNs hold for data analysis has led them to be applied in the field of forensic science from the analysis of human skeletal remains [15] to digital forensic investigation [16]. They have also been utilised in the field of entomology. A study by Bianconi et al. [17], applied three different types of ANNs on datasets obtained from the blowfly species *Chrysomya megacephala* in order to predict the number of larvae that matured to adult flies based on the food quantity, number of larvae and duration of the immature life stage. ANNs have also been used for insect hydrocarbon data in a study by Bagnéres et al. [18]. Data was extracted from four termite species (*Reticulitermes*) with the overall objective of trying to classify the caste for each insect. The results showed enhanced performance in comparison to multivariate techniques.

Results presented shall examine the potential that ANN analysis could have for improving age estimations for a forensically important blowfly in the larval stage

7.1 Aims and Objectives

Empty puparial cases of three forensically important blowfly species from the USA were analysed at JEOL USA, Inc. (fellowship funded by Winston Churchill Memorial Trust). These species were taken from Texas A&M University and included *Lucilia cuprina*, *Lucilia sericata,* and *Cochliomyia macellaria*. Hereafter, this research was expanded to examine population differences within the species for *C. macellaria,* which were compared to samples collected from Dayton University, Ohio.

The preliminary ANN results presented in this chapter were applied to a dataset, consisting of the peak areas of hydrocarbons extracted from the cuticle of *L. sericata* larvae. The overall aim was to examine whether a SOM is suitable as an ageing tool for blowfly species and to establish if this particular technique holds any advantages over PCA.

7.2 Direct Analysis in Real Time

The advancement of ambient ionisation techniques has seen a significant increase in DART ionisation being utilised in many science laboratories across the USA, in particular, forensic toxicology laboratories [5]. One advantage of this technique, besides the very quick analysis time and minimal sample preparation, is that in some cases, DART-MS does not require the insect of interest to be killed. This allows for the repeated analysis of a particular insect which can be beneficial for method development as different experimental conditions can be applied, or for behavioural studies [8,19].

7.2.1 Instrumentation

7.2.1.1 DART Ion source

DART was developed for the purpose of being able to instantly analyse gases, liquids and solids in an atmospheric environment [1][20]. The technique shares key characteristics with Atmospheric Pressure Chemical Ionisation (APCI) and is considered a soft ionisation technique. The DART ion source can ionise a wide range

of samples directly from the sampling surface. DART minimises the need for any chemical extraction or high-vacuum conditions by using excited-state helium atoms (carrier gas) to desorb and ionise the compounds of interest from the surface of the sample [8].

Helium gas is passed around a needle electrode that is held at a high electrostatic potential (Figure 7.1). A glow discharge (plasma) is created between the needle and the grounded electrode, which creates charged and excited-state species of helium. The gas stream continues through the ion source where it is then heated in the gas heater tube. The temperature to which the gas is heated can be controlled and supports thermal desorption of the analytes from the surface of the sample [1]. Subsequently, the gas passes through a final exit grid electrode which is biased to a positive potential for positive ion analysis and a negative potential for negative ion analysis, thus preventing ion-electron recombination when exiting the DART source. Finally, the gas exits the system through the insulator cap, and the actual ionisation of the sample occurs in the sample gap, which is under ambient conditions. The ions formed are then directed by both the DART gas flow and the slight vacuum at the inlet of the mass spectrometer which in the case of Figure 7.1 is an AccuTOF time-of-flight mass spectrometer [2].
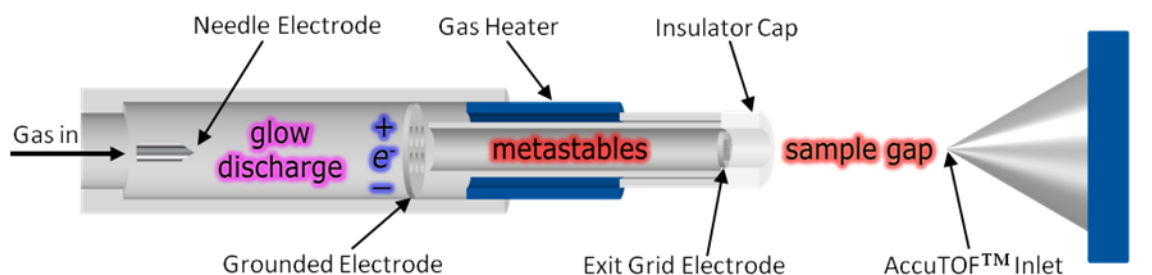
Figure 7.1: Schematic diagram of a DART ion source taken with permission (R. Cody) from JEOL USA.

Ionisation with DART can be carried out in two modes:

1) *Positive ionisation*

2) *Negative ionisation*

The positive ionisation mode involves the reaction of helium metastable states with atmospheric water. This leads to the formation of ionised water clusters which undergo proton transfer reactions with the analyte, giving rise to the formation of the largely unfragmented $[M+H]^+$ ion [21,22]. The positive ion formation mechanism below dominates when helium is used in the DART ion source [23].

$$He(2^3S) + H_2O \rightarrow H_2O^{+\bullet} + He(1^1S) + e^-$$

$$H_2O^{+\bullet} + H_2O \rightarrow H_3O^+ + OH^\bullet$$

$$H_3O^+ + nH_2O \rightarrow [(H_2O)_{n+1} + H]^+$$

$$[(H_2O)_{n+1} + H]^+ + M \rightarrow [M + H]^+ + (n+1)H_2O$$
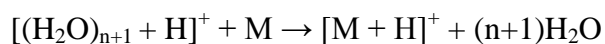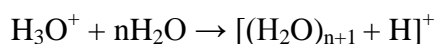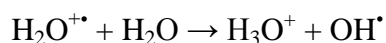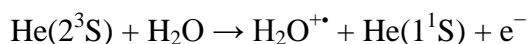
In the negative ionisation mode (used for results presented in this thesis), metastable helium atoms react with a neutral atom (N), to form electrons through Penning ionisation (Equation 7.1)

$$N* + M \rightarrow M^{+\bullet} + e^-$$
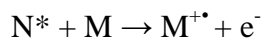
Equation 7.1 Penning ionisation [23]

The electrons formed are then rapidly thermalised by collisions with atmospheric gases (G). Afterwards, the electrons react with gaseous oxygen to produce oxygen anions.

$$e^- * + G \rightarrow G* + e^-$$

$$e^- + O_2 \rightarrow O_2^{-\bullet}$$
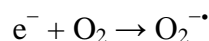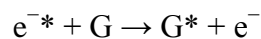
These oxygen anions can then react with sample molecules (M) to produce analyte anions:

$$O_2^{-\bullet} + M \rightarrow [M - H]^- + OOH^\bullet$$

$$O_2^{-\bullet} + M \rightarrow M^{-\bullet} + O_2$$

$$O_2^{-\bullet} + M \rightarrow [M + O_2]^{-\bullet}$$
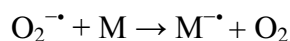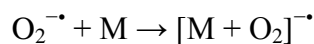
In this work, the last negative ionisation scheme (O_2 adduct formation) was used for the DART analysis of the cuticular hydrocarbons [2].

7.2.1.2 Mass Analyser

DART is especially powerful when it is coupled to a high resolution mass analyser because it will provide the exact molecular weight and the matching molecular formula of the ionised compounds [24]. The DART-AccuTOF-MS was used for the results presented in this thesis.

Time of Flight:

In Time-of-Flight (TOF), ions are separated according to their velocity. The kinetic energy is held constant so as the masses get larger their associated velocities get smaller. As a result, the smaller ions reach the detector faster than the larger ions. An added benefit to TOFs is that unlike the quadrupole mass analyser, all ions are detected all the time (i.e. no scanning occurs). The ions are accelerated under the influence of an electric field to achieve the same kinetic energy [25]. Once the ions have passed through the acceleration region they travel into the drift flight-tube region. The smaller ions travel through the flight-tube faster as they are lighter and have a higher velocity, therefore reaching the detector before the heavier ions. The velocities of ions are characteristic of the *m/z* ratio which is calculated by measuring the time taken for each ion to move through the flight-tube [26]. The velocity of the ions is proportional to the square root of the *m/z* ratio [27].

TOF is a highly sensitive mass analyser because all ions produced are analysed. It also has a high upper mass limit and gives a very high mass resolving power [28][26].

7.2.2 Materials and Methods for DART

Empty puparial cases were extracted in the usual method of being submerged in hexane for 10-15 minutes. The extract is then removed and added to a clean 2 mL GC vial. The closed end of a melting point tube is used for sample introduction into the DART stream. The melting tubes are mounted to a linear rail autosampler and 3 μL was

pipetted onto the tips, which are positioned 1 cm away from orifice 1. Each sample is exposed to the helium gas stream for 6 seconds.

The methodology and parameters were the same used for Cody and Dane [29] and have been taken and adapted with permission. All mass spectra were acquired with a JEOL (Tokyo, Japan) AccuTOF mass spectrometer equipped with an IonSense (Saugus, MA) DART-SVP ion source. The AccuTOF mass spectrometer has an atmospheric pressure ionisation (API) interface consisting of two off-axis skimmers, a ring lens and a bent RF ion guide [17]. The outer skimmer has a 400 μm i.d. sampling orifice (orifice 1) through which ions are introduced from atmospheric pressure into the first pumping region. The off-axis skimmer design coupled with a bent RF ion guide is highly resistant to contamination even when liquid solutions are introduced directly into orifice 1.

The mass spectrometer was operated in negative-ion mode with an RF ion guide voltage of 800V. Alkane mass spectra were acquired for the mass range 80-800 amu with a spectral storage rate of one spectrum per second. The mass spectrometer resolving power was 6000 (FWHM). Polyethylene glycol (average molecular weight 600) and/or perfluorotributylamine were used as external mass reference standards for exact mass determination. The API interface potentials were set to relatively low values (orifice 1 = -10V, ring lens = orifice 2 = -3V) to minimize in-source collision-induced dissociation of the weakly bound oxygen adducts of the alkanes. The orifice 1 temperature was 120^0C. JEOL Mass Centre software was used to control the mass spectrometer and acquire data, which were subsequently calibrated and processed by using TSSPro3 software (Shrader Analytical, Detroit, MI). Mass Spec Tools software (ChemSW Inc., Fairfield, CA) was used to examine and interpret the mass spectra.

The DART-SVP ion source was operated with an exit grid voltage of -530V to maximize the relative abundance of O_2^- in the negative-ion background mass spectrum. Helium was used as the DART gas at the factory-pre-set flow rate for the DART-SVP. The gas heater was set to 350^0C. The DART exit grid was aimed directly at the mass spectrometer sampling orifice positioned at 4.2 cm on the DART SVP railing guide. This corresponds to a distance of approximately 1.5 cm from the mass spectrometer sampling orifice.

7.3 DART Results

Preliminary results were obtained from a different DART instrument, with an Accu-TOF mass analyser (data not shown). Hydrocarbons are difficult to detect using DART analysis, especially the alkanes as they do not readily protonate and they usually require a high energy ionisation (EI) technique in order for them to become ionised. Therefore, the more readily ionised compounds (i.e. fatty acids, lipids etc) appeared to be much more abundant and although hydrocarbons may have been present in the mass spectrum, it is likely they were masked by compounds which were easily ionised in comparison.

Figure 7.2 shows the adapted sampling method used for analysing hydrocarbons. Experiments carried out at JEOL, USA led to some very novel results. The combination of the adapted parameters (lower orifice 1 and orifice 2 voltage which helps to keep the O_2^- adducts intact by reducing the collision energy with gas molecules in the atmospheric pressure interface), an altered sampling position and the coupling of the DART to an AccuTOF, alkanes were stabilized into holding their charge, thus enabling their detection by DART for the first time using negative ion analysis.
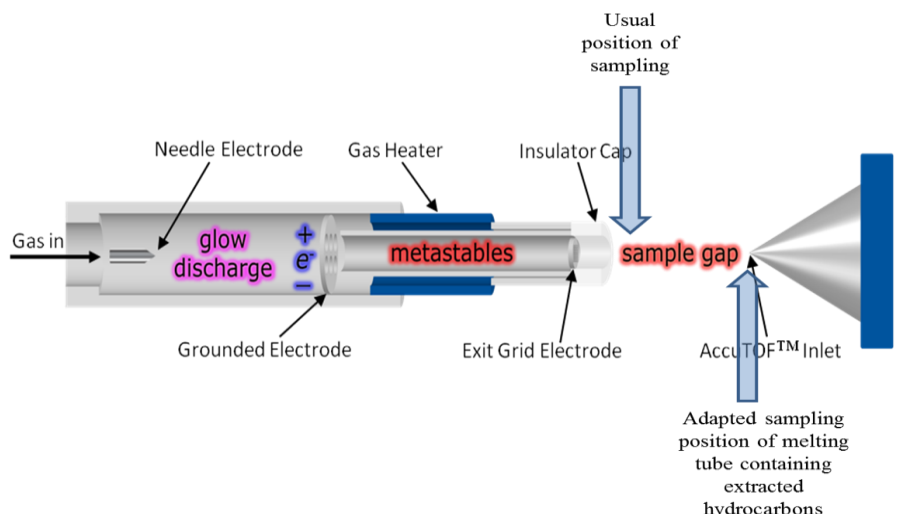
Figure 7.2: Schematic diagram of a DART ion source showing the adapted sampling position, taken with permission (R. Cody) and adapted from the JEOL USA website.

If the DART had an interfaced with any other MS other than an AccuTOF, a flange and ceramic tube would be needed, thus furthering the distance and time required for the alkanes to hold their charge. Figure 7.3 shows the mass spectrum taken from *C. macellaria*, showing $C_{26}H_{34}O_2^{-\bullet}$ to $C_{36}H_{34}O_2^{-\bullet}$. It is not possible to determine if the ions that are detected are methyl branched alkanes or linear alkanes. For example, an ion with a mass of 454 *m/z*, could be a MeC29:H or C30:H as they both hold the same mass. These ions shall therefore be referred to as alkanes, rather than *n*-alkanes.

The results were obtained from the empty puparial cases of forensically important blowflies in the USA. Furthermore, when using these ions for PCA and LDA, species identification was readily achieved for each analysis. More importantly, the two different *C. macellaria* groups from Texas and Ohio grouped in the lower right part of the plot (Figure 7.4), with a slight separation between each clustering, thus allowing

population differentiation. Table 7.1 lists the ions (alkanes and alkenes) used for LDA, as shown in Figure 7.4.
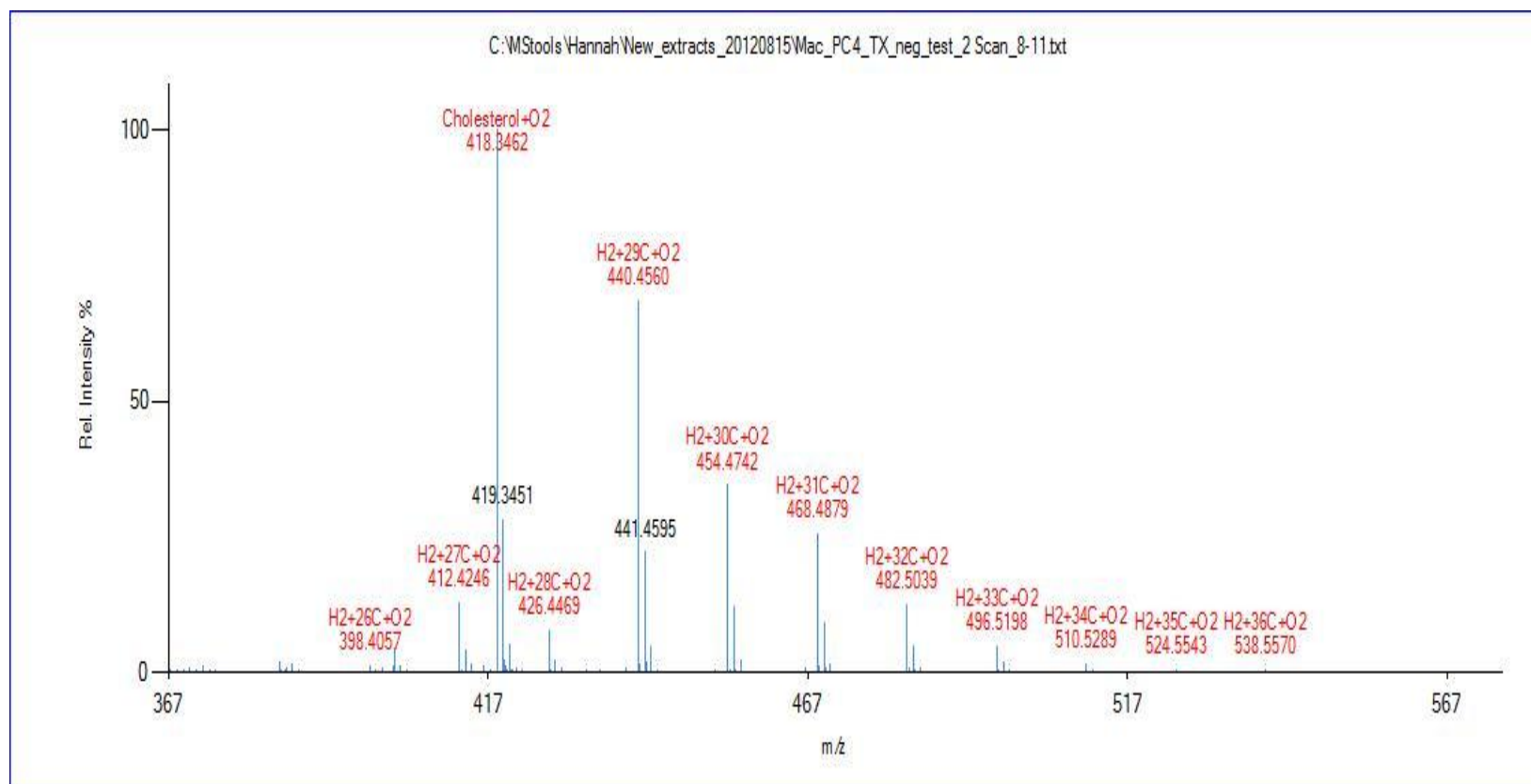
Figure 7.3: Mass spectrum of *C. macellaria* (Texas) using AccuTOF-DART, with the alkanes plus O_2 adducts labelled

Table 7.1: List of ions used for LDA plot

Selected m/z values:	
410	C27:1
412	C27:H
426	C28:H
438	C29:1
440	C29:H
454	C30:H
468	C31:H
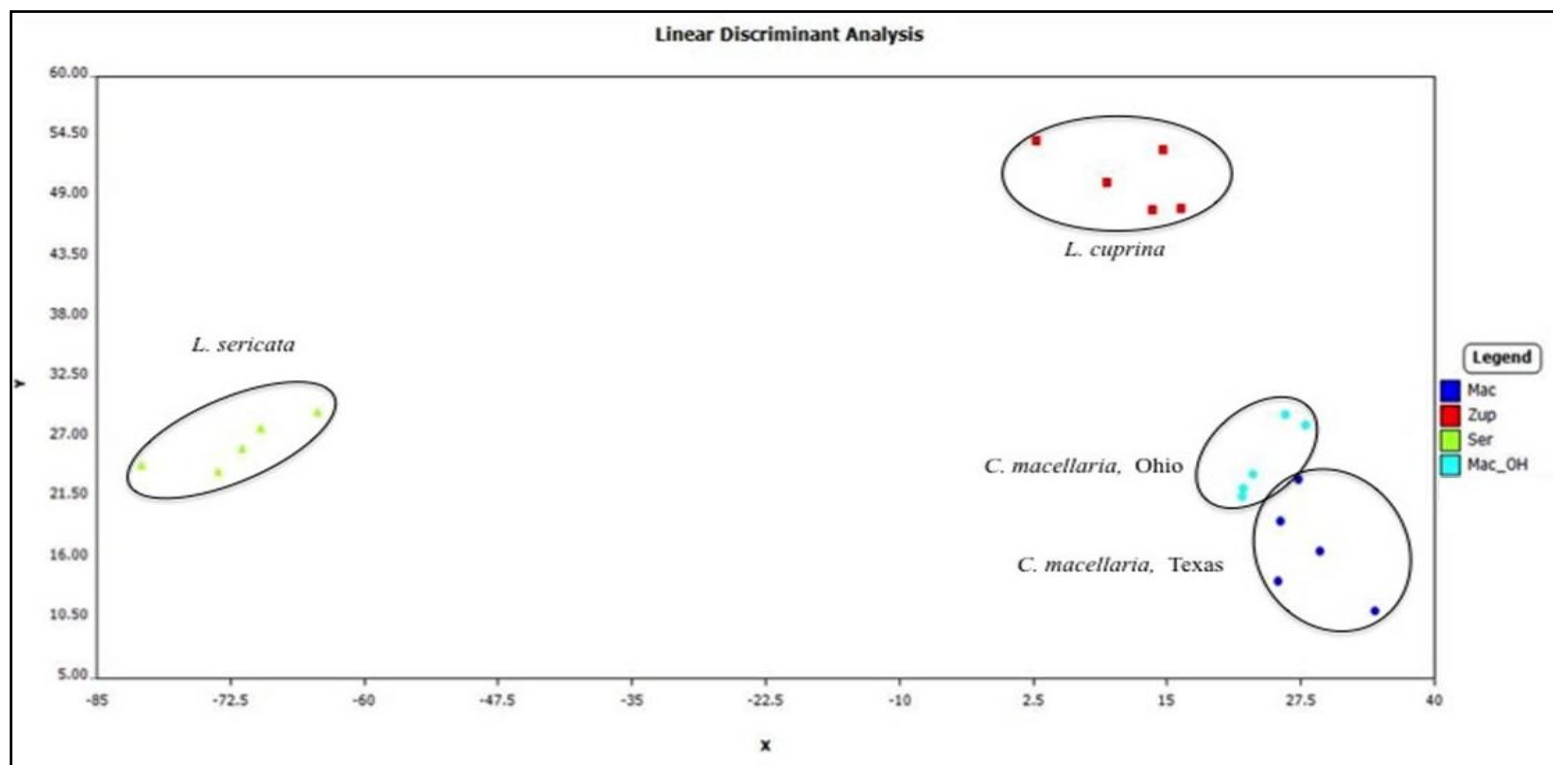
Figure 7.4: LDA plot formed using diagnostic ions taken from negative ion mode mass spectra of *C. macellaria,* Texas, *L. curpina*, *L. sericata* and *C. macellaria*, Ohio

7.3.1 DART Discussion and Conclusion

The preliminary results presented in this chapter for DART-MS highlight this technique as having great potential in the field of forensic entomology, enabling real-time data analysis and therefore rapid results for insect identification. Results also revealed the potential for analysing cuticular hydrocarbons from insects in general, as it was the first time alkanes have been detected using a DART. The population difference was also a very exciting result that was obtained and could hold a lot of forensic relevance, as it could indicate whether a body has been moved.

The differences within the hydrocarbon profiles of *C. macellaria* Texas and *C. macellaria* Ohio could be due to the different climates these two species inhabit. Texas is very dry with much lower humidity in comparison to Ohio, therefore the alkanes could be slightly different to protect the insects from desiccation in the Texas climate. The number of samples analysed for each species was relatively small ($n = 5$). Therefore, an increased sample size is required for further studies to assure any variation present within the empty puparial cases is being accounted for.

Although DART was successfully able to distinguish between the three species analysed using mainly saturated hydrocarbons, there are disadvantages to this technique. DART can detect methyl branched hydrocarbons (personal communication with Dr John Dane) but it cannot distinguish the position of the methyl groups along the backbone of the molecule nor from linear hydrocarbons containing an equivalent number of carbon atoms. Further method development using pure methyl branched hydrocarbons as well as linear hydrocarbons would be advantageous. From the work presented in chapters 4 to 6, it is clear to see how abundant the methyl hydrocarbons are in the three species used for this thesis. Technique validation of *n*-alkane standards

have already been carried out by Cody and Dane [29] which successfully detected and identified *n*-alkanes ranging from C26:H to C36:H using the adapted parameters (stated in section 7.3). However, in the case of *Calliphora vicina*, the *n*-alkanes often had to be removed from the final PCA analysis to obtain the best results for ageing. The various positions of methyl branched groups present in the profiles of the three species used in this research appear to be very influential in the ageing of all of the life stages. Therefore, DART may well offer a rapid form of species identification, but it is unlikely to be of any use for ageing studies.

In conclusion, the technique of DART-MS has proven to show great potential for rapid identification of the three species analysed. DART-MS provides real-time mass spectra, which drastically cuts down the analysis time in comparison to GC-MS, which has a typical run time of 40 minutes per sample. However, GC-MS remains to be the optimum analytical instrument of choice for its all-round ability of being able to analyse saturated, unsaturated and methyl branched hydrocarbons, which have all proven to be influential in either species identification (*n*-alkanes – chapter 4) or ageing (alkenes and methyl branched hydrocarbons - chapters 5 and 6).

7.4 ANN

Computational intelligence techniques are unique as they are based on the computer system's ability to "learn" rather than to be programmed [30]. One field of computation intelligence is Artificial Neural Networks (ANN) which are abstract models based on biological neurons found in the human brain [11]. Neural networks are an assembly of

units (neurons) which independently hold limited computing capabilities but in combination, are capable of processing complex data from a variety of domains.

As mentioned in the introduction, ANN comes in the form of supervised and unsupervised learning. For the results presented in this thesis, the latter was applied to the dataset. In the unsupervised form, a Self-Organising Map (SOM) is employed to cluster the dataset and works on the basis of training the system using a dataset of known patterns, based on competitive learning [13]. This competitive-learning process results in a single neuron being active at any one time [13]. The neurons of a SOM are placed in the nodes of a one or two dimensional lattice whose configuration is determined by key statistical characteristics within the input dataset [13]. Once trained, the SOM can be used to organise unknown patterns, based on what it has learned from the training dataset, and is therefore able to cluster input patterns according to the underlying characteristics of the dataset [31].

7.4.1 Materials and Methods for ANN

The data presented to the SOM for analysis was the hydrocarbon peak areas from *L. sericata* larvae, extracted from day 1 to day 9 (chapter 5, section 5.3). The ANN results presented in this chapter were applied to the data which had been transformed using PCA. The reasoning for using the PCs rather than the raw peak area data obtained from the chromatograms was to reduce the dimensionality of the data and PCA itself is very quick to analyse a dataset. It is the plotting of the PCs which can be the time consuming process for this technique.

Half of the replicates for each day were averaged and used as a training dataset. The reasoning for this was to overcome variability within the data. There was two test approaches. The first presented the SOM with the remaining five replicates averaged, and the second method fed the SOM the five samples individually. As seen from the data presented in chapter 5, section 5.3.1 for *L. sericata* larvae, six PCs described the majority of variance within the dataset (96.1%). Figure 7.5 shows the PCA plot taken from chapter 5, showing the clustering groups of larvae corresponding to age.
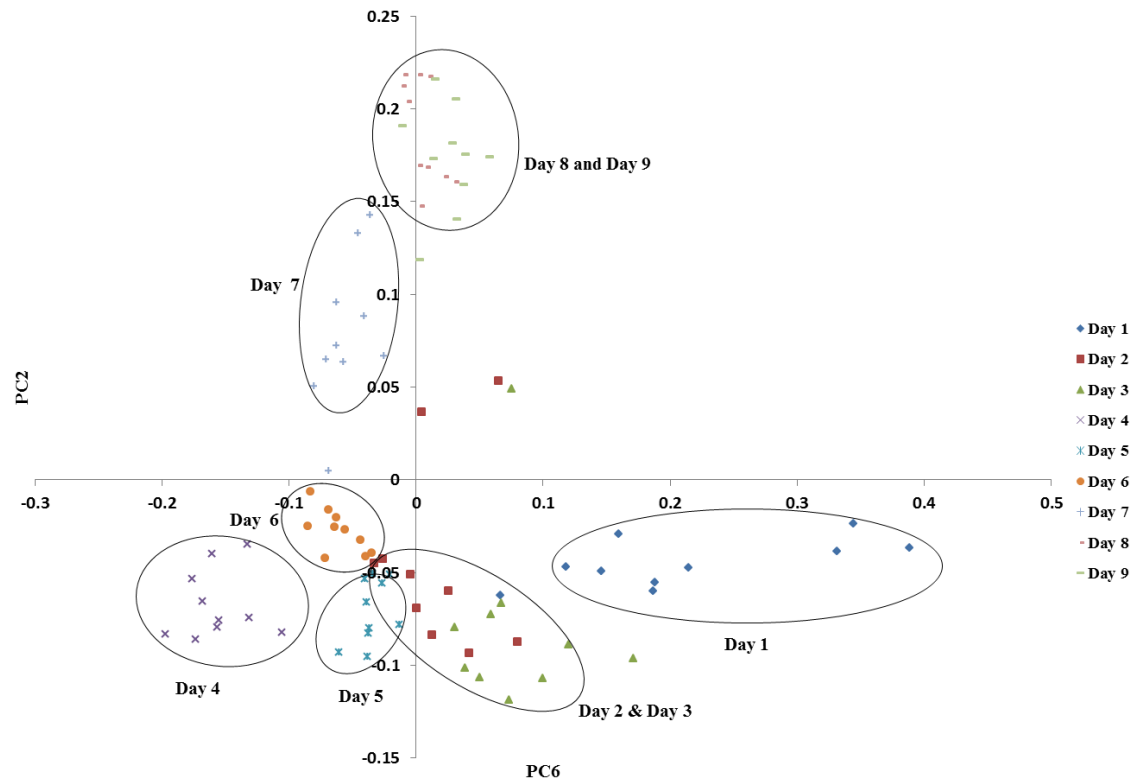
Figure 7.5: PCA plot showing PC2 against PC6 for *L. sericata* larvae with clustering days circled

All six PCs were combined for the training and test dataset, which is one of the major advantages ANN holds over PCA, as no important information contained within the PCs is excluded. The best output layer size was found by increasing the layer each time

by 2 until optimised performance is given. An output layer consisting of 12x12 output neurons produced the best results. Once the training was completed, labelling of the output layer nodes was carried out. For a well-trained SOM, the input patterns with similar characteristics are clustered together in the output layer so by labelling the data, an indication of the larval age can be established. During the labelling process, the training input pattern will determine what label the winning output neuron is assigned with. For example, the output neuron which has been classified as the winning neuron when presented with the training input pattern representing day 1 old larvae is labelled as such. The nearest neighbour approach was then applied, where the output neurons around the winning neuron (whose Euclidean distances were most similar to the winning neuron) were assigned the same label. This technique ensures that all output neurons are labelled.

7.4.2 ANN Results

The best results were obtained when inputting the average of the 5 remaining samples that were not used for training and therefore those results will be discussed in more detail. When tested, this approach gave an almost perfect classification for day 1 to day 7 larvae, incorrectly classifying a test pattern of day 2 larvae as day 6 and a day 4 larvae as day 5 (Table 7.2). The SOM also confused most of day 8 with day 9 larvae but PCA could not classify day 8 and day 9 either and grouped them into a single cluster (Figure 7.5). This is the late post-feeding larval stage and the hydrocarbon profiles are very similar with little chemical differences between them (Figure 7.6). The PC plot also grouped day 2 and day 6 replicates very close to each other and Euclidean distances had to be calculated to show there was a difference between them

(chapter 5, section 5.3), so it is not unexpected for the SOM to get one misplaced pattern wrong between these two days. This shows improvement over PCA results.
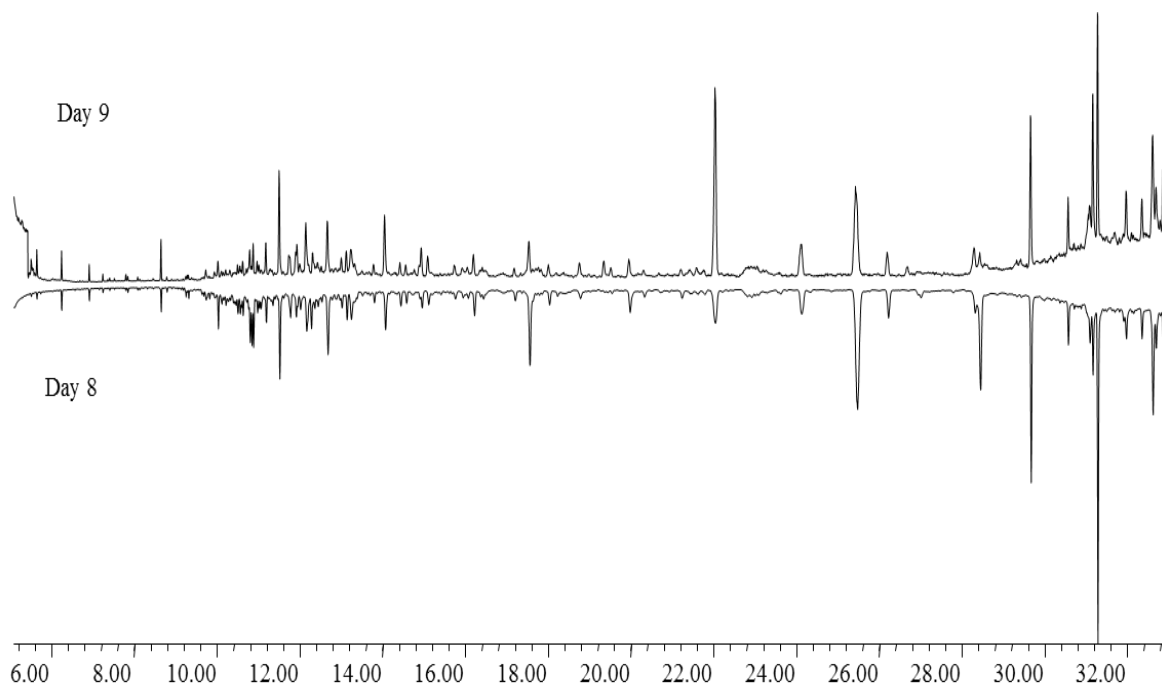
Figure 7.6: GC-MS chromatograms of day 8 and day 9 larvae, shown for comparison

Table 7.2: Table showing the confusion matrix of the SOM for each fold of cross-validation as well as the overall classification performance for each day when tested using the average of the remaining five input patterns

		Input pattern tested								
		D1	D2	D3	D4	D5	D6	D7	D8	D9
SOM Classification	D1	10								
	D2		9							
	D3			10						
	D4				9					
	D5				1	10				
	D6		1				10			
	D7							10		
	D8								3	2
	D9								7	8
% correct		100	90	100	90	100	100	100	30	80

Overall, the results produced classification scores of 87% for the averaged test data and 84% for the individually presented test data, which are very positive results given the dataset was very small.

7.4.3 ANN Discussion and Conclusion

The preliminary results presented in this chapter for DART-MS highlight this technique as having great potential in the field of forensic entomology, enabling real-time data analysis and therefore rapid results for insect identification. The results also revealed the potential for analysing cuticular hydrocarbons from insects in general, as it was the first time *n*-alkanes have been detected using DART analysis in negative ion mode. The population differences was also a very exciting result that was obtained and could hold a lot of forensic relevance, as it could indicate whether a body has been moved.

The results presented on ANN analysis also show the great potential of this data analysis approach in the field of forensic entomology and it is the first time a SOM has been applied to this domain in terms of ageing. Given the dataset was very small, the results are encouraging and once the training has been established, there is know need for retraining, as any unknown samples can simply be added to the model for an indication of age to be established. The main advantages of ANN over PCA is that all of the important PCs can be used (in the case of the results presented, all six PCs were used) and therefore most of the variance within the dataset is accounted for, removing the need for the judgment of the analyst to decide which PCs give the best result, hence a more objective approach. ANN would be highly advantageous for the analysis of

other datasets such as the empty puparial cases which contains substantially more samples and could be classified quicker by a trained ANN. Subtle chemical changes that happen over a much longer period of time also make the use of ANNs attractive, as data contained in all PCs becomes more important.

References

[1]   R.B. Cody and J.A. Laramée, Versatile New Ion Source for the Analysis of Materials in Open Air under Ambient Conditions, Journal of Analytical Chemistry 77 (2005) 2297–2302.

[2]   R.B. Cody, J.A. Laramée, J.M. Nilles, and H.D. Durst, *Direct Analysis in Real Time (DART) Mass Spectrometry*, JEOL, 2007.

[3]   J. Hajslova, T. Cajka, and L. Vaclavik, Challenging applications offered by direct analysis in real time (DART) in food-quality and safety analysis, TrAC Trends in Analytical Chemistry 30 (2011) 204–218.

[4]   H.J. Kim, W.S. Baek, and Y.P. Jang, Identification of ambiguous cubeb fruit by DART-MS-based fingerprinting combined with principal component analysis, Food Chemistry 129 (2011) 1305–1310.

[5]   R.R. Steiner and R.L. Larson, Validation of the direct analysis in real time source for use in forensic drug screening., Journal of forensic sciences 54 (2009) 617–22.

[6]   A.H. Grange and G.W. Sovocool, Detection of illicit drugs on surfaces using direct analysis in real time (DART) time-of-flight mass spectrometry., Rapid communications in mass spectrometry : RCM 25 (2011) 1271–81.

[7]   R.B. Cody, Observation of Molecular Ions and Analysis of Nonpolar Compounds with the Direct Analysis in Real Time Ion Source, Analytical Chemistry 81 (2009) 1101–1107.

[8]   J.Y. Yew, R.B. Cody, and E. a Kravitz, Cuticular hydrocarbon analysis of an awake behaving fly using direct analysis in real-time time-of-flight mass spectrometry., Proceedings of the National Academy of Sciences of the United States of America 105 (2008) 7135–40.

[9]   S. Haykin, *Neural Networks: A comprehensive Foundation*, Prentice Hall, New Jersey, USA, 1999.

[10]   J.B. Butcher, H.E. Moore, C.R. Day, F.P. Drijfhout, and C.D. Adam, Artificial Neural Network analysis of hydrocarbon profiles for the ageing of Lucilia sericata for Post Mortem Interval estimations, (2012).

[11]   J.B. Butcher, M. Lion, C.R. Day, and P.W. Haycock, A low frequency electromagentic probe for detection of corrosion in steel-reinforced concrete, in: M. Grantham, C. Majorana, and V. Salomoni, eds., Concrete Solutions, CRC Press, NL, 2009, pp. 417–424.

[12]   T. Kohonen, Self-organising map, in: Proceedings of the IEEE, 1990, pp. 1464–1480.

[13]   S. Haykin, *Neural Networks and Learning Machines*, Pearson, USA, 2008.

[14]   T. Nacnna, R.A. Bress, and M.J. Embrechts, DNA Classifications with Self-organizing Maps (SOMs), IEEE International Workshop on Soft Computing in Industrial Applications (2003) 151–154.

[15]   A. Prescher, A. Meyers, and D.G.V. Keyserlingk, Neural net applied to anthropological material: A methodical study on the human nasal skeleton, Annals of Anatomy - Anatomischer Anzeiger 187 (2005) 261–269.

[16]   B.K.L. Fei, J.H.P. Eloff, M.S. Olivier, and H.S. Venter, The use of self-organising maps for anomalous behaviour detection in a digital investigation., Forensic science international 162 (2006) 33–7.

[17]   A. Bianconi, C.J. Von Zuben, A.B.D.S. Serapião, and J.S. Govone, Artificial neural networks: a novel approach to analysing the nutritional ecology of a blowfly species, *Chrysomya megacephala*, Journal of insect science (Online) 10 (2010) 58.

[18]   A.-G. Bagneres, G. Riviere, and J.-L. Clement, Artificial neural network modeling of caste odor discrimination based on cuticular hydrocarbons in termites, Chemoecology 8 (1998) 201–209.

[19]   J.Y. Yew, K. Dreisewerd, C.C. de Oliveira, and W.J. Etges, Male-specific transfer and fine scale spatial differences of newly identified cuticular hydrocarbons and triacylglycerides in a Drosophila species pair., PloS one 6 (2011) e16898.

[20]   M. Curtis, M. a Minier, P. Chitranshi, O.D. Sparkman, P.R. Jones, and L. Xue, Direct analysis in real time (DART) mass spectrometry of nucleotides and nucleosides: elucidation of a novel fragment [C5H5O]+ and its in-source adducts., Journal of the American Society for Mass Spectrometry 21 (2010) 1371–81.

[21]   R.J. Hurtubise, Adsorption Chromatography, in: J. Cazes, ed., Encyclopedia of Chromatography 2004 Update Supplement, Marcel Dekker Inc., USA, 2002, pp. 17–20.

[22]   H.M. McNair and J.M. Miller, *Basic Gas Chromatography*, Wiley, UK, 2009.

[23]   R.B. Cody, Observation of Molecular Ions and Analysis of Nonpolar Compounds with the Direct Analysis in Real Time Ion Source, 81 (2009) 1101–1107.

[24]   S.W. Kim, H.J. Kim, J.H. Kim, Y.K. Kwon, M.S. Ahn, Y.P. Jang, and J.R. Liu, A rapid, simple method for the genetic discrimination of intact Arabidopsis thaliana mutant seeds using metabolic profiling by direct analysis in real-time mass spectrometry., Plant Methods 7 (2011) 14.

[25]   M. Guilhaus, Essential elements of time-of-flight mass spectrometry in combination with the inductively coupled plasma ion source, Spectrochimica Acta Part B: Atomic Spectroscopy 55 (2000) 1511–1525.

[26]   A. Langford, J. Dean, R. Reed, D. Holmes, J. Weyers, and A. Jones, *Practical Skills in Forensic Science*, Pearson, UK, 2005.

[27]   M. Guilhaus, Principles and instrumentation in time-of-flight mass spectrometry. Physical and instrumental concepts, Journal of Mass Spectrometry 30 (1995) 1519–1532.

[28]   E. Hoffmann, J. Charette, and V. Stroobant, *Mass Spectrometry: Principles and Applications*, Wiley, UK, 1999.

[29] R.B. Cody, Soft Ionization of Saturated Hydrocarbons, Alcohols and Nonpolar Compounds by Negative-Ion Direct Analysis in Real-Time Mass Spectrometry, Journal of the American Society for Mass Spectrometry (2013).

[30] R. Callan, *The Essence of Neural Networks*, Prentice Hall, UK, 1999.

[31] R. Callan, *Artificial Intelligence*, Palgrave Macmillan, UK, 2003.

Chapter 8

Summary, Conclusion and Future Work

The two main objectives of this study were to determine whether cuticular hydrocarbons could be utilised to firstly, identify to species level and secondly age all six developmental life stages of three forensically important blowflies.

The work presented in chapters 4 to 6 contain the principal data for this thesis, focusing on developing analysis of cuticular hydrocarbons with GC-MS and applying the technique in the field of forensic entomology. The studies carried out concerned preliminary laboratory based experiments, combining three main aspects; cuticular hydrocarbons, GC-MS and PCA.

The first stage of the research was to establish if hydrocarbons could be used as a means of taxonomy. The three blowfly species used for the research were *C. vicina*, *C. vomitoria* and *L. sericata*. The hydrocarbon profiles were extracted from all of the life stages and compared to establish if each species had a unique "fingerprint" profile which would make them distinguishable.

The second stage of the research was to establish if the hydrocarbon profiles change with time and therefore if they can be used to age the six life stages of the three blowflies mentioned. The current method of ageing larvae involve accurately recording the length and weight which is then compared to temperature and growth charts, since larvae growth is dependent on temperature.

Chapter 7 explored new developments that could be used to complement the work presented in chapters 4 to 6. DART-MS offers rapid analysis for taxonomy purposes whereas artificial neural networks (ANN) show great potential for being able to age the life stages and could provide a good alternative to PCA, with its ability to cope with large quantities of data.

Identification

When a forensic entomologist is called to a cadaver at a crime scene it is likely there will be an abundance of larvae evidence present. They provide the most useful amount of information for the PMI estimation. Entomological evidence can only be applied for PMI estimations when correct identification down to species level has been obtained. Correct identification is therefore vital because different species have different life cycle timings and accurate ageing cannot be established unless the correct developmental charts are utilised.

The morphological features that are currently used to establish larvae identity have been explained in chapter 4, section 4.2. However, hydrocarbon analysis was proven to offer a major advantage over current morphological techniques because it can be accomplished at any instar stage of the larval life cycle whereas current techniques

require larvae to be in the 3rd instar stage due to their size and still require the time consuming step of rearing to adult flies for species confirmation. However, a hydrocarbon profile extracted from newly emerged 1st instar larvae provided a GC chromatogram that can provide identification. Results presented in chapter 4 showed that for each life stage, identification was established for all three species examined, using GC-MS and PCA. The main advantage of using hydrocarbon analysis for taxonomy purposes is the speed in which identification can be accomplished. However, a database of hydrocarbon profiles for forensically important insects should first be constructed. The overall aim of a hydrocarbon database would be to upload a hydrocarbon profile and obtaining a species match.

It is important to note that results presented in chapter 4 do not necessarily "identify" the species, but they can be used to distinguish between the three species used, implying the hydrocarbon profiles are species-specific and show the potential for hydrocarbon analysis to be used in taxonomy. There are two distinguishing results (presented in chapter 4) that could be most beneficial in forensic entomology. Firstly, the three species examined are distinguishable from their chemical profiles in the 1st instar larval stage which could drastically cut time in criminal investigations if species identification can be established at this very early phase. Secondly, a full chemical profile can be obtained from partially intact empty puparial cases allowing for species identification. Using current morphological techniques, a whole puparial case with all of the morphological features intact is needed to establish identification to species level. The preliminary data presented for DART-MS also shows huge potential for providing rapid identification of empty puparial cases. For the three species analysed, the LDA plot showed excellent separation allowing for the species to be distinguished

without the need of relying on morphological features. The results were also able to show differences within the chemical profiles of the two *C. macellaria* species (one set of samples from Ohio and another from Texas). This shows considerable promise of being able to determine species from different geographical locations. As these slight differences were detected from the hydrocarbon profiles, there could potentially be differences within the chemical composition due to the different climates these two species inhabit.

The main potential of hydrocarbon analysis lies with species that are notoriously difficult to identify such as Sarcophagidae species or Coleoptera species. Results presented in this thesis show a proof of concept that this technique can be used to distinguish between the three species analysed. In order to prove whether hydrocarbons can be used for species identification, more species need to be analysed, with emphasis on the morphologically similar species.

Ageing

Age determination is the basis for determining the estimation of the PMI in criminal investigations. When presented with a crime scene, a forensic entomologist must be able to establish the age of the oldest insect present to acquire a time since colonisation, which in turn enables a PMI estimation to be calculated. Current ageing techniques combine many variable factors from the species of insects present with the temperature and humidity at the crime scene. Factors such as clothing/wrapping of the body, part burial, location (urban or rural/indoors or outdoors), substance intoxication of the deceased, can all have a significant effect on the developmental rates of insects and

must therefore be taken into consideration. Chapter 5 examined the potential for using cuticular hydrocarbons to age the different life stages of *L. sericata*, *C. vicina* and *C. vomitoria*. Results were obtained from the empty egg cases, larvae, pupae, empty puparial cases and adult flies. As with the identification results, the empty egg cases results were tentatively presented and show potential for this technique to be applied for ageing to be established, but more sampling replicates are required to confirm the results, as any variation within the samples is not been accounted for with only 2 replicates per age.

The larvae results show ageing can be established to the instar, even to the day in most cases when reared in the laboratory. Results from all three species were extremely encouraging, especially the data obtained from *C. vomitoria*, which allowed for the post-feeding stage to be aged to the day, for the first time.

The empty puparial cases and adult flies also gave very promising results. As with the identification results, a full profile of an empty puparial case can be obtained from a partially intact case, allowing for young cases to be differentiated from old.

The relevance of adult ageing can be used to classify flies that eclose on the decomposing remains from those that have been attracted by the odour. Previous results presented on hydrocarbon analysis of adult flies have only been able to distinguish between young and old flies, but this study allowed for ageing to be established at eclosion, day 5, day 10, and day 20 and 30, allowing for much more accurate ageing estimations. This could be particularly useful for indoor crime scene where they are unable to escape.

Table 8.1 summarises the ageing results presented in chapters 5 and 6.

	Larvae					Pupae		Adult flies				
	1st instar	2nd instar	3rd instar	Post-feeding young	Post-feeding old	Young	Old	D1	D5	D10	D20	D30
L. sericata	——	——	– – –	——	——	✖	✖	——	——	——	Not tested	Not tested
C. vicina	——	——	– – –	——	——	✖	✖	——	——	——	——————	
C. vomitoria	——	——	——	– – –	– – –	Not tested	Not tested	——	——	——————		

—— Age to the criteria

– – – Age to the criteria and to the day

	Empty egg cases		Empty puparial cases										
	Young (D2/D5)	Old (D8/D12)	Wk 1	Wk 2 to Wk 5	Wk 6	Wk 7	Wk 8	Mth 3	Mth 4	Mth 5	Mth 6	Mth 7	Mth 8	Mth 9
L. sericata	——	——	——	——	————————			——————————				
C. vicina	——	——	——	——	————————			——————————				

—— Age to the criteria

– – – Age to the criteria and to the day

Table 8.1: Two tables summarising the ageing results presented in this thesis (chapter 5 and 6) for larvae, pupae, adult flies, empty egg cases and empty puparial cases.

For the blowflies studies in this thesis, the chain length typically ranges from 16 to 33 carbons. However, a study from Akino [1] suggested the chain lengths detected by GC-MS may not be the longest that is present on the insects' cuticle, and maybe a case of instrument limitations. Akino presented results from the ant, *Formica truncorum*, and analysed the hydrocarbon profile using a new higher temperature GC column. The profile of the ant published in previous studies [2] usually ranges from 23 to 33 carbons. However, using the higher temperature column, they were able to detect up to 48 carbon atoms. Another group of researchers [3] were also able to detect higher chain lengths in insects by adopting the analytical technique of Matrix-Assisted Laser Desorption/ Ionisation (MALDI) Time of Flight (TOF) mass spectrometry. They were able to detect hydrocarbons with up to 70 carbon atoms in the chain from the profiles of different termite species. Although it would be advantageous to extract a full profile of the three blowflies species studied in this thesis, being restricted to examine the compounds up to C33:H has not had an affect on the results. It has been proved that all distinguishes can still be made between all three species from the different classes of hydrocarbons present and the ratios that hydrocarbons are present in as well as the unique double bond positioning within the alkenes.

Conclusion

Overall, a wealth of information was obtained from the experimental work carried out for this thesis. The field of forensic entomology could greatly benefit from a technique that facilitates identification information as well as age, from one chemical profile of an insect. The presented methodology is simple to execute, allowing a non-expert to

follow and perform the extraction procedures. In comparison to DNA, GC-MS analysis is inexpensive and the analysis time is short.

GC-MS has been the analytical technique of choice for hydrocarbon analysis for many years due to its ability to separate these non-polar compounds in order of increasing boiling point, followed by relatively simple mass spectrometry identification. However, advancements in other analytical techniques are being exploited in many areas of science, especially forensic science. DART-MS offers real-time analysis and has the potential to cut time even further in criminal investigations through rapid species identification. Although GC-MS was the main analytical technique for this research, DART-MS shows great potential in the field of forensic entomology due to its high sensitivity and prompt results. The practical methodology required for this type of work is relatively simple. The extraction method is straightforward. A set programme can be used on any GC-MS and the resulting chromatogram from each sample can be used to distinguish the hydrocarbon profiles. The chromatogram data can then be inputted into a PCA model giving an indication of the insect's age.

This study has shown that hydrocarbons hold the possibility of being used to determine the age of the insect in each of the life stages. The combination of using the analytical technique of GC-MS for chemical identification using cuticular hydrocarbons and the statistical analysis with PCA means an indication of age can be established for the empty egg shells, larvae, puparial cases and adult flies of *L. sericata*, *C. vicina* and *C. vomitoria*.

Results presented on DART-MS and ANN analysis offer alternatives to the main techniques used for the thesis. DART-MS has many advantages which have already been discussed and ANN is capable of coping with large domains and it does not require the analyst to make subjective decisions. The results presented in this thesis have successfully shown the potential of hydrocarbon analysis for species identification and ageing of three forensically important blowfly species in the UK.

Future Work

The next stage to validate hydrocarbon analysis fully in forensic entomology is to obtain some field based samples to test the practicalities of the technique. All of the experimental data presented in this thesis were obtained under standard laboratory conditions. Work needs to be done to examine the stability of the hydrocarbons under various temperatures (stable and fluctuating) [4] to see if this has an effect on the chemical profiles. Further work needs to done in the area of food sources as this will vary when larvae feed on a cadaver as they tend to feed from the head downwards (if no wounds present), therefore ingesting various bodily tissues and organs. Most studies published in the field of forensic entomology use liver as a food source to rear the larvae, but studies have shown their growth can be accelerated when feeding on other tissues such as heart, lung, kidney and brain [5]. It would also be useful to look into the effects that drugs may have on the hydrocarbon profile to see if it alters it and if so, can the chemical profile still be accurately utilised for identification and ageing purposes. If larvae feed on a cadaver that ingested drugs prior to death, this can have an effect on their development and can either accelerate or retard growth [6,7], which could have potential implications of reliable PMI estimations.

Results on ageing empty puparial cases (chapter 6, section 6.3) show changes observed over time. Where possible, and explanation of these changes has been proposed for the living samples, but they cannot be explained for the empty puparial cases and egg cases. For the purpose of this study, the aim was simply to determine if changes occurred with time and therefore show potential to be used for ageing. However, further investigation into whether the effects are due to physical, chemical or bacterial influences would be advantageous.

A hydrocarbon database of all forensically important insects could be created and, for the wider picture, a chemotaxonomy database of insects in the UK would be highly beneficial for identification purposes. More work using DART-MS is intended on being developed using morphologically challenging blowflies as well as flesh flies.

References

[1]   T. Akino, Cuticular hydrocarbons of *Formica truncorum* (Hymenoptera: Formicidae): Description of new very long chained hydrocarbon components, Applied Entomology and Zoology 41 (2006) 667–677.

[2]   J. Nielsen, J.J. Boomsma, N.J. Oldham, H.C. Petersen, and E.D. Morgan, Colony-level and season-specific variation in cuticular hydrocarbon profiles of individual workers on the ant *Formica truncorum*, Insectes Sociaux 46 (1999) 58–65.

[3]   J. Cvacka, P. Jiros, J. Sobotník, R. Hanus, and A. Svatos, Analysis of insect cuticular hydrocarbons using matrix-assisted laser desorption/ionization mass spectrometry, Journal of Chemical Ecology 32 (2006) 409–34.

[4]   S. Niederegger, J. Pastuschek, and G. Mall, Preliminary studies of the influence of fluctuating temperatures on the development of various forensically relevant flies, Forensic Science International 199 (2010) 72–78.

[5]   G. Kaneshrajah and B. Turner, *Calliphora vicina* larvae grow at different rates on different body tissues, International Journal of Legal Medicine 118 (2004) 242–244.

[6]   F. Introna, C.P. Campobasso, and L.M. Goff, Entomotoxicology, Forensic Science International 120 (2001) 42–47.

[7]   B. Bourel, V. Hedouin, L. Bouyer-Martin, A. Becart, G. Tournel, M. Deveaux, and D. Gosset, Effects of Morphine in Decomposing Bodies on the Development of *Lucilia sericata* (Diptera : Calliphoridae), Journal of Forensic Sciences (1999) 354–359.

Appendices

Appendix 1: Table showing all compounds extracted from the cuticles of the empty egg cases for *L. sericata, C. vicina* and *C. vomitoria*.

Peak no.	Peak Identification	Kovats iu	L. sericata n=2 %	C. vicina n=2 %	C. vomitoria n=2 %
1	Tricosane	2300	Present	Present	Present
2	2-Methyltriconsane	2463	ND	Present	Present
3	Tetracosane	2400	Trace	Trace	Present
4	Pentacosene	2469	Present	Present	Present
5	Pentacosene	2476	ND	ND	Present
6	Pentacosane	2500	Present	Present	Present
7	11+9-Methylpentacosane	2535	Present	ND	Present
8	Hexacosane	2600	Present	Trace	Present
9	2-Methylhexacosane	2662	Present	Present	Present
10	Heptacosene	2668	Present	ND	Present
11	Heptacosane	2700	Present	Present	Present
12	11+13-Methylheptacosane	2730	Present	Present	Present
13	Octacosane	2800	Present	Present	Present
14	3-Methylheptacosane	2773	Present	Present	Present
15	2-Methyloctacosane	2873	Present	Present	Present
16	Nonacosene	2877	Present	Present	Present
17	Nonacosene	2882	ND	Present	Present
18	Nonacosane	2900	Present	Present	Present
19	2,6-Dimethyloctacosane	2906	ND	Present	ND
20	13+11-Methylnonacosane	2938	Present	Present	Present
21	9-Methylnonacosane	2943	Present	Present	Present
22	7-Methylnonacosane	2950	Present	Present	Present
23	5-Methylnonacosane	2958	Present	Present	2.82±0.97
24	9,17-Dimethylnonacosane	2971	Present	ND	ND
25	3-Methylnonacosane	2981	Present	Present	Present
26	5,x-Dimethylnonacosane	2989	ND	Present	Present
27	Triacontane	3000	Present	Present	Present
28	14+16-Methyltricontane	3041	ND	Present	Present
29	2-Methyltricontane	3041	Present	Present	Present
30	Hentriacontene	3076	Present	ND	Present
31	Hentriacontane	3100	Present	Trace	Trace
32	2,14-Dimethyltriacontane	3106	ND	Present	Present
33	2,6/2,8/2,10-Dimethyltriacontane	3111	ND	Present	Present
34	11-Methylhentriacontane	3144	Present	Present	Present

35	11,19-Dimethylhentriacontane	3143	Present	ND	ND
36	7,x-Dimethylhentriacontane[1]	3147	ND	ND	Present
37	9,21-Dimethylhentriacontane[1]	3174	ND	Present	Present
38	17-Methyltritriacontane+4,8/4,10-Dimethylhentriacontane[1]	N/A[2]	ND	Present	Present
39	2,10/2,12-Dimethylhentriacontane[1]	3339	ND	Present	Present

[1] Tentative identification based on Kovats Index values and match with NIST08 Library database
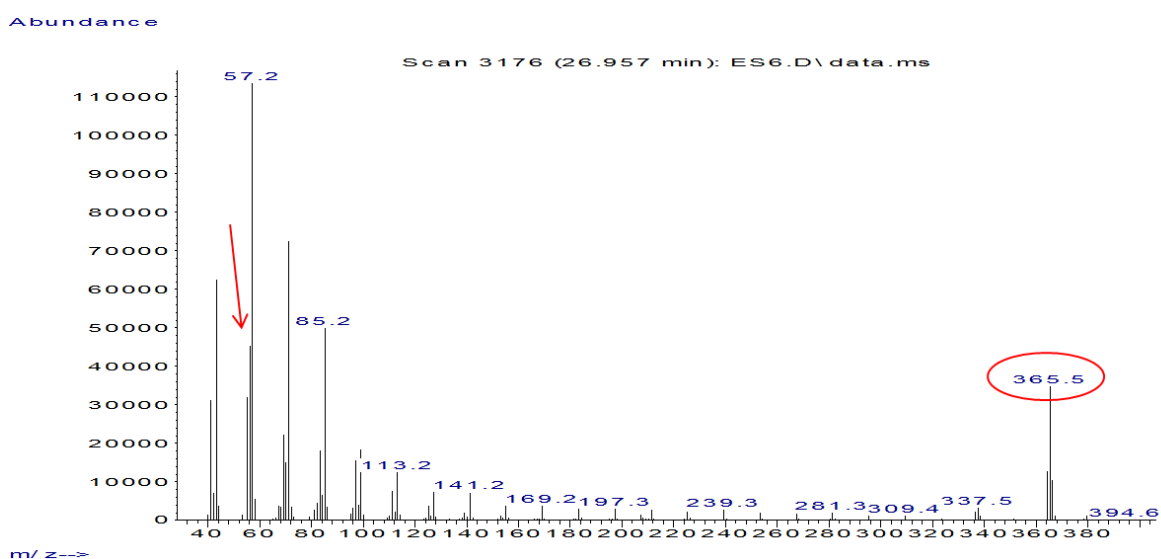
[2]Kovats not available due to co-eluting peak

ND = Not Detected

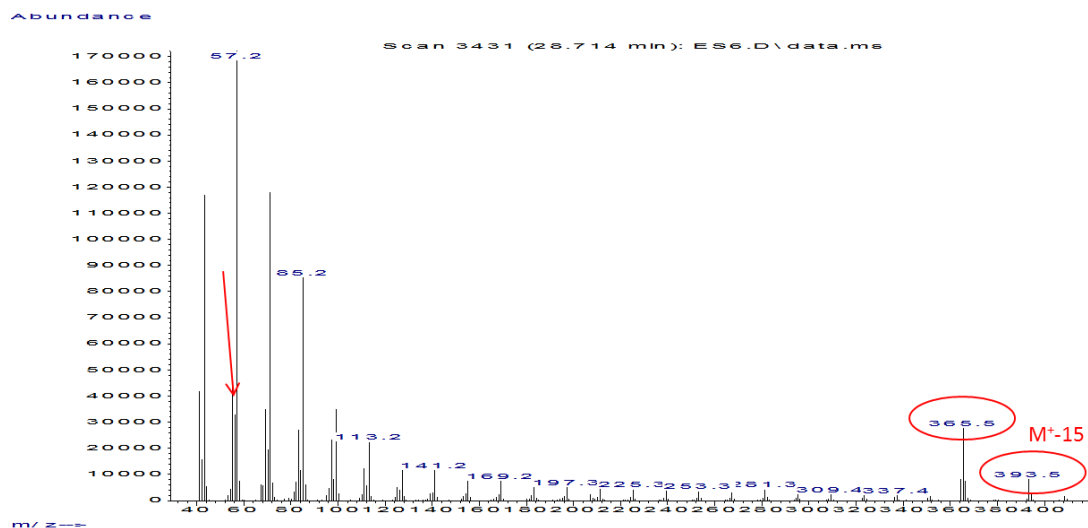Present = Present above a peak area of 0.5%

Trace = Present below a peak area of 0.5%

Appendix 2: Mass spectra of 3-Methylheptacosane with, diagnostic ions to aid identification circled.

321

Appendix 3: Mass spectra of 2-Methyloctacosane, with diagnostic ions to aid identification circled.

Appendix 4: Mass spectra of 11+13-Methylheptacosane, with diagnostic ions to aid identification circled.

Appendix 5: Mass spectra of 2,6-Dimethyloctacosane, with diagnostic ions to aid identification circled.

Appendix 6: Mass spectra of 9,17-Dimethylnonacosane, with diagnostic ions to aid identification circled.
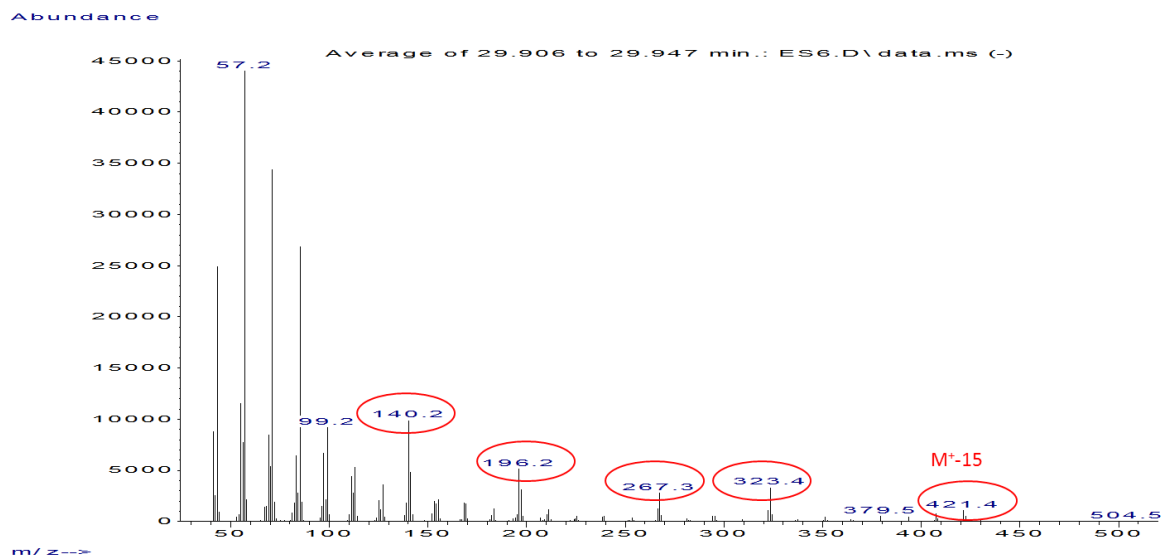
Appendix 7: Mass spectra of pentacosene, with diagnostic ion to aid identification circled.
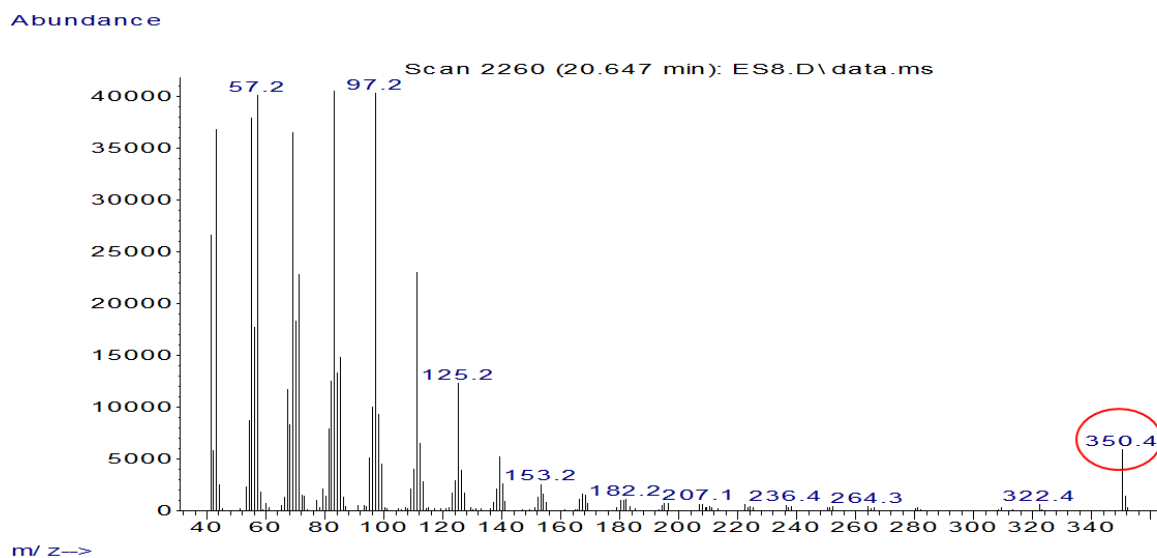
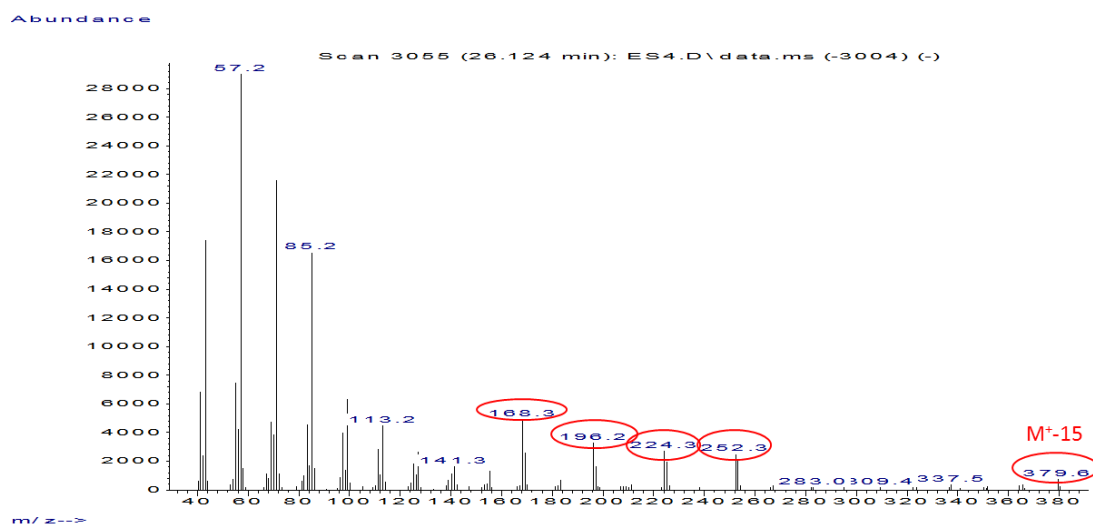

Appendix 8: Mass spectra of heptacosene, with diagnostic ion to aid identification circled.
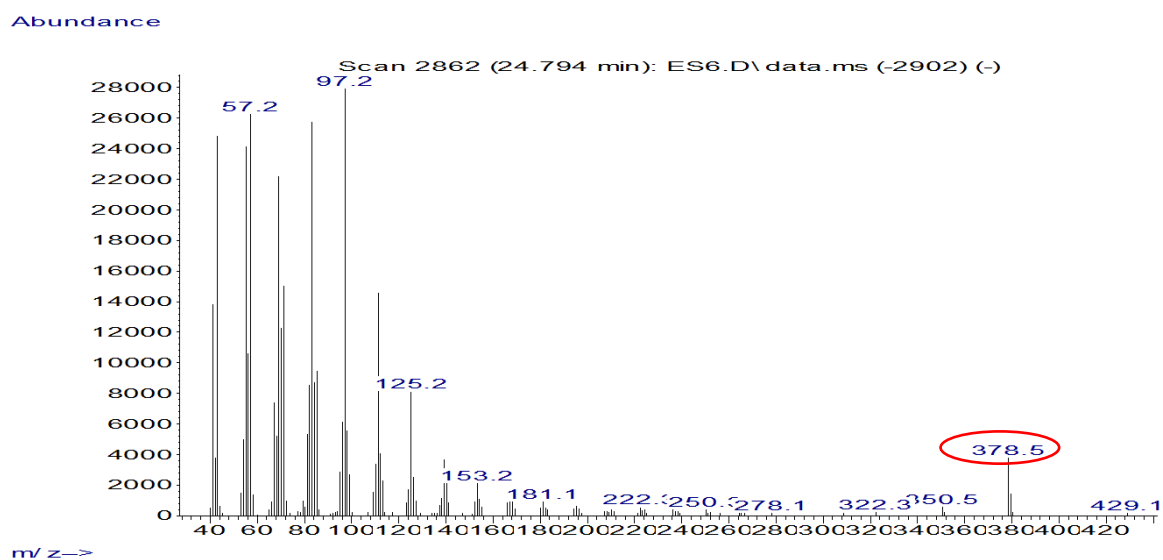
Appendix 9: Mass spectra of nonacosene, with diagnostic ion to aid identification circled.

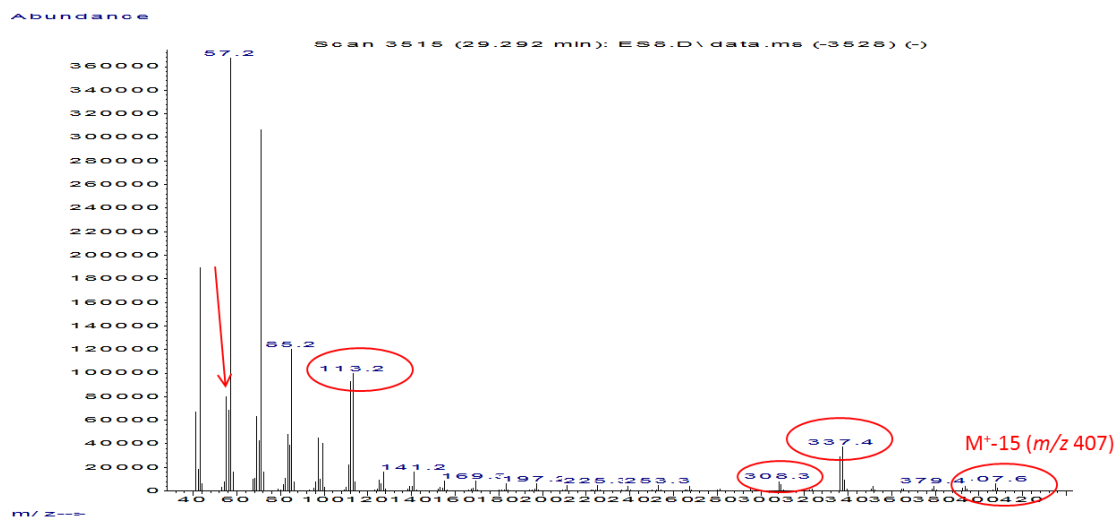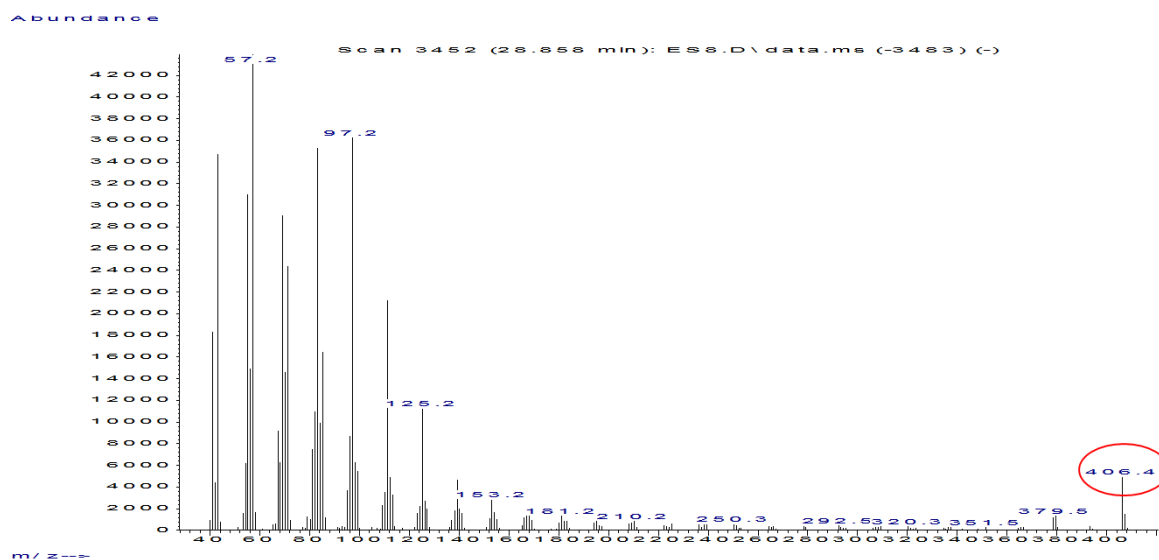**Appendix 10**: PCA table for species identification of *C. vicina, C. vomitoria* and *L. sericata* empty egg cases

PCA - Principal Components Analysis (Standardised)

N. PCs	Eigenvalues	
	E-value	*%*
Total SS	180	100
#1	140.7393205	78.1885
#2	34.86348457	19.3686
#3	2.836520897	1.57584
#4	0.984729076	0.54707
#5	0.478141918	0.26563
Total		99.9457

Appendix 11: PCA table for species identification of day 1 larvae of *C. vicina, C. vomitoria* and *L. sericata*

PCA - Principal Components Analysis (Standardised)

N. PCs	Eigenvalues	
	E-value	*%*
Total SS	1410	100
#1	660.904	46.87259
#2	368.415	26.128703
#3	279.69	19.836175
#4	26.9036	1.9080577
#5	24.1368	1.7118266
#6	19.2434	1.364777
Total		97.8

Appendix 12: PCA table for species identification of *C. vicina* and *L. sericata* pupae

PCA - Principal Components Analysis (Standardised)

N. PCs	Eigenvalues	
	E-value	*%*
Total SS	260	100
#1	190.6500185	73.32693
#2	66.21410059	25.466962
#3	1.292485047	0.4971096
#4	1.024608168	0.3940801
#5	0.398508596	0.1532725
#6	0.178726628	0.068741
Total		99.907095

Appendix 13: PCA table for species identification of *L. sericata, C. vicina* and *C. vomitoria* empty puparial cases

PCA - Principal Components Analysis (Standardised)

N. PCs	Eigenvalues	
	E-value	*%*
Total SS	290	100
#1	260.422	89.8007
#2	25.58847	8.82361
#3	3.362511	1.159486
#4	0.484975	0.167233
#5	0.090399	0.031172
#6	0.022753	0.007846
		99.99

Appendix 14: Mass spectra of *Z7C27:1*, with diagnostic ion to aid identification circled.

Appendix 15: Mass spectra of Z9C27:1, with diagnostic ion to aid identification circled.
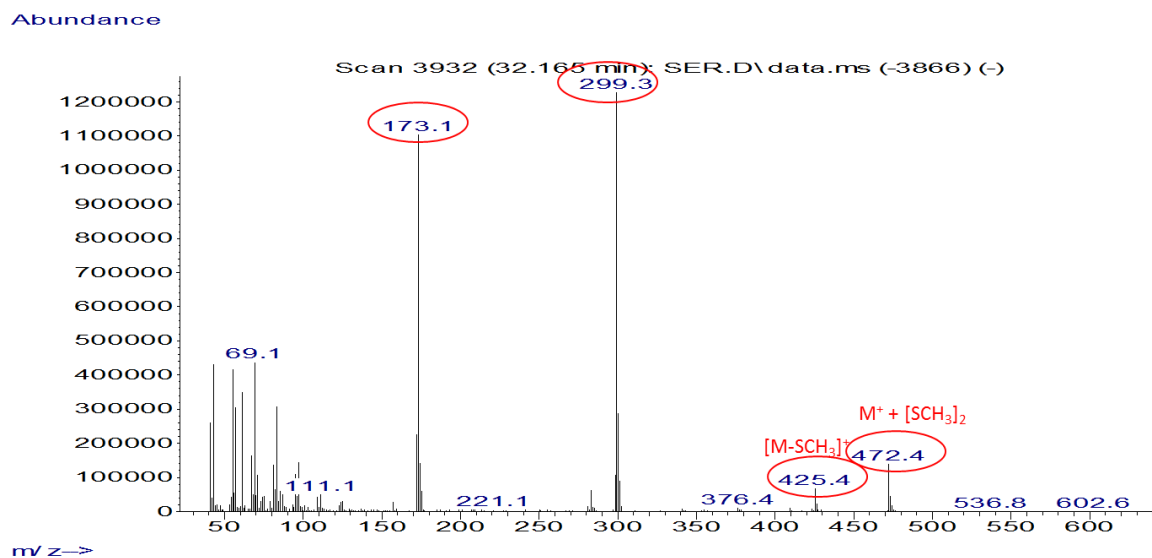
Appendix 16: Mass spectra of co-eluting Z9 & Z10C29:1, with diagnostic ion to aid identification circled.

Appendix 17: PCA table for species identification of *C. vicina* and *C. vomitoria* adult

fly

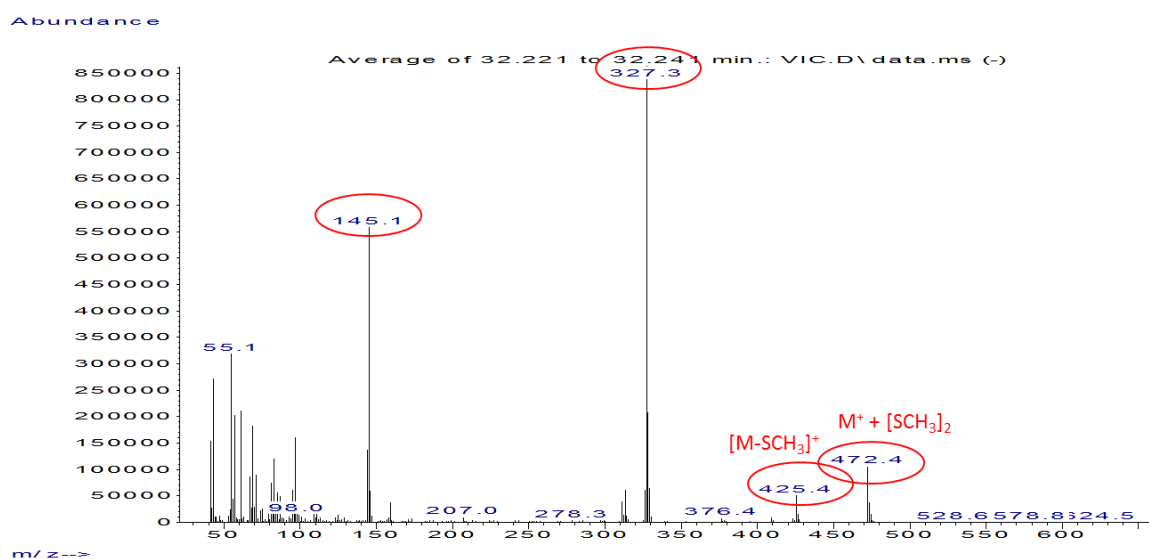**PCA - Principal Components Analysis (Standardised)**
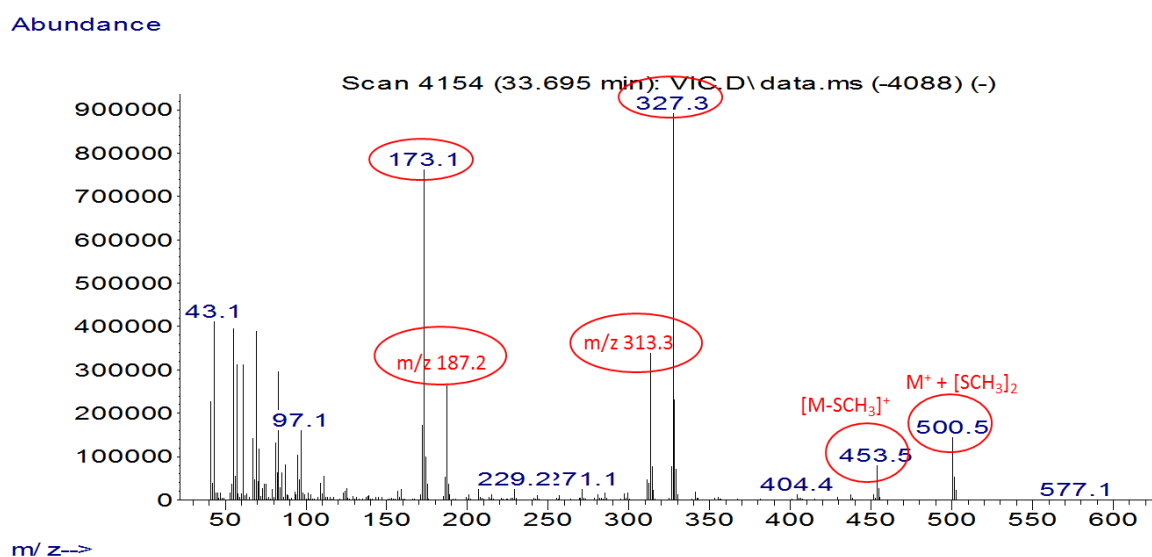
N. PCs	Eigenvalues	
	E-value	*%*
Total SS	160	100
#1	134.0728983	83.79556146
#2	24.49676123	15.31047577
#3	1.25885051	0.786781569
#4	0.109408232	0.068380145
#5	0.053796551	0.033622844
#6	0.008285143	0.005178214
Total		100

Appendix 18: PCA table for the ageing of *C. vomitoria* empty egg cases

PCA - Principal Components Analysis (Standardised)

N. PCs	Eigenvalues	
	E-value	*%*
Total SS	170	100
#1	141.9617739	83.5069258
#2	25.85792369	15.21054334
#3	1.84192313	1.083484194
#4	0.254556547	0.149739145
Total		99.95

Appendix 19: PCA table for the ageing of *C. vicina* empty egg cases

PCA - Principal Components Analysis (Standardised)

N. PCs	Eigenvalues	
	E-value	*%*
Total SS	108	100
#1	103.4168966	95.75638578
#2	3.182178095	2.946461199
#3	1.23919942	1.147406871
Total		99.9

Appendix 20: Graph of the average percentage peak area of each methyl branched hydrocarbon in relation to instars for *C. vomitoria*
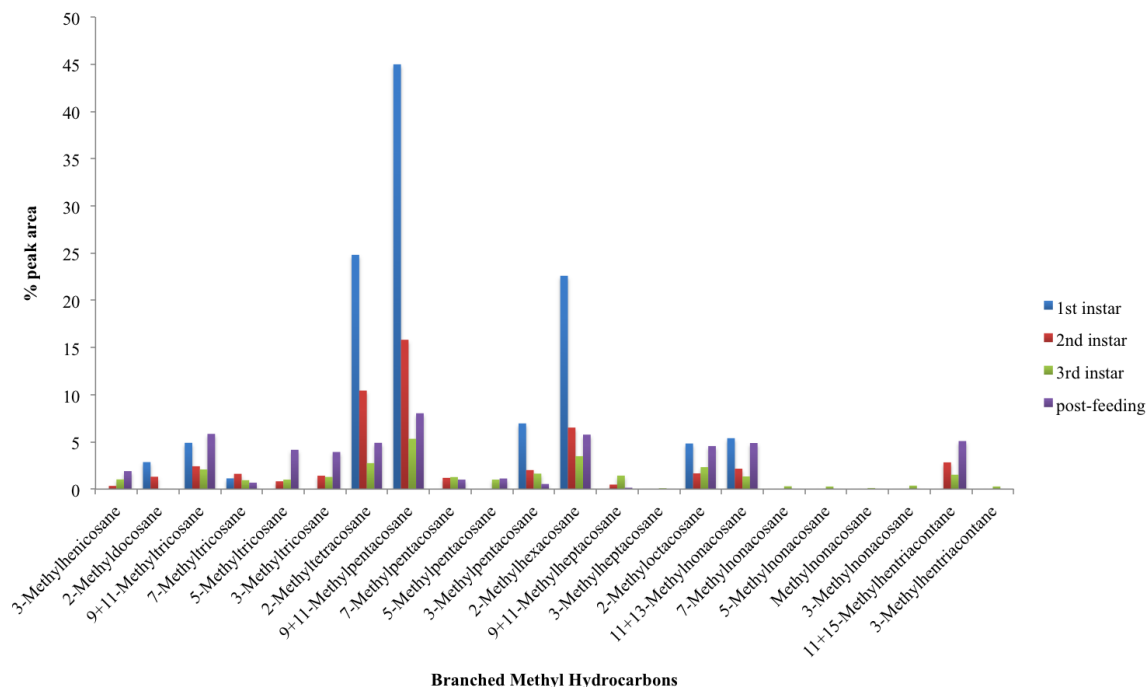
Appendix 21: PCA table for the ageing *C. vomitoria* larvae

PCA - Principal Components Analysis (Standardised)

N. PCs	Eigenvalues	
	E-value	*%*
Total SS	2346	100
#1	1719.85165	73.30995951
#2	200.8827956	8.56277901
#3	155.8546183	6.643419365
#4	96.37611478	4.108103784
#5	71.45009633	3.045613655
#6	26.28108452	1.120250832
Total		96.8

Appendix 22: Euclidean distances from PCA data of *C. vomitoria* larvae

vomitoria	Day 1	Day2	Day 3	Day 4	Day 5	Day 6	Day 7	Day 8	Day 9	Day 10	Day 11	Day 12	Day 13	Day 14
Day 1														
Day 2	0.0842													
Day 3	0.2900	0.2298												
Day 4	0.3744	0.3630	0.3490											
Day 5	0.2926	0.2564	0.2267	0.3303										
Day 6	0.2385	0.2274	0.2070	0.3295	0.1304									
Day 7	0.2314	0.2374	0.2511	0.3361	0.1593	0.0517								
Day 8	0.2383	0.2542	0.2675	0.3408	0.1987	0.0813	0.0415							
Day 9	0.2650	0.2977	0.3157	0.3546	0.2776	0.1576	0.1234	0.0823						
Day 10	0.2172	0.2340	0.2776	0.3130	0.1974	0.1204	0.0847	0.0865	0.1318					
Day 11	0.2606	0.2442	0.2635	0.3386	0.1504	0.1594	0.1549	0.1822	0.2478	0.1242				
Day 12	0.3172	0.2897	0.2531	0.3914	0.2232	0.2212	0.2271	0.2451	0.2986	0.1982	0.1148			
Day 13	0.2877	0.2831	0.2715	0.3524	0.3155	0.2585	0.2535	0.2494	0.2628	0.1977	0.2037	0.1605		
Day 14	0.2429	0.2458	0.2454	0.3584	0.3366	0.2515	0.2499	0.2377	0.2354	0.2120	0.2567	0.2347	0.1080	

Appendix 23: Graph of the average percentage peak area of all methyl branched hydrocarbons and alkenes in relation to instars for *C. vicina*

Appendix 24: PCA table for the ageing *C. vicina* larvae

PCA - Principal Components Analysis (Standardised)

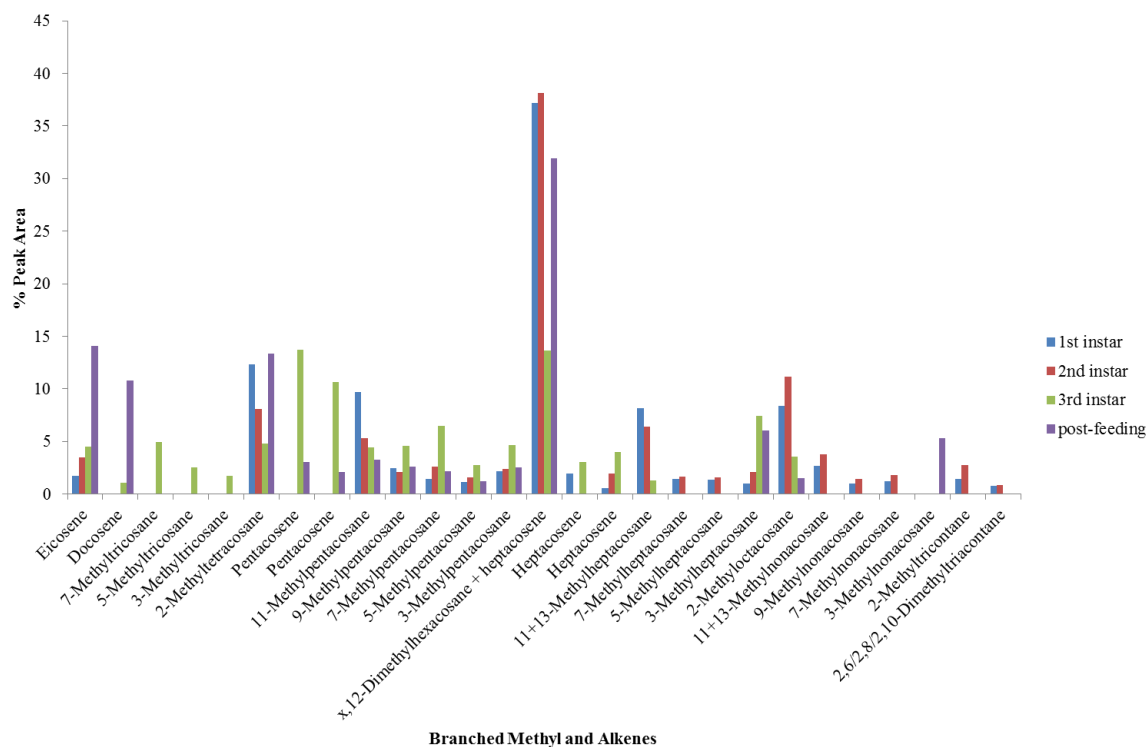| N. PCs	Eigenvalues	
	E-value	*%*
Total SS	2808	100
#1	1699.315248	60.51692478
#2	568.9978374	20.26345575
#3	248.6416931	8.854761149
#4	137.6304278	4.901368513
#5	38.33352011	1.36515385
#6	28.42507936	1.012289151
Total		96.9

Appendix 25: Euclidean distances from PCA data of *C. vicina* larvae

vicina	Day 1	Day2	Day 3	Day 4	Day 5	Day 6	Day 7	Day 8	Day 9	Day 10	Day 11
Day 1											
Day 2	0.1692										
Day 3	0.2537	0.2004									
Day 4	0.2935	0.2607	0.1263								
Day 5	0.3363	0.3648	0.2398	0.1517							
Day 6	0.3422	0.3266	0.2415	0.2906	0.3218						
Day 7	0.3058	0.2991	0.3133	0.3081	0.3298	0.2129					
Day 8	0.2888	0.3036	0.3363	0.2941	0.2769	0.3503	0.2113				
Day 9	0.2917	0.3094	0.2809	0.3104	0.2918	0.2839	0.3085	0.2483			
Day 10	0.3132	0.2819	0.2565	0.2939	0.3102	0.2954	0.3253	0.2666	0.0908		
Day 11	0.2673	0.2104	0.2206	0.2423	0.2883	0.3123	0.2980	0.2188	0.1576	0.1017	

Appendix 26: Graph of the average percentage peak area of each methyl branched

hydrocarbon in relation to instars for *C. vicina*

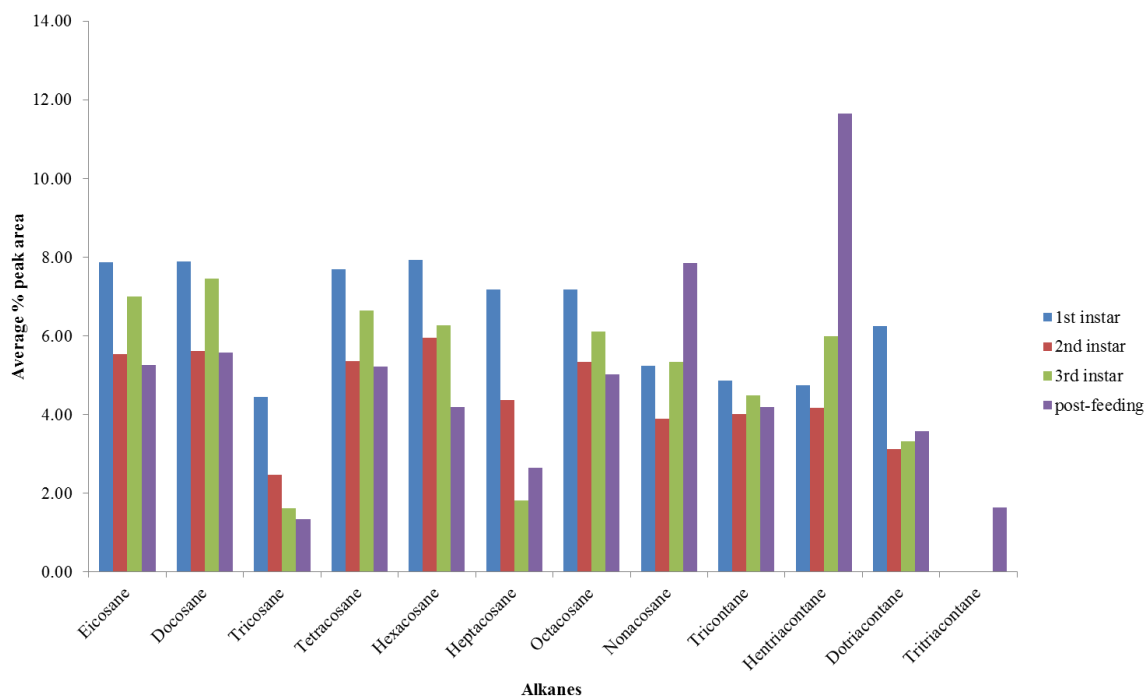**Appendix 27**: PCA table for the ageing *L. sericata* larvae

PCA - Principal Components Analysis (Standardised)

N. PCs	Eigenvalues	
	E-value	*%*
Total SS	2610	100
#1	1642.219098	62.92027197
#2	428.2377957	16.40757838
#3	180.1818773	6.903520204
#4	102.6936448	3.934622407
#5	88.64279246	3.396275573
#6	66.38528444	2.543497488
Total		96.1

Appendix 28: Euclidean distances from PCA data of *L. sericat*a larvae

	Day 1	Day2	Day 3	Day 4	Day 5	Day 6	Day 7	Day 8	Day 9
Day 1		0.2694	0.3848	0.4134	0.2846	0.3406	0.3730	0.3659	0.3397
Day 2			0.2401	0.2852	0.1717	0.2106	0.2135	0.2808	0.2832
Day 3				0.3474	0.2790	0.4027	0.3795	0.3386	0.3526
Day 4					0.1692	0.3378	0.3273	0.3265	0.3342
Day 5						0.2176	0.3080	0.2711	0.2576
Day 6							0.3169	0.3306	0.3106
Day 7								0.2994	0.3274
Day 8									0.0592
Day 9									

Appendix 29: PCA table for the ageing *L. sericata* pupae

PCA - Principal Components Analysis (Standardised)

N. PCs	Eigenvalues	
	E-value	*%*
Total SS	520	100
#1	492.925115	94.79329135
#2	17.77438759	3.41815146
#3	4.044619127	0.777811371
#4	3.499245493	0.672931826
#5	1.017619343	0.195696028
#6	0.394761043	0.075915585
Total		99.9

Appendix 30: PCA table for the ageing *L. sericata* puparial cases

PCA - Principal Components Analysis (Standardised)

N. PCs	Eigenvalues	
	E-value	*%*
Total SS	2960	100
#1	2835.408462	95.7908264
#2	96.3068758	3.253610669
#3	16.98851771	0.573936409
#4	5.359923119	0.181078484
#5	2.919330788	0.09862604
#6	0.88117459	0.029769412
Total		99.9

Appendix 31: PCA table for the ageing *C. vicina* puparial cases
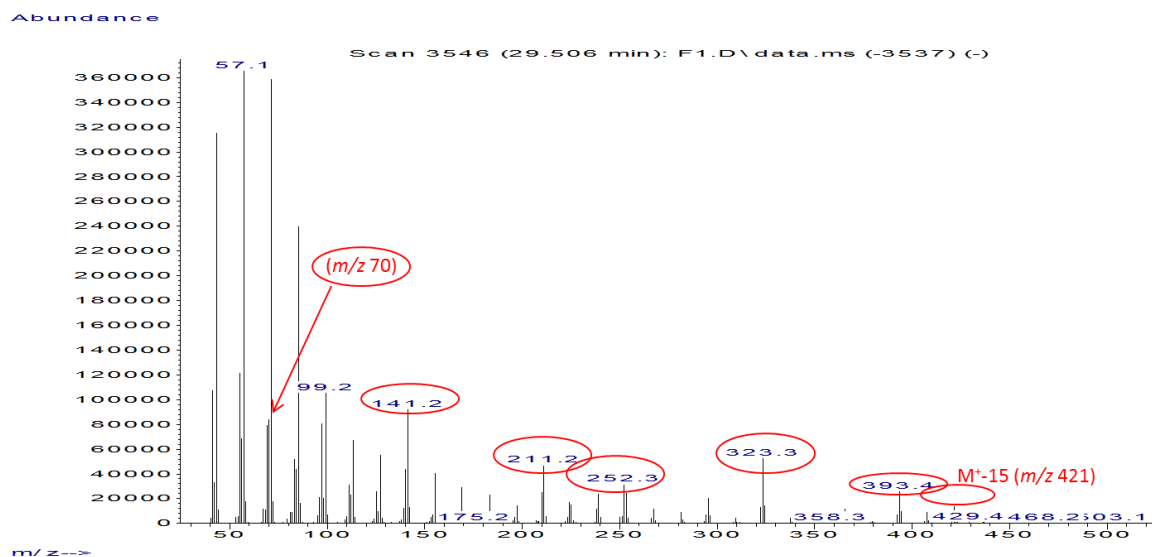
PCA - Principal Components Analysis (Standardised)

N. PCs	Eigenvalues	
	E-value	*%*
Total SS	3278	100
#1	3006.219136	91.70894254
#2	125.5828698	3.831082057
#3	73.27608649	2.23539007
#4	21.90452788	0.668228428
#5	17.62194096	0.537582092
#6	15.84948746	0.483510905
Total		99.5

Appendix 32: PCA table for the ageing *L. sericata* adult flies
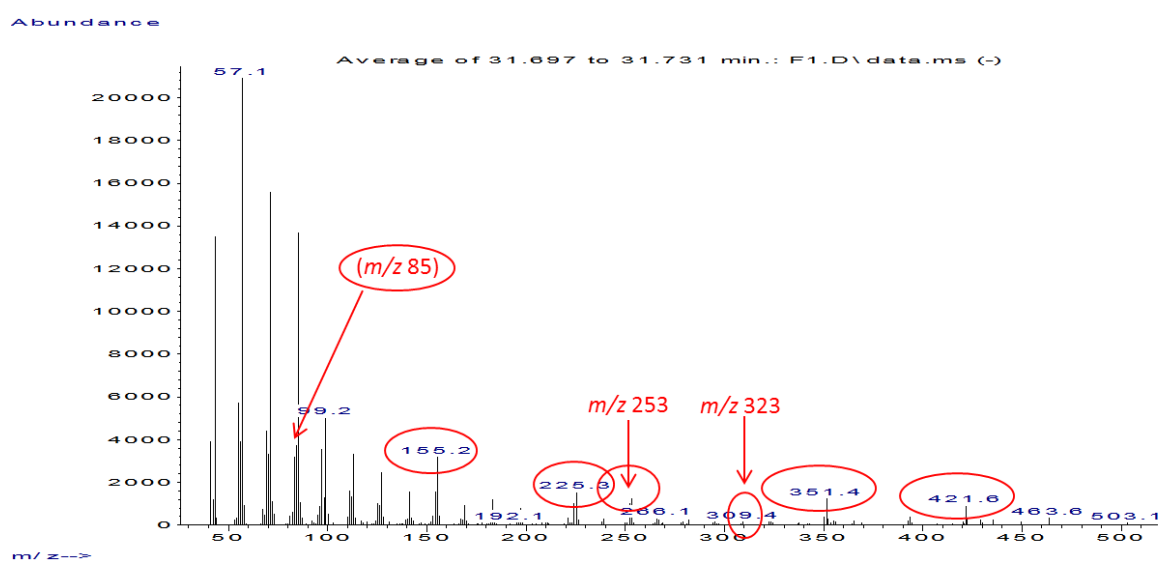
PCA - Principal Components Analysis (Standardised)

N. PCs	Eigenvalues	
	E-value	*%*
Total SS	1440	100
#1	942.7629878	65.46965193
#2	350.0192629	24.30689325
#3	52.93421735	3.675987316
#4	46.33162896	3.217474233
#5	22.07564691	1.533031036
#6	11.10264032	0.771016689
Total		99.0

Appendix 33: Mass spectra of 4,8,12/4,8,14-Trimethyloctacosane, with diagnostic ions to aid identification circled.

Appendix 34: Mass spectra of 5,9,13/5,11,15-Trimethylhentriacontane, with diagnostic ions to aid identification circled.

Appendix 35: PCA table for the ageing *C. vicina* adult flies

PCA - Principal Components Analysis (Standardised)

N. PCs	Eigenvalues	
	E-value	*%*
Total SS	2940	100
#1	2088.306934	71.03084811
#2	449.5575547	15.29107329
#3	183.107191	6.22813575
#4	60.17350378	2.046717815
#5	49.87722263	1.696504171
#6	41.13250506	1.399064798
Total		97.7

Appendix 36: PCA table for the ageing *C. vomitoria* adult flies

PCA - Principal Components Analysis (Standardised)

N. PCs	Eigenvalues	
	E-value	*%*
Total SS	2695	100
#1	1726.885169	64.07737175
#2	536.9184823	19.92276372
#3	284.7059783	10.56422925
#4	93.16489081	3.456953277
#5	26.58335937	0.986395524
#6	6.527062203	0.242191547
Total		99.2